MEMOIRE DE GEOSCIENCES

n° 143

Jo DE RIDDER

Réponse des processus biochimiques d'une tourbière soumise à des fluctuations du niveau d'eau

Thèse de Doctorat de l'Université de Rennes 1

soutenue le 1er février 2012

Géosciences – Rennes
UMR 6118
CNRS - Université de Rennes 1
Campus de Beaulieu
35042 - Rennes Cedex
(France)

2012

ISSN 1240-1498

ISBN 2-914375-84-0

Année : 2012

Auteur : Jo DE RIDDER

Titre : Réponse des processus biochimiques d'une tourbière soumise à des fluctuations du niveau d'eau.

Collection : Mémoires de Géosciences, n° 143

Disponible en archive ouverte au format PDF :

http://www.geosciences.univ-rennes1.fr

http://tel.archives-ouvertes.fr/

- -

Légende photo de couverture :

Dispositif expérimental en colonnes

Editeur :

Editions de Géosciences Rennes
Université de Rennes 1 - Campus de Beaulieu
35042 RENNES Cedex (France)

Directeur de publication :
Philippe Davy

Responsable d'édition :
Catherine Bertin (02 23 23 65 43 – catherine.bertin@univ-rennes1.fr)

N^o d'ordre : 4484 ANNÉE 2012

UNIVERSITÉ DE RENNES 1

THÈSE / UNIVERSITÉ DE RENNES 1
sous le sceau de l'Université Européenne de Bretagne
pour le grade de
DOCTEUR DE L'UNIVERSITÉ DE RENNES 1

Mention : Sciences de la Terre
Ecole doctorale des sciences de la matière
présentée par

Jo DE RIDDER

préparée à l'unité de recherche n^o 6118
Géosciences Rennes

Réponse des processus biochimiques d'une tourbière soumise à des fluctuations du niveau d'eau

Thèse soutenue à l'Université de Rennes 1 le 1/02/2012
devant le jury composé de :

Gilles BILLEN Directeur de Recherche - UMR SYSIPHE/rapporteur

Gunnar LISCHEID Professeur - Leibniz Centre for Agricultural Landscape Research / rapporteur

Gilles PINAY Directeur de Recherche - UMR ECOBIO/examinateur

Jean-Baptiste WETTON Responsable du pôle technique - PNR/examinateur

Pierre MARMONIER Professeur - Université de Lyon 1/examinateur

Luc AQUILINA Professeur - Université de Rennes 1/directeur de thèse

André-Jean FRANCEZ Maître de Conférence - Université de Rennes 1/co-directeur de thèse

Mélanie DAVRANCHE Maître de Conférence - Université de Rennes 1/co-directrice de thèse

Remerciements

Mes remerciements vont à Luc Aquilina, pour son agréable collaboration tout au long de ces années d'étude, où j'espère nous avons assemblé quelques pièces du grand puzzle de l'eau du Cotentin. Merci Luc d'avoir enrobé la cacahouète pour contrebalancer ma tendance au "the better, the shorter ".

Merci à Mélanie Davranche et André-Jean Francez pour l'encadrement de ce travail aux multiples facettes chimico-bio-hydro-géo-pédo-statistico-physico-bactériochampignonesques . Merci Mélanie, à ta manière franche et directe, pour les coups de pouce tout au long de cette étude. Merci André-Jean pour ton soutien, ta disponibilité, et pour rendre à César les quadruplicats c'est bien de toi !

Merci ensuite aux nombreux collaborateurs de l'équipe Eau, des plate-formes techniques de l'OSUR, qui ont chacun à leur manière, contribués à ce travail.

Merci à Jean-Pierre Caudal pour son support à l'ingénierie des colonnes. Je retiendrai, Jean-Pierre, que travail bien fait et convivialité font bon ménage.

Merci à Odile Hénin pour son support analytique et ses facultés de dénicher le truc qu'on ne trouve jamais.

Merci à Antoine Guéron, à deux c'est mieux pour monter les colonnes, et toutes les autres tâches chimiquesques.

Merci à Thierry Labasque, devant qui madame l'eau ne peut pas cacher son âge. Je tâcherai, Thierry, de préserver des petits coins à la Roche pour nos amis les petits oiseaux et les petits insectes.

Merci à Antoine Armandine les Landes pour sa belle mise en scène 3 D des écoulements, dont je retiendrai qu'homme fiable donne modèle fiable.

Merci à Pascal Goderniaux, ex-compatriote de la patrie du maneke pis, pour son aide précieuse.

Merci à Didier Michot de lINRA pour les petits piquets et les mètres et mètres de fils. Certes le Cotentin est un peu moins exotique que les bords du Nil, mais la vache du coin (et le taureau) vaut le détour.

Merci à Julien Lacombe "mon grand petit stagiaire" très doué avec les fils.

Merci à Patrice Petit Jean et Martine Bouhnik-Le Coz pour leur support analytique de précision en eau trouble (eh oui il y a de la tourbe).

Merci à Noémie Chateauret, "une femme de cœur et de passion" et jespère que tu vogues à présent sur une belle route.

Merci à Nathalie Le Bris-Josselin, dont je retiendrai que douceur, sourire et efficacité (et concentration, sinon c'est vite la foire dans les flacons) font bon ménage.

Merci à Marie-Paule Briand, dont je retiendrai que gentillesse, malice et efficacité (non je ne radote pas) a fonctionné.

Merci à Flavia Nunes, notre multilingual, multicultural chercheur de service, dont je retiendrai qu'il vaut mieux "essayer autre chose quand cela ne marche pas plutôt que de sentêter" (a vaut aussi pour l'informatique).

Merci à Virginie Vergnaud, dont je retiendrai que pragmatisme et bon sens ne nuisent pas à la rigueur scientifique.

Merci à Emilie Jardé, je garderai en souvenir les séances tire-lait et les bons conseils écolo-un-peu-bobo.

Merci à Laurent Jeanneau, et vive la Révolution !

Merci à Nadine Fouillé, pour avoir si bien géré la bourse en bonne mère de famille.

Merci à Isabelle Dubigeon pour m'avoir dévoilé les secrets de la biblio.

Merci à Alain-Hervé le Gall avec qui la fête de la science c'est un peu tous les jours.

Merci à Jonathan Thierry-Collet du Parc, et les divers intervenants du Comité de Pilotage du Cotentin, grâce à qui cette recherche est ancrée dans une socio-écono-agro-écolo réalité.

Contents

Introduction et problématique

Introduction et problématique

Les tourbières remplissent une importante fonction de régulation des cycles biogéochimiques, en tant que puits, sources et transformateurs de nutriments et autres contaminants chimiques. Elles ont donc un impact sur la qualité générale des eaux et sur la productivité des écosystèmes. **L'altération de leur fonctionnement engendre des processus de dégradation chimique, biologique et physique de la tourbe et déstabilise donc l'écosystème global**. L'assèchement des tourbières peut en outre contribuer à l'émission de gaz à effet de serre (CO_2, N_2O) (Reddy and Delaune, 2008).

Les tourbières sont très sensibles à des modifications mêmes légères du régime hydrologique qui peuvent résulter de variation du climat ou de pressions anthropiques. La position relative du niveau d'eau contrôle l'équilibre entre accumulation et décomposition de la tourbe. A l'échelle planétaire, la diminution des niveaux d'eau et la réduction des périodes d'inondation, notamment induite par le drainage, est aujourd'hui associée à divers problèmes (Holden et al., 2004). **Les effets négatifs se répercutent à la fois sur la structure physique de la tourbe et sur la qualité des eaux du milieu**. Par exemple, quand l'aération de la tourbe augmente, sa décomposition est accrue par l'action des bactéries aérobies qui décomposent bien plus efficacement la matière organique qu'en condition anaérobie. Un impact visible de ce processus est la subsidence qui entraîne une baisse de la densité dans la couche supérieure en quelques années suivant la baisse du niveau d'eau (Silins and Rothwell, 1998). L'oxygène accroît la minéralisation des nutriments, en particulier l'azote et le soufre liés au carbone. La tourbe contient de grandes quantités d'azote, de soufre et de carbone qui peuvent donc potentiellement générer des exports en nutriments importants.

Les zones humides sont des écosystèmes complexes, dont les fonctions sont supportées par de nombreux processus physiques, chimiques et biologiques. Les progrès de la recherche scientifique dans ce domaine ont mis en évidence qu'une approche interdisciplinaire est requise pour correctement décrire ces milieux. Le travail présenté dans cette thèse applique cette **approche interdisciplinaire en combinant hydrologie, géophysique, hydrochimie, biochimie et modélisation numérique.**

Le site d'investigation est une prairie tourbeuse située dans la presqu'île du Cotentin, en Normandie au NW de la France (Figure 1).

Les zones humides de Normandie se situent sur les départements de la Manche et du Calvados et couvrent 30 000 ha. Elles sont composées d'une multitude de milieux, abritant une diversité d'espèces animales et végétales dont certaines sont emblématiques à l'échelle nationale et internationale. Situés sur l'axe migratoire Europe du Nord - Afrique, les marais constituent une halte indispensable pour des milliers d'oiseaux. Leurs caractéristiques écologiques sont reconnues au titre de la convention Ramsar et des directives européennes habitat et oiseaux. A ces atouts s'ajoute l'existence d'une importante ressource en eau potable d'intérêt régional. Afin de préserver au mieux ce riche ecosystème tout en maintenant des équilibres entre acteurs du territoire, un Parc Naturel Régional a été créé en 1991. Cinq grands enjeux ont été identifiés à l'horizon de la décennie à venir dans la charte 2009-2021: (1) préserver et conforter la biodiversité (2) assurer une gestion équilibrée de la ressource en eau (3) impulser un éco-développement (4) valoriser les différents patrimoines comme facteur d'attractivité et (5) cultiver la démocratie participative pour mieux mettre en oeuvre le projet de territoire.

Les marais du Cotentin se sont développés sur une couche limono-argileuse, elle même supportée par des roches calcaires et sableuses qui hébergent un aquifère capacitif exploité pour l'eau potable. Cette zone humide a déjà subit un long historique de drainage, auquel s'ajoute aujourd'hui l'impact

de l'extraction d'eau potable dans l'aquifère sous-jacent. La conséquence majeure est que le profil tourbeux est sujet à de plus courtes périodes d'inondation, exposant la tourbe à des conditions plus aérées.

Du fait d'une demande croissante en eau potable de bonne qualité sur le département de la Manche, une implantation de nouveaux pompages est prévue à court terme. Eaux souterraines et de surface sont en connexion, donc un impact sur les zones humides est prévisible (Auterives et al., 2011). D'autre part, une ancienne carrière d'extraction de tourbe de type bombée (tourbière de Baupte) est soumise à un abaissement des eaux et a aussi un impact sur les niveaux actuels de la zone humide. Enfin, le changement climatique, dans ces milieux hautement sensibles, est présumé avoir un impact significatif (Gitay et al., 2001).

Dans ce contexte, **la présente étude a été initiée par le Parc Naturel Régional afin notamment de répondre aux questions suivantes:**

1. **Mieux comprendre le fonctionnement hydrologique des zones humides dans le bassin hydrologique global, incluant la nappe souterraine et les eaux de surface.**

2. **Mesurer l'impact d'une augmentation du pompage dans la nappe, sur les zones humides (prévue à court terme).**

3. **Mesurer l'impact du changement climatique sur les zones humides, à l'horizon de la fin du siècle.**

4. **Etudier l'impact de ces changements sur la biochimie de la tourbe.**

Pour répondre à ces questions, l'analyse de la bibliographie (reprise dans chacune des parties qui suivent) met en évidence plusieurs points qui restent à préciser. Le contrôle hydrologique sur le fonctionnement biogéochimique des tourbières est bien connu, mais les effets de variations de flux, notamment sur les communautés microbiennes, a été peu étudié (Bougon et al., 2009). L'effet des répétitions des variations de niveaux d'eau reste une question ouverte. De plus, les échelles de temps pertinentes et les effets rétroactifs des mécanismes mis en jeu sont peu connus. Ceci est d'un enjeu primordial dans les stratégies de restauration des tourbières. La présente étude a donc été menée pour évaluer l'effet des variations de niveau d'eau sur le fonctionnement biogéochimique de la tourbière. Ces effets sont étudiés à trois échelles par analogie avec les variations sur le terrain (Figure 2): (1) la Partie I est à l'échelle du bassin versant sur des variations de niveau d'eau moyennes sur l'année (2) la Partie II est à l'échelle de quelques jours relatif à des conditions statiques (3) la Partie III est à l'échelle de variations de niveaux d'eau ou de changement de flux hydrologiques à long terme (plusieurs années).

Ce rapport se divise donc en trois grandes parties:

1. **Une étude sur l'hydrologie du système intégrant l'impact des pressions anthropiques**

2. **Une description des processus biochimiques en jeux et l'impact de cycles répétés de mise en eau et de drainage.**

3. **Une étude de l'altération de ces processus en réponse à des changements environnementaux.**

La première partie a pour but de comprendre le fonctionnement hydrologique du système dans sa globalité pour ensuite prédire l'impact d'une augmentation des pompages et du changement climatique à l'horizon de la fin du siècle. Trois axes d'investigation sont présentés: (1) une description de la zone humide complétée par une étude géophysique de l'épaisseur des tourbes (2) une caractérisation de l'aquifère par datation des eaux et analyses chimiques et (3) une modélisation numérique en 3 dimensions pour déterminer les impacts respectifs d'une augmentation du pompage et du changement climatique.

La deuxième partie s'intéresse aux processus biochimiques de l'eau au contact de la tourbe en réponse à une alternance de cycles aérobies/anaérobies. Trois axes d'investigation sont présentés: (1) une description du comportement du sulfate et du carbone organique dissous en réponse à ces alternances (2) les différences de comportement globales en s'intéressant aux effets de fluctuations de nappe dynamiques versus des conditions de stagnation (3) l'impact des conditions testées sur les biomasses et communautées microbiennes.

La troisième partie étudie l'impact de deux changements environnementaux sur les processus biochimiques, mis en avant par l'étude hydrologique : (1) la dessiccation de la tourbe suite à un assèchement prolongé et (2) la recharge de la tourbière par deux types d'eau, soit une eau de surface (cours d'eau) et une eau souterraine.

Le rapport est finalisé par une synthèse générale conduisant à souligner quelques points de vigilance et à émettre quelques recommendations à destination des gestionnaires de ce milieu.

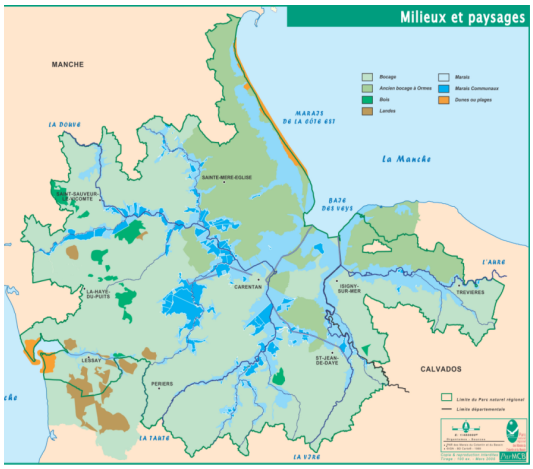

Territoire du Parc Régional des Marais du Cotentin

Figure 1: *Localisation du site d'étude dans la presqu'île du Cotentin*

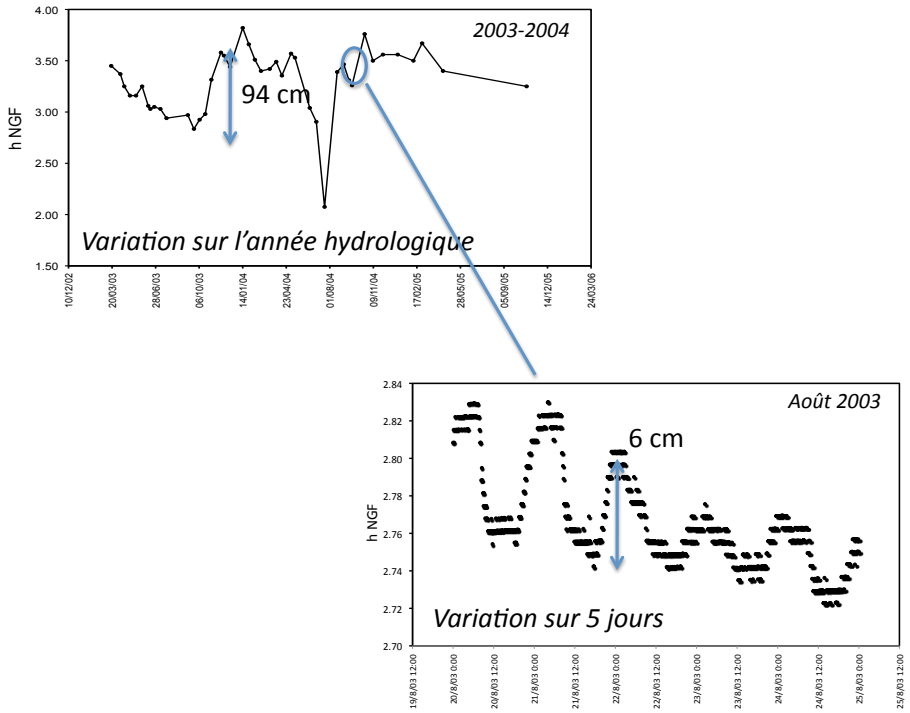

Figure 2: *Les variations de niveaux d'eau dans la zone humide à différentes échelles. Données issues d'une étude précédente (Auterives, 2006)*

Part I

Hydrology of the system

This first Part aims to understand the global system hydrological functioning (wetland and underlying connected aquifer) and then to predict the impact of increasing pumping and climate change at the end of this century.

Three Chapters are presented:

The first Chapter provides a global description of the wetland completed by a geophysical investigation to determine the depth of the peat/aquifer interface.

The second Chapter provides a characterization of the aquifer by water dating and chemical analyses in order to gain knowledge in the aquifer functioning and vulnerability and the potential wetland influence.

The third Chapter presents a numerical 3D modelisation to reproduce the global hydrological functioning and then to predict the respective impacts of increasing pumping in the aquifer and climate change on the wetland hydrology.

Chapter 1

Wetland history and extension and peat thickness

Collaboration team: Didier Michot (UMR SAS INRA Rennes) and Julien Lacombe (Licence student University of Rennes 1). The geophysical technical skills are provided by the INRA. In this Chapter, geophysical methods and results will be synthetically presented.

Figure 1.1: Wetland landscape in un-flooded and flooded conditions

The wetlands of Normandy are extending on two french departments, the Manche and the Calvados and cover 30 000 ha. They integrate a mosaic of water meadows forming a drainage network converging towards the sea. They exhibit a great biodiversity and are an important stop for migratory birds. These wetlands are included in the list of the Ramsar convention since 1991. In order to preserve this unique ecosystem while maintaining the agricultural activity, a Natural Regional Park was created in 1991. Four major issues are pointed out for the next 10 years: (1) preserve and reinforce the biodiversity (2) insure a sustainable management of the water resource (3) encourage an eco-development and (4) make the territory attractive.

A major issue is to maintain a sustainable equilibrium between environmental protection, water needs and the agricultural activity.

In this context, the study presented in this first Part was aimed to gain knowledge in the aquifer and wetland hydrological functioning and their potential vulnerability to pollution. In addition, a major issue was to determine the wetland sensitivity to increasing groundwater abstraction and climate change.

The peatlands of Normandy have developed over the last 5000 years from the anaerobic decomposition of feather mosses. The plant assemblage is mostly composed of phanerogams including trees and shrubs whose woody skeleton is well preserved in the peat (Provost, 1982). Most of the Cotentin peatlands are now at the end of the active turf-forming phase. Peats have almost entirely ceased accumulating organic matter, in spite of frequent and persistent flooding (Provost, 1982). The wetland ecosystem has evolved in equilibrium with human activities, preserving a rich biodiversity (Provost, 1982) (Provost, 1993).

This widely extended wetlands have undergone numerous disturbances. In the XVIII century the wetland was flooded 9 months per year (Bouillon-Launay, 1992). Since 1712 a human controlled drainage system was gradually installed. It presently consists in a network of channels and ditches in which the water level is set low in spring to minimize flooding and high at the end of the summer to act as wet-fencing. Since the 1950s, due to agricultural constraints, the flooding season has decreased to only 3 months on average. The top peat profile is thus subjected to longer periods of dessication.

The study area is limited by the Sainteny-Marchesieux basin where the wetlands extend over approximately 30 % of the total area (Figure 1.2).

The investigated peatlands are mesotrophic freshwater fens with slightly acid to neutral pH. They are nowadays classified in the meadow peatland type with plant communities dominated by *Dactylus glomerata* L., *Holcus lanatus* L., *Agrostis stolonifera* L., *Festuca arundinacea* S. and F., *Carex spp*. and *Juncus effusus* L.(Bouillon-Launay, 1992). The peat thickness is roughly known by locally distributed data (Bouillon-Launay, 1992): available values range between 1 and 7 m. The peatlands overlie: (1) a clay-rich layer of variable thickness (available data provides values from 1 to 6 m), although not always present and (2) a Miocene to Quaternary sandy formation 50 to 100 m thick (Baize, 1998). Peat hydraulic conductivity was measured locally by sludge tests and covers several orders of magnitude, ranging from $1.4.10^{-9}$ to $1.5.10^{-5}$ m.s^{-1}, mainly depending on the depth (Auterives et al., 2011). The clay-rich layer hydraulic conductivity was also measured locally and values range between 10^{-7} and $3.3.10^{-8}$ m.s^{-1}. The deeper peat and the clay-rich layer hydraulic conductivities are thus not very distinct. The underlying Miocene to Quaternary aquifer has much higher hydraulic conductivities ranging from 8.10^{-3} to $5.5.10^{-4}$ m.s^{-1} (Auterives et al., 2011).

The understanding of the hydrological wetland functioning, in particular the first modellisation

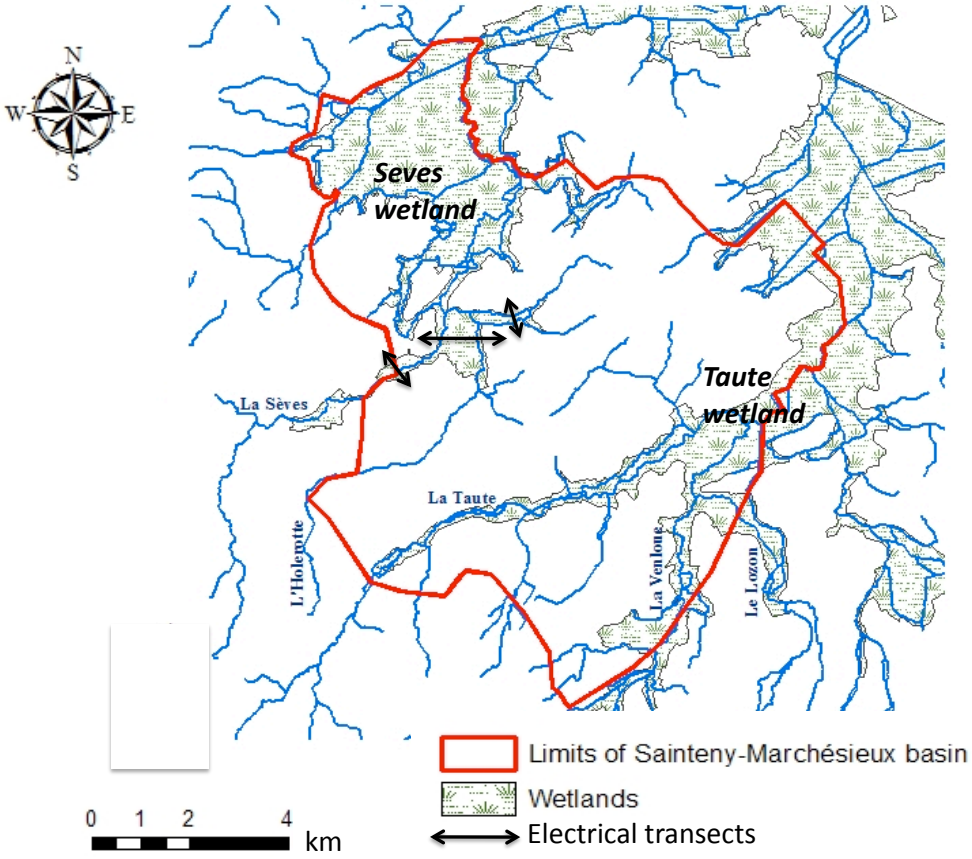

Figure 1.2: *Sainteny-Marchesieux basin and wetland extension*

attempt (Auterives et al., 2011) (see also Chapter 3), has pointed out the need to better know the peat thickness. The present study investigated the peat thickness by a geophysical electrical method on 3 transects in the Seves wetland (localisation on Figure 1.2). A short overview of the results is presented.

Resistivity method Soils and rocks have a resistance to electric current determined by the nature of the material (clay, quartz, sand, laterite, organic matter), the texture of the material (pore size, contact surfaces) and the medium contained in the pores (air, fresh or salt water, contaminants, etc.). The resistivity method provides a vertical and lateral mapping of the electrical resistance along the investigated soil profile. Consequently, altered zones, highly hard rocks, limits between layers can be detected. In this study, distinction between peat, clay and underlying sandstone/limestone/marshes is investigated.

In order to investigate around 20 m depth, 64 electrodes spaced every 5 m, were placed into the soil along the transect and connected to a resistivity meter (Wenner configuration). Measures

were done between two pairs of electrodes: an electrical current (in Amperes) is injected in two electrodes and a difference in potential (in Volts) is measured in two other electrodes, located in between the injection electrodes. The resulting resistance is then calculated by the ohms law. A series of measurements is done by gradually spacing the distance between electrodes to obtain a complete 2D vertical profile. A specific data treatment is needed (use of a resistivity model to inverse the apparent values to specific values, integration of a fine scale topography, adapted discretisation...) to finally obtain an interpretable profile.

Peat depths The transect localisations are reported in Figure 1.3. The transect vertical profiles after treatment are illustrated in Figure 1.4. Several hand measured peat depths, by use of a long auger 15 m length, are reported on the transects. The resistivity method was successful, as the difference in resistivity between peat and the underlying more resistant layer made discrimination possible. The hand depth measurements correlated well with the resistivity profiles. Peat resistivity was thus estimated between 0 and 50 Ohm.m. However, the peat and the clay-rich layer could not be distinguished. Globally, peat thickness is relatively variable along the transects ranging from a few centimetres in the borders to more than 15 meters at some locations. Peat is deeper in transects 2 and 3 and thinner in transect 4. On average, the peat thickness is locally higher than formerly estimated by the available data, as well as the thickness variability.

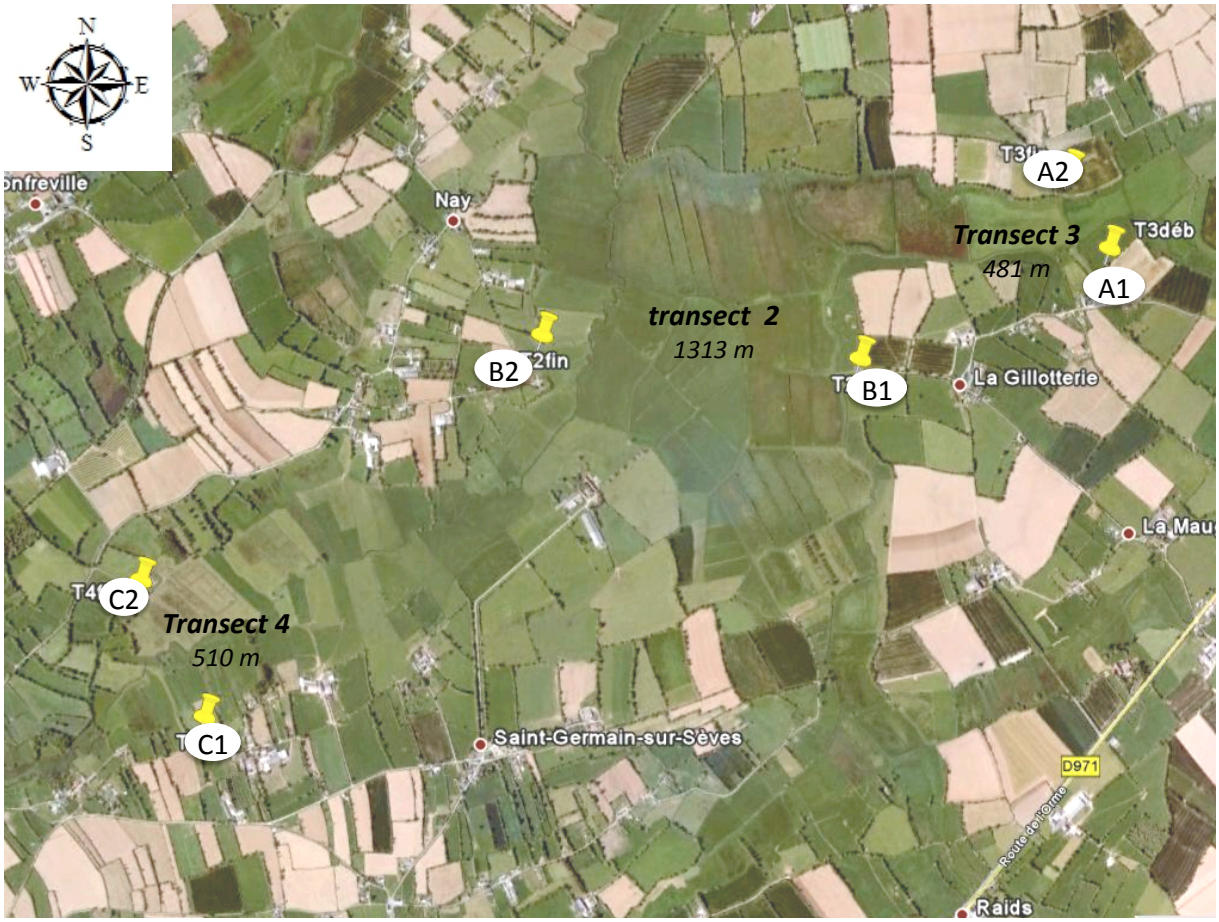

Figure 1.3: *Location of the transects*

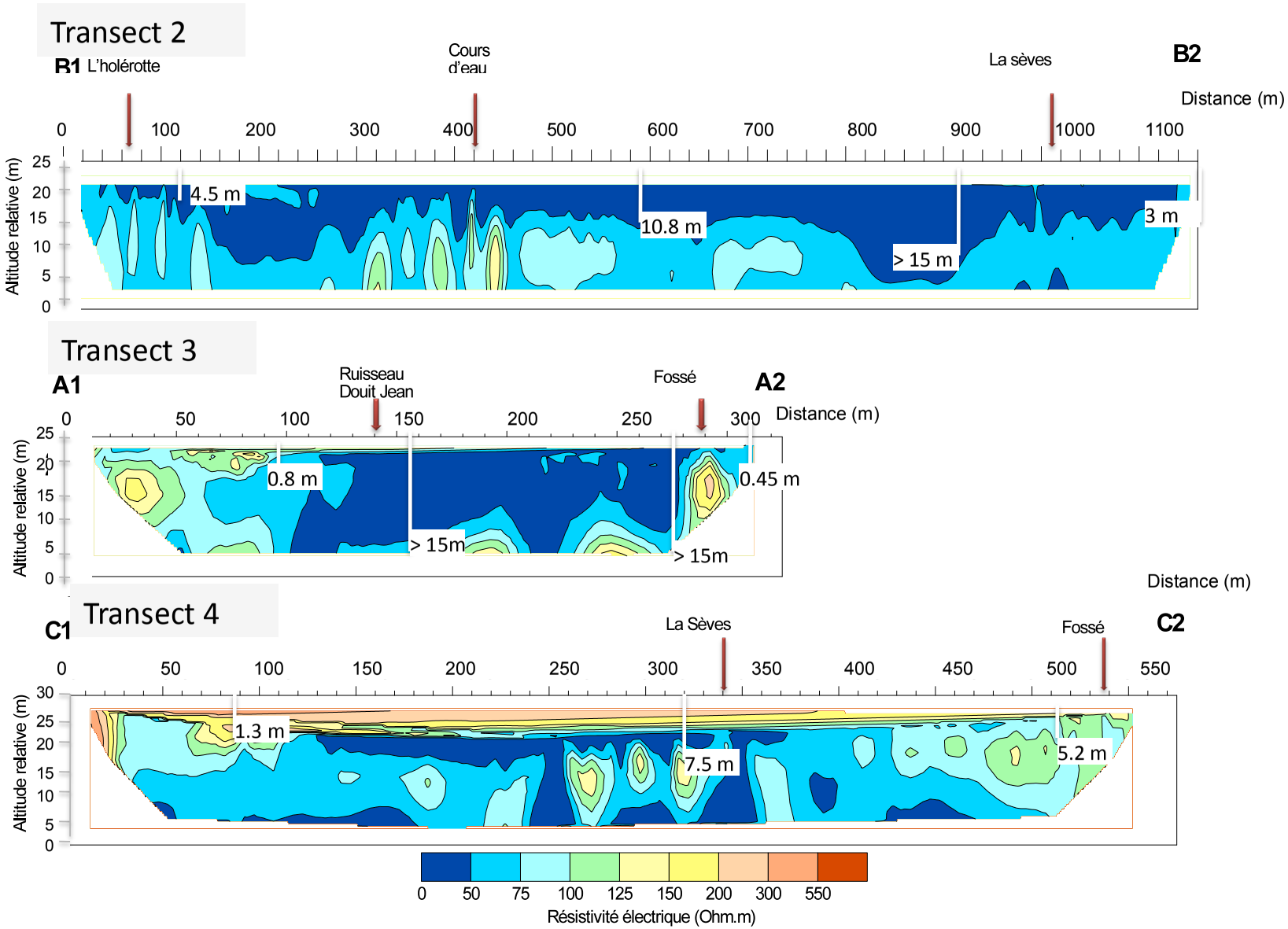

Figure 1.4: *Vertical 2D profile of the interpreted resistivity. The vertical white lines (3 or 4 per transect) figure the hand made peat thickness measures*

Chapter 2

Aquifer characterization

Collaborating team: Thierry Labasque for technical support and expertise, Odile Henin for field and analytical support, Martine Bouhnik-Le Coz and Patrice Petitjean for analytical support

Introduction

The hydrological catchment of Sainteny-Marchesieux is located in North Normandy and extends on 135 km^2. The Cotentin peatland has developed on top of a clayey bed which is supported by a highly transmissive aquifer used for drinking water supply. Due to an increasing demand in good water quality, the authorities plan to increase the extraction.

The objective of this study is to characterize the aquifer by : (1) a synthesis of available data provided by the authorities (2) field measurement of water residence times by age dating using CFCs et SF_6 tracers (3) a hydrochemical characterization to access chemical knowledge and vulnerability within the aquifer.

2.1 Study site

The Sainteny-Marchesieux basin extends over approximatively 135 km^2 and culminates at 30m (Figure 2.1). Vast wetlands are located in lowlands along rivers and made of peat soils.

The basin geology was studied by Baize (1998) (Baize, 1998): it is a graben, bounded by NE-SW oriented faults (South limit of the sub-catchment of Marchesieux and separating limit between Marchesieux and Sainteny in the centrum) and NNW-SSE faults (see Figure 2.2). This basin can reach 150 meters depth and lies on Permian pelites. It is limited by impermeable bedrocks: Precambrian rocks (paleovolcanites, quartzite diorites, sandstones and arkoses) to the South, Trias and Permian rocks to the East and the North and Paleozoic schist and sandstones to the West (Vernoux et al., 2000) (Baize, 1998).

Two sub-catchments, which make up two main aquifers, can be distinguished:

- Sainteny in the North-West, extending on 35 km^2. Dominated by limestones and sandy shell limestones (Faluns du Blehou) with gross grain size making this rocks very permeable. Max-

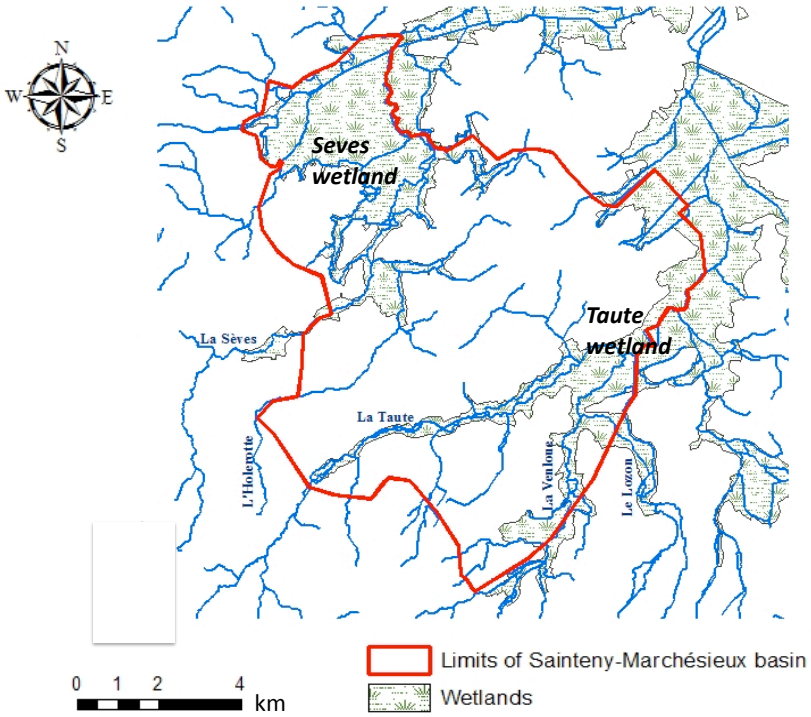

Figure 2.1: Sainteny-Marchesieux catchment

imum thickness is about 100 meters. Depending on the presence of a clayey bed or peat, the aquifer is locally confined, semi-confined or unconfined.

- Marchesieux in the South, extending on 100 km^2. The geology is more heterogeneous with an inter-layering of clayey marshes (of Saint Nicolas), clayey-sandy-silty marshes (of the Bosq d'Aubigny), clayey siltite and finely grained sandstone (of Marchesieux). The hydraulic conductivity is approximately 10 times lower than in Sainteny. Thickness is greater with a maximum around 150 meters. The aquifer is dominantly unconfined.

Finally, sands (of Saint-Vigor) overly the whole geological formations. They are locally completed by Holocene peats and Quaternary alluvial material.

At present, water extraction is predominantly affecting the sub-catchment of Sainteny, with around 5 millions m^3 pumped per year (supplying 90 000 inhabitants). Five pumping wells are used, 3 working since 1992, and 2 since 2002 (see Figure 2.1). The other sub-catchment is only poorly exploited by one well, with a pumping rate of around 0.14 millions m^3/year since 1999. Mean annual rainfall and temperature are 923 mm and 11.2 $^\circ C$, respectively (average 1946-2009 Meteo France). Run off was already calculated in a previous study (SOGREAH PRAUD, 2001) by taking into account the ratio river discharge:precipitation. The resulting average evapotranspiration is 70 % of the precipitation (Auterives et al., 2011). Groundwater extraction represents approximately 9 % of the recharge.

These sub-catchments are drained by a dense water surface network. Subsurface flow is globally

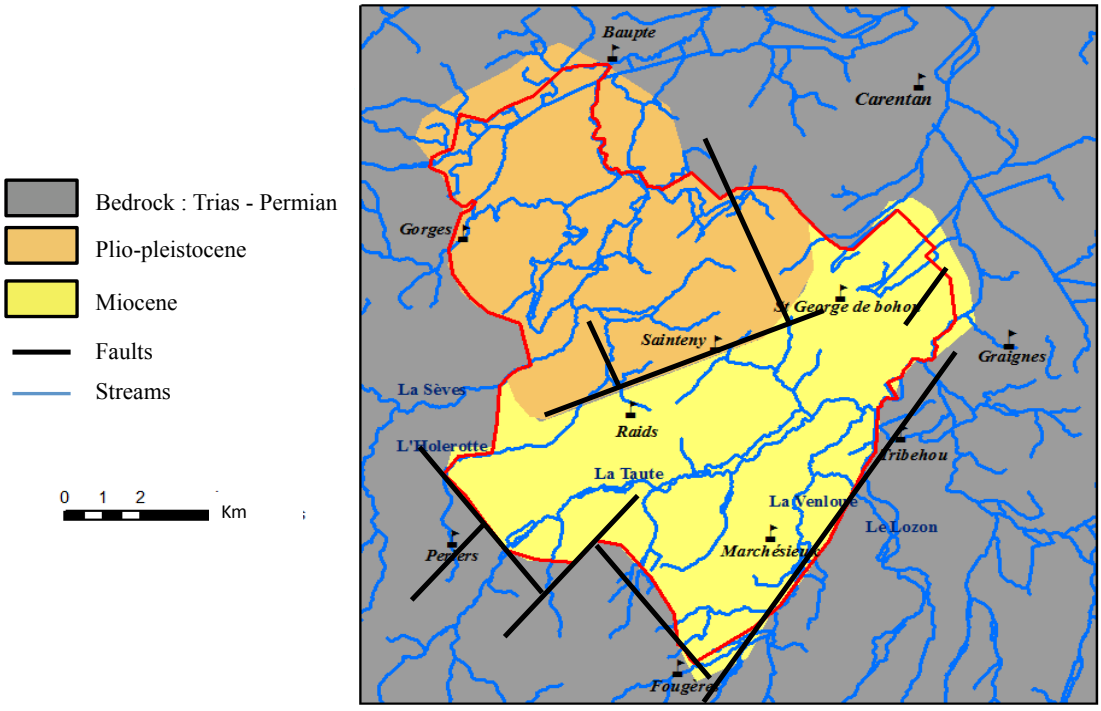

Figure 2.2: Structural diagram of the catchment geology

from South-west to North-east according to 3 main rivers : The Seves (in the North) which feeds the wetlands of Baupte, the Holerotte (in the middle) affluent of the Seves and the Taute which feeds the wetlands in the East (see Figure 2.1). The wetlands are mainly located in peat formations which thickness are between 5 and 15 m (chapter 1). These wetlands are hydrologically connected with the deeper aquifer (See Chapter 3).

Land use is mainly agricultural, with cattle breeding as dominant practice. More than half of the area is dedicated to meadow and crops (mainly corn). Wetlands (dominantly peatlands) cover approximately 30% of the area. The basin is at 30 m above see level at its highest point. In the peatlands and along the streams the average altitude is between 1 and 5 m.

2.2 Materials and methods

2.2.1 Sampled wells and waters

Fourteen wells located in the aquifer were sampled twice: in April during high water levels and in October 2009 during low water levels. The sampling was replicated (i) to increase the measurement reliability (ii) to check if the hydrological period had an impact on water chemistry and ageing. The criteria to choose the wells were as follow:

- a good spatial distribution to cover the land
- a good spatial distribution to cover the flow directions based on the piezometric map
- a good representation of the different lithographies within the aquifer

Figure 2.3 shows the well locations. Information about the wells, i.e. lithographic and technical features, were provided by the public authorities (DDAF Manche) (CDHAT, 2008).

Rain water samples analysed in 2004 (Auterives, 2006) were also used in order to quantify the salinity supply (expressed as NaCl) within the aquifer, originating from the rain water. Finally, 4 streams were sampled in order to compare their chemistry with the aquifer which may be helpful to evaluate connections with the aquifer and surface water pollution. Figure 2.3 shows the stream sampling locations.

2.2.2 Defining the sampling depth

The different lithologies presented in section 2.1 result in different transmissivities between wells but also within the vertical profile of a well. Consequently, within a well, some sections will dominantly contribute to its productivity. Some useful data is available to detect this:

- well lithological diagrams on all the wells
- flow meter measures on two wells
- diagraphies on two wells

In order to choose relevant sampling depths (i.e. a sample representative of a productive zone avoiding transition zones), these data were completed by multiparametric vertical profile measurements (Multi-Parameter TROLL 9000 Equipt. Scient.). This probe measures simultaneously pressure (converted to depth), temperature, conductivity, oxygen, pH and redox potential. The probe is slowly rolled down to the bottom of the well with a winch. The parameters are loaded when going down and again when the probe is moved up, for better reliability. 45 minutes are needed to achieve this. Interpretation of the profiles can be done directly to select relevant depths.

After defining the relevant sampling water depth, water is pumped with a Grunfoss MP1 pump. Sampling is done when chemical parameters are stabilized, i.e. temperature, O_2, conductivity, redox potential and pH (measured with probes).

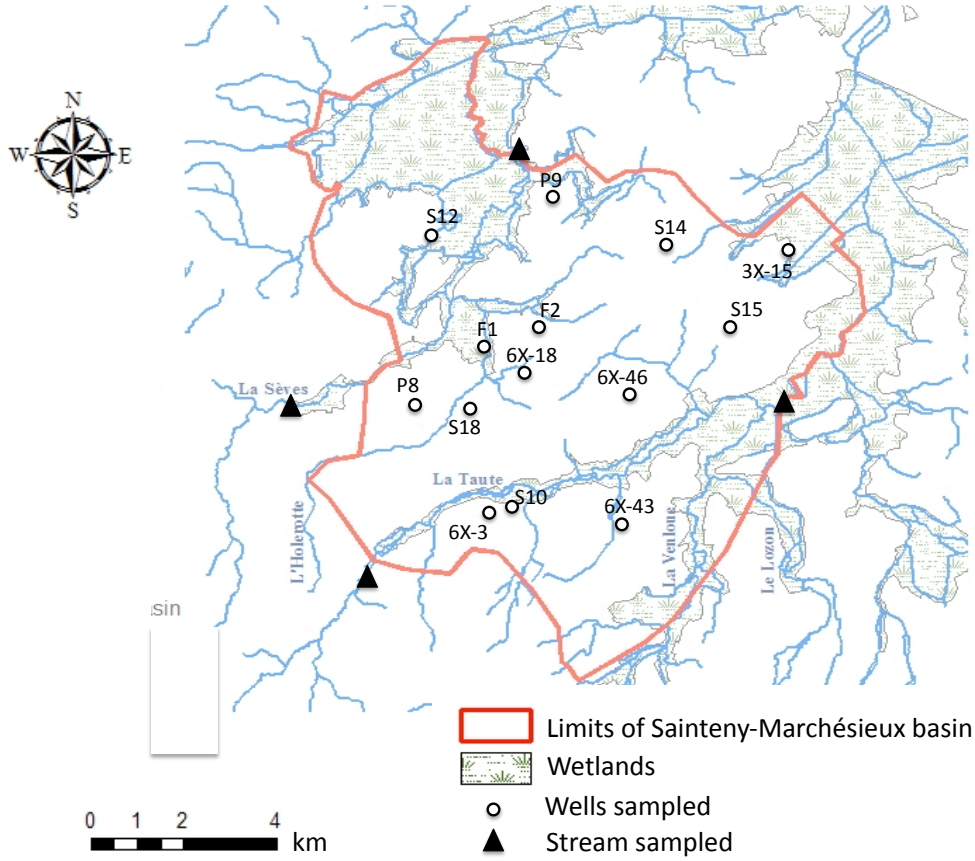

Figure 2.3: Sainteny-Marchesieux catchment and samples location

2.2.3 Water dating by CFCs and SF_6

The dating method is based on the analysis of the chlorofluorocarbons (CFC) and the sulfur Hexafluoride (SF_6). These gases originate from anthropogenic sources and their concentration in the atmosphere are well known (Figure 2.4). They are present since the middle of the XX^{th} century. Measuring these elements in the water allows to estimate when the water entered the aquifer. Coupling the three CFCs and the SF_6 provides a range of ages of about 3 years. Measuring the noble gas Ne is needed to correct the SF_6 concentrations for excess air. It should be taken into account that the computed ages are apparent ages. A good understanding of the hydrological system is needed to interpret the ages, notably because of the mixing processes between various flow lines.

Sampling protocol and analysis were developed in the laboratory of Geosciences-OSUR Rennes (Labasque et al., 2006) (Ayraud et al., 2008). Water is sampled in vessels directly connected to the pump tube to avoid atmospheric contact. To analyse the CFCs and SF6, water is degassed and trapped ('purge and trap') at freezing temperature. Consequently, the gases are isolated, further desorpted at boiling temperature and analysed by gas chromatography with an EDC detector. Uncertainty is attached to the analytical gas measure and reported in Table 2.1. For the noble gases, water samples

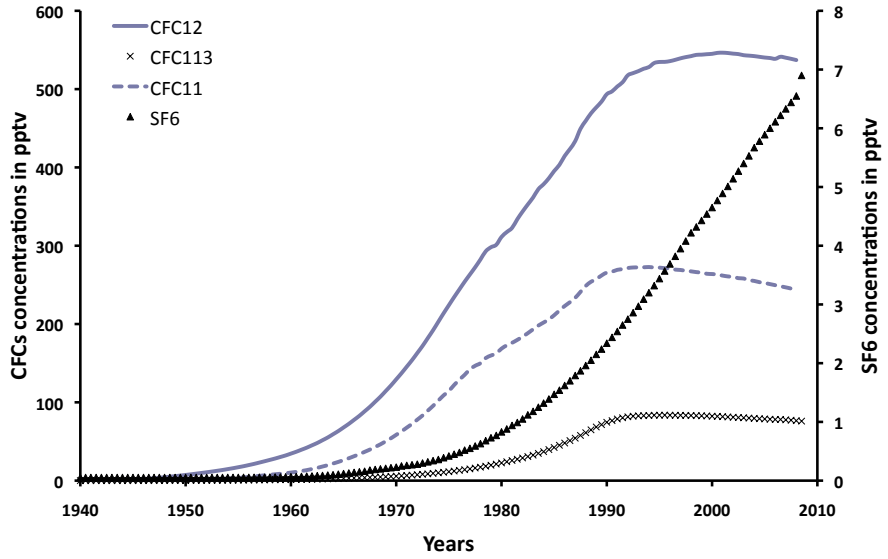

Figure 2.4: Atmospheric CFCs and SF6 concentrations since 1900

Table 2.1: Quantification limits of the dating tracers

	CFC-12	CFC-11	CFC-113	SF6
pptv	26	6	5	0.86
Dating possible after	1956	1956	1980	1980

are taken by overflow in glass bottles, to avoid contact with the atmosphere and trap of gas bubbles. A head space is then created in the bottle by injection of an inert gas (the equivalent volume of water is transmitted to a syringe). The gases within the water equilibrate with this gaseous phase and are further analysed by chromatography with a catharometric detector. The original gas contents are then computed based on the fractionation laws between liquid and gaseous phases (Labasque et al., 2006). Additionally, N_2 is analysed: a high value may indicate denitrification.

2.2.4 Anions, cations and carbon

The pH was measured in the field, with a combined Mettler InLab electrode after a calibration performed with WTW standard solutions (pH 4.01 and 7.00 at 25 C). The accuracy of the pH measurement is 0.05 pH units. The electrical conductivity (EC) was measured in the field, by a Consort electrode C533 with an accuracy of 0.01 μ S/cm. The redox potential (Eh) was measured in the field by a Mettler Platinium 4805 electrode with an accuracy of 1 mV.

Major anion (Cl^-, NO_3^-, NO_2^-, PO_4^{2-}, SO_4^{2-}) concentrations were measured by ion chromatography (Dionex DX-120): the uncertainty was below 4%. Major cation (Ca^{2+}, Na^+, K^+, Mg^{2+}, Mn^{2+}, Fe) concentrations and 31 tracers were determined by ICP-MS (Agilent 4500), using indium as an internal standard. The international geostandard SLRS-4 was used to check the validity and reproducibility of the results. Typical uncertainties including all error sources lay between 2 and 5%, depending on the concentration.

Dissolved organic carbon was analysed with a Total Organic Carbon analyser (Shimadzu TOC-5050A). The accuracy of DOC measurement was estimated at 3% (by using a standard solution of potassium hydrogen phthalate). Dissolved inorganic carbon was also measured with the Shimadzu TOC-5050A with an accuracy of 0.2%.

2.3 Results

2.3.1 Well description

Wells are described in Tables 2.2 and 2.3 for Marchesieux and Sainteny basin respectively.

The depth indicated in the second column is the maximal depth measured. In some wells the original depth (technical data) is not reached, presumably because of clogging (termed "blocked" in the table). The third column termed "Shift" means that there is a sudden change in the chemical parameters along the vertical profile (measured by the multi-parameters probe). These "shifts" correlated with the other available data (see section 2.2.2) provide information about specific productive zones. They are thus used to choose sampling depths.

Practically, the profiles often show a homogeneous water column. This suggest that the most transmissive zone contributes predominately to the well supply or alternatively that the totally screened wells mix all the flow lines in the well. Consequently, 9 wells were sampled at one depth, around the middle of the screened well (no shift); 3 wells were sampled at 2 different depths: S14, F1 and F2 (one shift); 2 wells were sampled at regular depths: S18 (5 depths) and 0015 (6 depths) to further investigate the vertical variations in recharge and discharge zones. An example of temperature profile for the well F2 is given in Figure 2.5.

Conductivity ranges between 380 and 807 μS/cm. The highest values are correlated to the most carbonated lithology (faluns de Bohon and faluns de Blehou). pH is close to neutrality and O_2 is generally low.

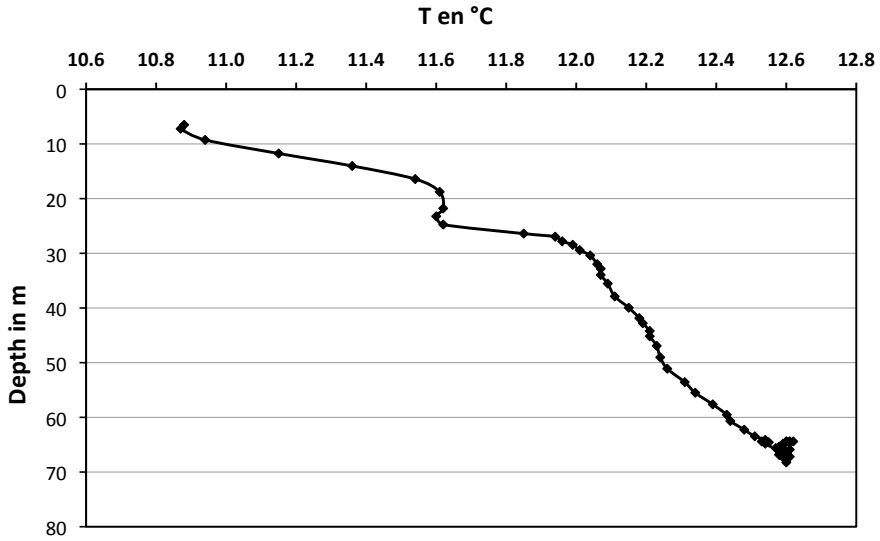

Figure 2.5: Temperature profile in well F2 measured by the multi-parametric probe

Table 2.2: Overall description of the wells in Marchesieux catchment

Well	Depth (m)	Shifts	Sample depth (m)	Lithology	Date	Piezo. level (m)	T (C)	EC (μS/cm)	O_2 (mg/L)	pH	Eh (mV)
3X-15	47	homog.	10	faluns de Bohon	jun.2010	0.85	12.5	714	0	7.1	46
			30	faluns de Bohon	apr.2008	0.82	12.7	716	0	7.2	50
					oct.2008	0.93	13.4	709	0	7.2	195
			45	faluns de Bohon	jun.2010	0.85	12.9	709	0	7.2	156
S15	31 (bl)	homog.	30	faluns de Bohon	apr.2008	14.6	12.5	537	0.80	6.6	376
					oct.2008	14.9	12.9	556	0.01	6.6	388
S10	100 (bl)	homog.	80	grès de March.	apr.2008	7.4	13.1	711	0	7.9	16
					oct.2008	8.3	13	709	0	7.8	239
6X-43	45 (bl)	homog.	40	faluns de Bohon	apr.2008	9.77	13.4	451	0.34	7.1	71
					oct.2008	9.95	13	446	0	7.6	313
6X-18	52	homog.	38	yellow shelly sand	apr.2008	8.6	13.5	570	4.4	6.5	98
					oct.2008	9.08	12.3	572	0.91	6.8	294
S14	75	66 m	40	faluns de Bohon	apr.2008	21.3	13.3	778	0	7.1	33
					oct.2008	21.5	12.9	766	1.1	7.3	317
			73	grès de March.	apr.2008	21.3	13	689	0	7.4	30
					oct.2008	21.5	12.4	807	0	7.4	73
S18	82	homog.	55	marne du Bosq	jun.2010	7.4	13.5	367	0.26	7.5	14
			65	marne du Bosq	apr.2008	7.5	12.8	418	0.48	7.1	21
					oct.2008	7.72	12.3	382	0	7.3	86
			77	marne du Bosq	jun.2010	7.4	13.5	360	0.5	7.5	52
6X-46	40 (bl)	homog.	35	grey clay	apr.2008	8.3	12.9	711	0.6	7.2	27
					oct.2008	9.32	12.5	713	0	7.1	304
6X-3	22	homog.	19	sand of St Vigor	oct.2008	/	12.2	392	2.44	6.3	535

Table 2.3: Overall description of the wells in Sainteny catchment

Wells	Depth(m)	Shifts	Sample depth (m)	Lithology	Date	Piezo. level (m)	T (C)	EC (μS/cm)	O_2 (mg/L)	pH	Eh (mV)
S12	25	homog.	17	yellow sand and clayey sand	apr.2008	1.84	12.7	650	1.17	7.1	208
					oct.2008	2.32	12.85	585	0.45	6.7	334
F2	65 (mou)	homog.	55	faluns de Bléhou	apr.2008	4.5	12.3	654	0.2	7.0	77
					oct.2008	4.8	12.5	658	0	7.1	187
			15	?	oct.2008	21.3	12	421	2.55	6.4	470
F1	73.7	58 m	32	faluns de Bléhou	apr.2008	2.3	13.5	592	6.82	6.8	186
					oct.2008	2.88	12.3	592	2.2	7.2	198
			65	faluns de Bléhou et argiles rouges	apr.2008	2.3	12.9	631	0.93	7.0	117
					oct.2008	2.88	12.4	628	0	7.2	209
P9	68	/	40	faluns de Bléhou	oct.2008	8.05	11.9	524	1.40	7.5	403
P8	22.5(bl)	/	20	fine sand (de St Vigor?)	oct.2008	4.50	13.2	380	3.14	5.9	395

2.3.2 Water age

Dating results from CFCs and SF_6 analysis, corrected for excess air, are synthesized in Tables 2.4 and 2.5. Ar and Ne results are reported in the Appendix B. The estimated recharge dates are listed in the last column of the table, with an uncertainty of 2 years.

As a first insight, the waters range between 1955 and 1993, in other words the apparent age is between 15 and 58 years relative to present.

Main results are:

- The four tracers are in good agreement an support similar ages in most cases.
- In 3 sample CFC113 concentrations are higher than what is normally predicted by equilibration with the atmosphere (003, S12 and F1 at 30 m). As contamination by pesticides may be expected, this tracer is not taken into account in the age estimation of these 3 wells.
- There are no significant age differences between Sainteny and Marchesieux catchments. Apparent ages around 1960 are encountered in the two basins.
- The two sampling campaigns give similar ages (in average a difference of 2.6 years) and can thus be considered as replicates
- Half of the samplings (28 to 77 m depth) result in apparent ages around 1960. These wells show a homogeneous water column.
- The other samples result in younger ages and a vertical stratigraphy is sometimes present
- Regarding the vertical profiles within the wells, 2 wells (F1 and F2) show an evident ageing stratigraphy. In contrast, no vertical difference is visible in S14 and 3X-15, which are located in a discharge zone. S18 shows some small age contrasts, although this well is located in a recharge or intermediate zone.

Figure 1.1 reports the spatial mapping of the ages, superimposed on a piezometric map (data from high water levels in may 1999 (CDHAT, 2008)).

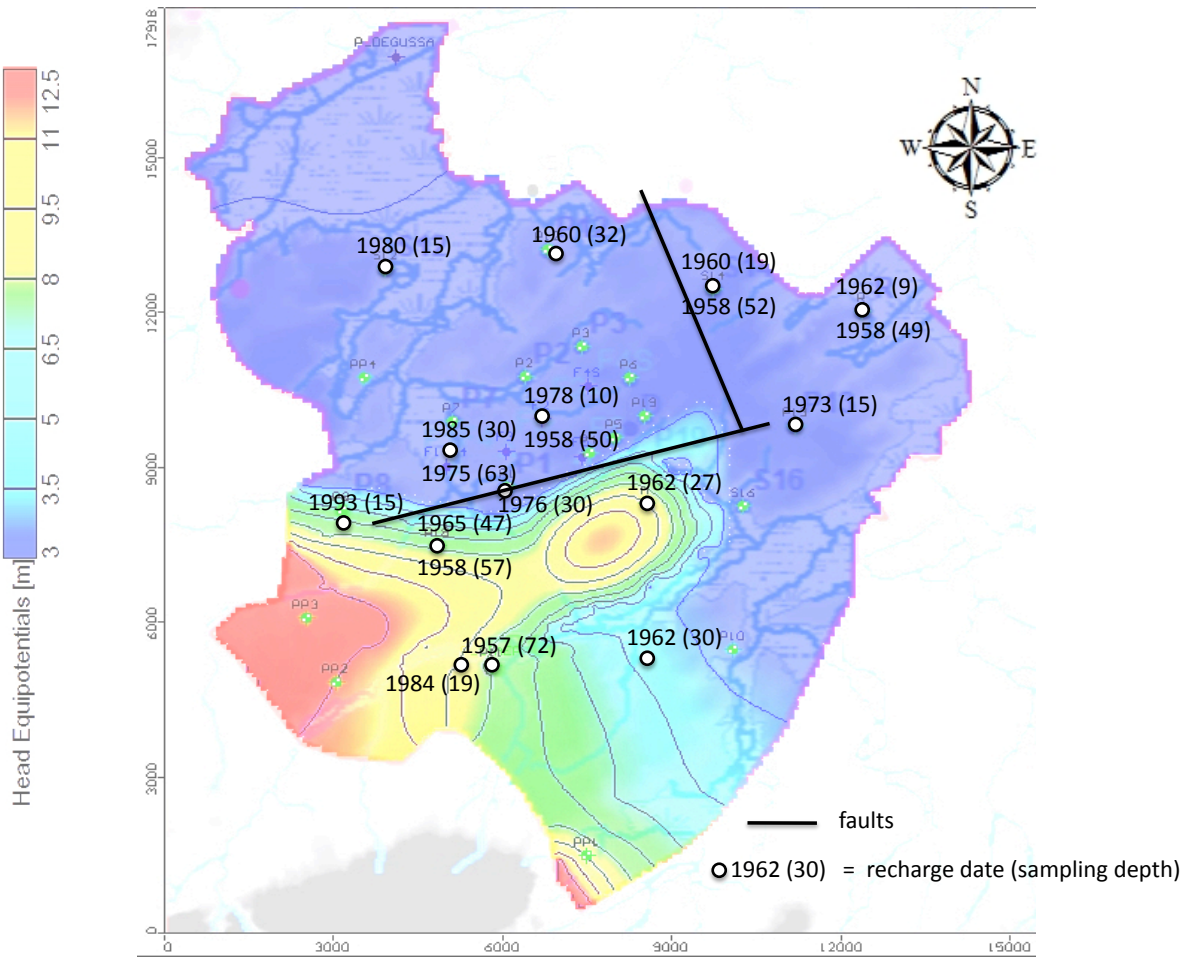

Figure 2.6: Recharge dates (in brackets sampling depths relative to piezometric level and corrected for altitude) superimposed on the piezometric map

Table 2.4: Age results from CFCs and SF_6 tracers in Marchesieux catchment

Well	Sampling depth (m) / piezo. level	Period	CFC 12		CFC11		CFC113		SF_6		Estimated age
			pptv	date	pptv	date	pptv	date	pptv	date	
3X-15	9.2	jun.	21.40	1956	16.5	1962	5.5	1969	/	/	1962
	29.2	apr.	49.2	1962	12.9	1961	15.2	1976	0	< 1975	1962
		oct.	18.7	1956	6.2	1957	/	/	0.8	1979	1957
	44.1	jun.	19.4	1955	5.5	1956	4.8	1968	/	/	1956
S15	15.4	apr.	173	1972	117	1975	34	1983		< 1975	1974
		oct.	138.2	1971	105.4	1974	/	/	0	< 1975	1972
S10	72.6	apr.	32	1958	7.4	1958	15.2	1973	0	<1975	1958
		oct.	7.2	1950	5.7	1956	/	/	0.4	< 1975	1956
6X-43	30.2	apr.	81	1965	23.7	1964	35.3	1983	0	< 1975	1964
		oct.	14.6	1953	11.1	1960	/	/	0.5	1976	1960
6X-18	29.4	apr.	129.4	1969	77.2	1971	58	1988	0.5	1976	1976
		oct.	238	1976	110	1975	/	/	1.1	1982	1976
S14	18.7	apr.	18.1	1954	8.6	1958	26.7	1981	0	< 1975	1958
		oct.	39	1960	27.1	1965	30	1982	0.6	1977	1962
	51.7	apr.	24.2	1957	8.3	1958	18.2	1978	0.9	1983	1958
		oct.	18.7	1956	10.2	1960	/	/	0.5	1976	1958
S18	47.5	jun.	71.40	1965	25.9	1964	18.5	1978	0.36	1974	1965
	57.5	apr.	15.6	1954	3.7	1955	16.5	1977	0.2	< 1975	1955
		oct.	43.8	1962	11.4	1961	/	/	0.3	< 1975	1961
	69.5	jun.	14.54	1953	9.0	1959	38	1984	/	/	1960
6X-46	26.7	apr.	66	1964	23	1964	9.2	1973	0.7	1978	1964
		oct.	25.2	1958	11.2	1961	3.3	1966	0.6	1977	1960
6X-3	19	oct.	356.7	1983	204.7	1984	101.9	/	2	1988	1984

Table 2.5: Age results from CFCs and SF_6 tracers in Sainteny catchment

Well	Sampling depth (m) / piezo. level	Period	CFC 12		CFC11		CFC113		SF_6		Estimated age
			pptv	date	pptv	date	pptv	date	pptv	date	
S12	15.1	apr.	305	1979	120.7	1975	26.3	1981	1.2	1982	1980
		oct.	321.2	1981	163.7	1980	102	/	/	/	1980
F2	50.5	apr.	24	1953.5	7	1957.5	12.4	1975	b.d.l.	$<$ 1975	1957
		oct.	13.4	1953	9.3	1959	/	/	0.6	1978	1959
	10.2	oct.	533.5	1994	154.4	1978	842	/	0.6	1978	1978
F1	29.7	apr.	366.2	1983	217.1	1985	112.6	/	/	/	1985
		oct.	380.4	1984	196	1983	/	/	2.9	1992	1985
	62.7	apr.	144.4	1971	81.7	1972	38.4	1984	0.6	1977	1975
		oct.	233.3	1975	114.9	1975	28.6	1981	2	1988	1975
P9	32	oct.	15.1	1954	11.9	1960	/	/	0.8	1979	1960
P8	15.5	oct.	524.7	1993	265.3	1989	/	/	3.2	1994	1993

2.3.3 Water chemistry

Groundwater

Complete results are reported in Appendix A. The two sampling campaigns show similar chemical concentrations. The average uncertainty on the ionic balance is 2.7 %.

The chemistry of these waters is dominated by Ca^{2+} and HCO_3^-. The pH is near-neutral, with an average value of 7.0 and a standard deviation of 0.4. SO_4^{2-} are present at concentrations between 7.8 and 40 mg/L, except in the well S10 where it is not detectable. No PO_4^{3-} is present. NO_3^- concentrations are variable: some wells have no NO_3^- while others have around 30 mg/L with a maximum at 53.6 mg/L.

Organic carbon content is always under the quantification limit (0.41 mg/L). Inorganic carbon content ranges between 20 and 92 mg/L. One exception is encountered in well P8 where DIC is only 9.4 mg/L (and pH 5.9), a low value probably related to the sand lithology in this well. Iron is sometimes present at relatively high concentrations, ranging from 120 to 2680 μg/L. The maximum value is reached in the well 3X-15 whose diagraphy showed clogging and corrosion traces. These high concentrations may be related to specific mineralogies iron rich and redox conditions favourable to Fe^{2+} mobilisation.

Surface water

Complete data set is reported in Appendix A.

Cl^- concentration is markedly constant in the 4 streams (37.6 $\pm$ 1.1 mg/L) and thus behaving as a conservative element. pH is around 7.4 and NO_3^- ranges between 1.4 to 7.9 mg/L.

Water types

Results are compiled in a Piper diagram to categorize water types (Figure 2.7). It appears that the waters are in the "calcium bicarbonate" type, except for well S10 which has a "sodium and potassium carbonate" type (Ca(Na)(K)-HCO_3). The stream waters are also within the "calcium bicarbonate" type, although the bicarbonate facies is less pronounced. Rain water is within the "sodium chloride" type. Three water samples from the wetland (Auterives, 2006)) are also plotted on the Piper diagram. One sample comes from the saturated zone (ZS), one from the unsaturated zone (ZNS) and a last one from the unsaturated zone when recharge occurs (ZNS rech.). Water typologies are respectively in the "calcium bicarbonate" type, the "calcium" type and the calcium-(hyper)sulphate" type.

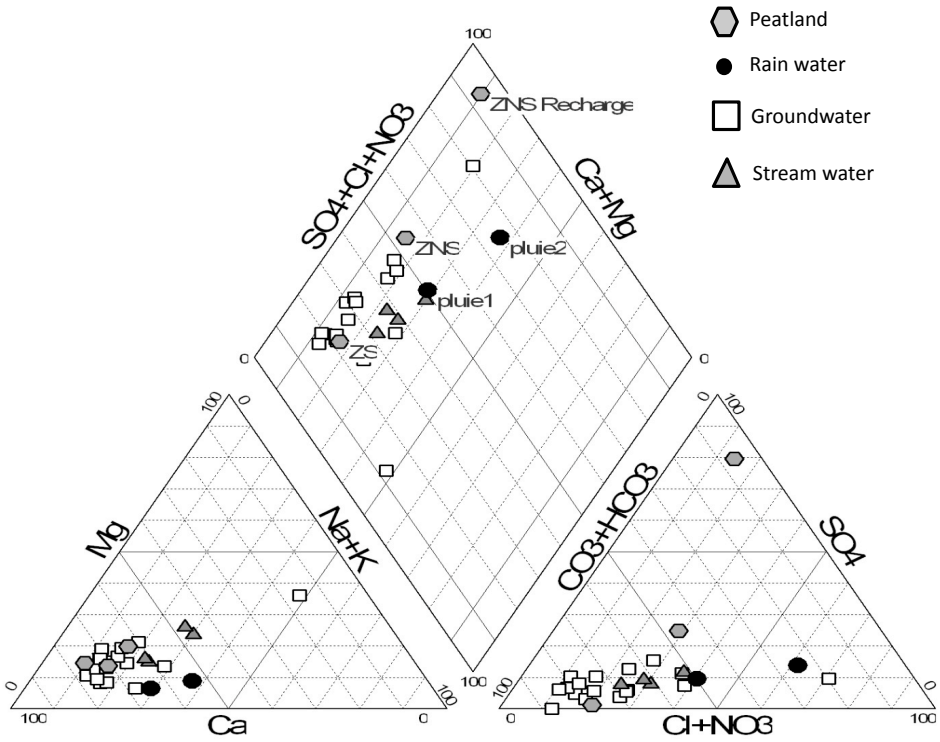

Figure 2.7: Water samples distribution in a Piper diagram

2.4 Discussion

2.4.1 Water dating: a tool to gain knowledge in the hydrological functioning

The interpretation of the water ages has to take into account two major points: (i) what is actually sampled and (ii) the occurrence of flow water mixing.

The aquifer is locally unconfined (where most of the recharge occurs) or semi-confined for instance in the wetland areas, or confined where clayey layers are important. A conceptual diagram illustrating the aquifer, with the flow, the hydraulic head network and the isochrones, is reported in Figure 2.8 (USGS). Some important information can be extracted from this conceptual diagram:

- in the unconfined aquifer, age distribution is described by (Domenico and Schwartz, 1998) :

$$t = \frac{L}{R\theta} ln \frac{L}{L - z}$$

z is the depth within the aquifer
θ is the effective porosity
R is the annual recharge
L is the total aquifer thickness

  Age distribution is independent of the horizontal location within the aquifer.

- the isochrones tighten with depth, in other words age differences with vertical distance are greater at the top of the aquifer.

- the flow lines tighten from the recharge zone towards the confined zone, meaning that the horizontal flow velocity increases.

- a water sample which integrates all the flow lines, i.e. a totally screened well where pumping enhances mixing of all the flow lines, will result in an integrated age which equals the water residence time. This residence time τ is described by:

$$\tau = \frac{L\theta}{R}$$

  Again this time is independent of the horizontal location within the aquifer. In other words, regardless the place in the catchment, in a homogeneous aquifer, an integrative water sample has the same age.

- in confined discharge zones, like the right part of Figure 2.8, the oldest flow lines can be intercepted, i.e. the oldest measured ages in a well.

Overall dating overview

In the study, the wells are screened on almost all their length down to the bottom of the aquifer. The samples collected in the middle of the productive wells are usually aged around 1960. Consequently, these ages may correspond to the mean residence time within the aquifer. This residence time seems to be similar in both sub-catchments, probably meaning that the effective porosity is also similar which agrees with available data providing an effective porosity of 0.25 and a recharge of 0.27 m/year (Auterives, 2006). Applying the residence time equation, a residence time of 55 years results in an aquifer thickness around 60 m. Actually, real thickness is variable in space, ranging from around 50 to 100 m. Some samples taken at shallow depth (S15, S12, F2 and P8 sampled around 15 m) provide more recent ages, ranging from 1974 to 1993. This suggest that the sampling has extracted the upper flow lines.

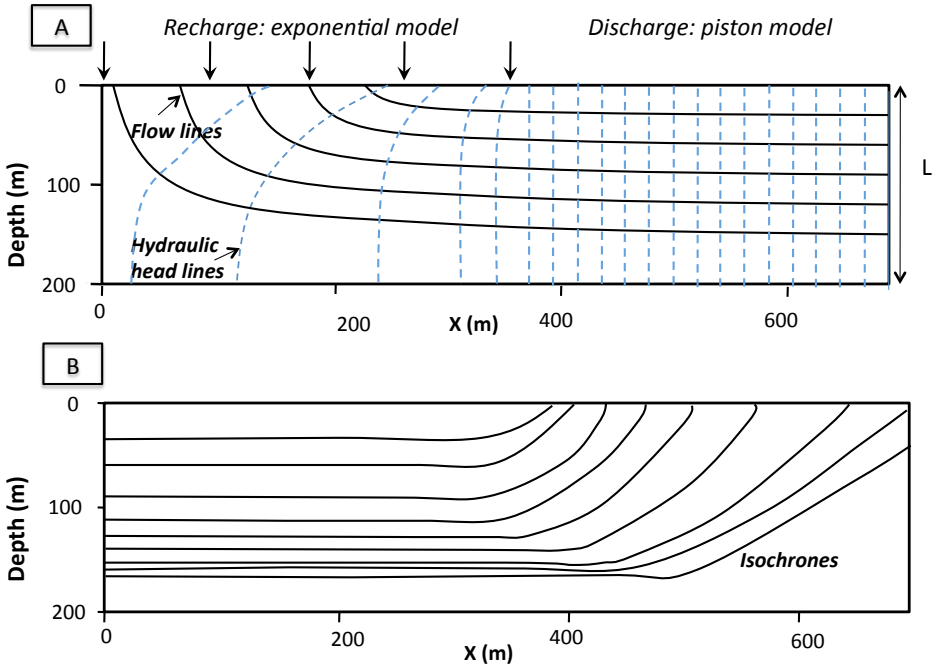

Figure 2.8: Confined aquifer of constant thickness (L) supplied by an unconfined adjacent aquifer with uniform recharge. The top figure shows the flow lines, the bottom figure shows the isochrones

Vertical temporal stratification

Regarding the vertical temporal stratification, wells 3X-15, S14 and S18 show almost no differences with depth, although a logical small age increase with depth is observed, but only of about 3 to 5 years, i.e. close to the method uncertainty. S14 and 3X-15 are located in a discharge zone (see Figure 1.1), i.e. in the right hand of Figure 2.8. In this part, older isochrones come up to the surface making the sampled water, in a fully screened well, a more or less mix of a few old flow lines, which agree with the measures. S18, however, is located in a recharge or intermediate zone of the aquifer where a temporal stratigraphy should appear. Probably the investigated depths (from 47.5 to 69.5 m) are not distant enough to isolate flow lines.

In contrast, F1 and F2 show a temporal stratigraphy: in F1 the age ranges from 1985 to 1975 on 33 m distance; in F2 from 1978 to 1958 on 40 m distance. These results agree with the piezometric map (see Figure 1.1): F1 is located in a recharge zone (left side of Figure 2.8), while F2 is still located in a recharge zone but more downwards within the catchment (left side of Figure 2.8).

Mixing evaluation

Evaluation of mixing is usually done by bi-variant graphs. A software developed by the U.S. Geological Survey Chlorofluorocarbon Laboratory was used to visualise and compute this mixing (USGS).

The underlying assumption is a flow network mathematically described as exponential or piston, i.e. like in Figure 2.8. Figure 2.9 reports the relation between CFC11 and CFC12 for all the samples. The samples plot more or less within the model, suggesting that the aquifer is indeed behaving as an ”exponential model” or ”piston flow” type. However, several points plot out of the zone limited by the model. This type of graph is very sensitive to uncertainty: a small error moves the point out of the model limit. The ”old” samples ageing around 1960 plot close to the graph origin, as the CFCs concentrations are low. In addition, these graphs are commonly used to quantify binary mixes between to water sources. Here, because of the sampling method (largely screened wells) and the low concentrations, several flow lines presumably mix. Therefore, quantifying a binary mixing is impossible (an infinite of solutions).

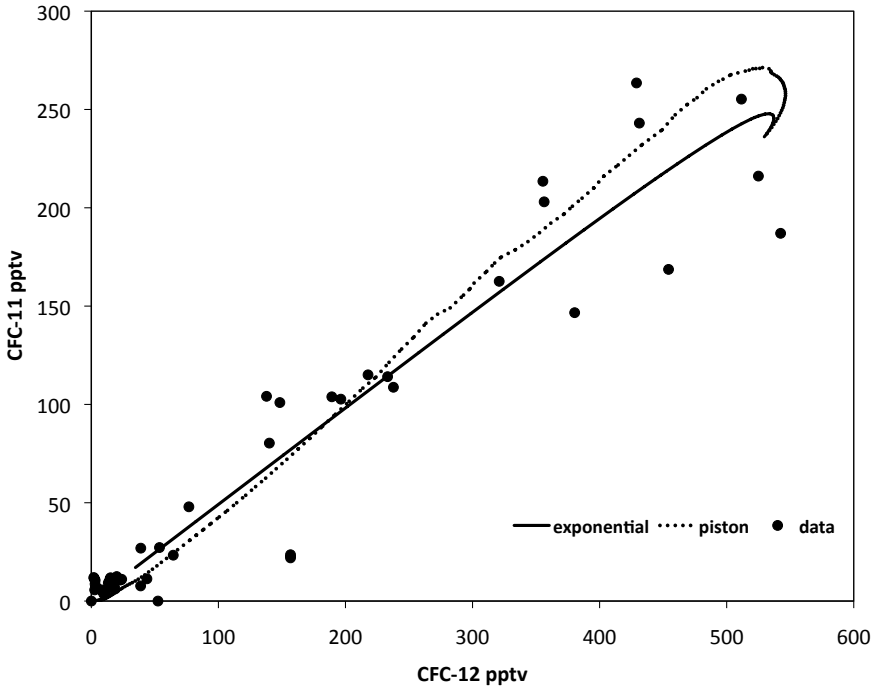

Figure 2.9: CFC11 plotted against CFC12 concentrations for all the samples

Synthesis on water dating

Based on all the previous discussed points, a schematic interpretation of the ages is presented in Figure 2.10, based on the conceptual model from Figure 2.8. The wells were placed on the diagram relative to their location on the piezometric map, i.e. in recharge, intermediate or discharge zones. Note that because of the hydraulic head lines (Figure 2.8 panel A), vertical flow is expected to preferentially go downwards in a well, in the recharge zone and do not move or potentially go upwards or downwards

in the discharge zone. The arrows on Figure 2.10 agree with this theory. This schematic interpretation appears to be very coherent with the theory on the hydrological functioning.

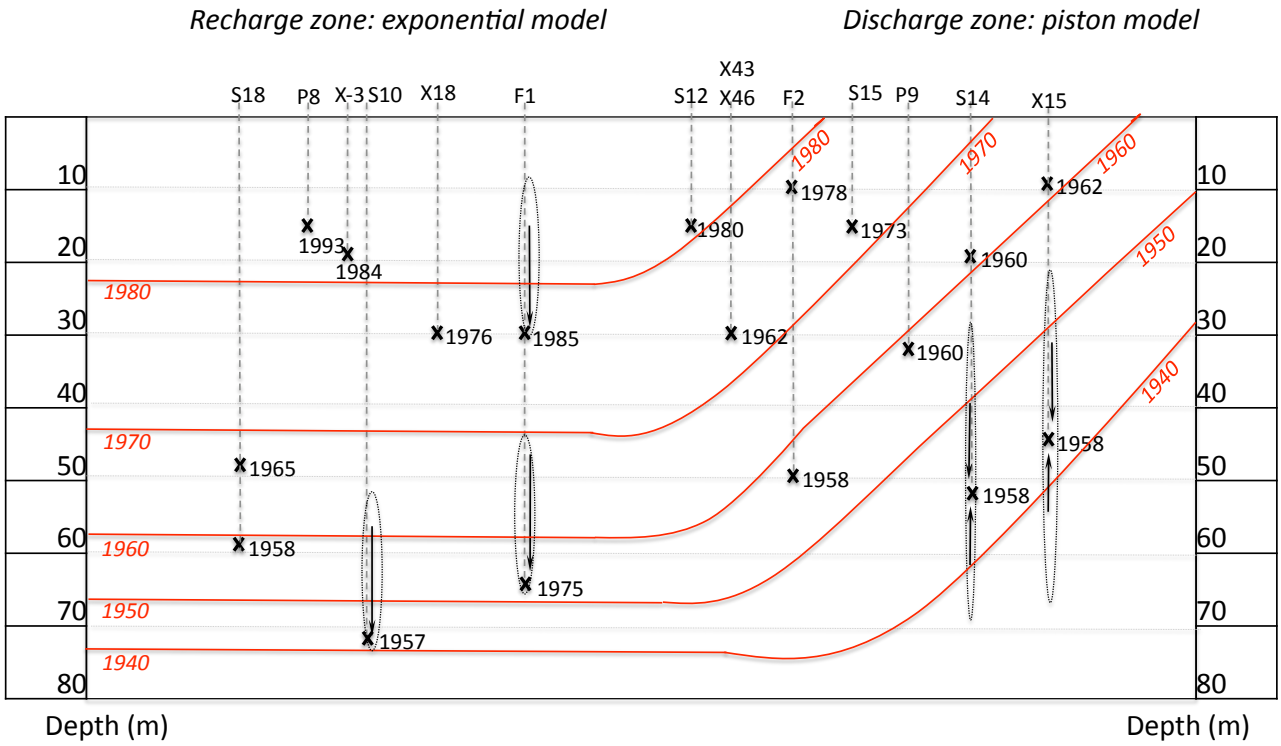

Figure 2.10: Dated samples plotted on a conceptual model : recharge zones agree with the exponential model and discharge zones agree with the piston model.

2.4.2 Chemical processes

Carbonate dissolution

The groundwater chemistry is dominated by carbonate dissolution, as evidenced by the plot of Ca^{2+} against HCO_3^- (Figure 2.11 panel A): the samples plot on the 1:1 dissolution line except for S10 well (Pearson coefficient is 0.75 when excluding S10). S10 has a "sodium and potassium carbonate" type (Ca(Na)(K)-HCO_3). This is probably related to the geological formation at this place which is a offshore clay-rich sandstone formation (Baize, 1998). An overall view of the samples show that the Ca^{2+} concentrations show a large concentration range. Although limestone rocks are dominant in Sainteny relative to Marchesieux, this has no effect on the water chemistry. This suggest that carbonate dissolution is largely controlled by CO_2 partial pressure (pCO_2) (Appelo and Postma, 2005). From the computed theoretical pCO_2 at equilibrium (Table 2.6), it can be noticed that a very large variation range is observed (0.5 to 4% CO2), which reflects various source mechanisms. The highest values are probably related to peatland production of CO_2.

Table 2.6: CO_2 partial pressure of groundwater, stream water, peatland water and rain water from the study

	pCO_2(atm)		
	min	average	max
Rain	0.003		0.006
Peatland	0.006 (ZNS rech)	0.02 (ZNS)	0.04 (ZS)
Groundwater	0.01	0.025	0.06

Cation exchange

A classical way in hydrochemistry to determine if cation exchange is significant, is to plot Na^+ against Cl^- and the evapotranspiration (EVT) line related to these two ions (Figure 2.11 panel B). The EVT line is defined as the line going from rain water (from the 4 rain water samples available on site) to rain water subjected to 70 % evapotranspiration (this rate was computed by the Penman equation by Meteo France (Auterives, 2006)). Almost all the samples plot more or less around the EVT line. It appears that globally Na^+ is not involved in cation exchange, and by extension that cation exchange is not a significant process in this aquifer. However, S10 well is enriched in Na^+ (3.3 meq/L), and in a lesser extend S15 and S14 at 73 m: the lithology data suggests that locally plastic grey clays may favour cation exchange in these locations (depletion in Ca^{2+} and enrichment in Na^+) (Appelo and Postma, 2005).

In addition, the graph shows that some samples are significantly enriched in Cl^-, relative to the 70 % averaged groundwater recharge rate of evapotranspiration (where Cl^- concentration is 0.7 meq/L). This suggest a Cl^- source.

Groundwater contamination

The presence of NO_3^- in some samples is most probably due to contamination by fertilizers. A plot of NO_3^- against Cl^- (Figure 2.11 panel C) highlights that when NO_3^- increases, Cl^- increases as well. This suggests that the previously discussed enrichment in Cl^- is also due to agricultural practices, fertilizers constituting a Cl^- source.

Figure 2.11 panel D reports SO_4^{2-} against Cl^- and the EVT line computed as previously: several samples plot above the line, which suggests an allochton enrichment in SO_4^{2-}. No relation is observed between NO_3^- and SO_4^{2-} which suggest that SO_4^{2-} is not coming from autotrophic denitrification which happens in particular when pyrite is present (Tarits et al., 2006) . Important SO_4^{2-} release is occurring especially when peat is subjected to dessication (further discussed in Chapter 1 in Part III). Moreover, flow through the peatland towards the aquifer has been observed (further discussed in Chapter 3). Consequently, the SO_4^{2-} excess may originate from the peatlands.

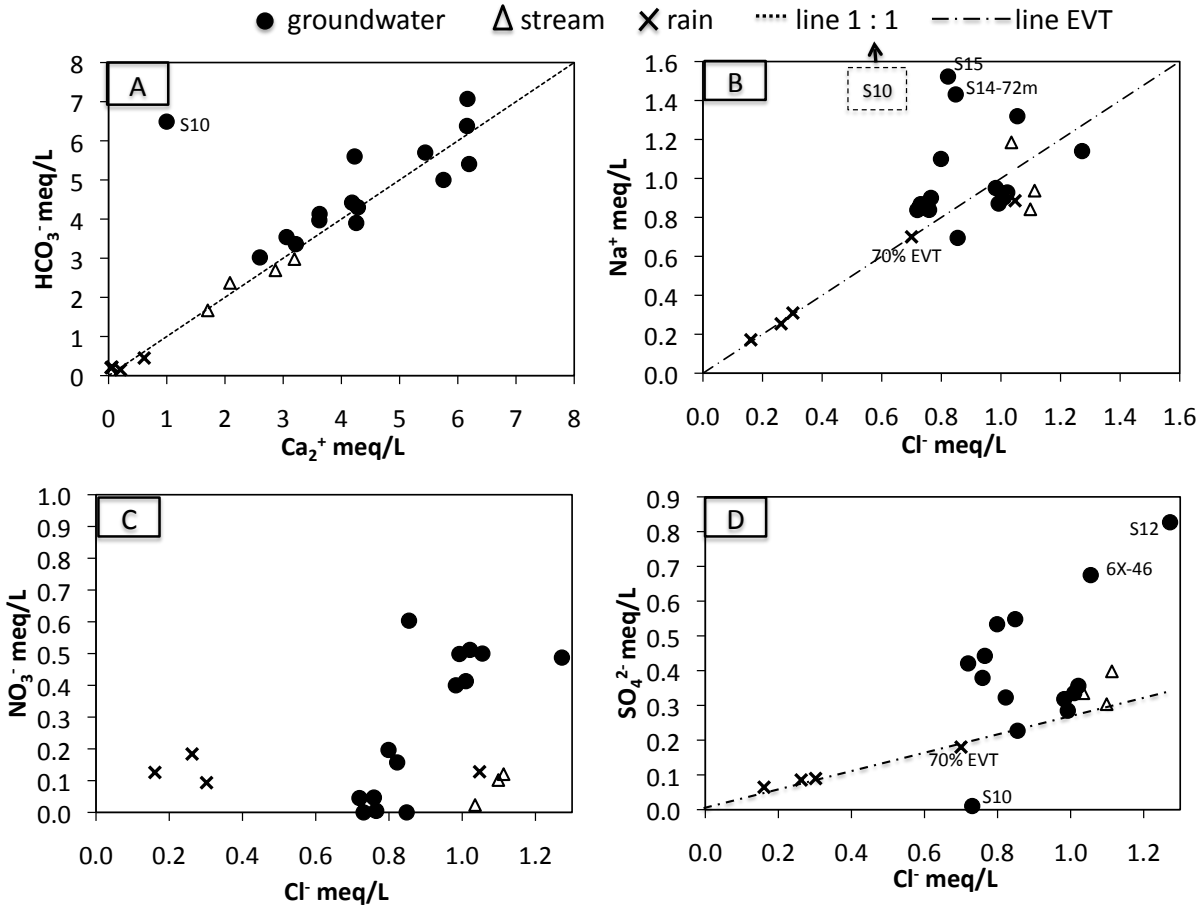

Figure 2.11: Binary graphs plotting the groundwater, rain water and stream water samples. Panel A: Ca^{2+} against HCO_3^- and the dotted line the 1 by 1 equivalence line; Panel B: Na^+ against Cl^- and the dotted line the evapotranspiration line; Panel C: Cl^- against NO_3^-; Panel D: Cl^- against SO_4^{2-} and the dotted line the evapotranspiration line

2.4.3 Relationships between chemistry and age

A Principal Component Analysis (PCA) was carried out on the groundwater chemical data and the estimated ages (Figure 2.12). It appears that NO_3^- and estimated ages are strongly correlated. As the data a assumed to follow a normal distribution (data not shown), computed Pearson correlation coefficients are presented in Table 2.7. This coefficient is of +0.91 between NO_3^- and estimated ages (see also the relation in Figure 2.13). As a conclusion, this linear relation clearly points out the fertilising practices intensification which impact on the groundwater quality started in the early seventies and linearly increased up to the last available value dated around 1993 where NO_3^- concentration was at 53 mg.L^{-1}. In addition, there is evidence that no (or almost no) denitrification occurs. Although a slight increase in N_2O is noticed correlated to the large NO_3^- increase, it remains very low and N_2 is not in excess (Figure 2.13 and graph reported in Appendix B).

The PCA and the Pearson correlation coefficients show that not only NO_3^-, but also other chemical elements are affected by the water age. As already discussed before, Cl^- correlates well with NO_3^- and consequently with ages (r=+0.63). It also appears that older ages are related to higher pH and higher alkalinity (and with higher conductivity and Fe content), suggesting that globally, the residence time favours water mineralisation. It can be noticed that age and SO_4^{2-} are not correlated (r=-0.04). In addition, as the ages were shown to strongly affect the NO_3^- concentration, a PCA was also carried out without NO_3^-: the overall trends are maintained and the "dendogram groups" are only slightly affected. To conclude, the sample distribution and the dendogram allows distinguishing groups related to "young" or "old" waters (Figure 2.12, Panel B and C). Consequently, the water residence time affects the overall water chemistry.

Table 2.7: Pearson correlation coefficients between the water age and chemistry. Only coefficients higher than $\mid 0.40 \mid$ are presented, in decreasing order.

	NO3	pH	Cl	F	HCO3	Mg	EC	Fe
Age	+0.91	-0.70	+0.63	-0.63	-0.60	-0.53	-0.42	-0.40

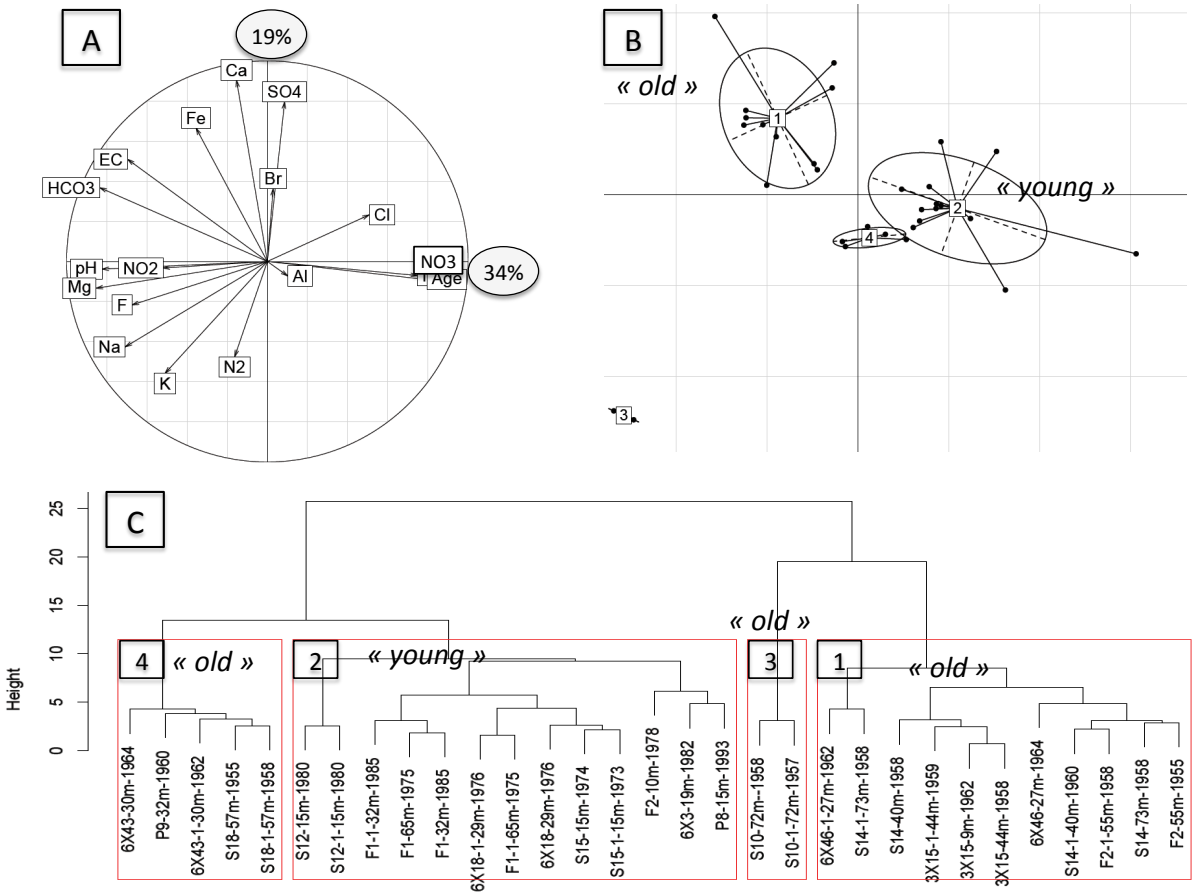

Figure 2.12: Scatter of the chemical data and the related estimated ages on the principal component analysis: Panel A plots the variables on the unit circle, component 1 explains 34% of the variance and component 2 explains 19 % ; Panel B plots the samples corresponding to the PCA and the groups based on the dendogram ward discrimination from Panel C.

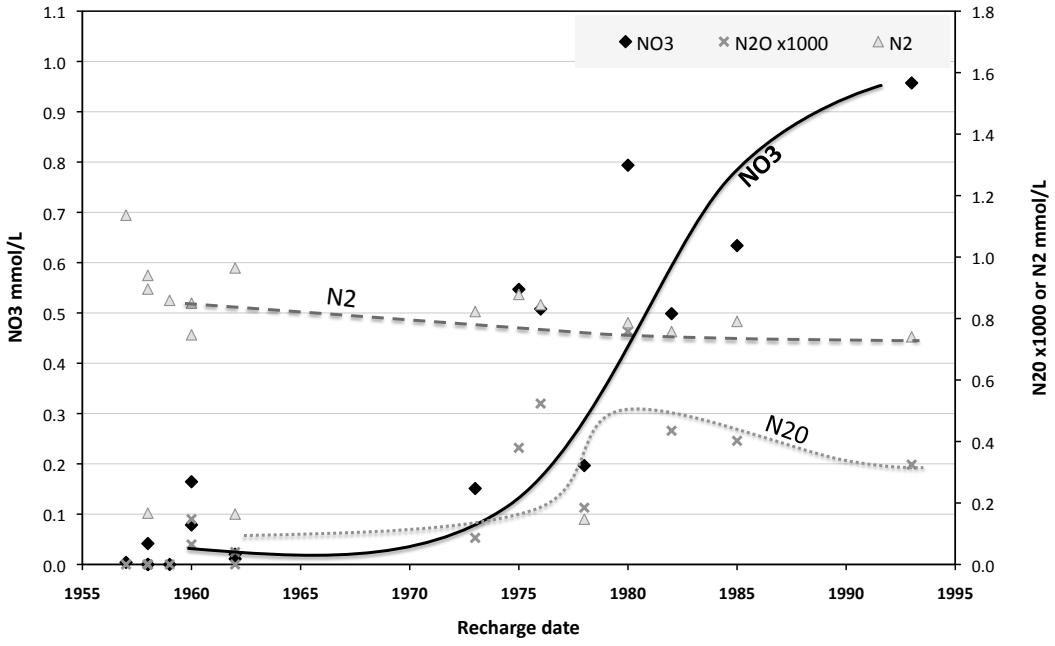

Figure 2.13: NO_3^-, N_2O et N_2 against the water recharge date

Conclusion

The dating and chemical analysis were done on two sub-catchements, belonging to the same basin, with different lithologies resulting in different transmissivities. Sainteny basin is dominated by sand and limestone while Marchesieux has an inter-layering of clayey marshes, sandy-silty marshes and sandstone. Sainteny aquifer has a high transmissivity around 0.1 $m^2.s^{-1}$ while in Marchesieux transmissivity is approximately 10 times lower.

Fourteen wells were sampled for dating and chemical characterization. Nine wells where sampled at one depth, while five where sampled at several depths. Vertical multi-parametric profiles, combined with technical data and dating results, show that most of the samples taken in the middle of the productive well are dated around 1960. These ages are interpreted rather (1) as mean residence times in totally screened wells where flow lines easily mix or (2) as old flow lines coming up to the surface, in discharge zones. No difference in mean residence time is noted between the two catchments, denoting that effective porosity, recharge (and thickness) controls water time renewal.

Regarding the vertical temporal stratification, some wells show no (or almost no) temporal gradients, while others show younger ages at the top and older at the bottom. Superposition with the piezometric map (i.e. the recharge, intermediate or discharge zones) shows good agreement with the dating results. Temporal gradients are found in recharge or unconfined places while homogeneous water columns are located in discharge zones.

The groundwater has a "calcium bicarbonate" water type. Cations exchange seems not significant and the chemical components mainly originate from carbonate dissolution. The water vulnerability to contamination is evidenced by nitrate and chloride contents. Sulphate concentrations are in excess relative to rainwater inlet and evapotranspiration. They probably originate from the peatlands where sulphate release can be important (studied later in this report).

Finally, dating and chemistry data superposition clearly shows that the water residence time affects the overall water chemistry. Not only nitrate (and chloride) is strongly related to age estimation, showing a quasi linear relation since the early seventies, but basically the residence time favours water mineralisation.

Chapter 3

Sensitivity of wetland hydrology to pumping and climate change

Collaborating team: Antoine Armandine les Landes for modeling support and Pascal Goderniaux for his helpful support

Introduction

Peatlands or peat meadows are complex ecosystems which functions are driven by many physical, chemical, and biological processes. Because peat soils can serve as sinks, sources, and transformers of nutrients and other chemical contaminants, they have a significant impact on water quality and ecosystem productivity (Holden et al., 2004). Worldwide, lowered water tables, mainly induced by drainage, are now recognized to be associated with several problems affecting both the physical structure of the peat as well as water quality. They are also considered as taking part to green house gas emission (Global Environment Centre).

Wetland drainage developed, especially in the industrial countries, for several centuries. It became however more effective with the development of agriculture mechanization after the Second World War. More recently, other anthropogenic constraints have also impacted the wetland hydrology, such as water extraction in connected aquifers or climate change.

In this context, the restoration of wetland ecosystems gains interest. However, there is crucial need for a comprehensive understanding of the unique wetland hydrology. The inter-connexions between surrounding aquifers and surface water networks is particularly necessary to access the wetland vulnerability. Therefore, modelling this type of systems began to emerge (Wilsnack et al., 2001) (Frei et al., 2010) (Reeve et al., 2000) (Grapes et al., 2006) (Bradley, 2002) (van Roosmalen et al., 2009) (Lischeid et al., 2010).

The Cotentin meadow peatlands are of the minerotrophic type : connectivity with the underlying aquifer is evidenced both by hydrologic fluxes and chemical features (Auterives et al., 2011). This aquifer is highly transmissive and used for drinking water supply since 1992. The current abstracted volume is around 5 millions m^3 per year, corresponding to 9 $\%$ of the recharge. Due to an increasing demand in good water quality, the authorities plan to increase the groundwater extraction in the near

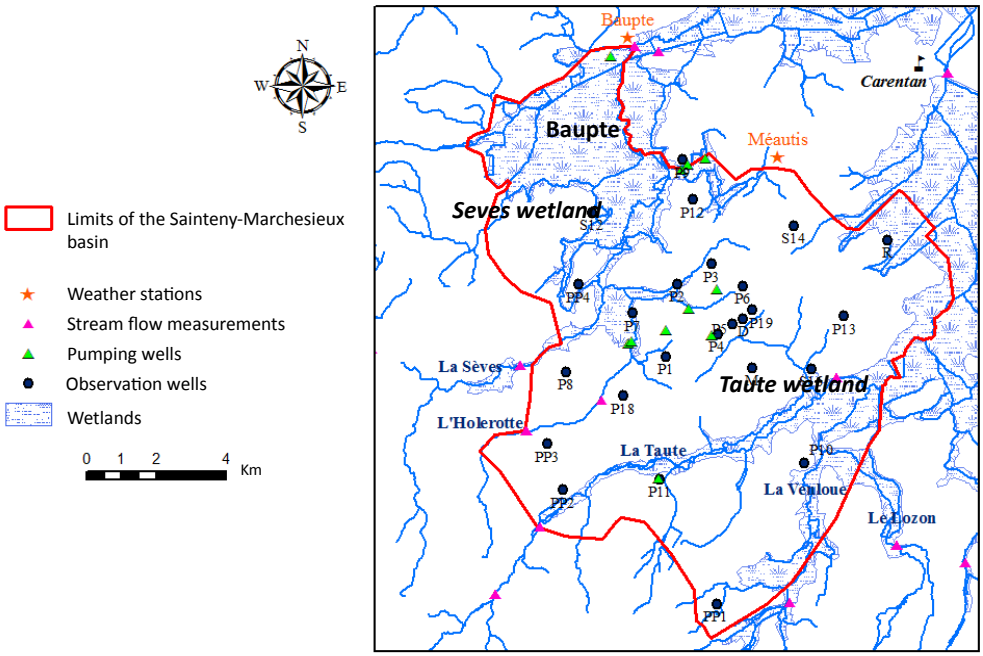

Figure 3.1: Sainteny-Marchesieux catchment and samples location

future. In addition, climate change is also expected to impact the wetland.

Consequently, the purpose of this work is threefold: (i) quantifying the connectivity between the wetland, the aquifer and the surface water network in order to define the vulnerability of these wetlands to (ii) increasing groundwater extraction and (iii) climate change at the end of this century. This goal will be accessed by a 3D physically-based modelling approach.

3.1 Basin hydrogeology

The Sainteny-Marchesieux basin extends over approximately 135 km^2 and culminates at 30 m (Figure 3.1). Vast wetlands are located in lowlands along rivers and made of peat soils.

The basin geology was studied by Baize (1998) (Baize, 1998): it is a graben, bounded by NE-SW oriented faults (South limit of the sub-catchment of Marchesieux and separating limit between Marchesieux and Sainteny in the centrum) and NNW-SSE faults (Figure 3.2). This basin can reach 150 meters depth and lies on Permian pelites. It is limited by impermeable bedrocks: Precambrian rocks (paleovolcanites, quartzite diorites, sandstones and arkoses) to the South, Trias and Permian rocks to the East and the North and Paleozoic schist and sandstones to the West (Vernoux et al., 2000) (Baize, 1998).

Two sub-catchments, which make up two main aquifers, can be distinguished:

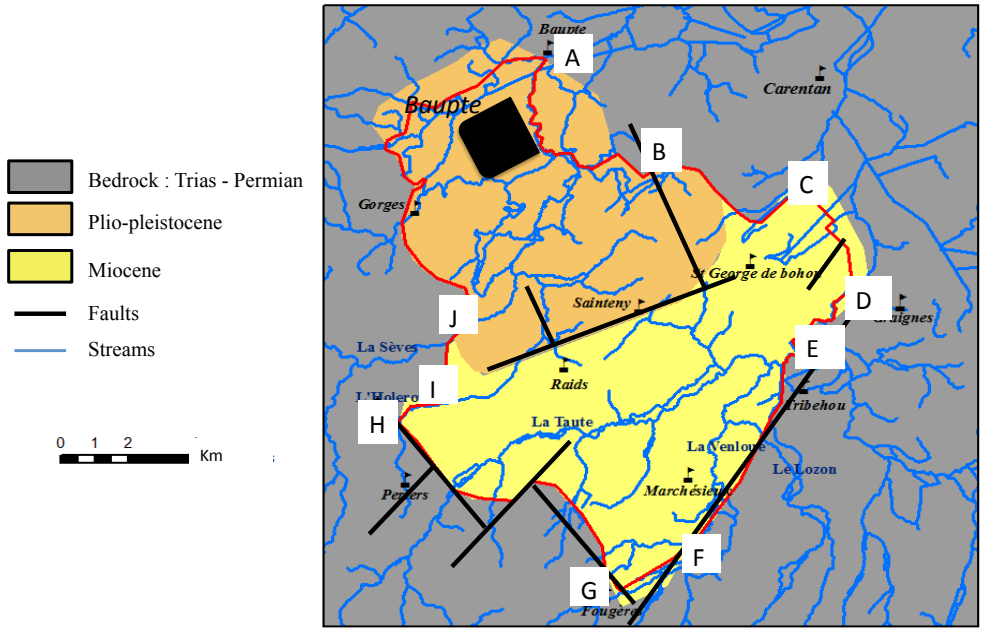

Figure 3.2: Structural diagram of the catchment geology

- Sainteny in the North-West, extending on 35 km^2. Dominated by limestones and sandy shell limestones (Faluns du Blehou) with gross grain size making this rocks very permeable. Maximum thickness is about 100 meters. Depending on the presence of a clayey bed, the aquifer is locally confined, semi-confined or unconfined.

- Marchesieux in the South, extending on 100 km^2. The geology is more heterogeneous with an inter-layering of clayey marshes (of Saint Nicolas), clayey-sandy-silty marshes (of the Bosq d'Aubigny), clayey siltite and finely granulated sandstone (of Marchesieux). The hydraulic conductivity is approximately 10 times lower than in Sainteny. Thickness is greater with a maximum around 150 meters. The aquifer is dominantly unconfined.

Finally, sands (of Saint-Vigor) overly the whole geological formations. They are locally completed by Holocene peats and Quaternary alluvial material.

At present, water extraction is predominantly affecting the sub-catchment of Sainteny, with around 5 millions m^3 pumped per year (supplying 90 000 inhabitants). Five pumping wells are used, 3 working since 1992, and 2 since 2002 (see Figure 3.1). The other sub-catchment is only poorly exploited by one well, with a pumping rate of around 0.14 millions m^3/year since 1999. Groundwater extraction represents approximately 9 % of the recharge.

These sub-catchments are drained by a dense water surface network. Subsurface flow is globally from South-west to North-east according to 3 main rivers : the Seves (in the North) which feeds the wetlands of Baupte, the Holerotte (in the middle) affluent of the Seves and the Taute which feeds the wetlands in the East (see Figure 3.1). The wetlands are mainly located in peat formations which thickness are commonly between 5 and 15 m (chapter 1). These wetlands are hydrologically connected with the deeper aquifer.

A peatland (bog type) was exploited in the North of the catchment (Baupte) from the 1950s to 2006 (Figure 3.1). Peat was extracted by lowering the water table. Presently, the intensive peat extraction results in a hole extending on about 400 ha. The precise topography is not known, but the average water level in this zone is around - 4.9 m relative to sea level.

Mean annual rainfall and temperature are 923 mm and 11.2 $^{\circ}C$, respectively (average 1946-2009 Meteo France). Run off was already calculated in a previous study (SOGREAH PRAUD, 2001) by taking into account the ratio river discharge:precipitation. The resulting average evapotranspiration is 70 % of the precipitation (Auterives et al., 2011).

The land is largely dedicated to agricultural use, with cattle breeding as dominant practice. More than half of the area is dedicated to meadow and crops (mainly corn). Wetlands (dominantly peatlands) cover approximately 30% of the area.

3.2 Modelling

3.2.1 Conceptual model

The Sainteny-Marchesieux hydrological catchment defines the boundaries of the modelled area (Figure 3.2). More precisely, the boundaries are defined by geological settings, hydrological features and the topography. Overall, there is no water exchange across the catchment boundaries. However, based on the piezometric maps, groundwater fluxes through the southern boundary have been taken into account. Along this border, hydrogeological and hydrographical limits differ, and groundwater flows northwards towards the basin. The two main streams are considered as the outlets of the catchment in the northern boundary. A topographically controlled drainage is considered to be the largest component of the total groundwater abstraction in the basin. The water supply pumping wells are aquifer outlets. They are mainly located in the center of the catchment (5 wells in Sainteny (SYMPEC) and 1 well in Marchesieux (SIAEP of Saint Martin d'Aubigny) (Figure 3.1). Finally in the peatland of Baupte a water level is maintained by pumping at -4.9 m : it constitutes an outlet of the superficial aquifer.

Inside the catchment, fluxes occur between three compartments: the hydrographic network, the wetlands and the aquifer.

Consequently, the catchment boundaries are defined as follow (Figure 3.2):

- No flow boundaries (from SOGREAH study (SOGREAH PRAUD, 2001)): geological impervious pelites (B to C; I to J; J to A); impervious faults (E to F; F to G); drainage by streams and/or wetland areas (A to B; C to D; D to E; H to L)

- Constant head boundaries: inlet zone in the south (G to H) with a head deduced from the

piezometric maps and fixed at 12.5 m; the peatland of Baupte where the water level is fixed at a certain height (-4.9 m on average).

- Drainage boundary: applied on the whole first layer and active when the water level reaches the topographical surface. The drains conductance (=DX*DY*SCOND with DX and DY the cell lengths in the X and Y directions and SCOND the conductance per unit surface) is largely higher than the layer permeability in order not to limit the drainage, which allows to the model to freely determine the drainage areas (wetlands and streams)

3.2.2 Mathematical and numerical model

MODFLOW

The Sainteny-Marchesieux basin hydrological model has been computed with the Visual MODFLOW 3D block-centred finite-difference model (McDonald and Harbaugh, 1988). The spatially-distributed model simulates 3D fully-saturated groundwater flow in porous anisotropic and heterogeneous media. Permanent or transient flow as well as confined or unconfined aquifers can be modelled.

Visual MODFLOW simulates the dynamic interactions between all sub-domains at each time step. It separates rainfall into components such as evapotranspiration, runoff and infiltration. The model also allows the calculation of water infiltration or exfiltration between vertical sub-domains (e.g. wetland and aquifer). These interactions are of great interest in the context of climate change as recharge is very sensitive to climatic variations and represents a crucial element for impact projections. The model solves the partial-differential equation of groundwater (McDonald and Harbaugh, 1988) :

$$\frac{\delta}{\delta x}(K_{xx}\frac{\delta h}{\delta x}) + \frac{\delta}{\delta y}(K_{yy}\frac{\delta h}{\delta y}) + \frac{\delta}{\delta z}(K_{zz}\frac{\delta h}{\delta z}) + W = S_s\frac{\delta h}{\delta t} \tag{3.1}$$

where

- $K_{x,y,z}$ are values of hydraulic conductivity along the x, y, and z coordinate axes, which are assumed to be parallel to the major axes of hydraulic conductivity (L/T);
- h is the potentiometric head (L);
- W is a volumetric flux per unit volume representing sources and/or sinks of water, with W negative for flow out of the ground-water system, and W positive for flow in (T-1);
- S_s is the specific storage of the porous material (L-1);
- t is time (T).

The numerical model solves this equation at every cell node, by using finite difference approximations (McDonald and Harbaugh, 1988).

Input files for MODFLOW were created using the ArcGIS geographic information system software. Moreover ArcGIS was used to exploit the output data of MODFLOW, especially to generate illustrative maps.

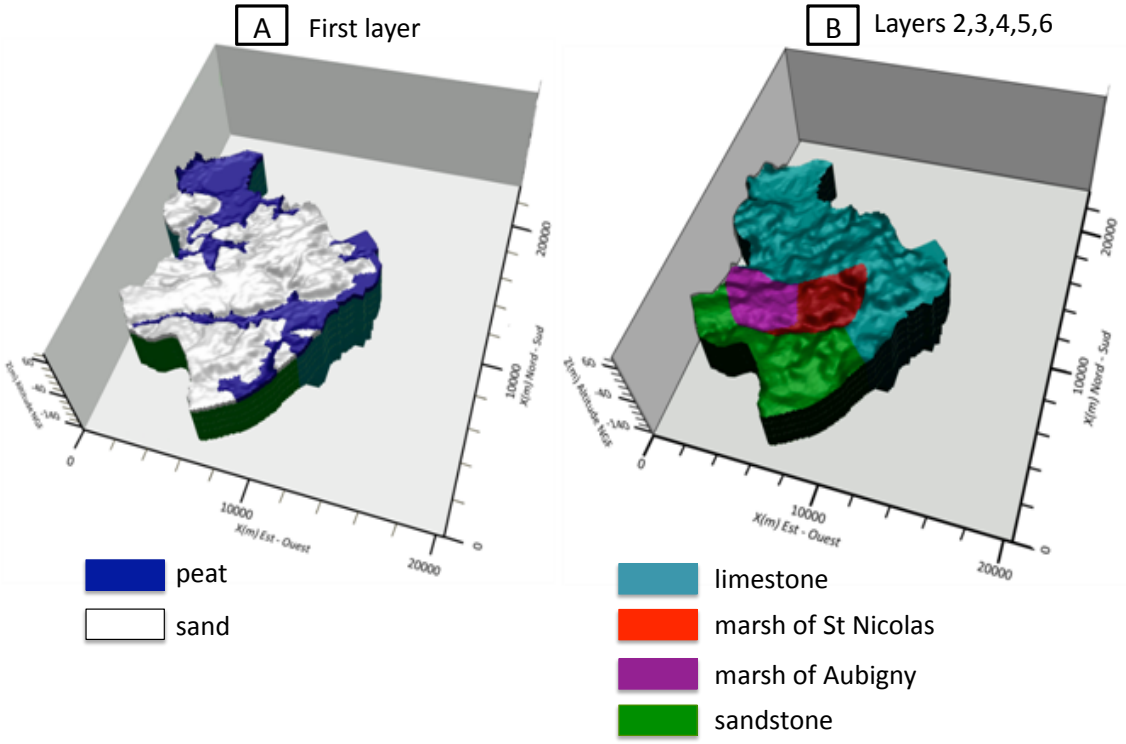

Figure 3.3: Spatial discretisation of the lithologies within the first layer (A) and the aquifer (B)

Discretisation

A three-dimensional finite element mesh, composed of 6 layers, was generated based on the conceptual model previously presented. Each layer has 16670 cells which size is 90x90 m. The top of the first layer represents the soil surface (the topography) generated form a the DTM (Digital Terrain Model), whose resolution is 25x25 m. This first layer (shallow aquifer) is 10 m in thickness and the bottom corresponds to the top of the aquifer. Within this layer, two lithologies are defined: peat and sands (Figure 3.3, panel A). The aquifer is sub-divided in 5 layers to keep a proportionality with the first layer thickness (Anderson and Cheng, 1993) (Wilsnack et al., 2001). The depth of the aquifer is variable depending on the drilling data (impervious Permian substrate) within the basin. Within the aquifer, 4 geological formations are defined: limestones and sandy shell limestones (of Blehou and Bohon), sandstones of Marchesieux, sandy loams of Aubigny and of Saint-Nicolas (Figure 3.3, panel B).

Specified fluxes

Specified hydrological fluxes within the catchment consist of recharge and groundwater abstraction by pumping wells. Historical climatic data are available for two weather stations located inside or near the basin (Figure 3.1). The stations have complete precipitation (P) and temperature (T) time series from 1946 to 2010. Potential evapotranspiration (PET) data, for the same time period, are calculated by Meteo France by the Penman method. Precipitation and PET data are distributed using Thiessen polygons. Groundwater volumes extracted from the production wells have been collected from the water supply companies and are updated annually since 1992.

Calibration

The model was calibrated to reproduce (1) observed aquifer hydraulic heads, (2) spatial distribution and total surface of the wetlands and (3) stream flow rates. Calibration was performed under steady state conditions, using the mean data of a particularly humid year (1999-2000) and a particularly dry year (2003-2004). A preliminary calibration was used to take into account the extension and the distribution of the geological units and to adjust the depth. The calibration was performed by PEST software coupled to MODFLOW. Hydraulic conductivities are adjusted automatically, during calibration, around ranges provided by tests conducted in the geologic formations given by previous studies (SOGREAH PRAUD, 2001) (Auterives et al., 2011). The model validation was made with another set of data from 2006-2007.

1. The aquifer hydraulic heads are considered the most reliable data, therefore residuals can be calculated. Residuals represent the match of the simulated values to the observations (year averaged hydraulic heads). We assumed a satisfactory calibration when residuals were between +1 and -1.

2. The occurrence of a wetland is considered in two ways, ranging from a more restrictive to a less restrictive definition: when the water level is between 0 et -0.5 m or 0 and -1 m. The later takes into account that a shallow water level, rather than flooding, can also be considered as a wetland. The surface area obtained in these two ways is compared to the cartographic wetland extend.

3. Finally, the volume of drained water is compared to the difference between inlet (Seves, Holerotte and Taute) and outlet (Seves and Taute) from the main streams which gauging stations are located in Figure 2.1. The goal is to reach the same range of values.

A sensitivity analysis is made to highlight the processes and parameters which highly impact the results. The sensitivity of a parameter is calculated as the percentage of variation (10, 20 or 50 %) normalized to the parameter value.

Calibration results The hydraulic conductivities resulting from the calibration procedure are synthesized in Table 3.1. The residuals for each well, from the calibration procedure, are illustrated in Figure 3.4. As a general overview, they are slightly over-estimated in wet periods (1999-2000) and under-estimated in dry periods (2003-2004). However they are distributed along the x axe (residual=

Table 3.1: Full saturated hydraulic conductivities values ($m.s^{-1}$) resulting from the calibration

		K_{xy}	K_z
Layer 1	Sands	1.10^{-6}	1.10^{-6}
	Peat	8.10^{-7}	7.10^{-8}
Layer 2, 3, 4, 5, 6	Limestone (Faluns)	8.10^{-3}	8.10^{-3}
	Sandstone	8.10^{-4}	8.10^{-4}
	Marshes of Saint Nicolas	$5.5\ .10^{-6}$	$5.5\ .10^{-6}$
	Marshes of Aubigny	2.10^{-5}	2.10^{-5}

0) and range between +1 and -1 which is considered as satisfactory. Two points (M and P18) do not meet this condition in the extreme periods, but are satisfactory for the validation period (2006-2007).

The simulation from the validation year gives a wetland area of 27 % (0 to -0.5 m) and 30 % (0 to -1 m) and a volume of drained water of $3.10^7 m^3$/year. The model is considered satisfactory.

The results from the sensitivity analysis are illustrated in Figure 3.5, for 4 model outputs. Each model input (parameters) are classified from the most sensitive to the less sensitive, e.g. their variation will significantly impact the model results. The most impacting parameters are the recharge and the hydraulic conductivity of the peat, while the less impacting are the hydraulic conductivities of the marshes and limestones and the drains conductance. Finally, the most sensitive output from the model is the volume of drained water (y axis is the highest).

Scenarios

The aim of the model is to predict the impact of groundwater extraction and climate change on the catchment, with a focus on the wetland water levels.

A reference model representing the present state is compared to the simulated scenarios. In the reference model, ETP is calculated with Thornthwaite equation from precipitation data from 1951 to 1981, on a monthly time step. The average recharge ends at 239 mm. Extracted groundwater volumes are fixed at 5 Mm^3 (current volumes).

Groundwater extraction 3 scenarios are simulated:

- scenario 1: no pumping
- scenario 2: doubled extracted volumes relative to current volumes, on the 6 current wells
- scenario 3: the 6 wells maintain the same extracted volumes as present + 2 new wells located in the Marchesieux sub-catchment close to Marchesieux and Saint George de Bohon localities (Figure 3.1). Total extracted volume is doubled. This scenario is inspired by new extraction wells potentially planned in the near future.

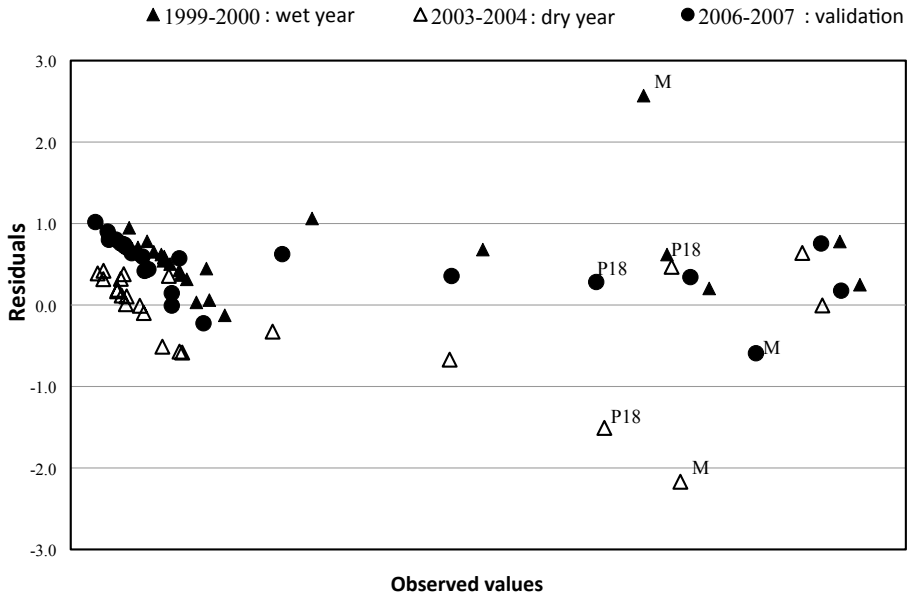

Figure 3.4: Residuals on the aquifer hydraulic heads, resulting from the calibration procedure

Climate change Regional Climate Model (RCM) output from the European Union Fifth Framework Programme (FP5) PRUDENCE project (Prediction of Regional scenarios and Uncertainties for Defining EuropeaN Climate change risks and Effects) (Christensen et al., 2007) was used. These dynamic climate models provide a series of high-resolution simulations of European climate for a control simulation (1961-1990) and for a future time period (2071-2100). The RMC is an average of 21 models derived from the A1B IPCC (Intergovernmental Panel on Climate Change) green house gas emission scenario. This medium-high scenario agrees with the recent observed increases in atmospheric carbon dioxide concentrations, in accordance with projections from high emission scenarios (Rahmstorf et al., 2007).

This scenario predicts an increase of 2.5°C at the end of this century (resulting in an increase of the ETP) and precipitation variations of $\pm 5\%$. In this work, 3 scenarios are simulated:

- scenario A: increase of 2.5°C and precipitation increase of 5% (results in a recharge decrease of - 8 %)
- scenario B: increase of 2.5°C and no change in precipitation (results in a recharge decrease of - 24 %)
- scenario C: increase of 2.5°C and precipitation decrease of 5% (results in a recharge decrease of - 40 %)

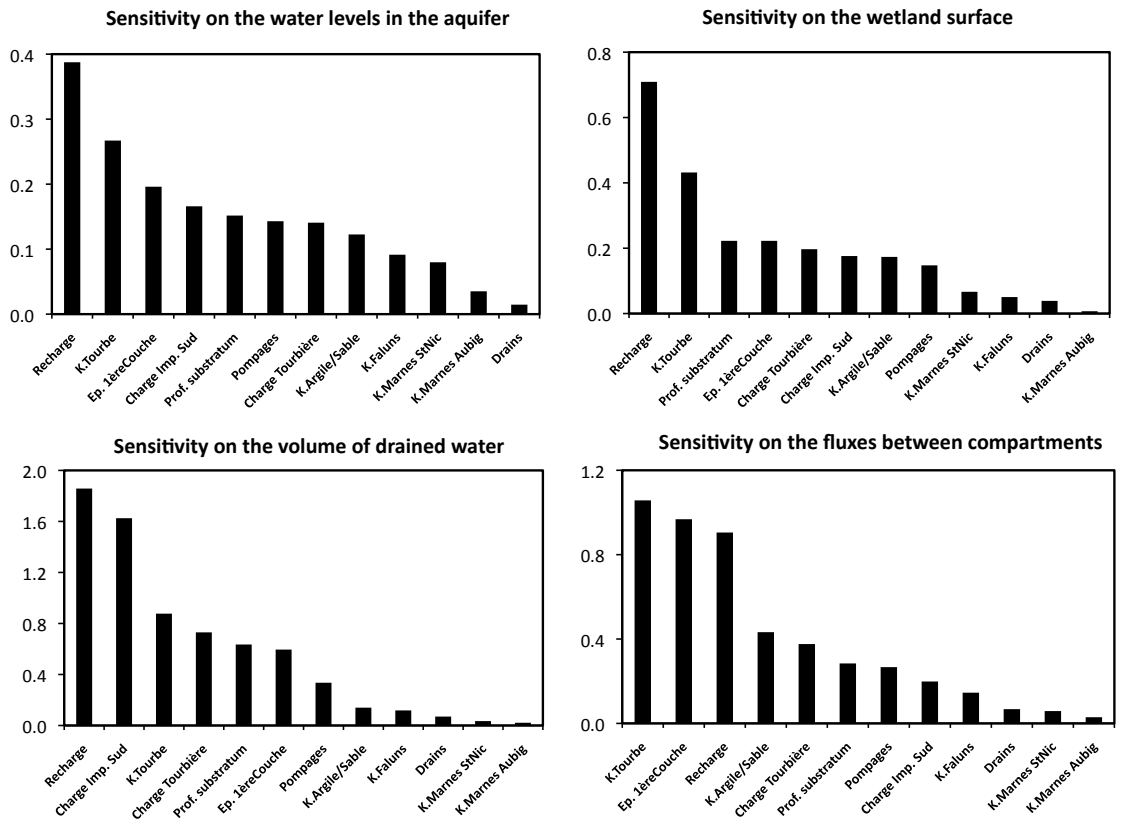

Figure 3.5: Results from the sensitivity analysis on 4 model outputs

All these scenarios result in a recharge decrease. Further, the climate change simulations will be coupled to the groundwater extraction scenarios 2 and 3.

3.3 Results

3.3.1 Current water budget

The modelling results on the reference model are synthesized in Figure 3.6, by illustrating the flows between compartments. Upward flow from the aquifer to the wetland is highly dominant relative to the reverse flow, supporting the fact that the wetlands behave as discharge zones.

3.3.2 Model result for groundwater extraction

Model results for the extraction scenarios are compared to the reference model (present conditions) and focus on (1) the water level changes in the first layer (2) the surface of wetlands and (3) the changes in water fluxes between compartments.

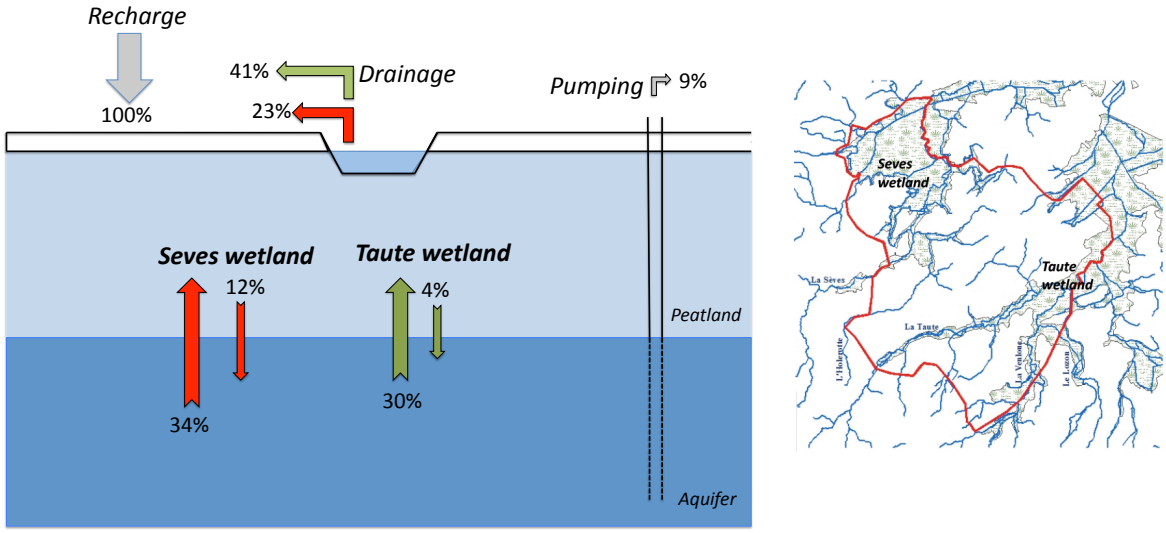

Figure 3.6: The reference model: upward and downward flow between the aquifer and the wetland and drained water by the draining network

Figure 3.7 illustrates the water level changes in the first layer, relative to the reference model. Main results are:

- As expected, without pumping, the water level in the wetlands from the North is increased, globally between 25 and 40 cm (scenario 1). The water levels in the South are not affected, except in local zones where small increases are observed (up to 15 cm).
- If the extraction rate of the current pumping wells is doubled, the Northern wetland water levels are decreased by about 35 to 50 cm (scenario 2). The South is not affected, except in lowland areas where a decrease up to 10 cm is observed.
- If the total extraction rate is doubled by 2 new wells in the Marchesieux sub-catchment, the Northern wetlands are still affected by a water level lowering of about 20 cm. The Southern wetlands are also affected, but lowering is localized in the wetland borders (up to 30 cm) while the inside wetland is not affected.
- The uncoloured grey zones correspond to dry model cells : important new dry surfaces are created in the scenario 2.

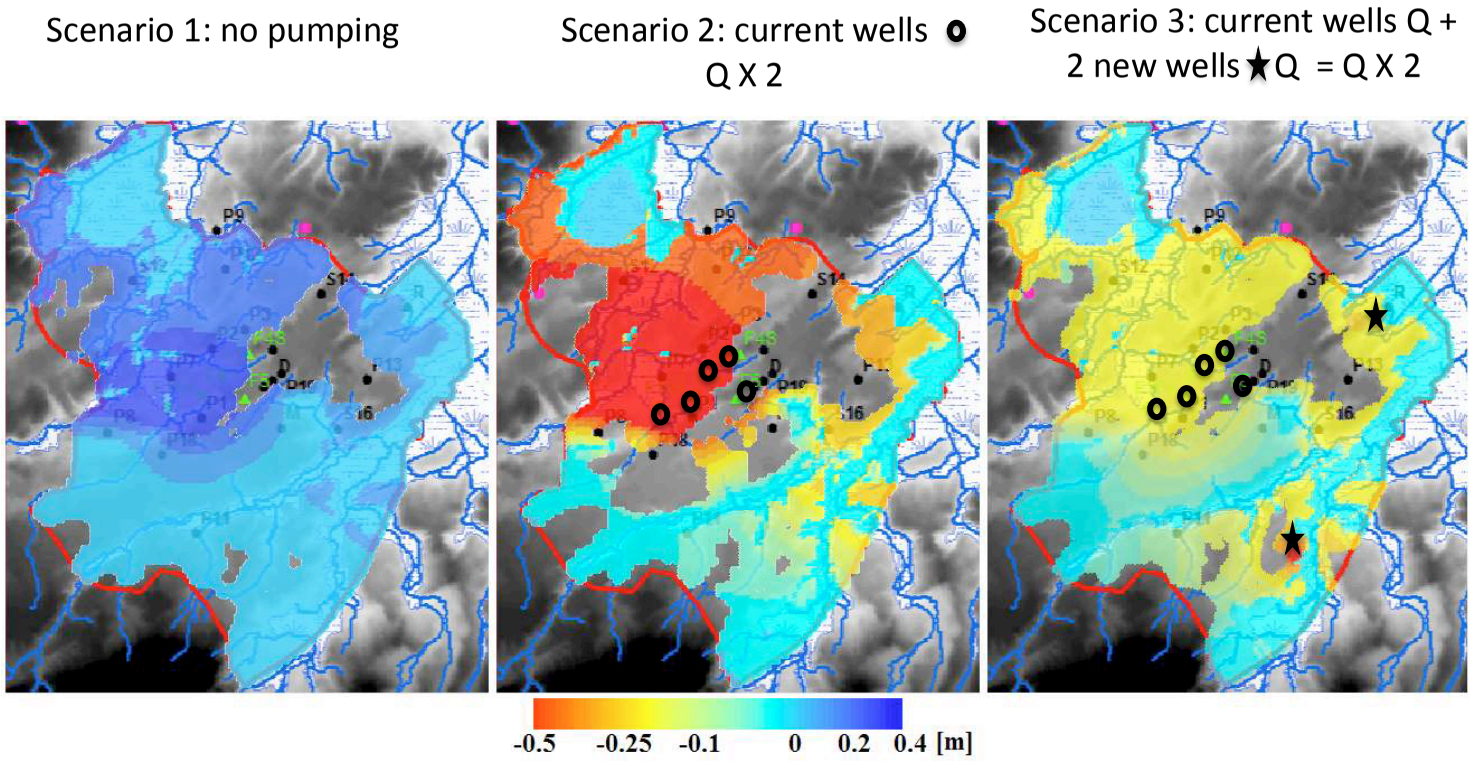

Figure 3.7: Water level variation (in m) in the first layer, relative to the reference model, for the 3 scenarios. Scenario 1: no pumping; scenario 2: the 5 current pumping wells extraction rates are doubled (Q X 2); scenario 3: the current pumping wells are maintained with the current pumping rates (=Q) but in addition water is extracted in 2 new wells (stars), each of them xtracting Q/2. The uncoloured zones (grey) are dry cells.

The wetland surfaces resulting from the 3 simulations are presented in Table 3.2. These results agree with the water level changes described previously: the most impacting scenario is again an increasing extraction from the present pumped area (scenario 2). The model predicts a decrease in wetland surface of 4.05 km^2 where the water level lowers under 50 cm relative to the surface. In the scenario without pumping (scenario 1), a wetland gain of 1.35 km^2 (0 to -0.5 m) is simulated. In contrast, scenario 3 with the 2 new wells, has no effect on surface wetland when the "0 to -0.5 m" definition is used.

Table 3.2: Surface of wetlands resulting from the 3 pumping scenarios (in %) and change in surface relative to the reference model (km^2). Two wetland definitions are taken into account (water level between 0 and -0.5 m and water level between 0 and -1 m) as explained previously

	—Wetland surface— 0 to -0.5 m		Wetland surface— 0 to -1 m	
	%	km^2	%	km^2
Scenario 1 (no pumping)	26	1.35	30	2.7
Reference (current pumping)	25	/	28	/
Scenario 2 (current pumping doubled)	22	-4.05	27	-1.35
Scenario 3 (current pumping+ 2 new wells = Q doubled)	25	0	27	-1.35

The impact of the scenarios on the changes in fluxes between compartments (aquifer/wetland/drained water (streams)) is synthesised in Figure 3.8. The two sub-catchments are taken apart. As a general behaviour, the fluxes are mainly upward (from aquifer to wetland). Increased pumping (scenarios 2 and 3) enhances downward fluxes and decreases upward fluxes. Pumping also impacts the volume of drained water, especially in the wetland drained by the Seves. The model predicts that scenario 2 decreases current stream water by 41 %! The model also highlights that the current groundwater extraction has already an impact on the volumes of water drained by the Seves: before the exploitation, the Seves may have drained 37 % more water.

3.3.3 Model result for climate change

The model simulations predict the possible changes in the hydrologic regime at the end of the century (2080 to 2099). Again, results are compared to the reference model (current conditions) and focus on (1) the water level changes in the first layer (2) the surface of wetlands and (3) the changes in water fluxes between compartments.

Figure 3.9 illustrates the water level changes in the first layer, relative to the reference model. Note that the systematic large lowering in the centre of the catchment (orange to red colours) is attributed to a bad calibration on the well "M", which residuals are not satisfactory (see chapter 3.2.2).

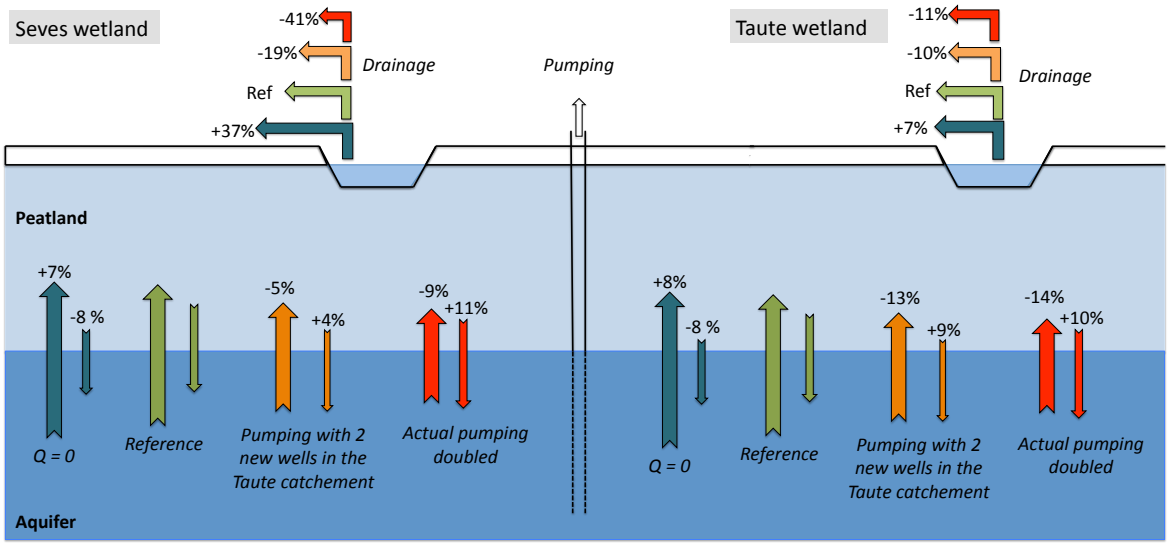

Figure 3.8: Groundwater extraction scenarios: upward and downward changes in the vertical fluxes relative to the reference model

Main results are:

- in scenario A (T and P increase), no changes are observed in almost half of the catchment surface, but the water level in the Seves wetland is decreased by around 20 cm. The Taute wetland is not impacted.
- in scenario B (T increase, P unchanged), the model predicts important changes, notably in the Seves wetland where the water levels are decreased by 50 to 70 cm. The recharge areas (West/South) at higher topographies, are also impacted by about - 20 cm. The Taute wetland is again almost not impacted.
- in scenario C (T increase, P decrease), the trends observed in scenario B are enhanced: all the catchment is highly impacted, except the Taute wetland which is only impacted locally and along the borders. The water level decrease in the Seves wetland is around 1 m, while the recharge areas show a decrease of around 30 cm.

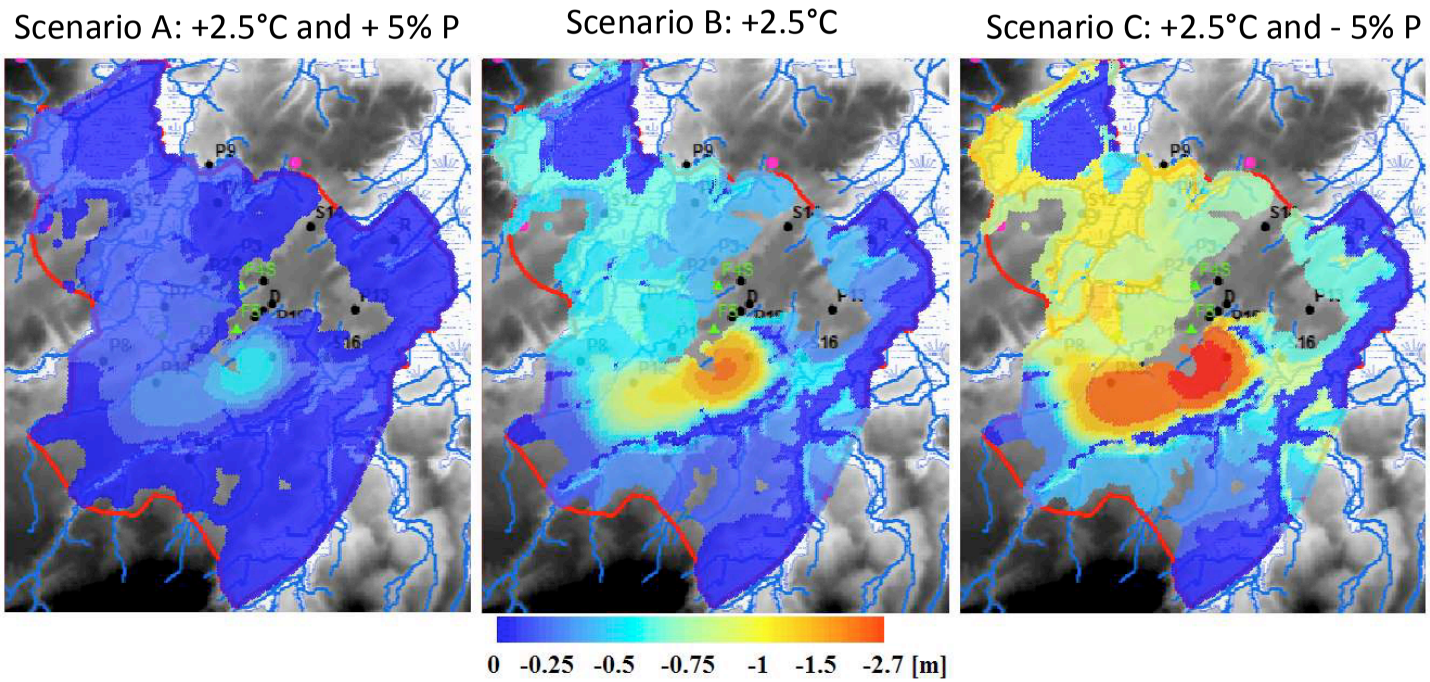

Figure 3.9: Water level variation (in m) in the first layer, relative to the reference model, for the 3 scenarios. Scenario A: T increase of 2.5 °C and P increase of 5 %; scenario B: T increase of 2.5°C and no change in P; scenario C: T increase of 2.5°C and P decrease of 5% .The uncoloured zones (grey) are dry cells.

The wetland surfaces resulting from the 3 simulations are presented in Table 3.3. These results agree with the water level changes described previously: the most impacting scenario is again C. The model predicts a decrease in wetland surface of 12.1 km^2 where the water level lowers b 50 cm relative to the surface. Even the most "favourable" scenario A predicts a surface decrease of 6.75 km^2, which is already more than the most "unfavourable" groundwater extraction scenario from the previous simulations (Table 3.2).

Table 3.3: Surface of wetlands resulting from the 3 climate change scenarios (in %) and change in surface relative to the reference model (km^2). Two wetland definitions are taken into account (water level between 0 and -0.5 m and water level between 0 and -1 m) as explained previously

	—Wetland surface— 0 to -0.5 m		Wetland surface— 0 to -1 m	
	%	km^2	%	km^2
Reference (current climate and pumping)	25	/	28	/
Scenario A (T and P increase)	21	-6.75	27	-1.35
Scenario B (T increase)	19	-9.45	24	-5.4
Scenario C (T increase, P decrease)	17	-12.15	21	-9.45

The impact of the scenarios on the changes in fluxes between compartments (aquifer/wetland/drained water (streams)), is synthesised in Figure 3.10. The two sub-catchments are taken apart. As a general behaviour, the fluxes are mainly upward (from aquifer to wetland). All the climate change scenarios predict a decrease in upward and downward fluxes (increasing groundwater extraction predicted an increase in downward fluxes). Although the decreasing rates are important in both catchments, the Taute upward fluxes are more impacted than those in the Seves: scenario C predicts a decrease of 32 % and 14 % respectively. In contrast, the Seves draining water volume is decreasing significantly more than the Taute: scenario C predicts a decrease of 82 % and 36 % respectively.

3.3.4 Model result for the combined effect of groundwater extraction and climate change

Figure 3.11 illustrates the water level changes in the first layer, relative to the reference model (present pumping) for 3 scenarios: Scenario B1: T increase of 2.5 °C and present pumping; scenario B2: T increase of 2.5°C and current pumping rates doubled (Q X 2); scenario B3: T increase of 2.5°C and current pumping wells and rates (Q) maintained, but in addition water is extracted from 2 new wells, each extracting Q/2. Notice that the systematic large lowering in the centre of the catchment (orange to red colours) is attributed to a bad calibration on the well "M", which residuals are not satisfactory (see chapter 3.2.2).

The previously described effects of groundwater extraction and climate change are added up. In the Seves wetland, scenario B2 results in a widely decrease of the water level by 100 to 150 cm. Scenario B3 maintains a water level lowering of about 70 to 100 cm in the Seves, while the Taute wetland is almost not impacted, except locally and along the borders.

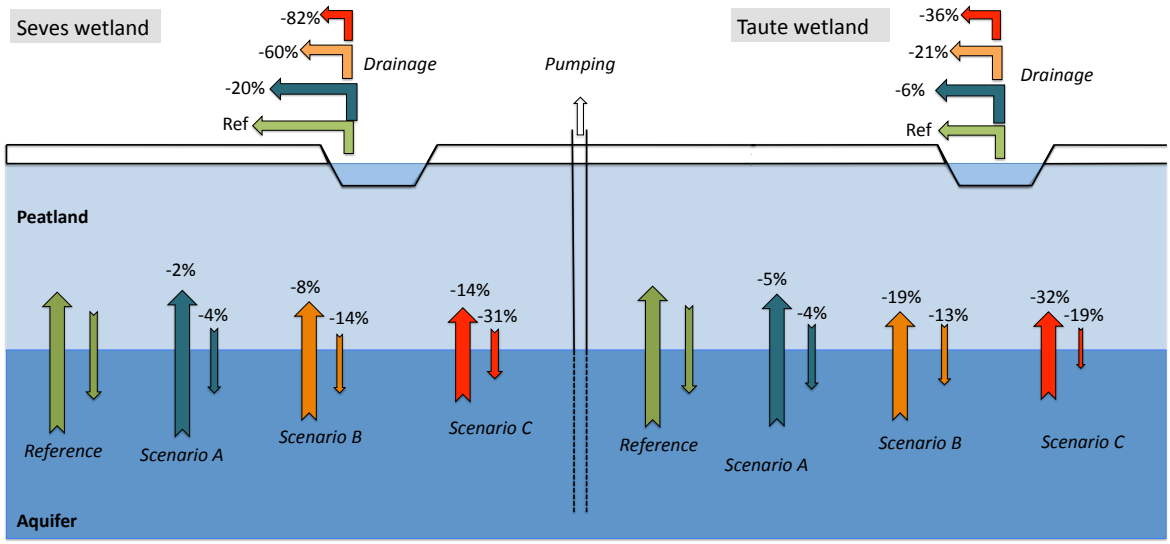

Figure 3.10: Climate change scenarios: upward and downward changes in the vertical fluxes relative to the reference site

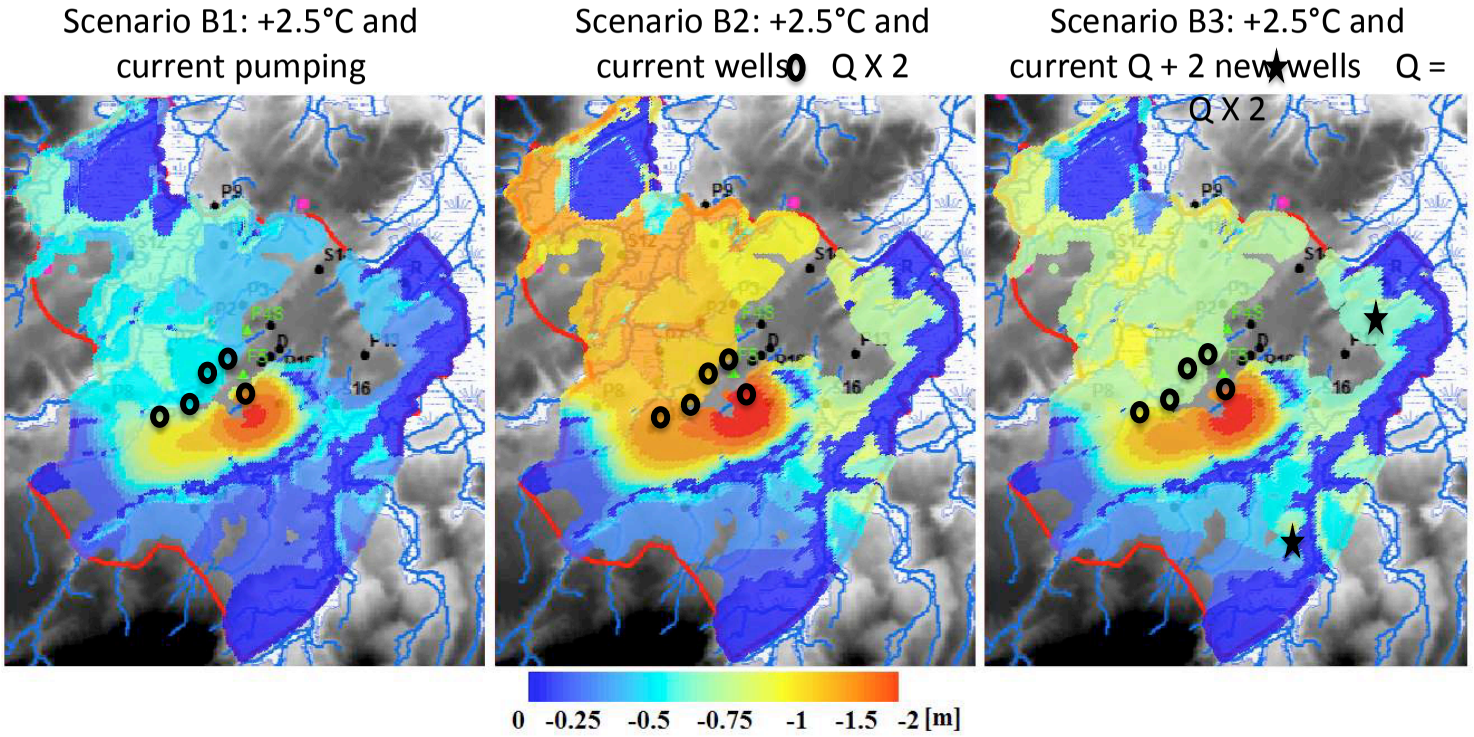

Figure 3.11: Water level variation (in m) in the first layer, relative to the reference model, for 3 scenarios. Scenario B1: T increase of 2.5 C and current pumping; scenario B2: T increase of 2.5C and current pumping rates doubled (Q X 2); scenario B3: T increase of 2.5C and current pumping wells and rates (Q) maintained, but in addition water is extracted from 2 new wells (stars), each extracting Q/2 .The uncoloured zones (grey) are dry cells.

3.4 Discussion

3.4.1 Model interest

According to the goals of this study, the available data and the basin scale, this steady-state and physically-based model approach is well adapted to the problematic. Classical wetland modelling takes into account an integrated surface-subsurface hydrological model, the unsaturated zone characteristics like vegetation and peat soil heterogeneity (Wilsnack et al., 2001) (Reeve et al., 2000). In contrast, our model is conceptually simple: it mainly takes into account the interactions between the wetland and the aquifer (which is well defined), the topography and the draining boundary. This draining boundary, applied on the whole first layer and active when the water level reaches the topographical surface, allows the model to freely determine the drainage areas. The calibration results show that the model is able to satisfactory simulate the annual variations in groundwater levels. In addition, the model predicts realistic wetland extends. The major uncertainty is on the volume of drained water but the error is difficult to estimate because of the partial stream discharge data available, which makes the river conductance calibration difficult.

3.4.2 Groundwater extraction and climate change scenarios

Groundwater extraction scenarios

The groundwater extraction scenarios were aimed to evaluate the sensitivity of the wetlands to future increasing demand. The two pumping simulations are inspired from realistic scenarios of future exploitation. The scenario without pumping simulates the original conditions before pumping started in 1992. It shows that the present pumping has lowered the Seves wetland water level by 25 to 40 cm, resulting from a 7 % decrease in vertical upward fluxes (from aquifer to wetland) and a decrease in the aquifer water level by 50 cm. As a general behaviour, the pumping decreases upward fluxes and increases downward fluxes. In addition to these changes in volumes of water transferred from one compartment to another, water and peat chemistry may be affected. Indeed, enhanced downward fluxes will bring different water qualities, and notably more oxygen, in deeper peat layers. The peat structure (e.g. mineralisation processes) as well as the catchment water quality may be affected. These hydrobiochemical impacts are the purpose of the next Part of this thesis report.

In order to limit the environmental impact, the pumping scenarios tend to favour the scenario including new extraction wells in the Marchesieux sub-catchment. Indeed, although this hydrological basin is less permeable (lower aquifer capacity), a similar water volume extracted (relative to present Sainteny extraction) results in a limited wetland water level lowering (see Figure 3.7). This lowering may almost affect the Taute wetland, only along its borders by around -10 cm, while the Seves wetland will be affected by a general lowering around 10 cm. On the other hand, the model predicts that a doubling of the extracted volumes in the Sainteny catchment, where exploitation is already important, will dramatically affect the wetland by a general lowering of about 40 to 50 cm.

Climate change scenarios

As stated in chapter 3.2.2, adopting a multi-model approach for the climate scenarios allows the uncertainty derived from climate model selection to be incorporated into the assessment of the impacts of climate change on the Sainteny-Marchesieux catchment.

Only projections using the SRES A1B emissions (medium scenario) are examined, thus uncertainty in future emissions is not addressed in this study. However, recent observed increases in atmospheric carbon dioxide concentrations agree with projections from high emissions scenarios (Rahmstorf et al., 2007) and significant divergence in green-house gas concentrations between scenarios in the second half of the 21st century are highlighted. This research field evolved rapidly these last years and a good perspective to this work would be to re-adapt our model to up to date new IPCC scenarios.

The 3 climate change scenarios predict a decrease in recharge from - 8 to -40% (from scenario A to C) resulting in water level decreases from 20 to 100 cm in the Seves wetland and stream discharge decreases from 20 to 82 %. As already noticed in the groundwater extraction scenarios, the Seves wetland is much more sensitive than the Taute wetland. The total Seves wetland surface is predicted to decrease by 5 to 9 %.

At long time scale (end of the century), the model shows clearly that climate change impact on the wetland water levels is much higher than the groundwater extraction projections. However, this must not lead to under-estimate the impact of increasing groundwater demand. The two processes are adding up and at short term (tens of years), groundwater extraction will be the first impacting process.

3.4.3 Model sensitivity and perspectives

It has been demonstrated that recharge is highly affected by climate change and is a very impacting contributor to the water balance. Therefore, a better knowledge on the recharge value and corresponding uncertainties is necessary. In addition, other parameters significantly impacted the hydrological modelling, and notably the hydraulic conductivity of the peat. Gain in knowledge on this parameter should improve the model. Finally more field data are needed to improve the model. E.g. less data are available in the Marchesieux sub-catchment : more distributed wells and a better knowledge of the geology should improve the model predictions in this area. In addition, more stream gauging are also necessary to better constrain the volume of drained water within the catchment. The possibility to move to a transient simulation to capture seasonal variations, which are also important in climate change scenarios (wetter winters and dryer summers are excepted), depends on the available data to satisfactory calibrate the model. In particular, no general water level monitoring, in time and space, is available in the wetlands, which should be needed for transient simulations.

Conclusion

The present simulation aimed to analyse the wetland sensitivity to groundwater extraction and climate change.

The constructed physically-based model works in a permanent regime and is based on saturated hydraulics, using the software Visual MODFLOW combined to ArcGis as a mapping tool. The conceptual model distinguishes a first layer made of peat or sands (finely spatially defined) and imple-

mented with the topography, and an underlying deep aquifer. This aquifer is exploited for drinking water supply, and therefore significant knowledge is available about the catchment geology, hydraulics and piezometry (from 1992 or 1995 to 2010). As drainage in this widely extended wetlands along the streams, is considered to be the largest component of the total groundwater abstraction, an original topographically controlled drainage boundary was used. This boundary allows to the model to freely determine the drainage areas. The model calibration was considered successful and simulates well the interactions between the wetland and the aquifer. The model highlights that upward fluxes (from aquifer to wetland) are indeed highly dominant. The sensitivity analysis points out the recharge as a very impacting contributor to the water balance and thus to the simulation results. Classical wetland modelling takes into account an integrated surface-subsurface hydrological model, the unsaturated zone characteristics like vegetation and peat soil heterogeneity. In contrast, our model is conceptually simple: it mainly takes into account the interactions between the wetland and the aquifer (which is well defined), the topography and the tographically-controled draining boundary. According to the goals of this study, this simplified approach is well adapted.

Simulations on groundwater extraction shows that the current exploitation has already a significant impact on the wetlands, the Seves wetland may have lowered by 25 to 40 cm. Future projects should favour groundwater extraction in the Marchesieux sub-catchment, as the other already exploited sub-catchment of Sainteny is more sensitive to wetland water level lowering.

Simulations on climate change, using the medium scenario A1B from the IPCC, show that the wetland water levels may be highly impacted by the end of this century, directly related to the resulting decrease in aquifer recharge. Nevertheless, the Seves wetland is again more impacted than the Taute wetland.

At long time scale (end of the century), the model shows clearly that climate change impact on the wetland water levels, is much higher than the groundwater extraction projections. However, this must not lead to under-estimate the impact of increasing groundwater demand. The two processes are adding up, and at short term (tens of years), groundwater extraction will be the first impacting process.

Part II

Biochemical processes in the peatland

Peatlands or peat meadows are complex ecosystems whose functions are driven by many physical, chemical, and biological processes. Because peat soils can serve as sinks, sources, and transformers of nutrients and other chemical contaminants, they have a significant impact on water quality and ecosystem productivity. Worldwide, lowered water tables, mainly induced by drainage, are now recognized to be associated with several problems affecting both the physical structure of the peat as well as water quality. As peat aeration increases, its decomposition is enhanced by aerobic bacterial processes which are approximately 50 times faster than under anaerobic conditions (Holden et al., 2004). A visible impact is subsidence causing bulk density to increase in the upper layer within a few years of water table lowering (Silins and Rothwell, 1998). Oxygen also enhances the mineralization of nutrients, particularly the carbon-bound nitrogen and sulphur. The top meter of peat soils can contain as much as 20 t nitrogen (N), 10 t sulphur (S) and 500 t of carbon (C) (Miller et al., 1996). Even an increase in mineralization of 1% yr^{-1} has the potential to generate large losses of these elements. In addition, water table lowering usually increases the leaching of Ca, Mg and K (Sundström, 2000) (Miller et al., 1996) (Kortelainen et al., 2006) as well as NH_4 (Holden et al., 2004). The hydrological anthropogenic impacts induced by drainage, pumping and climate change have been studied in the first Part of this report. They highlight a change in flows between the hydrological compartments and a decrease in wetland levels. The changed fluxes between compartments modify the respective water sources contributing to the wetland recharge. For example, the surface water or rain water contribution may increase while groundwater contribution may decrease. The water level lowering, depending on its intensity, may rather increase the desaturation period of the upper peat layer, or evolve to a perennial drying out leading to desiccation. These changes are expected to impact the wetland biochemical functioning. In addition, a comparative study between two peatlands (La Bergerie, close to a pumping station, and Le Marais) was carried out in 2003-2005 (Auterives, 2006). Downwards flows from the surface towards the aquifer appeared to be enhanced in the vicinity of an extraction well penetrating the aquifer, compared to areas outside the well drawn-down perimeter. The stream seepage towards the wetland was also increased. Consequently the peat is subjected to more oxygenated conditions throughout the year. **Based on these results, we investigated in Part II the influence of the water level fluctuations on biochemical processes in the peatlands. This Part II focuses on the biochemical processes in peat pore water in non extreme conditions, by comparing a dynamic fluctuating water table to stagnant conditions in laboratory experiments.** Two fluctuating conditions (3 days and 9 days cycles) of desaturation/rewetting are tested. Two peat types from La Bergerie (pumping station) and Le Marais are investigated. This site comparison provides a temporal perspective of the anthropogenic effects.

The first Chapter describes the Materials and Methods used and the peat physico-chemical characterization. **The second Chapter** focuses on the sulphate and dissolved organic carbon behaviour in response to the alternating aerobic/anaerobic conditions in peat samples from La Bergerie and Le Marais sites. **The third Chapter** investigates the overall impact of dynamic fluctuations relative to stable conditions on nutrients cycling to determine the potential impacts of each water table regime.

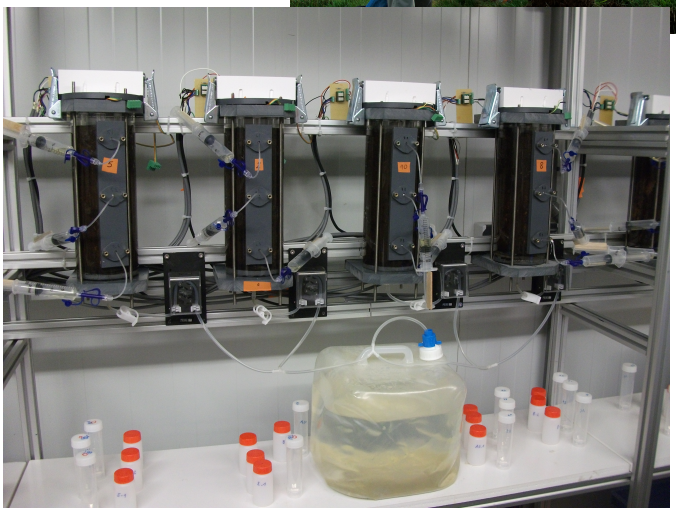

Chapter 1

Laboratory experiment: materials and methods and peat characterization

Collaboration team: Jean-Pierre Caudal, fabulous multifunctional engineer I worked with to build up these experiments. We had the ambition to make a fully automatic, repeatable designed experiment. Thanks to Jean-Pierre to have initiated me to electronics, computer tricks, machining pieces... and brain-storming about the best way to saturate peat! For peat characterization: thanks to Nathalie Josselin-Le Bris and Marie-Paule Briand (from the Ecobio team) and Martine Bouhnik-Le Coz (from Geosciences) for analytical support.

Two laboratory experiments were conducted, both with cores from La Bergerie and Le Marais (Figure 1.1). A full hydrological monitoring was conducted in these sites in a previous field study. La Bergerie is adjacent to a pumping well, which was shown to increase the downward fluxes through the peat profile (Auterives et al., 2011). This peat is thus subjected to more oxygenated conditions throughout the year. Le Marais is considered as a relatively undisturbed site.

The first experiment uses cores directly sampled from the field with their original moisture content (around 80 %). This experiment is reported in this Part II. The second experiment uses cores sampled in the same conditions as the first experiment, but stored in the laboratory for 5 months before the experiment (moisture content around 60 %). This experiment is reported in Part III Chapter 1.

1.1 Site description

The study area consists of a peaty meadow belonging to a wetland complex, located in the Cotentin Marshes in Normandy (49°18'20"N, 1°14'34"W). The plant communities are dominated by *Dactylus glomerata* L., *Holcus lanatus* L., *Agrostis stolonifera* L., *Festuca arundinacea* S. and F., *Carex spp.* and *Juncus effusus* L.(Bouillon-Launay, 1992). Mean annual rainfall and temperature were 923 mm and 11.2 $^{\circ}C$, respectively (average 1946-2009, from Meteo France (Meteo France, 2011)). The peatland has developed on top of a clay bed (1.5 - 6 m tick) which is supported by rocks rich in sand and limestone which constitute a 80 m thick aquifer. Peat accumulation in the investigated area is between 5 and 12 meters. This widely extended wetland has undergone numerous disturbances. In the XVIII century the wetland was flooded 9 months per year (Bouillon-Launay, 1992). Since 1712 a human

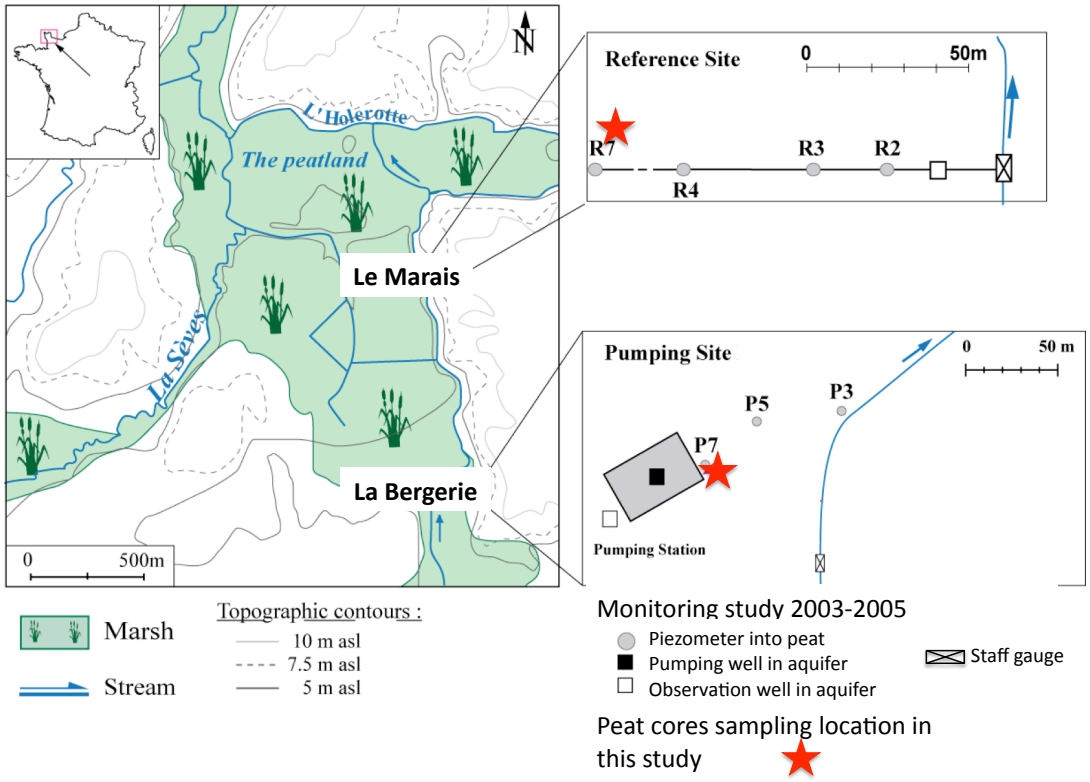

Figure 1.1: The two investigated sites: Le Marais is the reference site, La Bergerie is in the pumping well draw-down perimeter. Modified from (Auterives, 2006)

.

controlled drainage system was gradually installed. It presently consists of a network of channels and ditches in which the water level is set low in spring to minimize flooding and high at the end of the summer to act as wet-fencing. Since the 1950s, due to agricultural constraints, the flooding season has decreased to only 3 months on average. The top peat profile is thus subjected to longer periods of dessication. This wetland is connected with an underlying aquifer and the wetland behaves globally as a discharge zone from the aquifer (Auterives et al., 2011). But this does not exclude more local reversed flows between the deeper and surface aquifers. Localized seepage from the wetland to the aquifer have been observed in particularly dry years (Auterives et al., 2011). Moreover, reversed flow appears to be enhanced in the vicinity of an extraction well penetrating the aquifer, relative to areas outside the well drawn-down perimeter. Based on these results, the area of investigation focuses on two small plots of land within the peatland, separated by 1.5 km: Le Marais and La Bergerie. La Bergerie is adjacent to the pumping well, which was shown to increase the downward fluxes through the peat profile (Auterives et al., 2011). This peat is thus subjected to more oxygenated conditions throughout the year. Le Marais is considered as a relatively undisturbed site.

1.2 Peat cores

Samples where collected when relatively dry conditions were favourable for core collection. At this time the water level was at 65 cm and 75 cm below soil surface for Le Marais and La Bergerie respectively. Peat cores were collected at randomly selected plots on a 10 x 10 meters area, in the unsaturated zone, a few centimetres above the water table. This sampling layer is chosen because it is in the zone of water table fluctuation, i.e. this peat is saturated in winter time. Replicated samples were obtained directly into push cores (10 cm diameter, 30 cm height) that were further used in the experiments (see Figure 1.2). Caution was taken to minimize the disturbance of layers during collection and storage. The peat cores were thus bulk samples, preserving the field structure. The cores were put in polyethylene bags and returned to the laboratory within 6 hours.

The pH of the water samples from the below water table were measured on site with a Consort electrode C533.

Peat material was characterized initially, after sampling, for bulk density, soil moisture, Van Post index, total C, N, S and O content, mineral content expressed as the total cation content and microbial and active biomass: methods and results are reported in Section 1.5.

Microbial and active biomass are again analysed after the 5 months drying and at the end of the 45 days experiment in each core, by sampling a layer of peat 2 cm in thickness at the 3 heights of investigation (top, middle, bottom).

1.3 Draining-rewetting experiment

Two experiments were conducted where peat samples from the two sites (Le Marais and La Bergerie) were subjected to varying time periods of water saturation. The water used in the rewetting experiment was collected from the observation well at La Bergerie site at 40 meters depth (see Figure 1.1). The composition of this groundwater is presented in Table 1.1. This source of water was chosen because (i) it is a natural water contributing to the wetland recharge (ii) the water quality is stable

Figure 1.2: Core collection in the field, directly into push cores 10 cm diameter and 30 cm height

in time and can be re-used for several experiments (iii) this water has a relatively high hardness and around neutral pH which strongly differs from the peat water chemistry. The goal was to enhance the chemical processes (e.g. leaching or buffering processes) in order to make them easily visible as well as to highlight potential differences between the two peats.

Intact peat monoliths were sampled using PVC cores (30 cm height, 10 cm diameter). The experiment lasted 45 days. Figure 1.3 illustrates the column design. Water was sampled at three heights along the core by use of soil moisture samplers (Rhizon 19.21 from Eijkelkamp), reflecting the pore water characteristics at specific heights. Water was filtered at 0.10 μm directly through the moisture samplers. Drained water from the whole column was also analysed. Air-tight lids allowed for punctual incubation of the cores for measurement of CO_2. Depending on the experiment, several treatments were tested (Figure 1.4). Common to the two experiments :(1) a dry case, where no rewetting occurred throughout the experiment (2) a permanently saturated case, where the core was kept saturated during 45 days (3) a drained-rewetted cycle on a 9 day frequency. In addition, the first experiment tested a draining-rewetting cycle on a 3 day frequency. A temperature-controlled dark

Table 1.1: Chemistry of the water used in the core experiments. Concentrations are in mg.L^{-1}

pH	7.5	Ca^{2+}	76.0
Cl^-	30.6	Mg^{2+}	8.5
NO_3^-	36.9	Na^+	14.9
SO_4^{2-}	10.0	K^+	2.7
DOC	0.0	Fe	0.02
DIC	56.5		

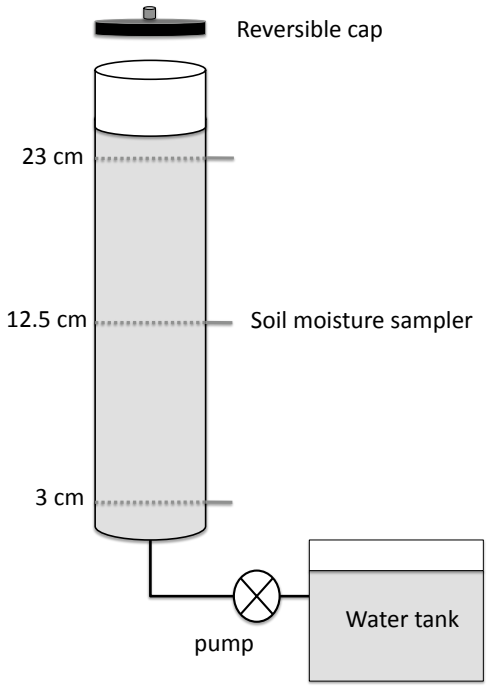

Figure 1.3: Column design: water inlet is from the bottom by help of a pump, pore water is sampled to micro-porous samplers, a reversible cap allows punctual incubation to analyse CO_2 production.

room was used for the experiments. The temperature was set to 15 $^\circ C$ in order to speed up the rate of nutrient mobilization. It is somewhat higher than the average field temperature (around 12 $^\circ C$) but still within the field range. The water inlet and outlet were located at the bottom of the cores (see Figure 1.6) to reproduce the field water level rise or drop and to fully saturate the peat pores. Inlet and outlet were controlled automatically by peristaltic pumps so that all cores underwent the same

hydraulic constraints both between cores and between each draining-rewetting cycles on a single core (Figure 1.5). Water tanks preserved from contact with the atmosphere were connected to the cores randomly distributed in the dark room. The automated design imposed a 5 seconds time step allowing water to enter (or exit) a core, one core at a time. Depending on the cores porosity and composition, rewetting (or draining) took approximately 2 hours. The vertical structure of the peat in the field was preserved, resulting in a certain degree of heterogeneity between cores. These differences are especially reflected in the effective porosity, measured by the volume of water needed to saturate (or empty) each core.

Water loss by evaporation or punctual water sampling resulted in a drop of the water level in the cores, especially for the permanently saturated treatment. To counteract this effect which otherwise would result in the desiccation of the top layer, water was allowed to enter the column (always by the bottom) at regular intervals.

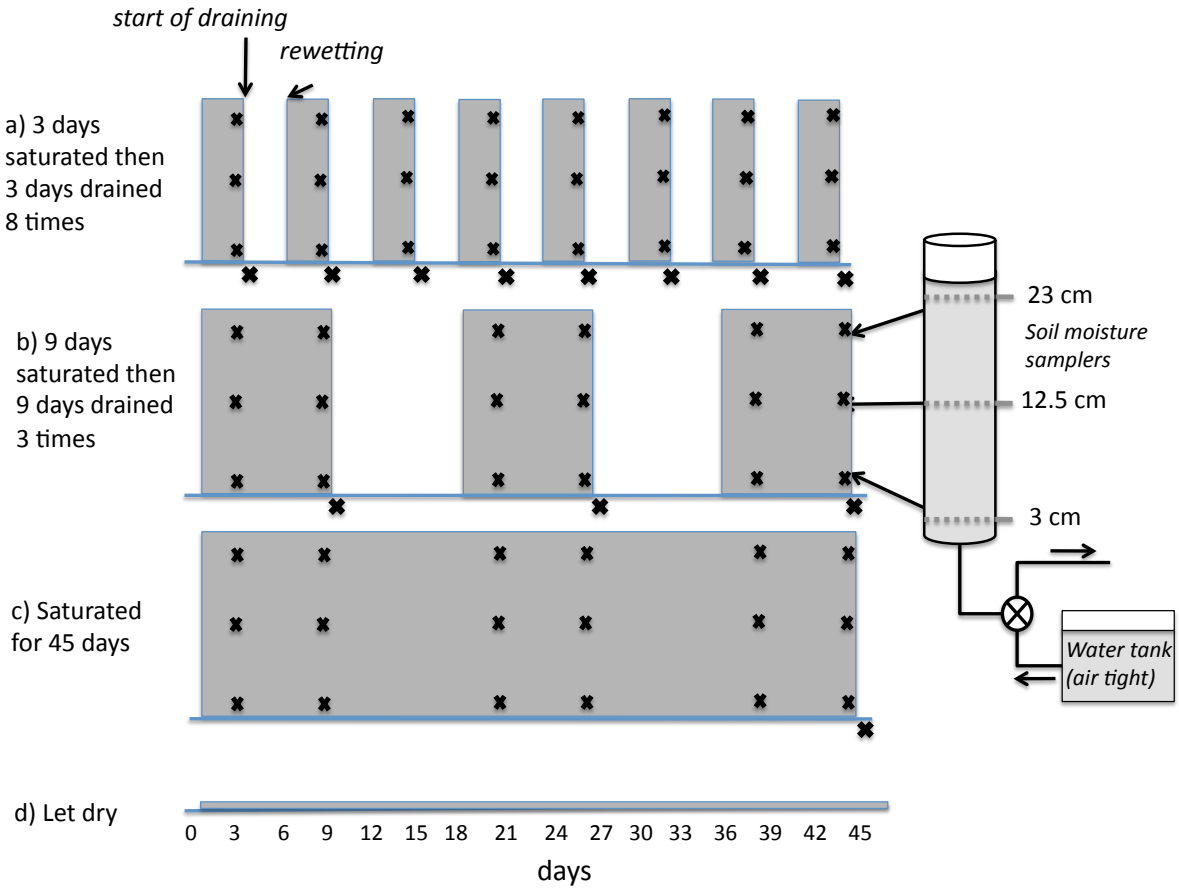

Figure 1.4: Diagram representing the experimental setup a) the cores are saturated for 3 days then drained for 3 days (first experiment) b) the cores are saturated for 9 days then drained for 9 days c) the cores are saturated for 45 days d) the cores are kept dry. The black crosses indicate where the water samples were taken at the 3 levels in the core and in the drained water.

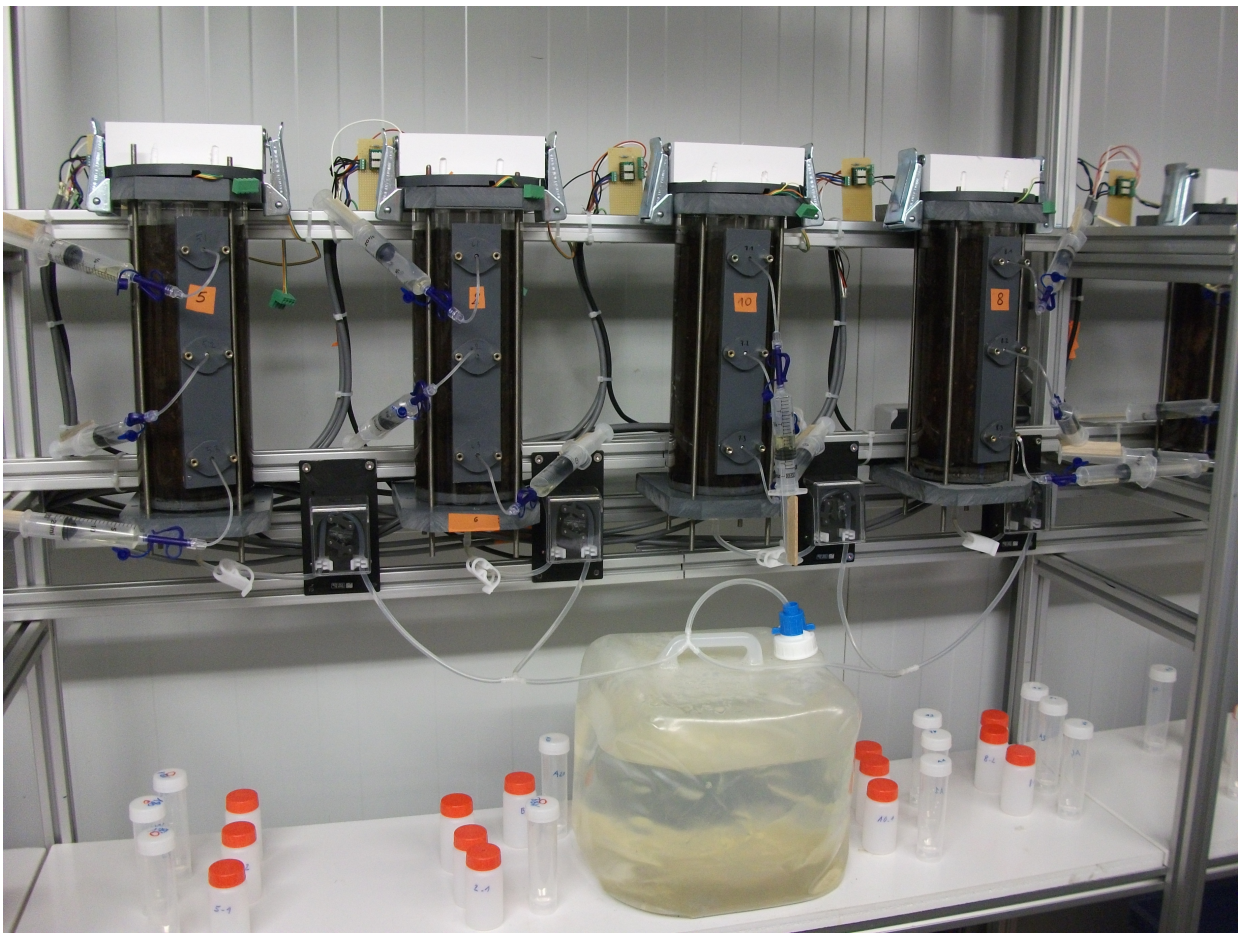

Figure 1.5: Picture of the column experiment

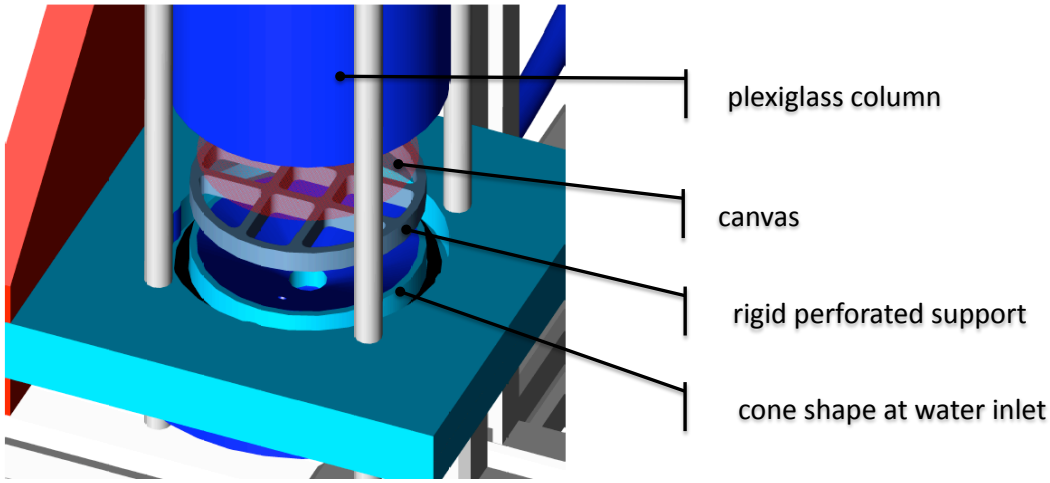

Bottom of the column: details

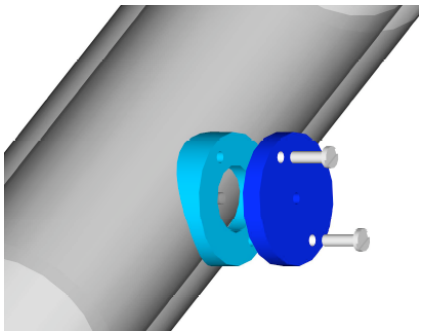

Middle of the column: piece to fix soil moisture sampler

Figure 1.6: Details on the design of the column

1.4 Peat pore water chemistry

The pH was measured with a combined Mettler InLab electrode after a calibration performed with WTW standard solutions (pH 4.01 and 7.00 at 25 ∘C). The accuracy of the pH measurement is 0.05 pH units. The electrical conductivity (EC) was measured by a Consort electrode C533 which accuracy is of 0.01 μ S/cm. The redox potential (Eh) was measured by a Mettler Platinium 4805 electrode which accuracy is 1 mV. Dissolved organic carbon was analysed with a Total Organic Carbon analyser (Shimadzu TOC-5050A). The accuracy of DOC measurement was estimated at 3% (by using a standard solution of potassium hydrogen phtalate). Dissolved inorganic carbon was also measured with the Shimadzu TOC-5050A with an accuracy of 0.2%.

SUVA (Specific UltraViolet Absorbance), strongly correlated with degree of aromaticity of organic matter (aromaticity = 6.52 * SUVA + 3.63) (Weishaar et al., 2003), was used as an indicator of the chemical composition and reactivity of dissolved organic carbon.

Major anion (Cl^-, NO_3^-, NO_2^-, PO_4^{2-}, SO_4^{2-}) concentrations were measured by ion chromatography (Dionex DX-120). The uncertainty was below 4%. Major cation (Ca^{2+}, Na^+, K^+, Mg^{2+}, Mn^{2+}, Fe) concentrations were determined by ICP-MS (Agilent 4500), using indium as an internal standard. The international geostandard SLRS-4 was used to check the validity and reproducibility of the results. Typical uncertainties including all error sources lay between 2 and 5%, depending on the concentration. Fe(II) concentration was measured by the 1.10 phenantroline colorimetric method, AFNOR NF T90-017 (AFNOR, 1997), using a UV visible spectrophotometer. Estimated uncertainty is 1%. NH_4 concentration was measured by the salicylic colorimetric method, DIN 38 406 part 23, section 2 and ISO/DIS 11732, using an automatic UV visible spectrophotometer No. G-102-93 Rev. 4 from Bran and Luebbe. Estimated uncertainty is 2%. Finally, CO_2 was analysed by a micro gas chromatograph 3000 (from SRA Instrument). Estimated uncertainty is 1%.

1.5 Peat characterization

This section describes the chemical and biological characterization of the initial peat material from Le Marais and La Bergerie.

Materials and methods

Initial peat characterization was done on four subsamples for bulk density, soil moisture and Van Post index. Peat material was characterized for bulk density, soil moisture and Van Post index. Total C, N, S and O content were measured with a carbon-sulphur analyser LECO SC 144 DRPC, with an accuracy of 5 %. The peat sample is oxidized at high temperature (1800°) with a catalyst and under oxygen. The emitted gases (CO_2, N_2, H_2O, SO_2) are separated on a chromatographic column (Porapack QS). After detection and signal amplification, the measured concentrations permit to quantify C, N, S and O. Mineral content, expressed as the total cation content, was determined by ICP-MS (Agilent 4500) after acid, drying and peroxide digestion. Microbial and active biomass were measured (i) initially on 4 peat subsamples before the experiment and (ii) at the end of the 45 days experiment in each core, by sampling a layer of peat 2 cm in thickness at the 3 heights of investigation (top, middle,

bottom). Microbial carbon was measured by the fumigation-extraction method, using a protocol modified for peat (Williams and Silcock, 1997) (Francez et al., 2000). C was analysed in 0.5 M K_2SO_4 extracts. Soluble organic C extracted from both fresh and fumigated peat was measured by using a OI-analytical TOC 1010. The values obtained from the non-fumigated samples are referred to as soluble organic carbon (SolOC) Microbial biomass C results from the difference between fumigated and non-fumigated samples, corrected with the recovery factor K_{EC} of 0.45 (Sparling et al., 1990). Potentially active biomass was measured by the substrate induced respiration method, by adding a pre-determined glucose solution (18 $mg.g^{-1}$ dry mass) and using a pre-determined incubation time (1 hour). The resulting respiration rate, i.e. CO_2, was measured by gas chromatography and further converted to C microbial biomass (Anderson and Domsch, 1978) (Sparling, 1995) .

Results

Peat characteristics are given in Table 1.2. These peats are moderately degraded (+ 40 % fibers) with macro-pieces of stringy wood. With respect to total nutrients, organic carbon content is higher in le Marais, 401.5 $g.kg^{-1}$(dry weight), compared to la Bergerie where C is 328.8 $g.kg^{-1}$. This difference is also visible on the total nitrogen content. Sulphur contents are similar (4.9 $g.kg^{-1}$).

Peat mineral content is expressed by the total major cations content. Mg is similar in the two peats. Ca is somewhat higher in peat from le Marais, while the other components are slightly lower.

With respect to extractable nutrients, nitrogen contents are similar between the two peats, but carbon is 2 times greater in le Marais compared to la Bergerie. This difference is also reflected in the microbial biomass and the microbial activity.

Peat from le Marais and la Bergerie are compared for C and N ratios in Figure 1.7. Peat from le Marais has a C:N ratio of 15.7 (SE: 1.03) and the microbial biomass carbon to soluble organic carbon ratio is (MBC/SolOC) 0.35 (SE: 0.02). Peat from la Bergerie has a C:N ratio of 17.5 (SE:0.42) and a MBC/SolOC of 0.14 (SE:0.03)[1].

1.6 Statistical analyses

A large range of chemical species were followed in our experiment to allow a comprehensive study of the inter-related reactions involved. To achieve data reduction and help categorize the set of chemicals a principal component analysis (PCA) was carried out with R (Foundation for Statistical Computing, 2010). Near-normal distribution was improved by log transformation of the data.

Another objective of the experiment was to test if short frequency draining-rewetting cycles (3 days and 9 days) have an effect on the resilience of the peat chemistry. To achieve this, an analysis of variance (ANOVA) was carried out to test the effect of the cycle frequencies. Before running the analysis, the assumptions underlying this test were checked: normal distribution of data (by Shapiro-Wilk test and histogram shape), equality of the variances (by Levenes test), and similar distribution shape (by Kolmogorov-Smirnov test). Near-normal distribution was improved by log transformation of the data. The pairwise comparisons of the means of pH, SO_4^{2-} and DOC were then tested with the Tukey-Kramer test, using the type of treatment as explaining variable (saturated, 9 days draining-rewetting

[1]SE: standard error

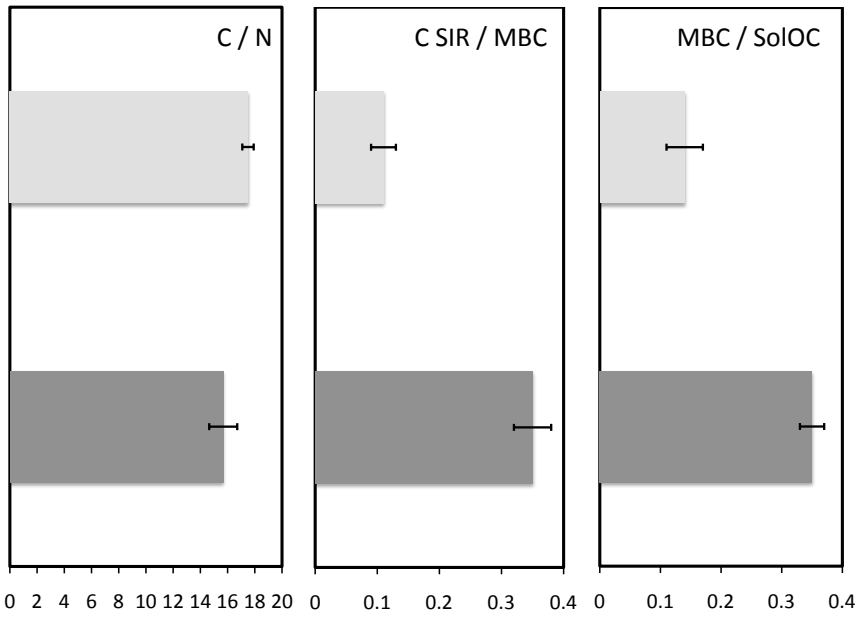

Figure 1.7: Comparison between peat from le Marais (grey bars) and la Bergerie (light grey bars) on carbon-nitrogen ratios. Error bars are standard errors, n=36.

Table 1.2: Peat properties. Average and standard error are given on four different samples from the same core

	Le Marais		**La Bergerie**	
	Value	Standard error	**Value**	Standard error
Humification (Van Post)	**H6/H7**		**H4/H5**	
Bulk density (g.cm^{-3})	**0.22**	0.001	**0.21**	0.002
Moisture content (%)	**85**	0.3 %	**84**	0.5 %
Total nutrients (g.kg^{-1} dry mass)				
C	**401.5**	1.0	**328.8**	0.4
N	**25.6**	0.1	**18.7**	0.02
S	**4.9**	0.05	**4.9**	0.006
Ca	**19.4**	0.24	**14.15**	0.29
Na	**0.60**	0.01	**1.88**	0.27
K	**2.28**	0.05	**5.00**	0.31
Mg	**1.61**	0.02	**1.96**	0.04
Fe	**9.3**	0.4	**11.7**	0.3
Extractable nutrients (g.kg^{-1} dry mass)				
Soluble organic carbon (SolOC)	**2.43**	0.07	**1.16**	0.04
Soluble organic nitrogen (SolON)	**0.33**	0.01	**0.34**	0.01
Biomass (g.kg^{-1} dry mass)				
C microbial (MBC)	**0.80**	0.06	**0.26**	0.04
N microbial (MBN)	**0.07**	0.01	**0.10**	0.02
C microbial activity (C SIR)	**0.28**	0.005	**0.03**	0.003
pH of the water at the sampling site	**6.1**		**5.4**	

frequency and 3 days draining-rewetting frequency). Likewise, all statistic tests were carried out with R.

Chapter 2

DOC and sulphate release under draining-rewetting constraints in peat

Abstract

Peat is very sensitive to changes in hydrology that may be brought about by climate or anthropogenic pressures. The study highlights the chemical processes involved in peatlands, focusing on sulphate and DOC release. Two peats undergoing different hydrological flows in the field - a site impacted by pumping of an underlying aquifer and an undisturbed site - were subjected to short periods of saturation and draining in a laboratory experiment. The study confirms that peat quality is a key control on its sensitivity to environmental changes such as changing water recharge quality or aeration status. The nutrients turnover in these peats is highly influenced by their state. A more degraded peat, i.e. depleted in nutrients and biomass, is more sensitive to oxidation processes. Release of sulphate (here dominantly iron sulphides, resulting in high dissolved iron concentrations) results in acidification which in turn enhances cation leakage and a decrease in DOC solubility. From this study, the most convincing explanation is that, instead of the total iron sulphide content (mainly pyrite), its degradation state is responsible for these different behaviours between sites.

The draining-rewetting experiment emphasizes the difference in S availability to oxidation. In the undisturbed peat, a 3 or 9 day draining-rewetting frequency or permanently saturated cores produce similar sulphate concentrations, while in the impacted peat, increasing the residence time of water leads to increasing sulphate release resulting in increasing acidity. The impacted site is more sensitive to alternating oxidation-reduction cycles. The buffering capacity of the peat, i.e. its efficiency to counteract environmental changes, is thus less maintained where peat is more degraded.

The peats differ mainly by their nutrient and biomass content. Microbial activity is expected to respond to relative rapid disturbances in the peat environment. Therefore we argue that the difference in peat quality between the two sites may be related to the different hydrological constraints experienced in the field. It is likely that 20 years of enhanced downward flow has contributed to degradation of the peat material. This downward flow is expected to bring more oxygenated waters into the peat, and thus enhance oxidizing processes.

Key Words: Peat hydrochemistry; Hydrological change; Short-term disturbance; Degradation dynamics; Acidity; Sulphate; DOC

Introduction

Contrasting mobilization-immobilization responses of peat soil to more aerobic conditions have been reported in the literature. Although sulphate (SO_4^{2-}) release is always observed, contradictory results are reported on dissolved organic carbon (DOC) and the dynamic of major cations (Blodau et al., 2004) (Blodau et al., 2002) (Clark et al., 2006) (Glaser et al., 1990). SO_4^{2-} turnover is highly documented (Krairapanond et al., 1991) (Chapman and Davidson, 2001) (Chapman, 2001) (Devito and Hill, 1999). Regardless of the source of sulphur, SO_4^{2-} reduces to a mineral form, i.e. FeS, FeS_2, H_2S and S. Under aerobic conditions this reduced form oxidises to SO_4^{2-}, generating an increase in acidity (Schiff et al., 2005) (Lamers et al., 2002). It is likely that some of the H^+ ions replace other cations on exchange sites or enhance carbonate dissolution resulting in the marked increase in Al or Ca concentrations in the drained water (Kadlec and Keoleian, 1986) (Skyllberg and Magnusson, 1995) (Eimers et al., 2008). In contrast to SO_4^{2-}, the response of DOC to different oxidation states has not a unique trend. In some cases, an increase in DOC has been observed in more aerobic conditions (Freeman et al., 2004a) (Silvola et al., 1996), possibly because drained peat soils have more humus compounds and substances that are readily hydrolysed. Other studies, however, have found no significant DOC changes or even declines in DOC following drainage most likely influenced by the hydrologic regime (e.g. dilution effect occurring with changes in stream flow) (Eimers et al., 2008). These studies suggest that mobilization or immobilization responses of nutrients in peat soils depend largely on the change in peat decomposition, which is regulated by factors related to the environment and substrate (Laiho, 2006). Environmental factors include (i) aerobic/anaerobic constraints which impact the redox potential (ii) the water quality recharging the wetland which notably impacts the pH and (iii) temperature. Substrate factors include stage of decomposition, organic matter quality, nutrient content, and the presence of chemical and biological inhibitors to microbial activity. The sensitivity of nutrient mineralization to oxidation depends on substrate characteristics related to the quality and quantity of organic matter. Therefore large heterogeneities in nutrient dynamics related to oxidation state across the landscape result in the interacting influence of environmental and substrate factors.

The present Chapter investigates the chemical processes in peats related to variable oxidation states as a response to variation in water table height. These wetlands have experienced two main land management practices resulting in changes to peatland water tables : progressive draining since the beginning of the XVII century and water extraction from an underlying productive regional aquifer. As a result, the top peat profile is subjected to longer periods of dessication. We hypothesize that anthropogenic impacts such as water pumping and drainage of the wetlands can lead to greater degradation of the peat. **The aim of this study is (i) to test the effects of peat substrate quality on DOC and SO_4^{2-} solubility - from a pumping site subjected to more oxygenated conditions throughout the year and an "undisturbed" site (ii) and to test if short frequency draining-rewetting cycles have an impact on the resilience of the peat chemistry.**

In order to test this hypothesis, laboratory experiments were conducted in peat cores, by repeated draining and re-wetting cycles at different frequencies (3 days and 9 days, beside steady controls), in controlled air conditions of temperature and humidity.

2.1 Materials and methods

Please refer to the general Materials and methods section of Chapter 1 in this Part II. In this experiment four treatments were tested on intact peat cores directly from field (around 80% water content) collected in the two sites - La Bergerie and Le Marais: (1) a dry case, where no rewetting occurred throughout the duration of the experiment (2) an always saturated case, where the core was kept saturated during 45 days (3) a drained-rewetted cycle on a 3 day frequency (4) a drained-rewetted cycle on a 9 day frequency. Each treatment was replicated four times, resulting in 16 cores per peat type.

2.2 Results

2.2.1 Peat pore water in the cores

Results are presented for the middle and the bottom of the cores. Results from the top of the cores show higher oxidation and higher variability between cores and between sampling days and will not be discussed here. Table 1.1 summarizes the monitored parameters and chemical concentrations in the middle of the cores, at the end of the experiment for the permanently saturated cores in Le Marais and La Bergerie. The "inlet water" column recalls the chemistry of the water used to saturate the cores.

Table 2.1: Comparison, over a set of parameters or elements, between Le Marais and La Bergerie. Average and standard error are given on four pore water samples from the middle of the always saturated cores, on day 45. Concentrations are in mg.L^{-}. The "inlet water" column recalls the chemistry of the water used to saturate the cores.

	Inlet water	**Le Marais**		**La Bergerie**	
		Value	Standard error	**Value**	Standard error
pH	7.5	**6.1**	0.02	**4.3**	0.02
Cl^-	30.6	**30.1**	0.5	**32.4**	1.0
NO_3^-	36.9	**0.5**	0.1	**0.9**	0.40
SO_4^{2-}	10.0	**63**	7	**439**	76
DOC	0.0	**110**	5.6	**36**	5
DIC	56.5	2.8	0.3	**1.2**	0.1
Fe^{2+}	0	**1.9**	0.3	**27.0**	2.6
Fe	0.017	**5.7**	1.3	**72.7**	25.6
Ca^{2+} + Mg^{2+}	84.5	**52**	2.8	**130**	53.3
Na^+ + K^+	17.5	**10.2**	0.4	**24.5**	5.3
SUVA		**3.39**	0.16	**3.57**	0.20

Relation between elements

A Principal Component Analysis was carried out on pore samples data from the middle and the bottom of all the cores and for each peats (Figure 2.1). The PCA for each site shows similar results, however the correlations among variables are stronger in La Bergerie (i.e. the explained variance by the two first components is higher). The PCAs do differentiate the groups SO_4^{2-}-Ca-Mg-Na on one side, and pH on the other side of a component. In La Bergerie Mg and K are correlated to Ca and Na respectively, and therefore were excluded from the PCA in order to not distort the analysis. In Le Marais Mg was correlated with Ca and was excluded for the same reason. For both peats, Fe and DOC are strongly correlated (very close and highly linked to a component) and anti-correlated with NO_3^-. It appears that in Le Marais the main process controlling the concentrations (first component) is

the redox state (from more oxidant with NO_3^- to more reduced with Fe) while in La Bergerie the first controlling process is the acidification (pH anti-correlated with SO_4^{2-}-Ca-Mg-Na-K). Although the two first components do explain 73.4 % of the variance in La Bergerie, it only explains 55.6 % in Le Marais. Therefore the third compoent was used (Figure 2.1). In this case, the correlation coefficients show a different pattern between some elements: (i) Fe and DOC are still strongly correlated and explain the major part of the variance in the first component (ii) Ca, Mg and K are linked to the first component and correlated with Fe-DOC (iii) pH-Na are on one side and SO_4^{2-} on the other side of the third component. The combination between component 2 and 3 (not shown) also maintains the couple Fe-DOC and the anti-correlation between SO_4^{2-} and pH. However the cations Ca, Na and K show a contrasting pattern. Ca is found together with SO_4^{2-}, while Na and K are coupled and anti-correlated with DOC-Fe.

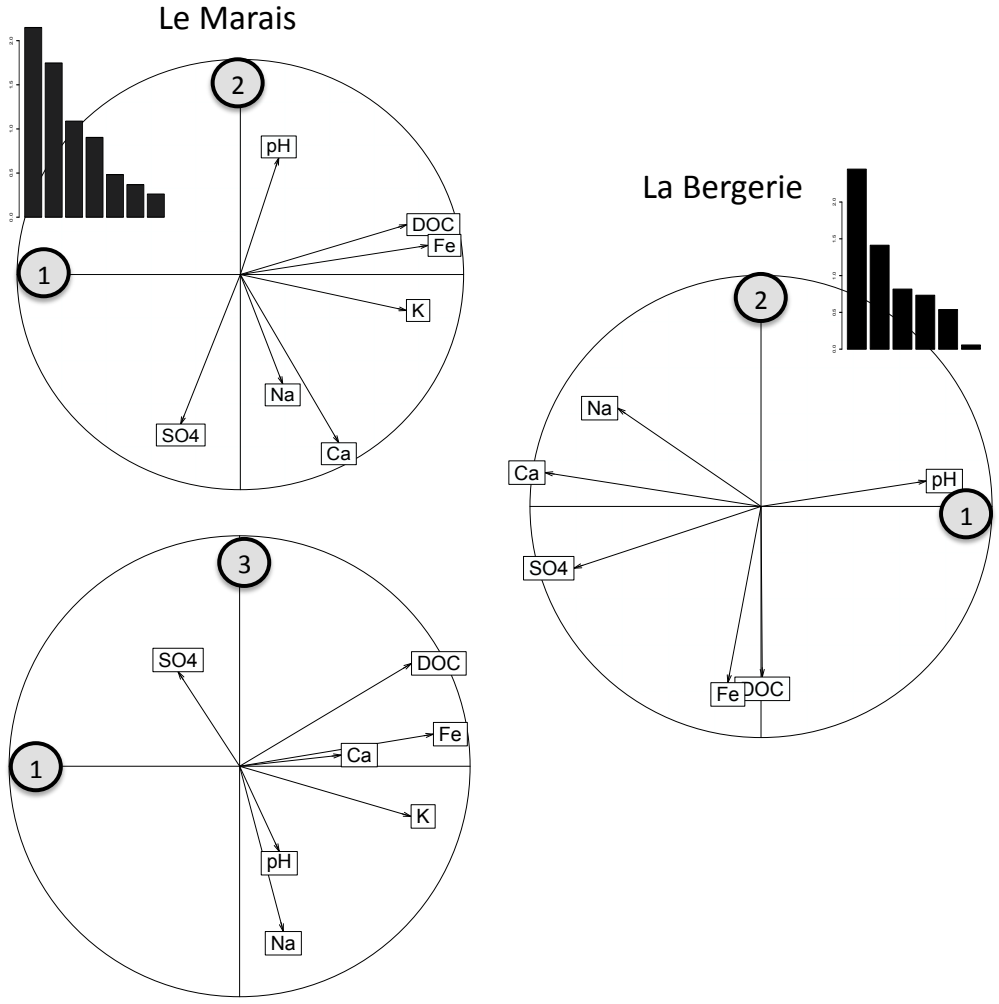

Order of component	Eigenvalue		Explained variance %		**Cumulative variance %**	
	Le Marais	La Bergerie	Le Marais	La Bergerie	**Le Marais**	**La Bergerie**
1	2.14	2.74	30.7	45.6	**30.7**	**45.6**
2	1.74	1.66	24.9	27.7	**55.6**	**73.4**
3	1.08	0.69	15.6	11.4	**71.2**	**84.8**
4	0.90	0.51	12.9	8.5	**84.1**	**93.3**
5	0.48	0.29	6.9	4.8	**91.0**	**98.1**
6	0.36	0.11	5.2	1.9	**96.2**	**100**
7	0.26		3.8		**100**	

Figure 2.1: Scatter of a set of elements plotted as their correlation coefficients between them and the principal components in the unit circle. Data are from the 45 days experiment on pore samples from the middle and the bottom of all the cores from Le Marais (on components 1-2 and 1-3) and La Bergerie (on components 1-2); n=170; the bar plots illustrate the variance expressed on each component

pH and cations

Figure 2.2 shows the pH trend for both peats over the three treatments.

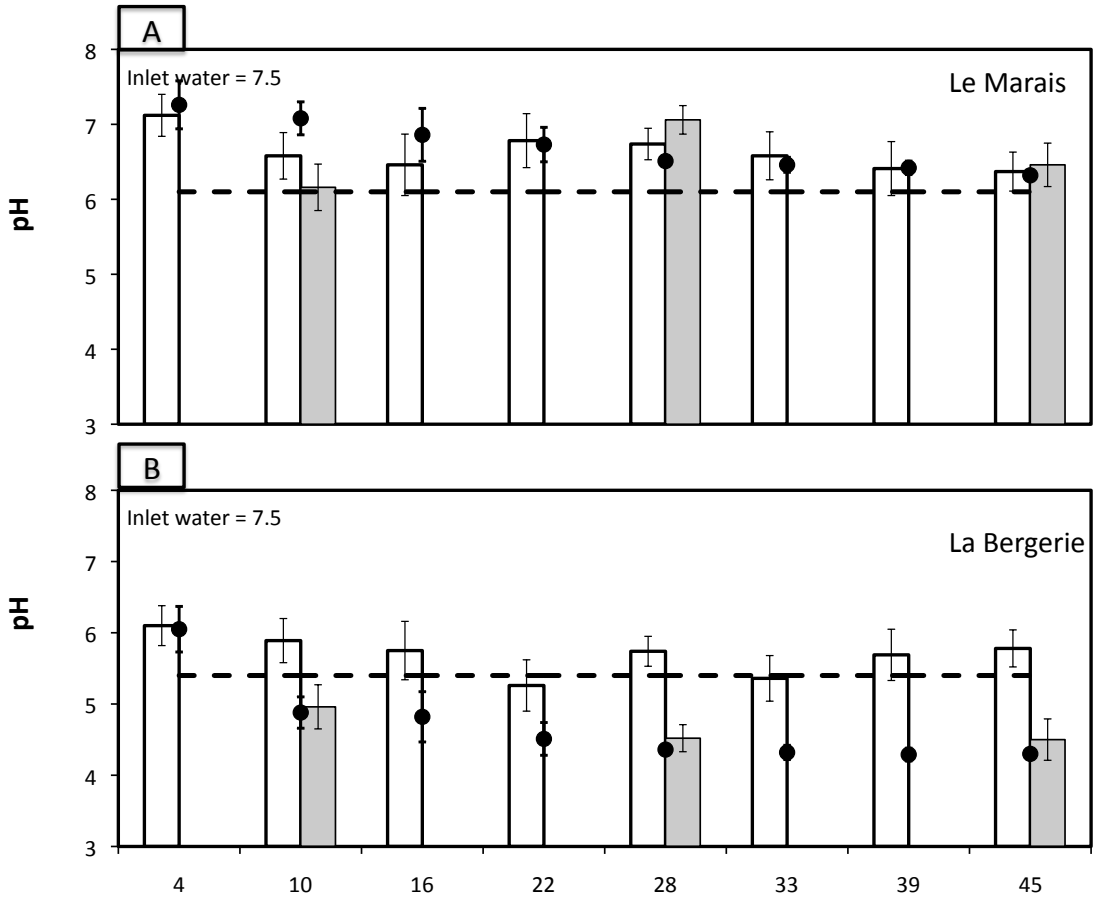

Figure 2.2: Temporal pH in the peat pore water from the middle of the column over the three tested treatments: saturated (black dots), drained-rewetted cycle on a 9 day frequency (grey bars) and drained-rewetted cycle on a 3 day frequency (white bars). The doted line figures the concentration level at the sampling site on sampling day. Error bars are the standard errors, n=4

The cores were all saturated with water at pH 7.5. The pH of the peat pore water was 6.1 (SE: 0.02) in Le Marais and 4.3 (SE: 0.02) in La Bergerie at the end of the experiment in the saturated cores. In the field, the pH below the wetland water tables were also different: 6.1 and 5.4 for Le Marais and La Bergerie respectively at the sampling location and at sampling date. Acidification in La Bergerie is thus important.

Rewetting and draining had contrasting results on pH behaviour between each site. In Le Marais pHs are not significantly different regardless the treatment (see variance analysis in Table D.1 and

Figure D.1 in Appendix D). Meanwhile, in La Bergerie, the saturated and drained-rewetted cycle on a 9 day frequency had similar pHs, approximately 1.4 unit pH lower compared to the drained-rewetted cycle on a 3 day frequency.

Cation behaviour showed contrasting results between the two sites (Table 1.1). While La Bergerie shows a net export of Ca^{2+}, Mg^{2+}, Na^{+}, K^{+} and Fe compared to the inlet concentrations, Le Marais shows net decrease, except for Fe.

Sulphate release

A release of SO_4^{2-} occurred for all the treatments after rewetting with higher concentrations in the peat from La Bergerie (maximum around 400 mg.L^{-}) (Figure 2.3, panel C, D). At the same time NO_3^{-} was always low, below 1.5 mg.L^{-} after 10 days of saturation in both peats (Figure 2.3, panel E, F).

Rewetting and draining had contrasting results on SO_4^{2-} behaviour between each site. In Le Marais SO_4^{2-} concentration were not significantly different regardless the treatment (see variance analysis in Tables D.2 and Figure D.1 in Appendix D). Meanwhile, in La Bergerie, the saturated and drained-rewetted cycle on a 9 day frequency had similar concentrations, approximately doubled compared to the drained-rewetted cycle on a 3 day frequency.

The release dynamics are also different. In Le Marais, the maximum SO_4^{2-} concentration is reached after 3 days, i.e. the short frequency cycle. In La Bergerie, the maximum SO_4^{2-} concentration, i.e. leading to a plateau, is visible only after 10 days. The cycling maintains important NO_3^{-} lowering (the inlet concentration is 37 mg.L^{-}), although after repeated draining (on the 3 days frequency) NO_3^{-} tends to increase relative to the previous cycles.

DOC release

Saturating the cores resulted in the immediate release of DOC (Figure 2.3, panel A, B), with the highest concentrations in peat from Le Marais. Most of the DOC was released within the first 3 days (first sampling date). The time to reach a plateau in DOC concentration in the saturated cores is within approximately 30 days. DOC stabilizes around 120 mg.L^{-1} in Le Marais and around 30 mg.L^{-1} in La Bergerie. Results are similar in the middle and the bottom of the cores.

Rewetting the peat cores after a period of drainage produced again DOC concentrations similar to the first wetting. Only the peat from La Bergerie has decreasing DOC concentrations in the three first rewettings. Afterwards the concentrations did not decline relative to the number of rewettings. A drained-rewetted cycle on a 3 day or a 9 day frequency did not result in significantly different DOC production both in Le Marais and La Bergerie (see variance analysis in Table D.3 and Figure D.1 in Appendix D). Increasing water residence time (seen in the permanently saturated treatment) leads to a maximum DOC level.

To complete DOC characterization, the Specific UV absorbance (SUVA) values are given in Table 1.1. The SUVA values are similar between the two peats (between 3.23 and 3.77; Table 1.1) .

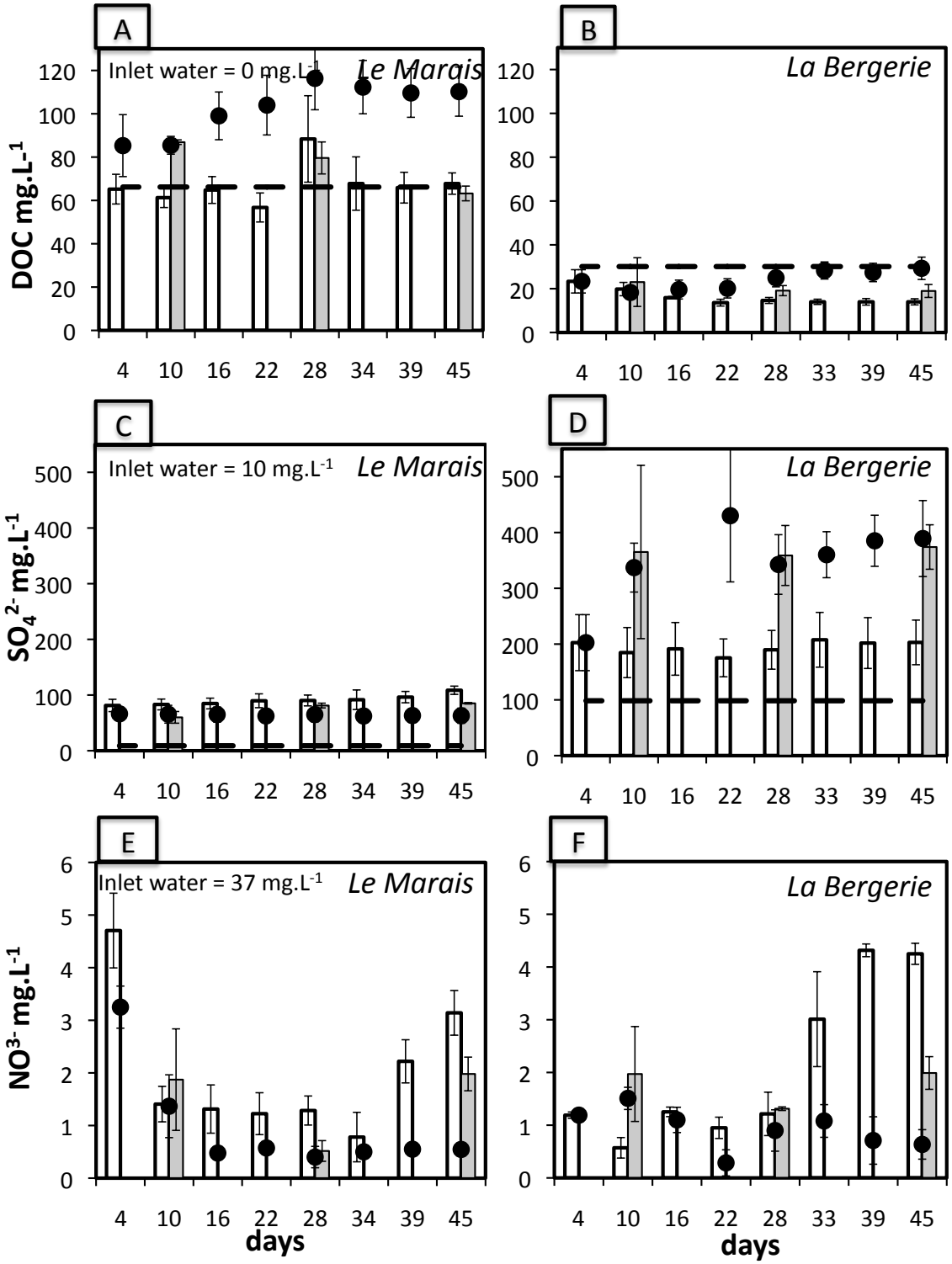

Figure 2.3: Temporal DOC and SO_4^{2-} concentrations in the peat pore water from the middle of the column over the three tested treatments: saturated (black dots), drained-rewetted cycle on a 9 day frequency (grey bars) and drained-rewetted cycle on a 3 day frequency (white bars). The doted line figures the concentration level at the sampling site on sampling day. Error bars are the standard errors, n=4

2.2.2 Biomass

The C biomasses are illustrated in Figure 2.4 for both peats. The results indicate that biomass is globally higher in Le Marais. Regarding the differences between treatments, results suggest that the microbial communities seems to be best adapted to anaerobic conditions in Le Marais as can be seen on the total C biomass content higher in the re-wetted cores relative to the "dry" case. However the active C biomass does not show any distinction between treatments. On the opposite, in La Bergerie, the "dry" conditions favour microbial aerobic grow, both visible in the total and active C content from the "dry" case.

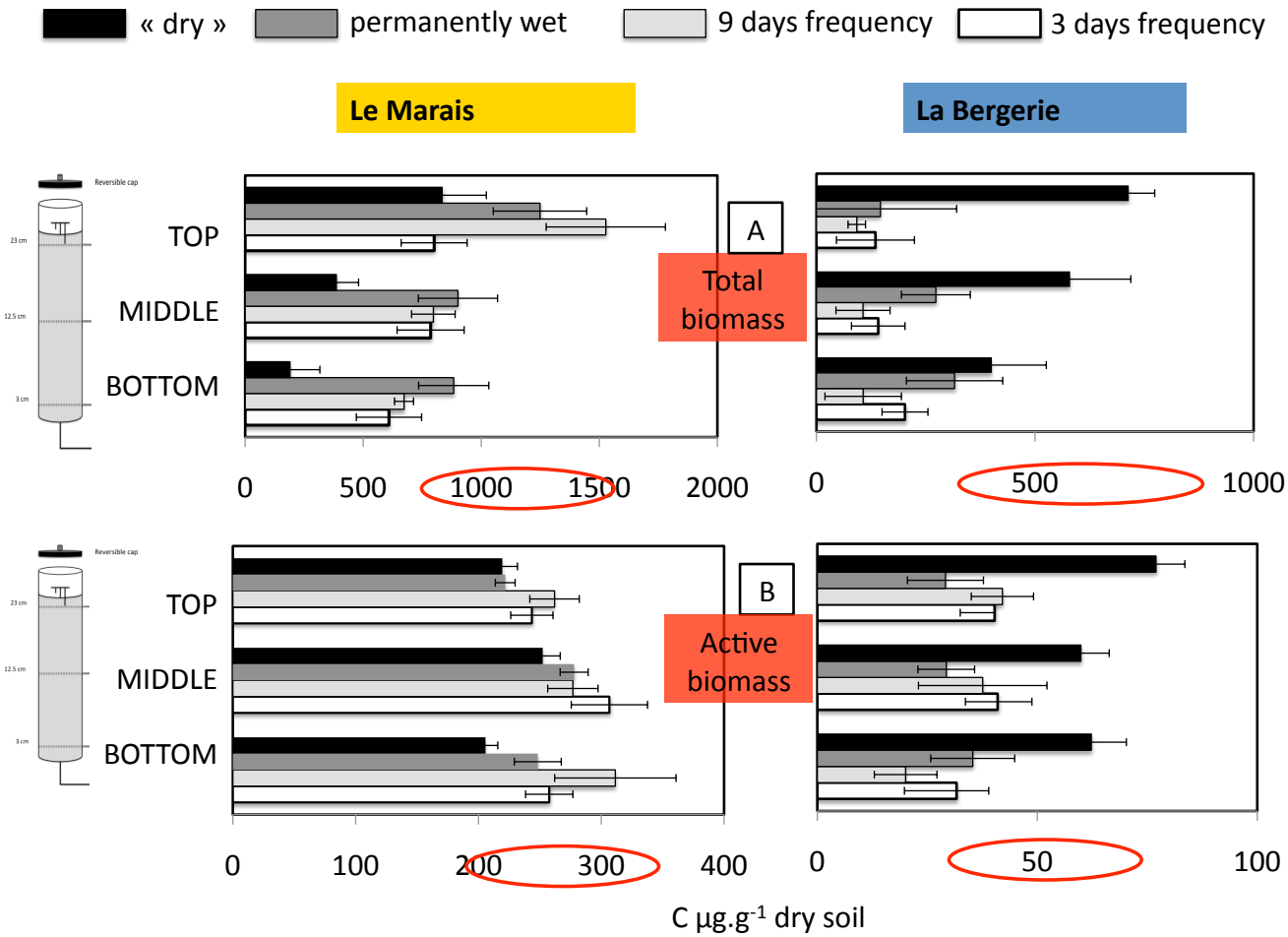

Figure 2.4: Total C biomass by the fumigation-extrcation method (panel A) and active C biomass by the SIR method (panel B) content in the two tested peats after the treatments

2.3 Discussion

2.3.1 Controls on sulphate release: oxidation processes

SO_4^{2-} release occurs in the two peats. The classical explanation is that reduced S compounds that formed during anoxic periods (dominantly FeS_2), are subject to re-oxidation during periods of oxic conditions (Paul et al., 2006a). SO_4^{2-} release is approximately four times greater in La Bergerie. The Principal Component Analysis (Figure 2.1) differentiates the groups SO_4^{2-}-Ca-Mg-Na on one side, and pH on the other side of the first component. As pH and SO_4^{2-} are shown to be strongly anti-correlated on the PCA, the lower pH in this peat pore water appears to be a result of a higher sulphur oxidation to SO_4^{2-} which produces H^+ (Appelo and Postma, 2005). This is also evident on Figures 2.2 and 2.3 where pH and SO_4^{2-} behave in the same anti-correlated way. The peats have similar total S (4.9 $g.kg^{-1}$ dry mass), but S availability to oxidation appears to be significantly different between the two peats. Nutrient and biomass content in peat from La Bergerie (Table **??** and Figure 1.7) clearly indicate a more degraded peat. In addition, a previous study of these peats, revealed differing nitrate reducer communities between the two sites (Bougon et al., 2009). Furthermore, in contrast with Le Marais, cation release is observed in La Bergerie. These results suggest that peat from La Bergerie is highly sensitive to oxidation processes.

Sulphur is involved in many biochemical processes, such as the synthesis of essential amino acids, proteins, and enzymes. It exists in soils in organic and inorganic forms in various oxidation states, ranging from -2 to +6. Sulphur speciation in peatlands have been documented in several studies. Wet-chemical methods based on sequential extraction of S fractions have already highlighted the large predominance of organic sulphur (Krairapanond et al., 1992) (Wieder and Lang, 1988a). Newly developed methods based on X-ray absorption have significantly improved the speciation. Fast sulphur turnover in peatlands is highly dominated by pyrite but ester sulfates may also contribute to SO_4^{2-} production in alternating oxidation-reduction cycles (Prietzel et al., 2009). These organic and inorganic contributions are discussed below.

Pyrite as a source of sulphuric acid In the experiment, Fe and S can be assumed to be correlated, as pore water Fe and SO_4^{2-} in La Bergerie are also approximately four times higher than in Le Marais. This suggests that a major part of Fe and SO_4^{2-} concentrations are the result of the oxidation of inorganic iron sulphur containing minerals, most likely pyrite FeS_2. Iron sulphur containing minerals (as well as elemental S) are known to be the most dynamic S constituents of peat (Wieder and Lang, 1988b). However, SO_4^{2-} and Fe are not coupled in the PCA, rather Fe is coupled to DOC suggesting that part of the Fe is then bounded to DOC in colloidal form (Grybos et al., 2009).

Pyrite accumulates in waterlogged soils where there is a supply of easily decomposed organic matter (Appelo and Postma, 2005). Bacteria, breaking down this organic matter under anaerobic conditions, reduce dissolved sulphate ions to sulphides and Fe(III) oxides to Fe(II). Pyrite is the stable end-product of these reactions, as long as anaerobic conditions are maintained. Peats from La Bergerie and Le Marais have similar total Fe and S content and have likely accumulated pyrite under similar anaerobic conditions over long time scales in the field.

Oxygen entering the soil oxidises pyrite, generating sulphuric acid. Overall, the oxidation of pyrite can be represented by Figure 2.5. The reaction of pyrite with oxygen is a slow process, but

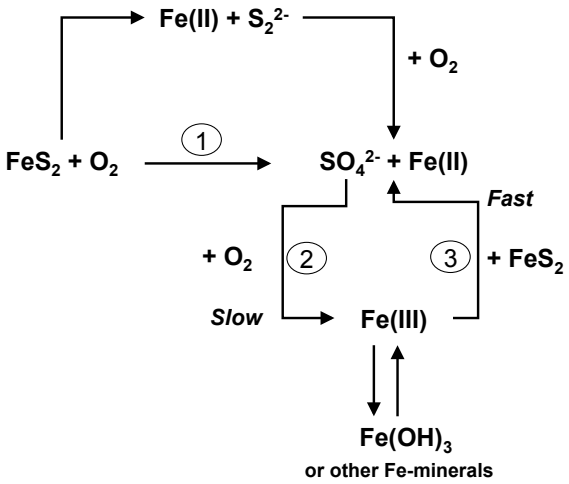

Figure 2.5: Reaction pathways in the oxidation of pyrite (after Stumm and Morgan, 1996)

pyrite is rapidly oxidised by Fe(III) in solution. Fe(III) is thereby reduced to Fe(II), but Fe(III) is then regenerated from Fe(II) by the bacteria *Thiobacillus ferrooxidans*. This catalytic oxidation of pyrite can take place only at pH less than 4, because Fe(III) is soluble only under these very acid conditions. In our experiment, La Bergerie releases a large amount of SO_4^{2-} and Fe, suggesting that pyrite oxidation may be explained by higher pyrite availability. In other words, greater degradation of the surfaces of pyrite minerals, rather than the total content, is the key factor responsible for the greater release of Fe, SO_4^{2-} and H^+ ions in La Bergerie. Indeed several studies have emphasized that iron-sulfide-like minerals, rather than crystalline pyrite-like compounds, are able to function as electron donors (Haaijer et al., 2007). In addition, pH is around 4 or even lower in La Bergerie, suggesting that the catalytic pyrite oxidation by Fe(III) takes place, resulting in even higher acidification.

Potential contribution of organic sulphur It is well known that the primary source of sulphur in freshwater peats is organic bounded sulphur (as ester sulphates or carbon-bounded S) which represents generally more than 70 % of total S (Krairapanond et al., 1991). Ester-sulphates are preferentially mineralized relative to carbon-bounded sulphur (Chapman, 2001). Prietzel et al 2009 (Prietzel et al., 2009) showed that the relative contribution of organic ester sulphates to the total S pool was higher in peat subjected to alternating oxidation-reduction cycles, relative to permanently wet peat. Thus, even if the fast S turnover is in the inorganic form through pyrite dissolution, organic ester sulphates may also contribute to S release, notably in the more degraded peat from La Bergerie. On the

other hand, the activity of the enzyme involved in ester linkage cleaving and release (arylsulphatases) is known to be inhibited by microbial biomass activity (Freeman et al., 1996) (Williams et al., 2000). This mechanism may partly explain a less available organic sulphur pool to be oxidized in Le Marais.

As a summary, the nutrients turnover in these peats seems to be highly influenced by the overall organic matter state. A more degraded peat seems to make more pyrite available for oxidation and eventually organic ester sulphates. Consequently, high release of SO_4^{2-} results in drastic acidification, which in turn enhances cation leakage.

2.3.2 Controls on DOC release: pH control

pH appears to have a major role in the release of DOC. pH reaches a lower value in La Bergerie: 4.3 compared to 6.1 in Le Marais. We suggest that this pH difference is only an indirect consequence for the rate of degradation of the peat, as previously explained by the sulphate release mechanisms (Coulson and Butterfield, 1978). pH is known to have a significant control on DOC solubility and sorption and consequently on metal complexation to organic matter (Grybos et al., 2009).

Both peats highlight a chaining mechanism which may be described as follow:

1. a pH rise, resulting from the peat wetting by water having a pH of 7.5, increases negative charges within the carboxylic or phenolic groups, leading to more hydrophilic organic carbon, i.e. higher DOC solubility (Reddy and Delaune, 2008). Indeed, both peats produce DOC when rewetted.

2. the concomitant SO_4^{2-} release by oxidation counteracts the pH rise, resulting in a pH decrease ending at 6.1 in Le Marais and 4.3 in La Bergerie. This difference in pH explains the difference in DOC concentrations, i.e. DOC is approximately 3 times higher in Le Marais, relative to La Bergerie.

3. the produced DOC enhances Fe^{2+} and slightly Ca^{2+} and Mg^{2+}) binding (Skyllberg and Magnusson, 1995), at least in Le Marais where balance between inlet and outlet in the peat pore water, after 45 days, shows a net bi-valent cation decrease (Table 1.1). By contrast, La Bergerie shows net cation release.

Finally, the organic matter aromaticity, reflected by the SUVA values around 3.5, is similar, which likely reflects a similar DOC composition in each peat. SUVA does not provide information about reactivity of DOC derived from different types of source materials (Weishaar et al., 2003). However, the value of 3.5 indicates more fulvic dominated acids, i.e. complexing molecules rather than metabolites (Ghabbour and Davies, 2005).

As a conclusion, the different behaviours between the two peats emphasize contrasting neutralising capacities. Commonly, the acid-neutralising capacity is provided by carbonates, exchangeable bases and easily-weatherable silicates (Dent, 1986). In this peats, carbonate dissolution does not seem to mainly contribute to the neutralizing capacity, as no linear correlation is observed (data not shown). The neutralising capacity seems to be mainly controlled by the exchangeable bases. In La Bergerie, the overall peat degradation state may notably decrease the exchangeable bases.

2.3.3 Peat sensitivity to draining-rewetting cycles

The draining-rewetting experiment was intended to study the peat sensitivity to rapid changes in water recharge quality.

Regarding SO_4^{2-} behaviour, it is evident that SO_4^{2-} release is impacted by the cycle frequency in La Bergerie, but not in Le Marais (for statistical significance see Table D.2 and Figure D.1 in Appendix D). In La Bergerie, SO_4^{2-} concentration is lower on a 3 day drained-rewetted frequency (Figure 2.3 C, D), while rewetting every 9 days or permanently wetting give similar higher concentrations. These differences are reflected in the pH values, which show similar trends (Figure 2.2 B). It appears that the dramatic pH decrease in La Bergerie gradually reaches its minimum value after 9 days, while in Le Marais stable conditions are reached after just 3 days. This may imply that the impacted peat from La Bergerie is more sensitive to fast water pulses. In addition, it is interesting to note that repeated rewettings result in similar SO_4^{2-} productions, from one rewetting to the other. Indeed, a leaching process (i.e. exponential decrease) may have been expected from these peat cores collected in the unsaturated zone, which is not observed. This suggest that the sulphur pool available to oxidation is not contracting even after 8 rewettings (for the 3 day frequency). In a recent study focusing on the impact of experimental drought and rewetting on redox transformations, Knorr et al (Knorr and Blodau, 2009) emphasize that it is not well known to what extent and at what time scale electron acceptors responsible for S turnover, are renewed and consumed during such events in peatland soils. Their incubation study suggest that the sulphate pool turns over in less than a day. In an other study, Paul and al (Paul et al., 2006b) showed that sulphur and iron constituents can provide electron accepting capacity for weeks to months if all oxidized species are reduced. Our results also suggest a rapid recycling mechanism. However, a detailed characterisation of sulphur species may be needed to confirm this assumption.

With respect to DOC behaviour, both peats are similarly impacted by the cycle frequency: the permanently saturated peats reach a maximum plateau concentration after approximately 28 days, while the 9- and 3-day cycles produce similar lower DOC level from one rewetting to the other. By contrast with the fast pyrite oxidation reactions, it appears that DOC kinetic solubilization is slower. Repeated rewetting results in similar DOC productions throughout the experiment, suggesting that like sulphur, carbon availability to solubilization is not limiting in the present experimental conditions. As a conclusion, although DOC kinetic solubilization is slower, repeated rewettings on both peats highly contribute to DOC export from the catchment.

Regarding NO_3^- behaviour, the kinetic reduction is fast in both peats. Draining and rewetting maintains reducing conditions, but repeated cycles (on the 3 day frequency) show that the reducing rate decreases (Figure (Figure 2.3 E, F). Although several studies have shown that denitrifying communities are well adapted to fluctuating redox conditions (Knorr et al., 2009) (Blodau and Moore, 2003), this might imply that the microbial community structure starts to loss its high adaptation capacity in extreme repeated fluctuation conditions.

2.3.4 Field implication

The results discussed in this paper correlate well with field observations made by Auterives et al (Auterives, 2006): e.g. peaks of SO_4^{2-} and Ca^{2+} were correlated with acidity increase after water level

rise and were more intense in the ”pumping site”. The study confirms that organic matter quality is a key control on peat sensitivity to environmental changes such as changing water recharge quality or oxidation state (Bauer, 2004). Indeed, the peat quality of the two studied sites differs, notably by their nutrient and biomass content. Biomass is expected to respond to relative rapid disturbances in the peat environment. Therefore we argue that the difference in peat quality between the two sites may be related to the different hydrological constraints experienced in the field. It is likely that 20 years of enhanced downward flow has contributed to degradation of the peat material in La Bergerie (Auterives et al., 2011). This downward flow is expected to bring more oxygenated waters into the peat, and thus enhance oxidizing processes. As an overall conclusion, long term aerobic conditions, even without extreme drying, has an important impact on peat biodegradation, and more globally on the ecosystem, by enhanced nutrient release and acidification.

The rewetting cycles performed in our experiments are analogous to highly fluctuating water tables in the field. The results confirm that, while anaerobic conditions must be favoured in peatland management, regular small water table fluctuations do not disturb the peat functioning, as a nutrient transformer. These results agree with nowadays guidelines on peatland restoration which favour dynamic water level fluctuations (Mitsch et al., 2005). Indeed, flowing conditions and flooding pulses enhance primary productivity and other ecosystem functions (which are depressed by stagnant conditions) like renewing materials (including toxic accumulation), energy and biota. Although some degree of water table fluctuation is beneficial, this study also shows that when levels of oxidation increase beyond a certain threshold, the cycling of chemical species such as Fe and S can be drastically altered.

Conclusion

The study highlights the chemical processes involved in peatlands, focusing on sulphate and DOC release. Two peats undergoing different hydrological flows in the field - a site impacted by pumping of an underlying aquifer and an undisturbed site - were subjected to short periods of saturation and draining in a laboratory experiment. The study confirms that peat quality is a key control on its sensitivity to environmental changes such as changing water recharge quality or aeration status. The nutrients turnover in these peats is highly influenced by the organic matter state. A more degraded peat, with lower nutrient and biomass content, is more sensitive to oxidation processes. The higher sulphate release in the ”pumping site” may be explained by higher pyrite availability, i.e. the degradation state of pyrite, instead of the total content, may be the key factor. Release of sulphate results in acidification which in turn enhances cation leakage and a decrease in DOC solubility. The draining-rewetting experiment emphasizes the difference in S availability to oxidation. In the undisturbed peat, a 3 or 9 day draining-rewetting frequency or permanently saturated cores produce similar sulphate concentrations, while in the impacted peat, increasing the residence time of water leads to increasing sulphate release resulting in increasing acidity. This suggest that the impacted site is more sensitive to rapid changes. The buffering capacity of the peat, i.e. its efficiency to counteract environmental changes, is thus less maintained where peat is more degraded.

The peats differ mainly by their biomass. Biomass is expected to respond to relative rapid disturbances in the peat environment. Therefore we argue that the difference in peat quality between the

two sites may be related to the different hydrological constraints experienced in the field. It is likely that 20 years of enhanced downward flow has contributed to degradation of the peat material. This downward flow is expected to bring more oxygenated waters into the peat, and thus enhance oxidizing processes. Information provided by this study may therefore be of relevance to the management of wetlands. Of major concern are the well extraction locations in order to optimize peat conservation and the potential impacts of climate change.

Chapter 3

Biochemical peat response to repeated draining and re-wetting cycles

In this part, full results from the experiment with peat cores from the reference site "Le Marais", already presented in Chapter 2 Part II, are presented. The interpretation goes deeper in the potential impacts of repeated wettings and drainages, compared to permanently saturated and non saturated conditions. The vertical conditions in the cores are also investigated.

3.1 Materials and methods

This chapter is based on the same experiments than the previous chapter and we decided to avoid the duplication of the Materials and Method section. Please refer to the general Materials and Methods section of Chapter 1 in this Part II.

3.2 Results

3.2.1 Relationship between elements and sample distribution

A Principal Component Analysis (PCA) was carried out on the peat pore water data from the 3 levels inside the cores and on the drained water. Figure 3.1 plots the PCA results for the middle core samples. Major part of the variables variance (Panel A) is explained by [SO_4^{2-};Ca^{2+}; Mg^{2+}; Mn^{2+}; Zn^{2+}; Al^{3+}; N-NH_4] on one side of the first component, and [pH] on the other side. On the second component, variance is mostly explained by [Fe or Fe^{2+} and DOC] on one side and NO_3^- on the other side. The main involved reactions were already presented in chapter 2. They indicate especially a significant acidification related to oxidation processes. Regarding the samples distribution (Panel B and C), most of the cores subjected to draining-rewetting cycles are together around the PCA centre. Specific samples from the 3 days frequency cycle plot more on the left and top sides, towards the pH pole and the Fe or Fe^{2+} and DOC pole. Most of the permanently saturated cores are together towards the [SO_4^{2-};Ca^{2+}; Mg^{2+}, etc...] pole. It can be noted that, in a given core, top, middle and bottom peat pore water exhibit different concentrations showing a classical redox gradient (see Figure 3.2). They

result however in a similar distribution in the PCA. The drained water also results in a similar variable distribution, but no group trends are highlighted relative to the tested treatments (PCAs not shown).

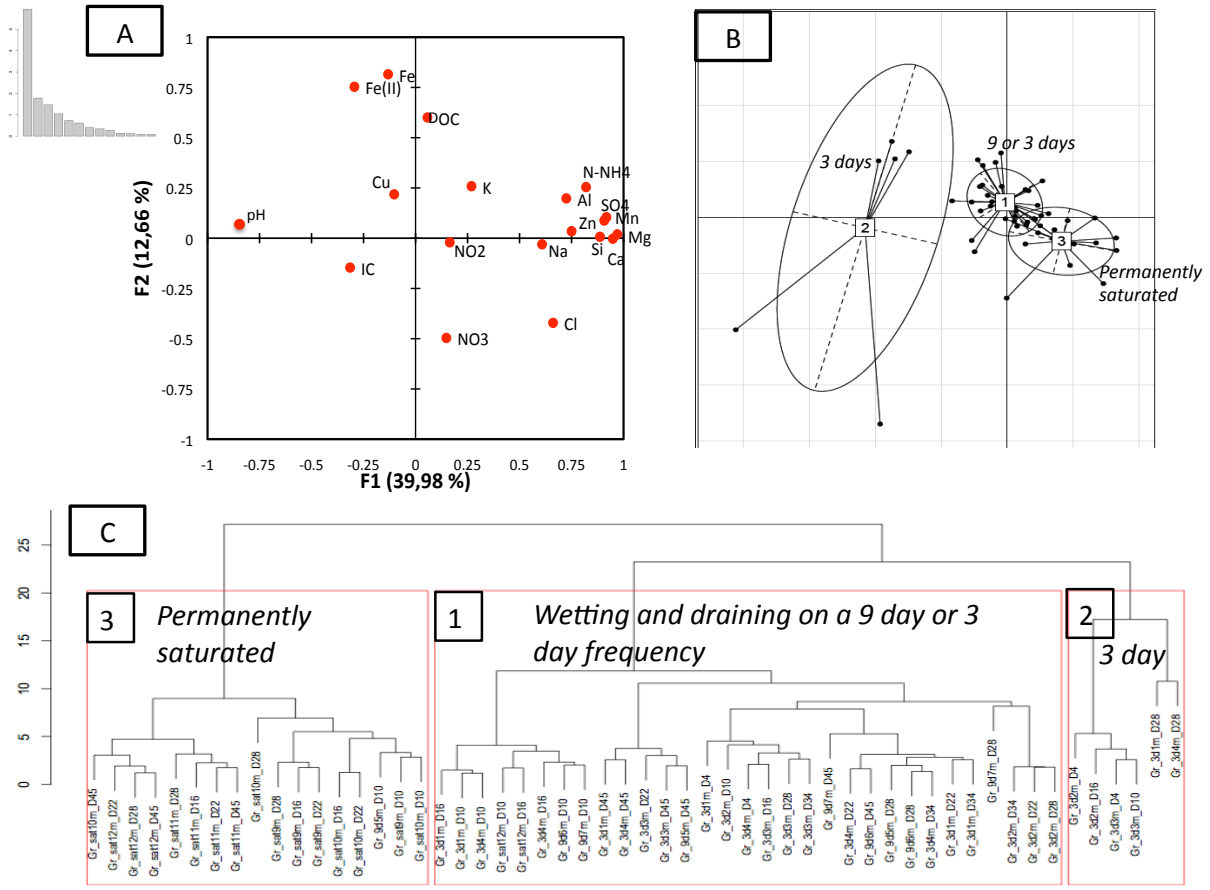

Figure 3.1: Graphical representation of the PCA analysis on the peat pore water data from the middle of the cores. Panel A: variables plotted on components 1 and 2; Panel B: related samples distribution; Panel C: related ward dendogram

3.2.2 Behaviour of the redox-sensitive elements

The tested treatments, by renewing the water inlet at a 3 day or 9 day frequency, relative to a permanently saturated case, are expected to impact the redox environment. Figure 3.2 illustrates the temporal trends of three redox-sensitive elements (NO_3^-, SO_4^{2-} and Fe^{2+}) relative to the tested treatments. The top, the middle, the bottom and the drained water are illustrated.

Regarding the vertical behaviours of these three elements, a redox gradient appears from oxic to more anoxic conditions, in both three treatments. For example, SO_4^{2-} is relatively high in the top and quite lower in the bottom.

Regarding the differences between treatments, it appears that the permanently saturated cores evolve towards a more anoxic environment (especially noticeable on the SO_4^{2-} concentration trends), while the fluctuating treatments maintain more oxic conditions. On the other hand, the drained water, which integrates the chemical "signature" of the entire column, clearly shows a different picture between treatments on the NO_3^- behaviour. The NO_3^- temporal trend shows higher concentrations in the fluctuating treatments.

Finally, regarding the impact of repeated saturations and drainages within the 9 days or 3 days frequency, it seems that the peat maintains a good ability to reproduce similar concentrations from one rewetting to the other. Except for NO_3^-, which concentration seems to gradually increase from one rewetting to the other in the top for the 9 days and 3 days frequency cycle, and in the drained water for the 9 days frequency cycle.

3.2.3 Nutrient cycling: import and export

The cumulative concentrations computed for the three treatments are plotted on Figure 3.3 for NO_3^-, SO_4^{2-}, DOC and Ca^{2+}. The vertical profiles as well as the drained water are reported. From this Figure it appears that the peat maintains a good ability to consume or produce nutrients even under repeated rewetting and draining cycles. A good proportionality is maintained relative to the number of repeated rewettings for most of the nutrients (on Figure 3.3 see the numbers on each bars which are the mean concentrations consumed or produced per rewetting, i.e. total concentration divided by the number of cycles). However an evolution can be seen for SO_4^{2-} and DOC concentrations relative to one rewetting. For the middle part of the column (the trend is similar for the top, bottom and drained concentrations), SO_4^{2-} increases from 52 to 67 and 79 mg/L ($\pm$14 mg/L) for the permanently saturated, 9 days and 3 days frequency, respectively. Regarding the DOC, the concentrations decrease from 110 to 77 and 67 mg/L ($\pm$11 mg/L), for the permanently saturated, 9 days and 3 days frequency, respectively.

3.2.4 Biomass and CO_2

Results from the biomass analysis at the end of the experiment are illustrated in Figure 3.4, panel A for the top, middle and bottom sampled peat cores, and for the four tested treatments. The C microbial biomass is lower in the permanently dry cores, and decreases from top to bottom. The rewetting treatments are not distinguished, both between treatments and within the vertical profile. The C active biomass is approximately 3 times lower than the total C microbial biomass. In addition, no differences between treatments are noticed.

Results from the entire CO_2 column incubation are presented in Figure 3.4, panel B. Note that CO_2 rates are converted to equivalent C production. The permanently dry cores show higher respiration rates, while the rewetting treatments do not show clear differences except that the short and frequent rewetting cycle (3 days) seems to produce more CO_2. Finally, it can be noticed that the equivalent C production from this CO_2 analytical method is much lower than the values reached in the "active biomass method".

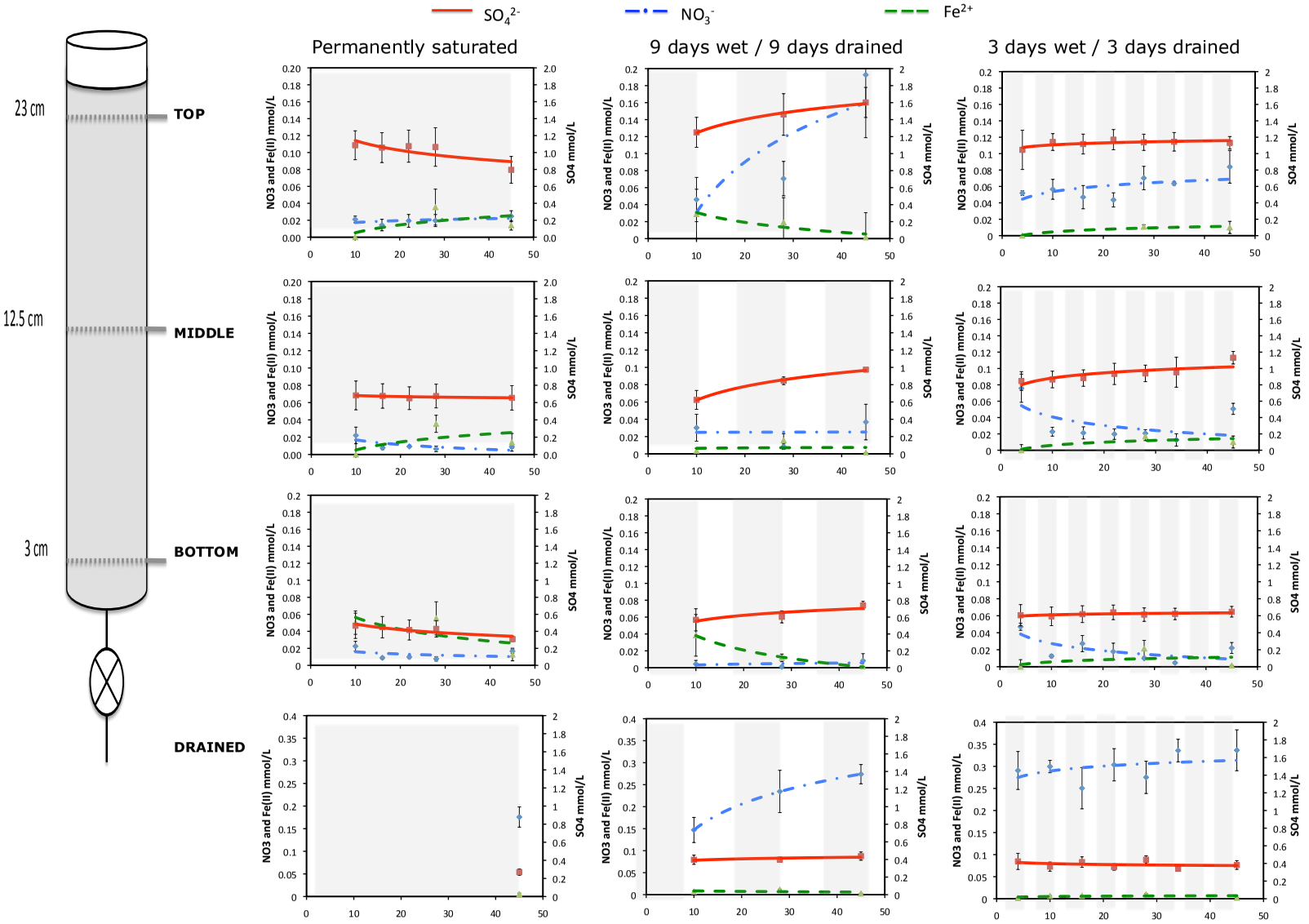

Figure 3.2: Temporal trends of three redox-sensitive elements (NO_3^-, SO_4^{2-} and Fe^{2+}) relative to the tested treatments n=4. The vertical distribution is illustrated by the top, middle and bottom peat pore water. The drained water is illustrated in the bottom graphs.

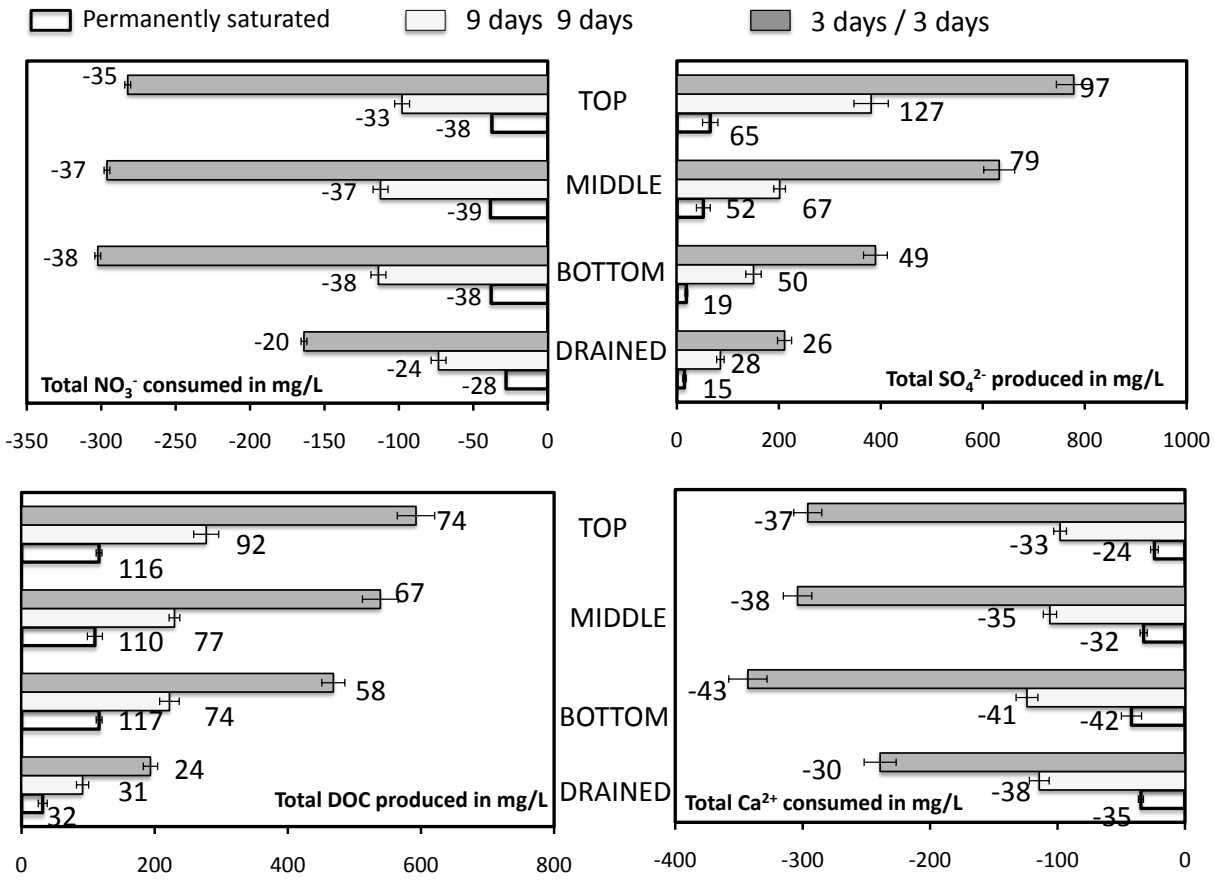

Figure 3.3: Illustrative bar diagram plotting the total nutrient turnover along the three tested treatments for NO_3^-, SO_4^{2-}, DOC and Ca^{2+}. The vertical distribution is illustrated by the top, middle and bottom peat pore water. The drained water is also illustrated. Errors bars are on four replicates. The numbers on each bar are the computed mean consumed or produced concentrations per rewetting (total concentration divided by the number of rewettings)

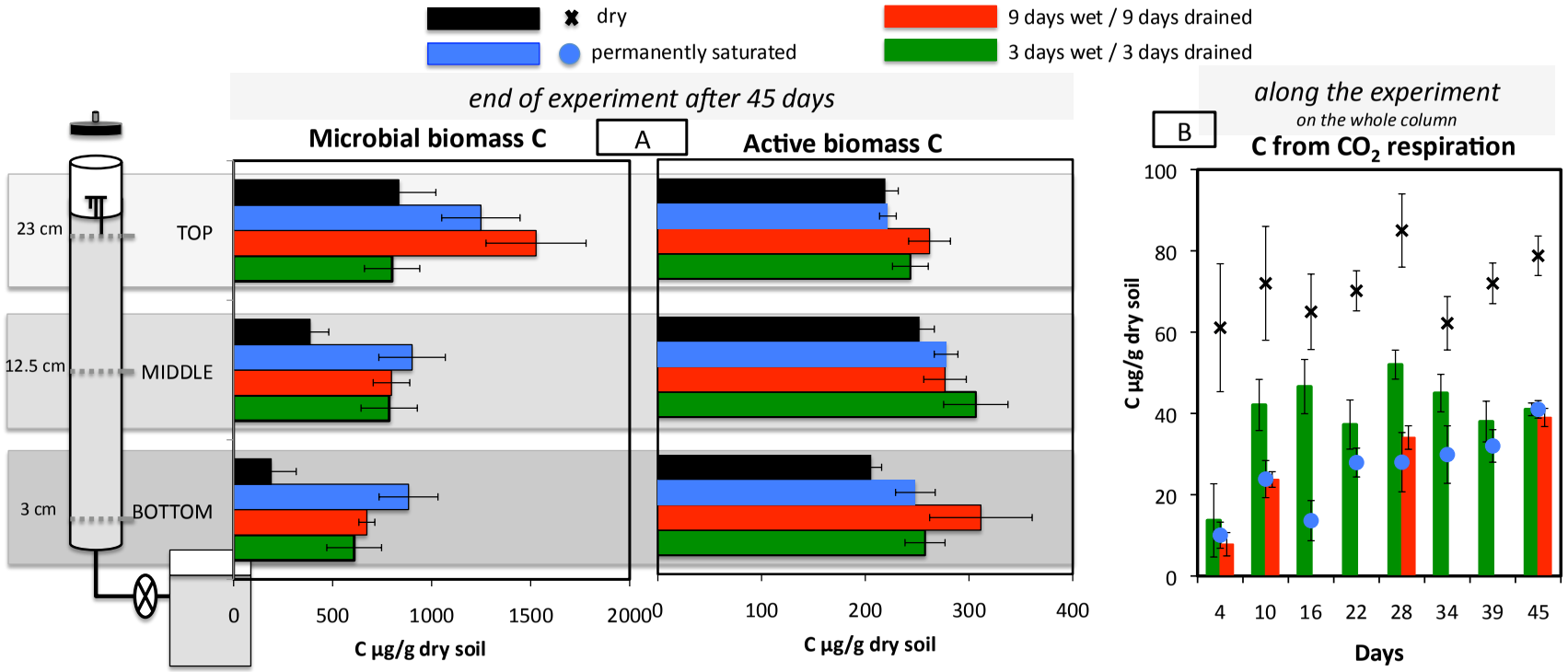

Figure 3.4: Panel A: illustrative diagram of the C microbial biomass (measured by fumigation-extraction method) and the C active biomass (measured by substrate induced respiration method) at the end of the 45 days experiment for the four tested treatments. Panel B: temporal trend of CO_2 respiration (converted to equivalent C) along the experiment four the four tested treatments. Bar errors on all diagrams are on four replicates.

3.3 Discussion

3.3.1 Overall treatment impact

The experiment shows the development of conditions that are close to the field ones (Auterives, 2006). A vertical redox gradient develops throughout the cores. The top of the cores equilibrates with the atmosphere which provides an oxygen source. It shows more oxidizing conditions when compared to the middle and the bottom parts. Deeper in the core, more reducing conditions are characterized by NO_3^- decrease and Fe^{2+} increase. Figure 3.5 shows how the vertical gradient correlates with the classical redox reaction sequence. Although the cores were collected below the top soil, the relative equilibrium with atmosphere is rapidly obtained while the rest of the core maintains highly reducing conditions throughout the experiment, despite the water level fluctuation. Within the deeper part of the core, peat clearly acts as a biogeochemical reactor with an efficient and extremely rapid O_2 consumption and NO_3^- reduction. The Fe increase and the SO_4^{2-} reduction also show the significant capacity of the peat medium, i.e. the microbial communities, to develop or maintain highly reducing conditions. The cycles do not modify this capacity. Although a large part of the water is renewed, the reducing conditions are always maintained except in the upper part of the column which is permanently exchanging with the atmosphere. As observed in Figure 3.3, the 3 days cycle allows very significant amounts of NO_3^- to be consumed.

3.3.2 Treatment impact on the redox reactions and the nutrient cycling

As a overall overview on the whole set of collected chemical data, the PCA shows that the saturated cores are distinguished from the "fluctuating cores". A small group of "3 days frequency treatment" (group 2 in the panels B and C from Figure 3.1) indicates that the "fluctuating cores" progressively evolved during the experiments, particularly the 3 days frequency. This is confirmed by the mean concentration comparison related to one rewetting (Figure 3.3). It however appears from the results illustrated in Figures 3.2 and 3.3, that the peat maintains a good ability to reproduce similar redox reactions and nutrient turnover, even under relatively rapid water fluctuations. The results confirm that regular small water table fluctuations do not disturb the peat functioning. If one considers the peat as a nutrient transformer reactor (analogous to constructed waste water treating wetlands), a dynamic fluctuating water level favours primary productivity and other ecosystem functions (which are depressed by stagnant conditions) like renewing materials (including toxic accumulation), energy and biota. The experiment can be interpreted in light of the cycle frequency that may occur in field conditions. If the 3 days cycle is considered as an analogue to the day/night cycle, it seems that the impact would be limited, especially because the amplitude of the day/night cycle (less than 10 cm) is more limited than the experiment amplitude (30 cm). However, as such cycles are repeated every 24 hours, the cumulative impact might be significant at the scale of the year. Furthermore, if water level variations induced by precipitation are integrated to this effect, the whole rapid water level variations throughout the year may clearly impact the peat functioning. These variations enhance nutrient recycling, as for example seen in the 3 days experiment for NO_3^-. On the opposite, if only one stable water level is maintained, the nutrient turnover is limited.

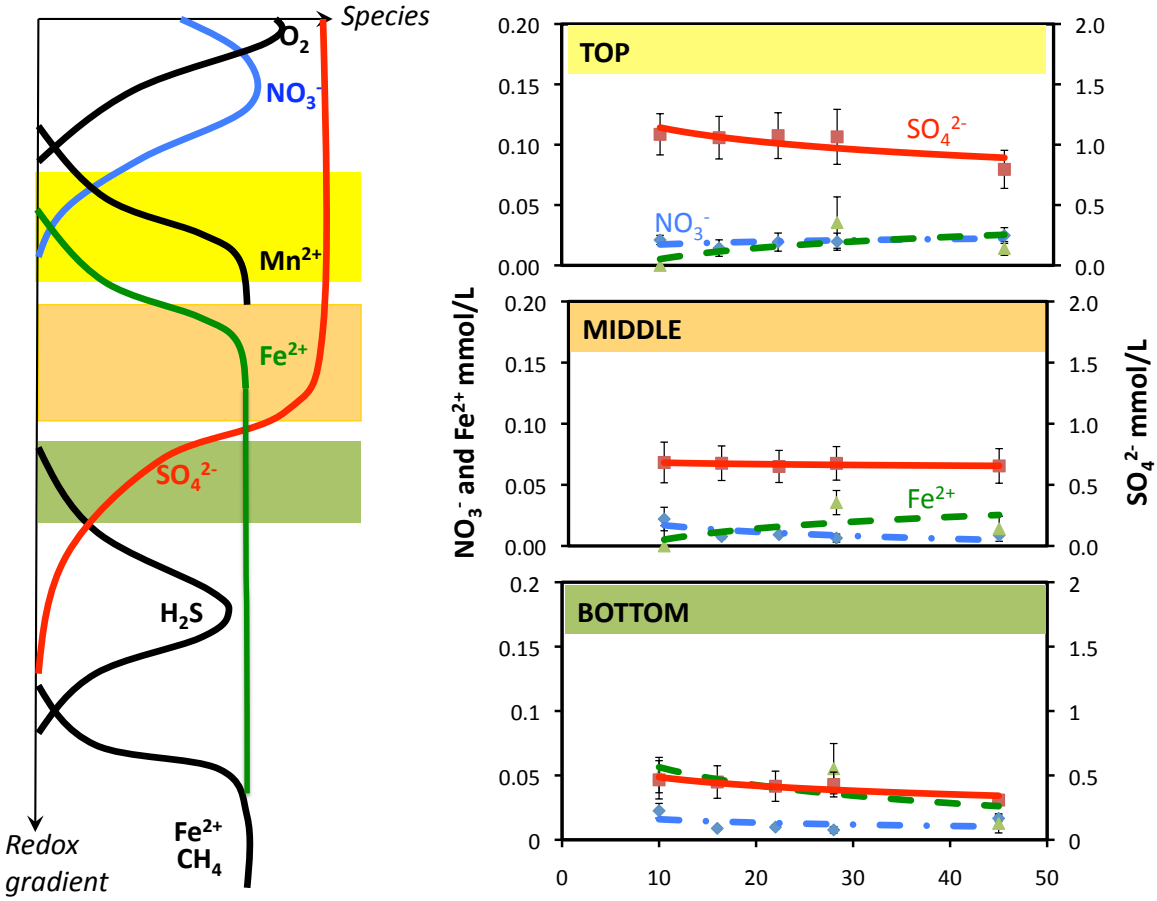

Figure 3.5: Illustrative diagram showing the good agreement between the vertical gradient of redox sensitive elements and the classical redox sequencing

3.3.3 Treatment impact on the microbial communities

It appears that in this peat, re-saturating the cores with groundwater inhibits the CO_2 respiration rate, relative to the pristine conditions (the "dry" cores). This may be explained by a solubility effect, i.e. produced CO_2 is "trapped" into the free water saturating the cores. On the other hand, the highly fluctuating treatment (3 days) produces some more CO_2 relative to the other rewetting treatments, suggesting that microbial communities are more activated.

On the opposite, the non discrimination between treatments on the active C biomass measurements (by the substrate induced respiration method), especially on the dry cores, may be related to the method. Indeed, this method is indirect, relative to the direct CO_2 measurement on the entire column, which does not disturb the cores. In other words, the potential variability between treatments is hidden by the method itself. However, it seems that the fluctuating treatments do not affect the active biomass suggesting that fluctuating conditions do not alter the microbial communities.

Finally, the total C microbial biomass shows a reversed trend, compared to the CO_2 respiration rate. It appears that the "dry" pristine cores are depleted in biomass and that anaerobic conditions favour biomass. It can be suggested that the original microbial community, present in this peat, is best adapted to an anaerobic environment. In addition, the total biomass is somewhat higher in the top of the cores which may indicate that an aerobic community develops but can not be maintained with time. This result is further confirmed by the desiccation experiment in Part III.

3.3.4 Effect of peat heterogeneity

As seen in Figure 3.2, a major difference is observed between the peat water in the pores (top, middle and bottom measurements) and the drained water, although these waters are extracted from the same core, at the same moment. In the drained water NO_3^- concentrations are higher and Fe^{2+} concentrations are lower. Only the SO_4^{2-} shows intermediate concentrations compared to the pore water. The drained water does not reach as reducing conditions than the pore water. The difference between drained and pore water is interpreted as reflecting the peat heterogeneity. The drained water represents the water which has the highest freedom degree in the peat, in other words it is less bounded to the peat pore-structure. It may represent either large pores or various heterogeneous voids. Analogous to the soil structure, it can be considered as the macro-porosity in a double-porosity concept (Simunek et al., 2003). This might be due to preferential flow phenomena, as already observed by (Lischeid et al., 2007). This has substantial implications for assessing, e.g., the dentrification capacity of wetlands. Within such structures, the water/peat surface ratio is much higher than in the micro-porosity, which explains the relatively slower chemical evolution and the less reducing conditions. As SO_4^{2-} is mainly explained by pyrite oxidation, the production is also limited if the water/peat surface ratio is low. Consequently, the pore water concentrations reflect the micro-porosity which can be considered as the "heart" of the biogeochemical reactor. However this water evolves towards slightly more oxidizing conditions in the alternating aerobic/anaerobic treatments (seen on the SO_4^{2-} concentrations), suggesting that the repeated rewettings and drainages progressively favour the "free" water in the macro-pores to impact the inner pore water.

Conclusion

Within this experiment, the effect of rapidly fluctuating water tables in peat was tested. Peat cores were collected on field and the water level was controlled in order to induce 3 days and 9 days cycles of drainages and rewettings.

The study highlights that rapid alternating aerobic/anaerobic cycles do not (or slightly) alter the peat functioning: a rapid redox gradient is established. In addition, regular small water level fluctuations (analogue to diurnal or short increases or decreases of the water table) favour nutrient cycling. In other words, the relatively highly moving unsaturated zone is a dynamic biochemical reactor. The fluctuations do not alter the biochemical functioning, however the frequent rewettings induce some more oxidizing conditions. Regarding the microbial communities, it appears that saturated or alternatively saturated peat has a higher biomass content, relative to the 45 days unsaturated cores. It suggests that the microbial community is best adapted to anaerobic conditions. The fluctuating condi-

tions tested in these experiments seems not to alter the microbial communities, although slightly more CO_2 respiration rates are observed in the 3 days frequency cycle. The comparison of the peat pore water (”inner water”) and the drained water from the entire core provides some insights to the peat functioning. A double porosity concept may be applied: the drained water has the highest freedom degree (macro-pore) and is less reductive while the inner pore water (micro-pore) is the most efficient biochemical reactor.

Part III

Peat biochemical response to environmental changes

Long term intensification of the anthropogenic impacts studied in the first Part showed that the peatland hydrology can be dramatically affected. Two major changes are pointed out: (1) a gradual evolution to perennial drying out leading to desiccation and (2) changes in water sources contributing to the wetland recharge.

The biochemical processes studied in Part II showed that: (1) The peat saturated by water with chemical characteristics which highly differ from the wetland, maintains a good buffering capacity. In other words, the alternating aerobic/anaerobic cycles do not (or slightly) alter the peat capacity to rapidly reach anaerobic conditions. However, repeated and rapid water level fluctuations contribute to a higher nutrients turnover. (2) The study confirms that the biochemical sensitivity of peat is highly dependent on the peat material quality. Indeed, the peat reactivity is affected by its state, i.e. its mineral, organic and biomass content. A more depleted peat is more sensitive to oxidation processes which result in higher acidification, sulphate production and cations leaching.
(3) The higher sulphate release in the cores from the "pumping site" and the resulting acidity may be explained by a higher pyrite availability. In other words the pyrite degradation state rather than the total pyrite content may be the key factor.

Illustration of the subsidence resulting from desiccation (near La Bergerie – Septembre 2010)

Consequently, this PART III investigates the impact of long term environmental changes on the biochemical processes described in PART II.

The first Chapter studies the impact of drying out leading to desiccation by use of an experimental setting similar to the previous experiments. Peat cores from La Bergerie and Le Marais were free to dry out during 5 months. Water loss was around 20 %.
The second Chapter studies the impact of two different waters recharging the peat, a stream water and a groundwater.

Chapter 1

Impact of desiccation on peat chemistry

Introduction

The hydrological regime is the principal factor controlling ecosystem processes in peatlands. Any change in water balance is expected to have important effects on biogeochemical cycles, productivity and community composition. Worldwide decreasing flooding periods in peatlands, mainly induced by systematic drainage of farmed organic soils, are responsible for severe subsidence effects. Subsidence can lower the peatland surface elevation by an amount that can reach several meters (Wosten et al., 1997). It is caused by desiccation of the peat surface, resulting in structural damage such as cracking and peat structure modification (Holden et al., 2006). This is supported by the worldwide subsidence rates that are recorded in drained peat areas and that range from few millimeters per year in boreal climates to several centimeters per year in tropical conditions (Deverel and Rojstaczer, 1996). Peat desiccation is due to increased aerobic decay in the surface layers of peatlands resulting in increased mineralization of organic compounds including nitrogen (N). The N is partly released in the form of nitrous oxide (N_2O), a powerful greenhouse gas (Alm et al., 2007). In addition, desiccation of peat surfaces is likely to make them more susceptible to erosion and extreme desiccation can lead to the point where rewetting is extremely difficult. Irreversible long term subsidence of drained peatlands is mainly due to (i) the consolidation of the saturated porous medium due to the effective stress increase following the lowering of the water table and (ii) the volume reduction of peat due to organic matter oxidation (Wosten et al., 1997). The latter is generally recognized as the main contributor to the overall land settlement (Armentano and Menges, 1986) (Deverel and Rojstaczer, 1996) (Price and Schlotzhauer, 1999).

Regarding the oxidation process, carbon-bounded nitrogen and sulphur are preferentially affected. The top meter of peat soils can contain as much as 20 t nitrogen (N), 10 t sulphur (S) and 500 t of carbon (C) per m^2 (Miller et al., 1996). Even an increase in mineralization of 1% per year has the potential to generate large losses of these elements. In addition, water table lowering usually increases the leaching of Ca, Mg and K (Sundström, 2000) (Miller et al., 1996) (Kortelainen et al., 2006) as well as ammonium (Holden et al., 2004).

The Cotentin peat meadows are severely impacted by long periods of lowered water tables as reported in a previous Chapter (Chapter 1 of Part I). Nowadays important soil subsidence is occurring in the peat, mainly around the pumping sites, even on a landscape scale, creating holes and bumps re-

sulting in serious agronomic problems. The modelling results presented in Chapter 3 have highlighted that the anthropogenic impacts affect the wetland water level. Pumping and climate change scenarios predict that desiccation will be of major concern in the near future. Within this scope, the present work aims to study the impact of peat drying out (desiccation) on peat pore water biochemistry. A compared study between peat cores subjected to natural drying out lasting for 5 months (ending at around 60 % humidity) and the previous experiment on peat cores directly from field (humidity was around 80 %) is carried out. The previous experimental methodology by re-wetting and draining cores by groundwater is re-used with the desiccated peats.

1.1 Materials and Methods

The experiment design was similar to the previous experiments, already explained in section Materials and Methods (Chapter 1 in Part II).

Similarly to the previous experiment, cores from the two sites (La Bergerie and Le Marais) were collected in October 2010 and stored for 5 months at 4°C before the experiment started. Cores were kept open to allow slow drying-out. To estimate the loss in water (i.e. the rate of drying-out), the cores were weighted after collection and at the beginning of the experiment, 5 months later. In addition, humidity was also checked (48h dry oven at 105°C) in 10 sub-samples directly collected from the field.

The experiment lasted again for 45 days, but only 3 treatments were tested: (i) a drained-rewetted cycle on a 9 day frequency with 3 replicates (ii) a permanently saturated case with 3 replicates and (iii) a dry control with 2 replicates. Cores were saturated with the groundwater used in the previous experiment. Peat pore water at the 3 levels and the drained water were monitored for the same parameters and elements used in the previous experiment. Extractable C and N and total and active biomass were also analysed in the same way (see Materials and Methods Chapter 1 of Part II).

1.2 Results

Initial humidity from the field was 79.6 % ((n=10, SE[1] = 0.9 %) in La Bergerie and 80.1 % ((n=10, SE= 1.2 %) in Le Marais. Humidity of the total cores after 5 months drying out was 64.4 % (n=8, SE =1.4 %) in La Bergerie and 59.6 % ((n=8, SE=2.6 %) in Le Marais.

As a first insight, some major differences are observed after 5 months drying-out, relative to the first experiment where the humidity was around 80%. Extractable soluble organic carbon (SolOC), total and active biomass and the final values or concentrations in the pore water from the middle of the permanently saturated cores are given in Table 1.1, relative to the first experiment.

1.2.1 Impact of desiccation relative to the non-desiccated experiment

Soluble organic carbon is not affected by the drying period, while total and active biomass are higher. SO_4^{2-} production in the cores is dramatically higher: around 5 times higher in Le Marais, reaching

[1] Standard error

Table 1.1: Comparison, over a set of parameters or elements, between Le Marais and La Bergerie for the two experiments. Average and standard error (SE) are given on six peat sub-samples before the experiments and on three pore water samples from the middle of the always saturated cores, on day 45. Water chemistry concentrations are in mg.L^{-}. The "inlet water" column shows the chemistry of the water used to saturate the cores.

	Inlet water	**Le Marais**				**La Bergerie**			
		80% humidity		60% humidity		80% humidity		60% humidity	
		value	SE	value	SE	value	SE	value	SE
Peat									
Extractable nutrients (g.kg^{-1} dry mass)									
Soluble organic carbon		0.74	0.03	0.74	0.07	0.39	0.03	0.35	0.03
Biomass (g.kg^{-1} dry mass)									
C microbial (MBC)		0.61	0.11	1.75	0.41	0.14	0.08	0.88	0.13
C active biomass (C SIR)		0.28	0.01	0.32	0.01	0.20	0.04	0.24	0.02
Pore water									
pH	7.52	6.13	0.02	5.43	0.04	4.29	0.02	3.78	0.09
Cl^{-}	30.6	30.1	0.5	38.2	2.7	32.4	1.0	33	1.3
NO$_3^{-}$	36.9	0.5	0.1	2.5	0.9	0.9	0.4	0	0
SO$_4^{2-}$	10.0	63	7	336	25	439	76	1767	137
DOC	b.d.l.	110.2	5.6	96.7	2.4	35.8	4.9	23.8	2.3
DIC	56.5	2.8	0.3	0.9	0.1	1.2	0.1	0.7	b.d.l.
NH$_4^{+}$ (on day 28)	b.d.l.	4.6	0.4	9.5	1.6	10.1	1.1	3.6	1.7
Fe^{2+}	b.d.l.	1.9	0.3	2.2	0.7	27.0	2.6	24.1	0.1
Fe	0.02	5.7	1.3	2.0	0.6	72.7	25.6	74.3	12.4
Ca^{2+} + Mg^{2+}	84.5	52	3	132	7	130	53	419.	40
Na^{+} + K^{+}	17.5	10.2	0.4	11.5	0.5	24.5	5.3	21.1	1.1
SUVA		3.4	0.1	3.8	0.4	3.6	0.2	3.6	0.2

330 mg/L and around 4 times higher in La Bergerie, reaching 1760 mg/L. Likewise, pHs are quite lower: from 6.1 to 5.4 in Le Marais and from 4.3 to 3.8 in La Bergerie. However, iron apparent concentrations (total and ferrous) are not affected and DOC concentrations are slightly lower. Ca^{2+} + Mg^{2+} are higher, both peats showing release (relative to the inlet concentration). Na^{+} + K^{+}, the final NO_3^- and DIC concentrations and the SUVA values are not affected.

Consistent with the non-desiccated experiment, there are significant differences between the two sites. Le Marais still maintains higher biomass levels relative to La Bergerie. Acidification is higher in La Bergerie, as well as the SO_4^{2-} and bi-valent cations release.

1.2.2 Relation between elements and sample distribution

A Principal Component Analysis (PCA) was carried out on the peat pore samples data from the 3 levels inside the cores : Figure 1.1 plots the variables of the PCA for Le Marais and La Bergerie together, and the two sites separated. In the 3 PCAs, Fe and Fe(II) are strongly correlated (superimposed): only Fe is thus kept in the analysis (as strong superimposition introduces a bias by giving an overestimated weight to this pair of elements). For the whole data set, major part of the variance is explained by [SO_4^{2-}; Ca^{2+}; Na^{+}] on one side of the first component, and [pH; DOC] on the other side. In the second component, variance is mostly explained by NO_3^- on one side and DIC on the other side. Projection on the third component gives similar results (not shown).

Taking the sites apart shows some common results, however differences are noticed. In Le Marais, [SO_4^{2-}; Ca^{2+}; Mg^{2+}] are anti-correlated with pH, but DOC is not associated with pH. The variance of the second component is mainly explained by [Na^{+}; K^{+}; Fe]. In La Bergerie, [SO_4^{2-}; Ca^{2+}; Mg^{2+}; Na^{+}; K^{+}] belong to the same component, pH belongs to the other side of this component, but DOC is again not associated with pH. The variance of the second component is mainly explained by NO_3^- on one side and DIC on the other side. Fe is somewhere in the middle, and does not clearly belongs to a specific component.

The individual samples, related to the variables in the PCA from Figure 1.1, are plotted on the principal components. Data are from the peat pore water extracted from the 3 levels in the cores, at the 3 sampling dates: in Le Marais and La Bergerie together (Figure 1.2), Le Marais alone (Figure 1.3) and La Bergerie alone (Figure 1.4). The two sites are distinguished: Le Marais plots towards the [pH;DOC] pole, while La Bergerie plots towards the [SO_4^{2-}; Ca^{2+}; Na^{+}] pole.

The cores subjected to draining-rewetting cycles are together towards the pH pole in Le Marais and the Cl pole in La Bergerie, while the permanently saturated cores are together towards the [SO_4^{2-}; Ca^{2+}; Mg^{2+};(Na^{+}; K^{+})] pole, regardless the site. In the dendograms (Figures 1.3 and 1.4), the drained-rewetted are clearly distinct from the permanently saturated samples.

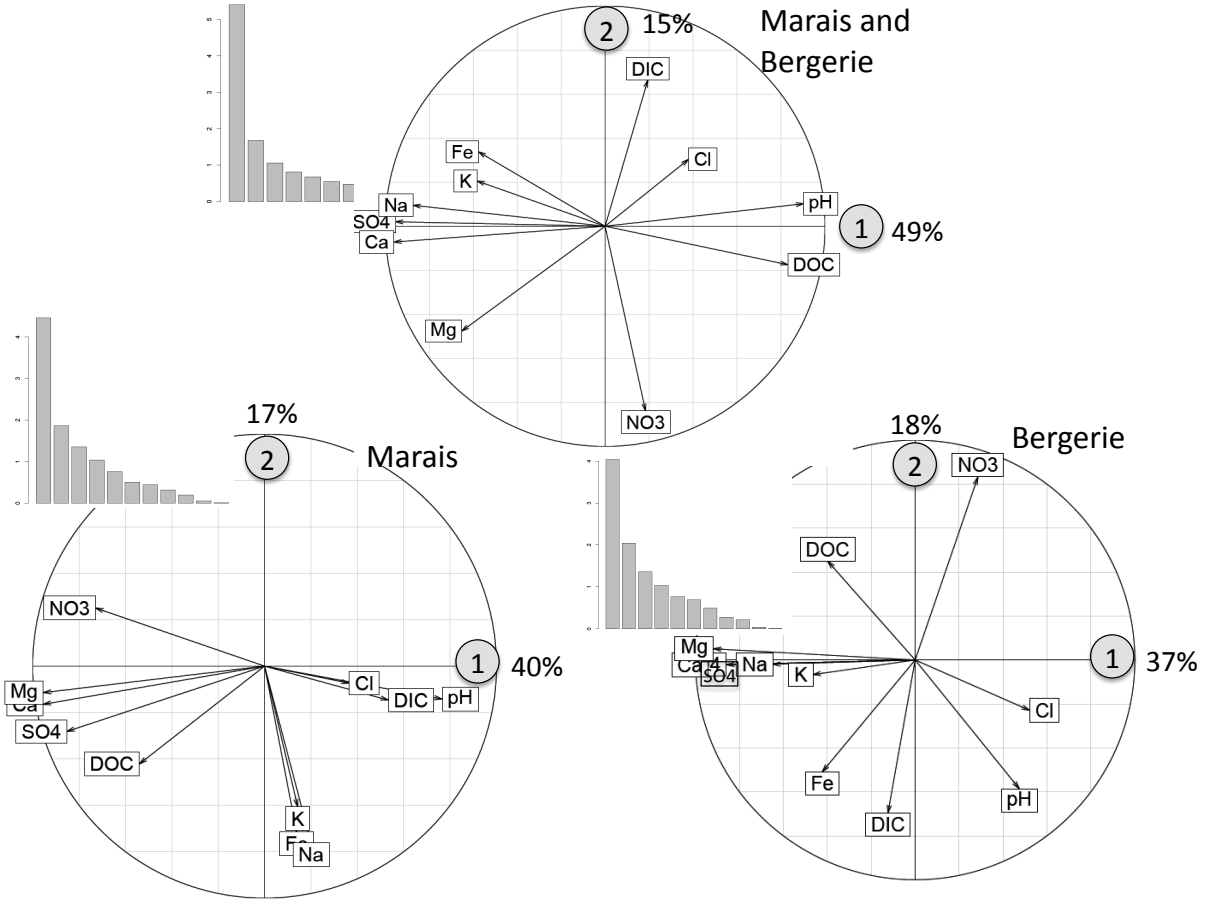

Figure 1.1: Scatter of a set of elements plotted as their correlation coefficients between them and the principal components in the unit circle. Data are from the peat pore water extracted from the 3 levels in the cores, at the 3 sampling dates. Le Marais and La Bergerie (n=100), Le Marais alone (n=50) and La Bergerie alone (n=50). The bar plots illustrate the variance projected on each different component

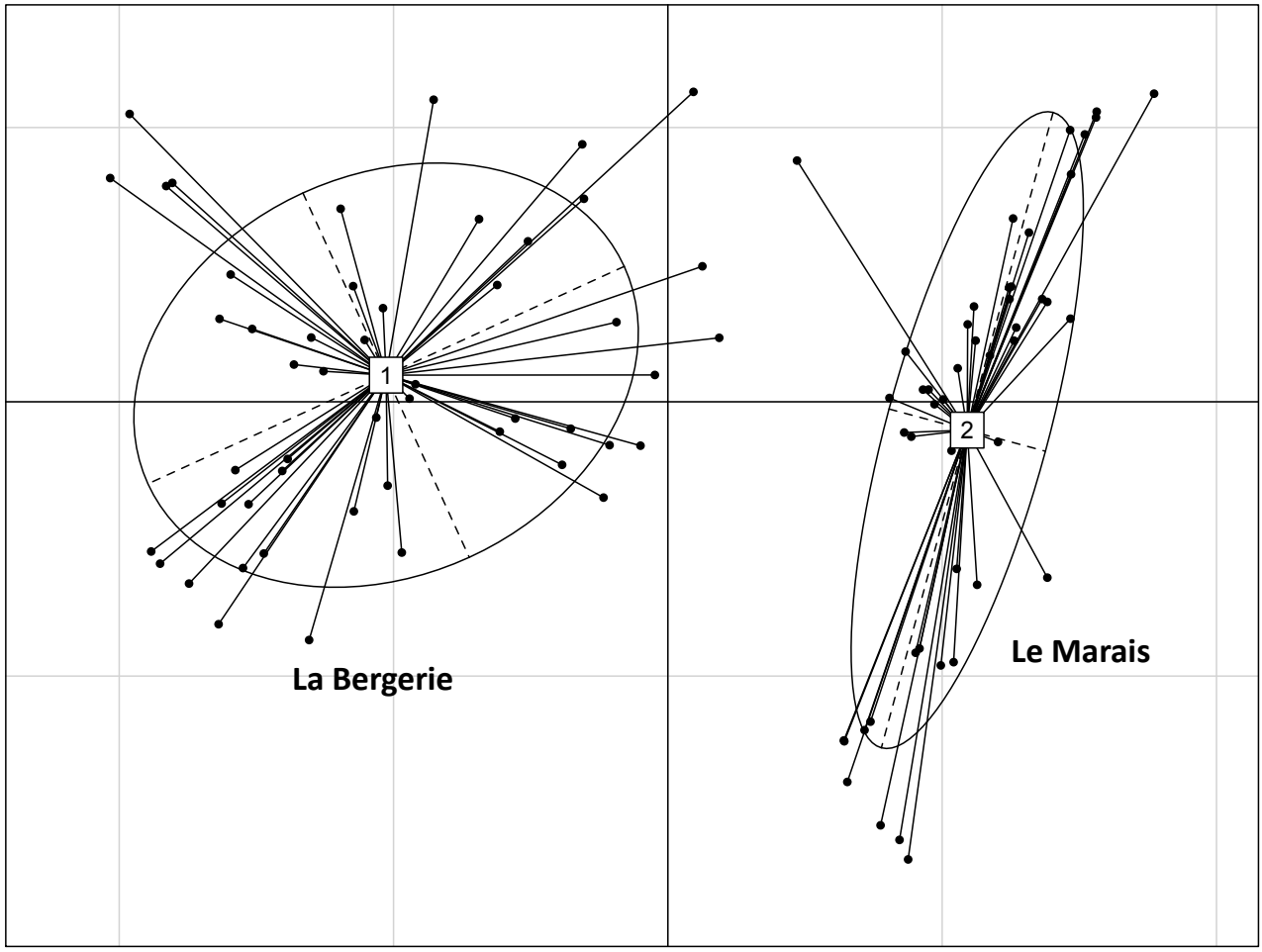

Figure 1.2: The individual samples plotted on the principal component. Data are from the peat pore water extracted from the 3 levels in the cores, at the 3 sampling dates for Le Marais and La Bergerie (n=100).

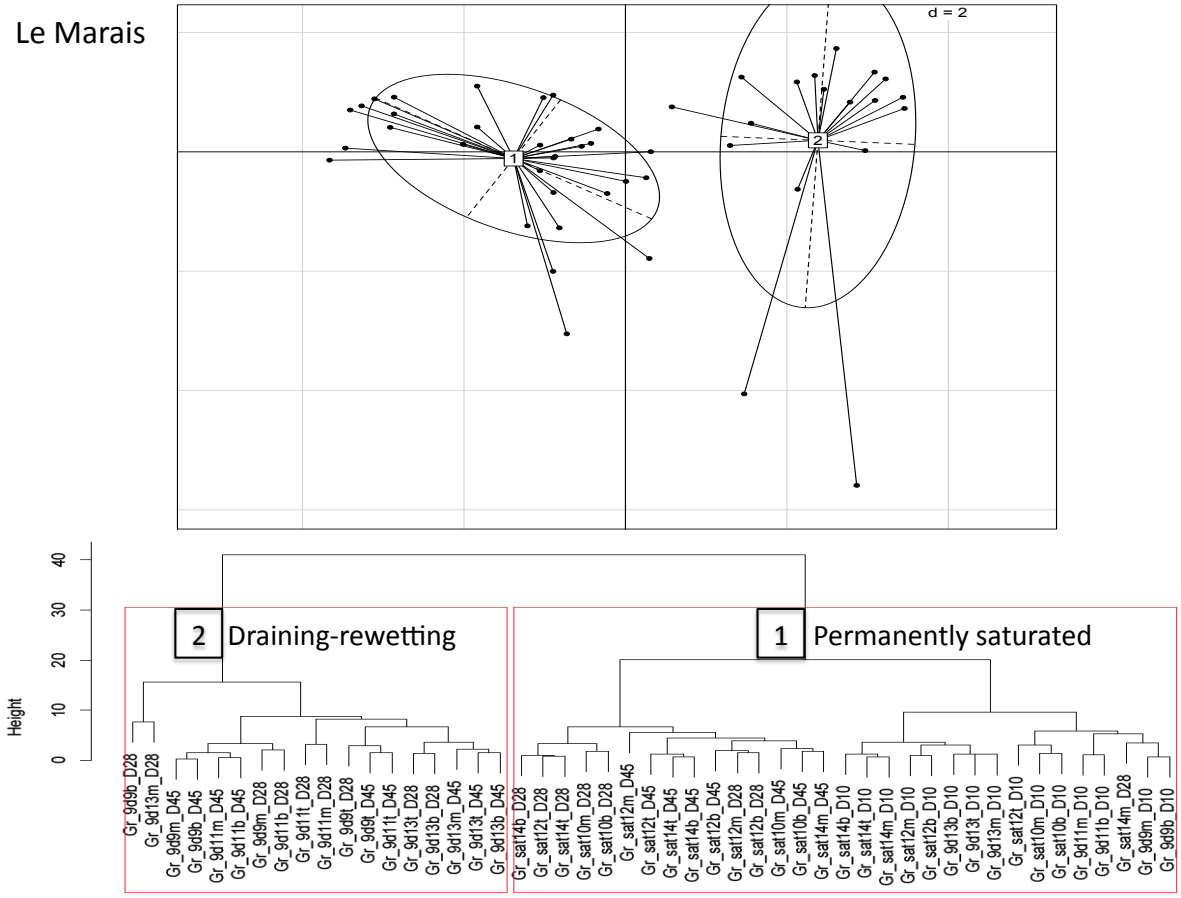

Figure 1.3: The individual samples plotted on the principal component and the corresponding ”ward” dendogram. Data are from the peat pore water extracted from the 3 levels in the cores, at the 3 sampling dates for Le Marais (n=50).

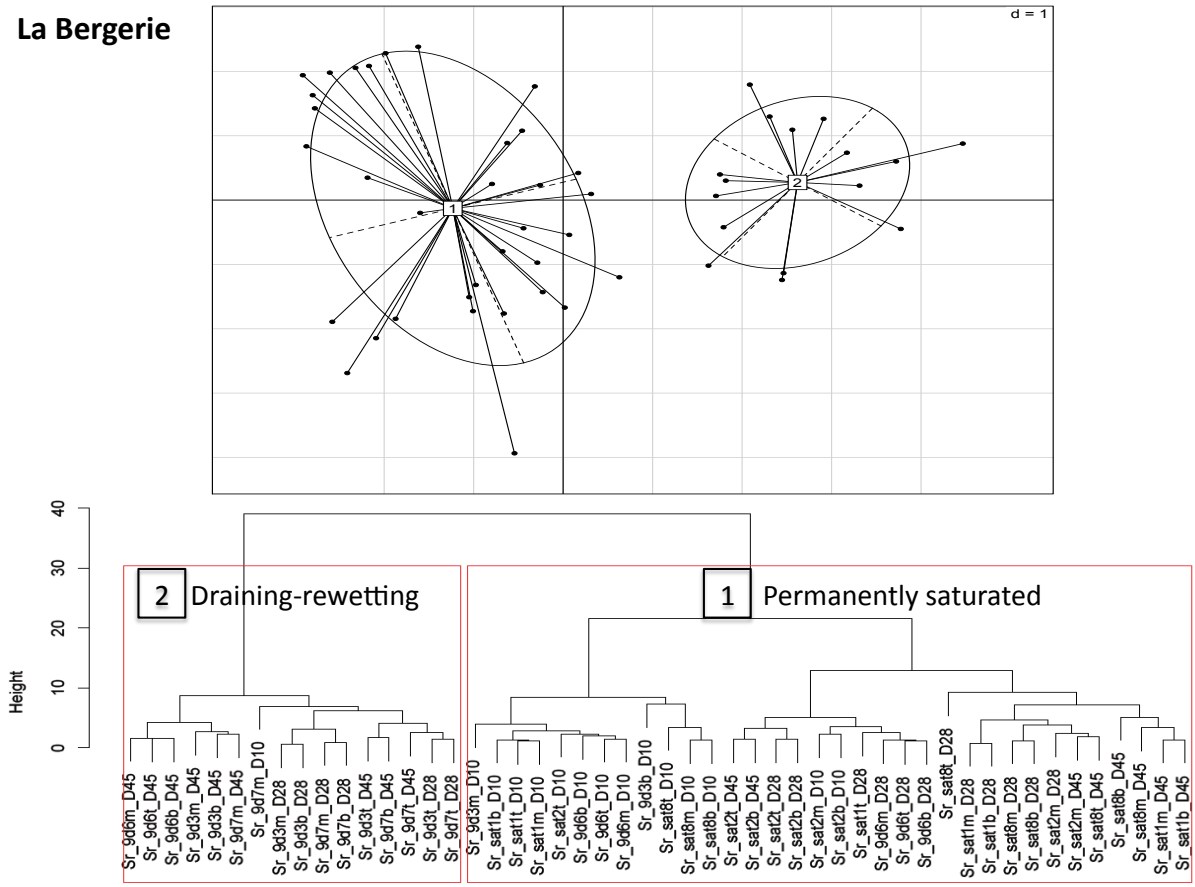

Figure 1.4: The individual samples plotted on the principal component and the corresponding ”ward” dendogram. Data are from the peat pore water extracted from the 3 levels in the cores, at the 3 sampling dates for La Bergerie (n=50).

1.2.3 Chemical temporal patterns

Temporal patterns for several parameters or elements, for the two tested treatments (saturated and draining-rewetting on a 9 day frequency), in the middle of the cores, are shown on the next Figures: Figure 1.5 for pH and SO_4^{2-}; Figure 1.6 for DOC and Fe; Figure 1.7 for Fe(II) and NH_4^+; Figure 1.8 for NO_3^- and Ca^{2+}.

pH, SO_4^{2-}. Figure 1.5. A minimum pH is reached after 9 days saturation and maintained at this level afterwards, in the permanently saturated case. A slight pH increase is observed after draining-rewetting, whatever the site. SO_4^{2-} high levels of concentration are also reached after 9 days of saturation and does not change for 45 days in the permanently saturated treatment. By contrast, the draining-rewetting treatment results in a gradual SO_4^{2-} decrease from one cycle to the other.

DOC, Fe, Fe(II) and NH_4^+. Figure 1.6 and 1.7. The maximum DOC production is reached after 9 days saturation and maintained at this level afterwards in the permanently saturated case. On the opposite, the draining-rewetting treatment results in a gradual small DOC decrease from one cycle to the other. Total dissolved Fe and Fe(II) behave exactly in the same way with low concentrations at day 9, increasing with time almost linearly, in the permanently saturated cores. On the opposite, the draining-rewetting treatment results in similar (or small increase in Le Marais) concentrations from one cycle to the other. NH_4^+ is produced in the cores with no significant differences between the saturated case and the cores subjected to a second rewetting, whatever the site. An increase with time is observed in all cores. Last rewetting data is missing (due to analytical problems).

NO_3^- and Ca^{2+}. Figure 1.8. After 9 days of saturation, NO_3^- in the cores is high, by contrast with the very low concentrations observed in the previous "non-dessicated" experiments. NO_3^- in Le Marais is even higher than the inlet concentration, indicating net production. Afterwards, NO_3^- decreases in a similar way in Le Marais down to very low values. The decreasing rate is lower in La Bergerie, in the cores subjected to rewettings: the third rewetting still remains around 13 mg/L NO_3^-. The maximum Ca^{2+} production is already reached after 9 days saturation and there is almost no change for 45 days in the permanently saturated treatment. On the opposite, the draining-rewetting treatment results in a gradual Ca^{2+} decrease from one cycle to the other.

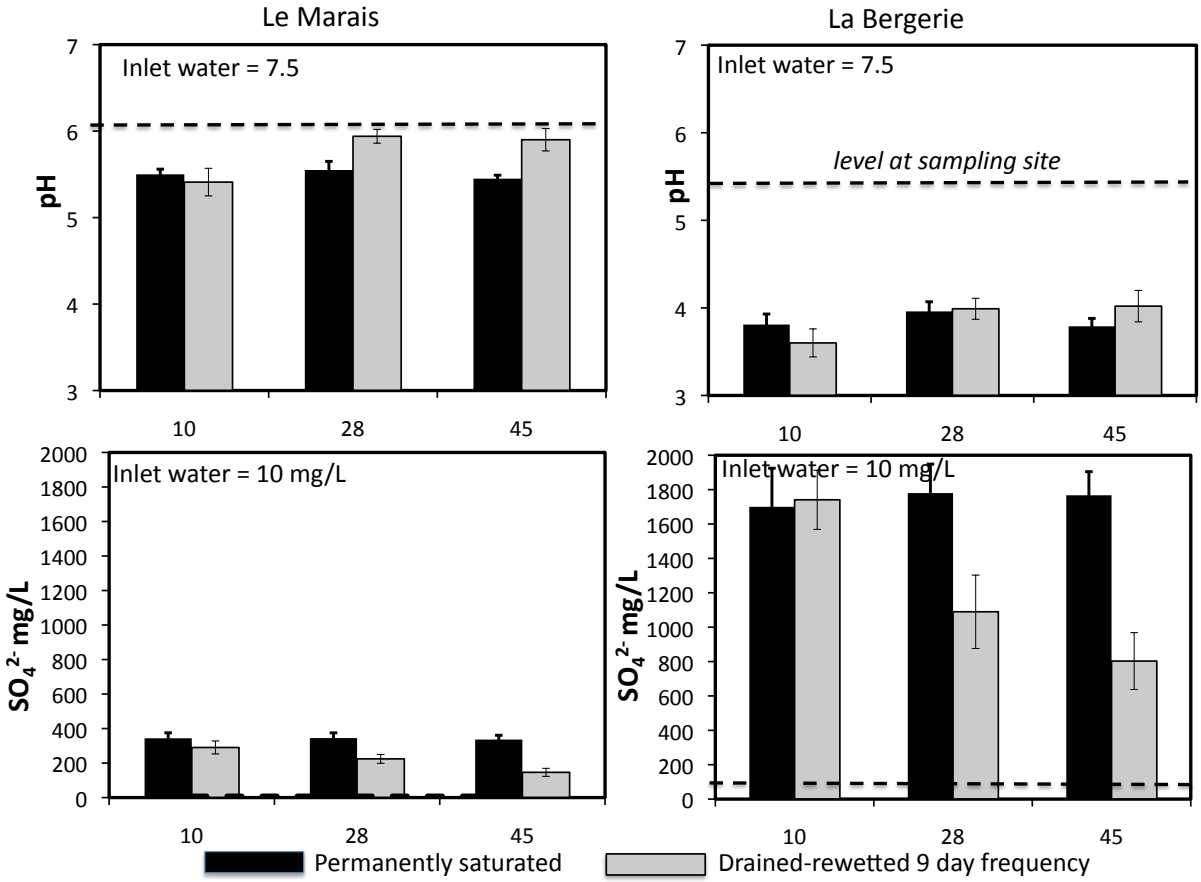

Figure 1.5: Temporal pH and SO_4^{2-} in the peat pore water from the middle of the column over the two tested treatments: saturated (black bars), drained-rewetted cycle on a 9 day frequency (grey bars). The doted line figures the concentration level at the sampling site on sampling day. Error bars are the standard errors, n=3

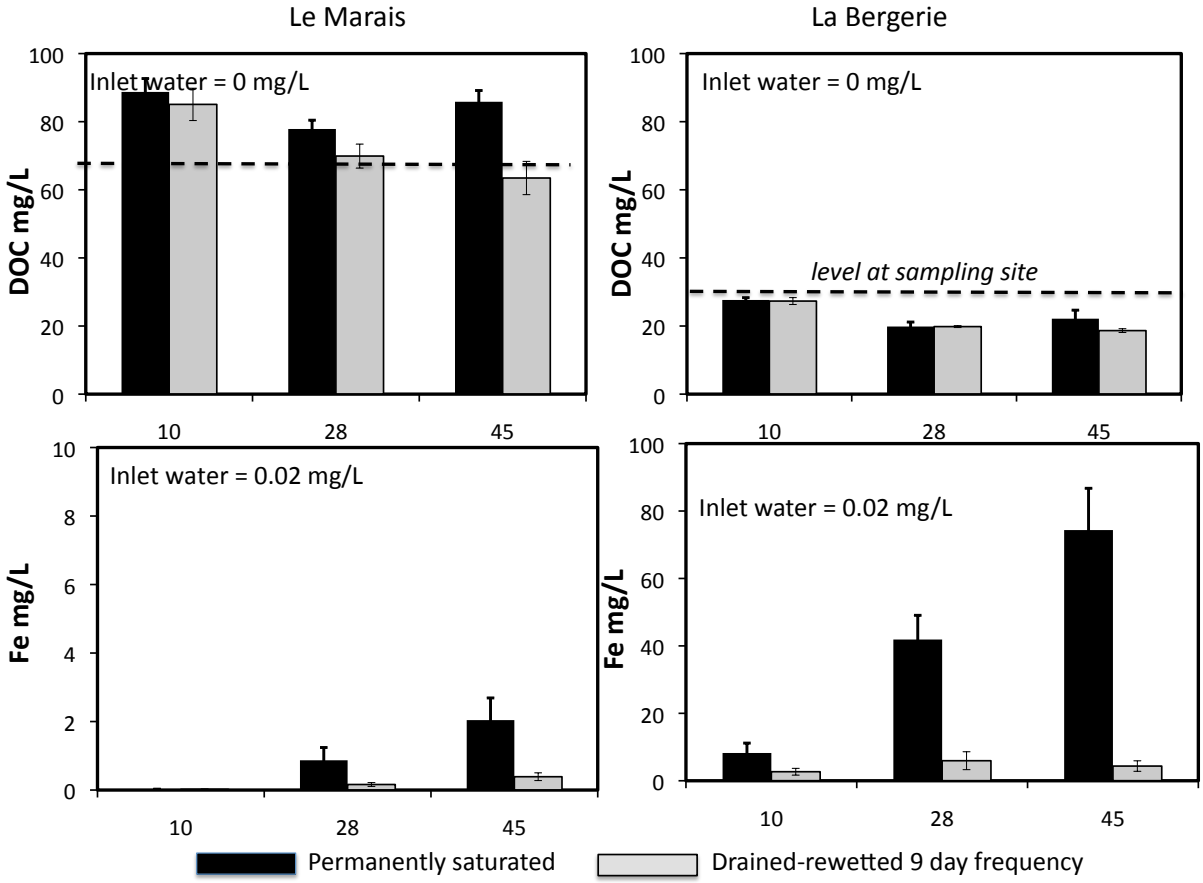

Figure 1.6: Temporal DOC and Fe in the peat pore water from the middle of the column over the two tested treatments: saturated (black bars), drained-rewetted cycle on a 9 day frequency (grey bars). The doted line figures the concentration level at the sampling site on sampling day. Error bars are the standard errors, n=3

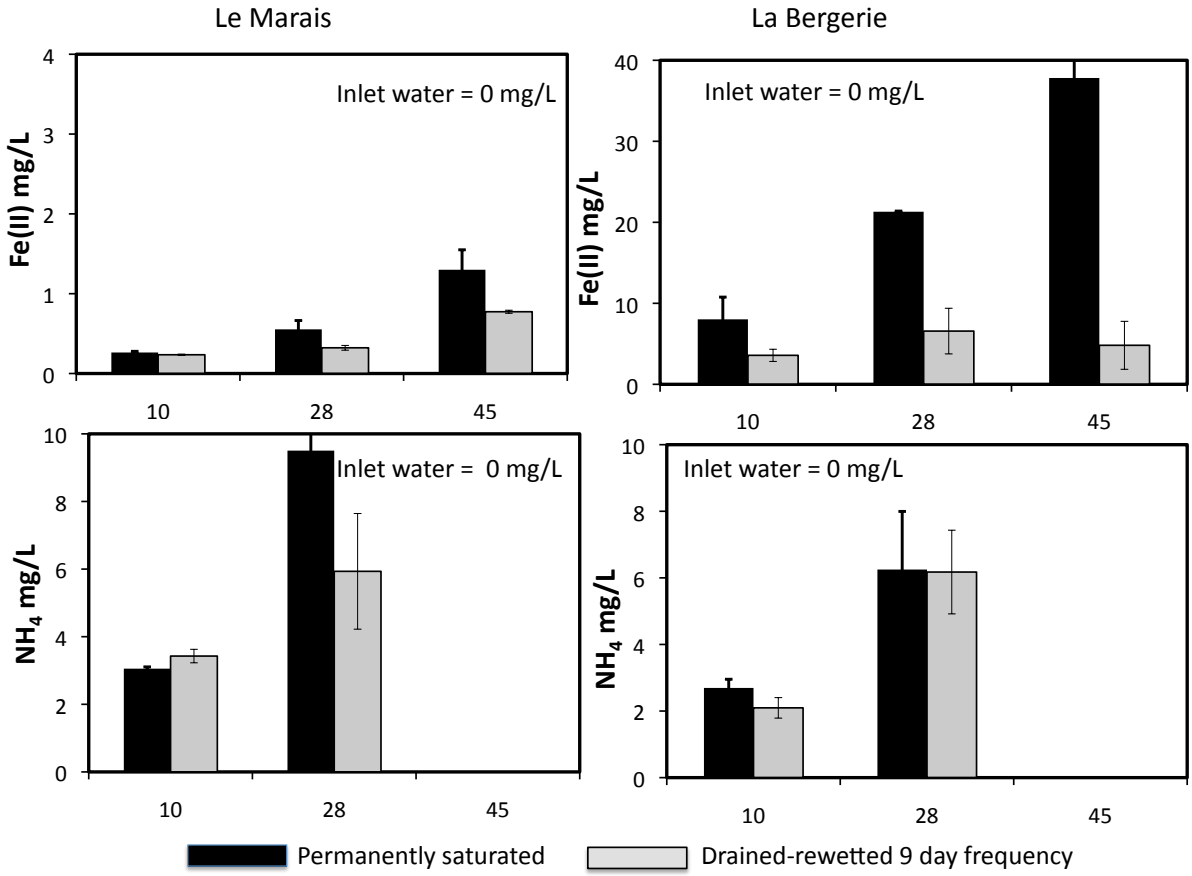

Figure 1.7: Temporal Fe(II) and NH_4^+ in the peat pore water from the middle of the column over the two tested treatments: saturated (black bars), drained-rewetted cycle on a 9 day frequency (grey bars). The doted line figures the concentration level at the sampling site on sampling day. Error bars are the standard errors, n=3. No data available for day 45 on NH_4^+

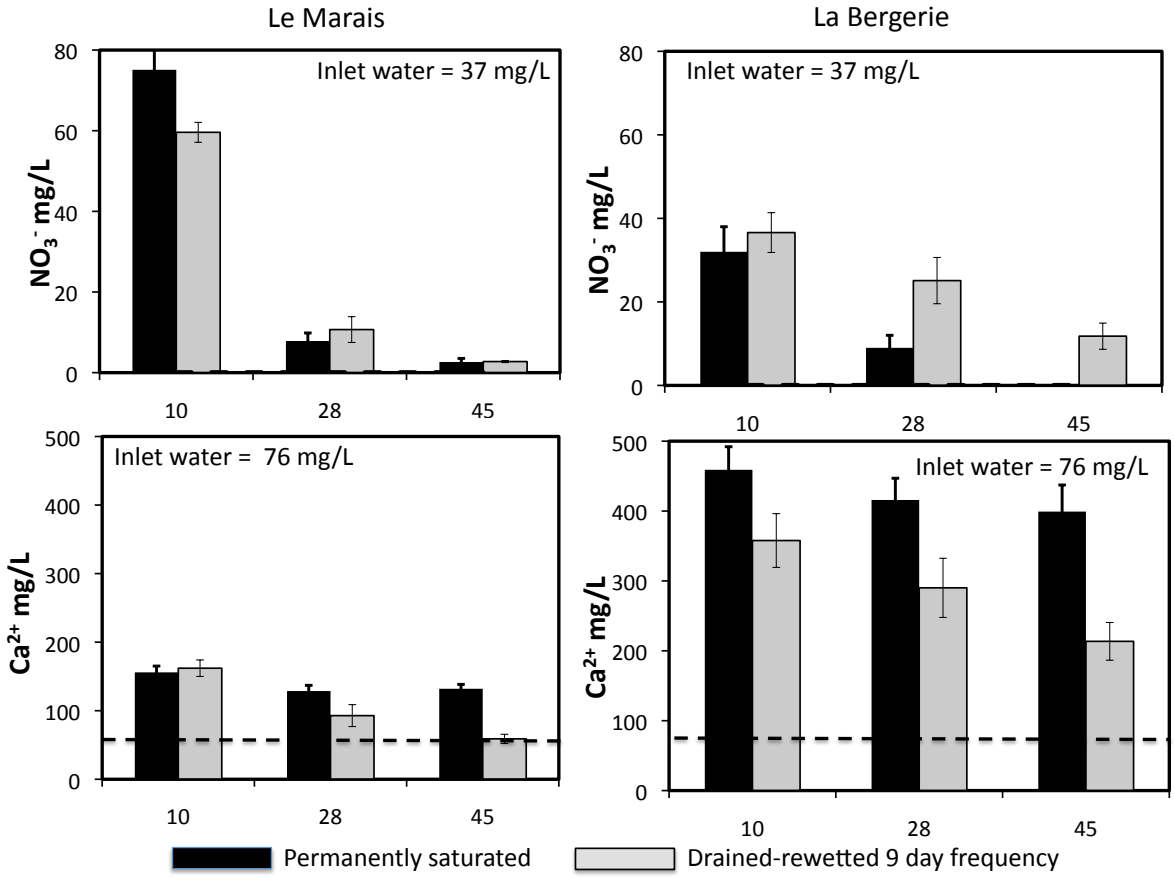

Figure 1.8: Temporal NO_3^- and Ca^{2+} in the peat pore water from the middle of the column over the two tested treatments: saturated (black bars), drained-rewetted cycle on a 9 day frequency (grey bars). The doted line figures the concentration level at the sampling site on sampling day. Error bars are the standard errors, n=3

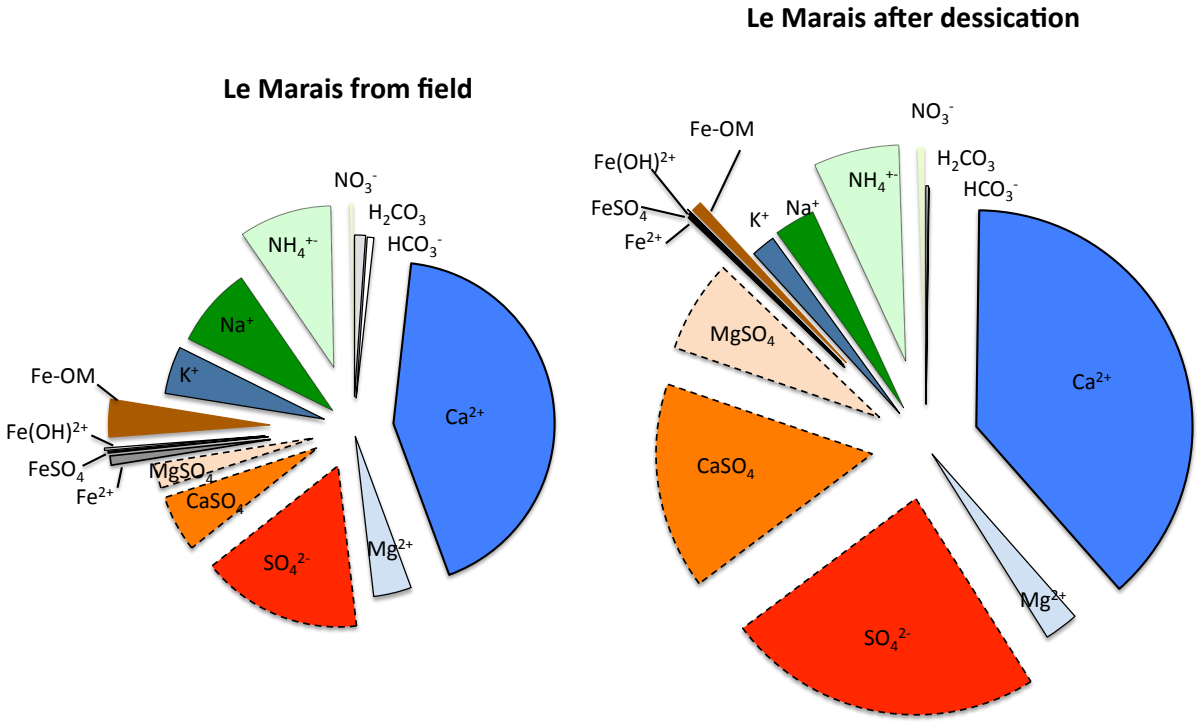

Figure 1.9: Aqueous speciation comparison between dessicated and non-dessicated experiment in Le Marais, modelled by PHREEQC, accounting for cation-humic acid binding reactions. Water chemistry is from the permanently saturated cores at the end of the experiment. Units are in meq.L^{-1}

1.2.4 Aqueous Speciation

The aqueous speciation within the water samples is accessed via modelling with PHREEQC (Parkhurst and Appelo, 1999) coupled to Model VI [Tipping, 1998]. The classical PHREEQC database "minteq.v4" was completed by a database created by Remi Marsac (Marsac et al., 2011), based on Model VI from Tipping (1998), to account for cation-humic acid binding reactions. Speciation was calculated on the water chemistry from the permanently saturated cores at the end of the experiment, for the non-dessicated ("from field") and the dessicated ("after desiccation") peats (data from Table 1.1). The ionic strength was determined based on the electrical conductivity and fixed at 0.01 mol.L^{-1}. The electron activity (pe) was not measured in the experiment and thus freely calculated by PHREEQC. Figures 1.9 and 1.10 illustrate the speciation of Le Marais and La Bergerie respectively.

The main results are:

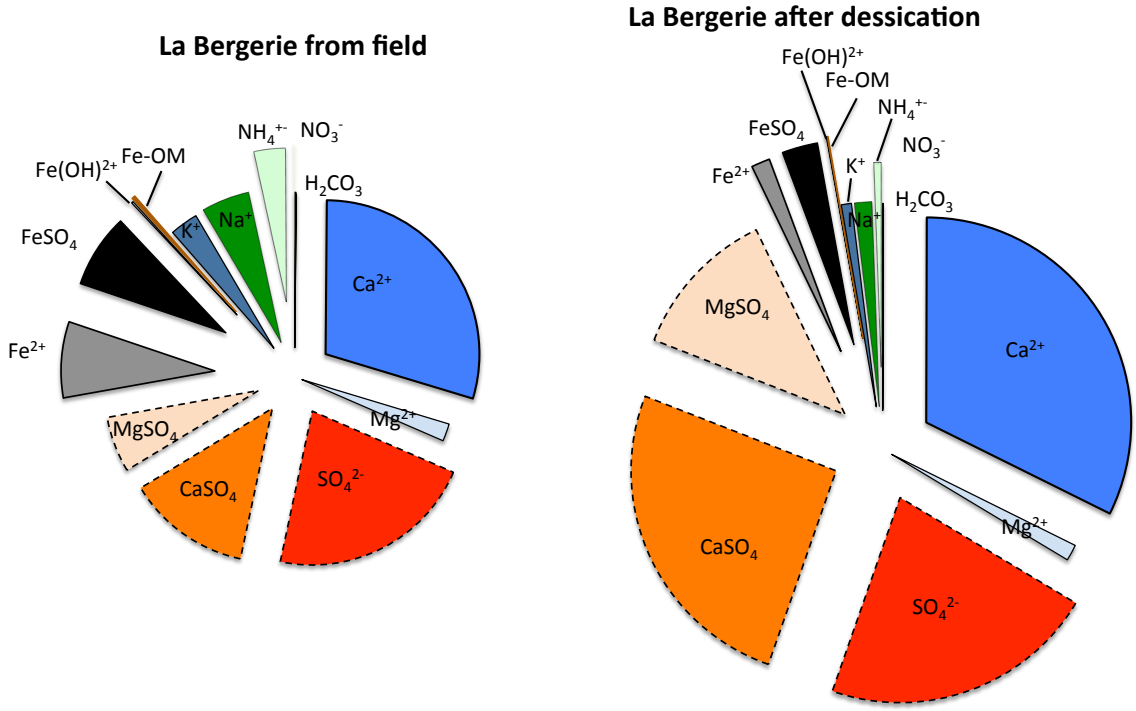

Figure 1.10: Aqueous speciation comparison between dessicated and non-dessciated experiment in La Bergerie, modelled by PHREEQC, accounting for cation-humic acid binding reactions. Water chemistry is from the permanently saturated cores at the end of the experiment. Units are in meq.L^{-1}

- desiccation increases the mineralization content by around 34 % in both peats.
- relative to the speciation distribution (i.e. relative proportions), desiccation increases the $CaSO_4$ and $MgSO_4$ complexes
- it decreases the Fe phases (Fe^{2+} and $FeSO_4$)
- it slightly decreases the relative proportions of Na^+ and K^+
- it maintains the relative proportions of Ca^{2+}, Mg^{2+} and SO_4^{2-}
- similarly to the first "non-dessicated" experiment, iron bonded to organic matter (Fe-OM) is maintained at a high level (around 70 % of Fe is bounded) in Le Marais and at a very low level (around 2 %) in La Bergerie

1.3 Discussion

1.3.1 Sulphur production related to desiccation

As pyrite is recognised to be the dominant form in rapid S turn-over, the question is : may pyrite oxidation totally explain the high level of sulphate? Iron concentration, as a product from the pyrite oxidation reaction, is indeed higher when sulphate is higher. However it is not a good indicator because Fe(II) does not remain in a soluble form at these low pH, but rather precipitates in iron oxides. This is suggested by PHREEQC speciation results: $Fe(OH)_3$ saturation index ranges from 0.13 to 2.41 in the four modelled waters. In this desiccation experiment, Fe concentrations are very similar to the non-dessicated experiments.

In the present peat cores subjected to drying-out, sulphate concentrations are very high, although decreasing with repeated draining. No anti-correlated relation is observed between nitrate and sulphate, contrarily to the previous experiments on non-dessicated cores. In the other experiments (both in the static batches and the dynamic draining and rewetting) (see for example Figure 2.9 from next Chapter 2 in this Part), a good agreement between the nitrate/sulphate stoichiometric ratio and the pyrite oxidation mainly driven by nitrate as a strong oxidizer, were observed.

Pyrite as a source of sulphuric acid Pyrite accumulates in waterlogged soils where there is a supply of easily decomposed organic matter (Appelo and Postma, 2005). Bacteria, breaking down this organic matter under anaerobic conditions, reduce dissolved sulphate ions to sulphides and Fe(III) oxides to Fe(II). Pyrite is the stable end-product of these reactions. It is stable only under anaerobic conditions. When oxygen enters the soil pyrite is oxidised, generating sulphuric acid. The reaction of pyrite with oxygen is a slow process, but pyrite is rapidly oxidised by Fe(III) in solution (Dent, 1986). Fe(III) is thereby reduced to Fe(II), but Fe(III) is then regenerated from Fe(II) by the bacteria *Thiobacillus ferrooxidans*. This catalytic oxidation of pyrite can take place only at pH less than 4, because Fe(III) is soluble only under these very acid conditions. Most of the Fe(III) ultimately crystallises as the reddish brown oxide goethite in mottles, coatings, and nodules within the soil. In our experiment La Bergerie releases a large amount of sulphate and pH is around 4 or even lower, which suggest that the catalytic pyrite oxidation by Fe(III) may take place. Moreover, PHREEQC modelling shows that the dominant aqueous Fe-phase is $FeSO_4$ (Figures 1.9 and 1.10) and that pyrite is strongly under-saturated (saturation index around -130) in both peats. There is thus evidence that pyrite is highly involved in the sulphate production in both peats.

Sulphur speciation in organic soils Sulphur (S) exists in soils in organic and inorganic forms in various oxidation states, ranging from -2 to +6. Table 1.2 lists the sulphur species and their oxidation state. Sulphur is involved in many biochemical processes, such as the synthesis of essential amino acids, proteins, and enzymes. It can be retained in organic topsoil horizons by microbial incorporation into organic compounds (Fitzgerald et al., 1982). In wetland soils, SO_4^{2-} is transformed into H_2S by microbial dissimilatory reduction (Wieder et al., 1987). Subsequently, it may be volatilized, precipitated as sulfide minerals (Wieder and Lang, 1988a), or incorporated into organic compounds (Casagrange et al., 1979).

Table 1.2: Sulfur species and their oxidation state. From Prietzel, 2009(Prietzel et al., 2009)

Sulfur species		Example	Electronic oxidation state
Inorganic sulfide Type I	S^2	Troilite	-2
Inorganic sulfide Type II	${S_2}^{2-}$	Pyrite	-1
Elemental sulfur	S^0	Cystine	0
Organic polysulfide	R–S–S–S–R′		+0.15
Organic disulfide	R–S–S–R′		+0.2
Thiol	R–SH	Cysteine	+0.5
Organic monosulfides	R–S–R′	Methionine	+0.5
Sulfoxide	R–S=O	Methionine sulfoxide	+2
Sulfite	SO_3^{2-}	Sodium sulfite	+3.68
Sulfone	$R–S(=O)_2$	Phenyl sulfone	+4
Sulfonate	$R–O–S–(O)_2$	Cysteinic acid	+5
Ester sulfate	$R–O–SO_3$	Sodium dodecylsulfate	+6
Inorganic sulfate	SO_4^{2-}	Sodium sulfate	+6

Although not analysed here, sulphur speciation in peatlands has been documented in several studies. Wet-chemical methods based on sequential extraction of S fractions have already highlighted the large predominance of organic sulphur (Krairapanond et al., 1992) (Wieder and Lang, 1988a). New methods based on X-ray absorption have significantly improved the speciation. Non destructive and able to work on bulk samples they allow distinguishing organic S compounds in much more detail. Prietzel et al. (Prietzel et al., 2009) showed that fast sulphur turnover in peatlands is highly dominated by pyrite but ester sulfates may also contribute to SO_4^{2-} production in alternating oxidation-reduction cycles.

In the desiccation experiment, although mineralization rates were not measured, the important nitrate production may suggest that mineralization occurs. Thus, organic ester sulphates may also explain the high sulphate concentrations. As a overall conclusion, we can hypothesize that inorganic S oxidation (mainly from pyrite) takes place, concomitantly to organic S mineralization.

In addition, this experiment agrees with the hypothesis made in Chapter 2 of Part II: the degradation state of pyrite, instead of the total content, is a key factor. Total S and Fe contents have close values in the two peats. Therefore, it is suggested that the two peats have accumulated an important pyrite content under similar anaerobic conditions, throughout long time scales. It is concluded that the drastically higher pyrite oxidation in La Bergerie is related to higher pyrite availability, i.e. more surface degraded minerals due to more oxidizing conditions in the field. The desiccation experiment makes sulphur more available in both peats and ends with higher acidities, suggesting that the oxidizing conditions during the 5 months drying have indeed enhanced pyrite oxidation.

1.3.2 Other consequences of desiccation

The high sulphate release results in higher acidity in these peats, which in turn contributes to bivalent cation desorption which counteract the high negative charges induced by the high sulphate release. Bivalent cation leaching is thus of concern after desiccation. PHREEQC modelling results show that desiccation increases the $CaSO_4$ and $MgSO_4$ complexes (Figures 1.9 and 1.10), suggesting that pyrite dissolution, by increasing SO_4^{2-}, and indirectly Ca^{2+} and Mg^{2+}, induces $CaSO_4$ and $MgSO_4$ complexation.

DOC solubility is clearly controlled (and lowered) by the low pH: while most elements are subjected to leaching, DOC is maintained at similar or even lower levels relative to the first experiment. The rewetting also results in nitrate loss, which decreases with repeated rewettings. High nitrate concentrations are present concomitantly to Fe(II) and NH_4, which suggest that the redox potential is not adapted to nitrogen oxidation. Rather, organic nitrogen mineralization may be the dominant process, which agrees with the hypothesis that mineralization occurs. Similarly to the first "non-dessicated" experiment, Fe bounded to organic matter (Fe-OM) is maintained at a high level (around 70 % of Fe is bounded) in Le Marais and at a very low level (around 2 %) in La Bergerie after desiccation. It appears that the low pH in La Bergerie explains these dramatic bounding differences. Peat from Le Marais has thus a high complexing efficiency, while desorption mechanisms dominate in La Bergerie.

The active and notably total biomass is higher in this desiccation experiment relative to the more humid previous experiment. Consequently, the 5 months drying-out has enhanced biomass growth. Although no measures were made to qualify this biomass, we can suggest that drying-out has favoured aerobic microbial communities which quantitatively exceed the formerly anaerobic communities. Linked to this observation, the organic matter mineralization suggested by the important leaching, may be enhanced by this newly developed aerobic communities. It is indeed well known that an increase in the air-filled porosity of the peat affects microbial processes and thus decomposition rates. Oxygen, acting as an optimal terminal electron acceptor for decomposition ((Freeman et al., 2004b) (Laiho, 2006)), allows aerobic decomposition to take place at a higher rate. Depending on the organic matter content, this rate has be shown to be twice faster (Geurts et al., 2010) to 50 times faster (Clymo, 1983) than anaerobic decomposition.

1.3.3 Field implication

As a overall result, the impact of desiccation in peats from le Cotentin (taking into account two representative peat sites) seems to severely impact the peat structure by oxidation and mineralization mechanisms, but also the catchment water quality by significant nutrient loss. Based on this study, the current degraded peat state in La Bergerie may be better understood. As already explained previously, La Bergerie is in the close vicinity of a pumping well working since 1992. It was evidenced that this peat layers are subjected to enhanced downward flow throughout the year (Auterives et al., 2011), bringing more oxygen into the soil. This phenomenon could impact the peat (although less intensively), similarly to desiccation which also enhances aerobic processes. The current peat state, depleted in C, N and Ca but somewhat enriched in Fe relative to the reference site, suggests indeed that nutrient leaching takes place (see Section 1.5 in Chapter 1 of Part II). In addition soluble organic carbon, total and active biomass are also lower in this peat (see Table 1.1) suggesting that long

term nutrient leaching has decreased the microbial communities. The observed biomass increase in the desiccation experiment, by growing aerobic micro-organisms, is thus not reflected in this site. A plausible explanation is that, while turning quickly from humid to more dry conditions enhances microbial growing, it is not maintained on larger time scales. Rather, nutrient depletion on long periods is a limiting factor to microbial aerobic growth. However, the peat pumping site is highly sensitive to desiccation, i.e. nutrient leaching occurs at a high level. These results correlate well with field observations (Auterives, 2006) (Bougon et al., 2009): e.g. peaks of SO_4^{2-} and Ca^{2+} were correlated with acidity increase after water level rise and were more intense in the "pumping site". Finally, important soil subsidence is occurring in the peat around the pumping site, even on a landscape scale, creating holes and bumps resulting in serious agronomic problems. This observation gives prominence to the mineralization occurrence.

Conclusion

This experiment aimed to study the impact of peat desiccation on overall pore water chemistry. Peat cores were allowed to naturally dry-out for 5 months in the laboratory at 4°C. Final humidity was around 60 %. Peat was then rewetted, and depending on the experimental design, subjected to repeated draining and rewettings. Comparison with the previous experiment on cores directly used from the field with an averaged humidity of 80 %, outlined significant differences.

Major results are:

- Very high sulphate release at first rewetting, decreasing gradually after repeated rewettings.
- As a result, pH values are lowered, i.e. until less than 4 in peat from La Bergerie.
- Bivalent cations (Ca and Mg) are highly released. The low pHs, may favour high bivalent desorption.
- DOC is similar to the 80 % humidity peat, explained by pH buffering (low pH maintains low DOC solubility).
- Nitrate is produced in the first rewetting, which was not the case in the 80 % humidity peat. Because of concomitant Fe(II) and NH_4 presence, nitrogen oxidation is not expected to occur, but rather organic nitrogen mineralization.
- C biomass is increased relative to the 80 % humidity peat, suggesting that drying-out has favoured aerobic microbial communities growth.
- The desiccation experiment agrees with the hypothesis that the degradation state of pyrite, instead of the total content, is a key factor to explain higher pyrite oxidation.

Temporal patterns, as well as the presence or absence of redox-sensitive elements which informs about the range of redox potential, support the idea that high sulphate levels are not only a result of pyrite oxidation, but rather that mineralization is also occurring, involving organic sulphate esters.

As a overall overview, desiccation in peats from le Cotentin, taking into account two representative peat sites, seems to severely impact the peat structure by enhancing oxidation and mineralization mechanisms, resulting in a dramatic acidification, significant nutrient loss and impacting the catchment water quality. In addition, the impact on the peat structure and the biochemical functions leads to perennial alteration and retro-active mechanisms inducing even more alteration.

Chapter 2

Sensitivity of peat chemistry to water recharge quality

Introduction

The modelling results presented in Chapter 3 of Part I have highlighted that the anthropogenic impacts (both pumping and climate change) affect the wetland water level but also the water budget partitioning. The Cotentin wetland behaves globally as a discharge zone from the aquifer but this does not exclude more local reversed flows and stream contribution. For example doubling the water extraction in Sainteny catchment results in a downward flow (from wetland to aquifer) increase of 11 % (see Figure 3.8 in Chapter 3 form Part I). The origin of the water contributing to the wetland recharge is thus modified and consequently the water quality differs.

Changes in wetland water recharge quality have important consequences for the preservation of these freshwater ecosystems. Previous studies on wetland restoration have stressed the need for the restoration of both water quantity and water quality to prevent unexpected chemical reactions, like (internal) eutrophication (Van Dijk et al., 2004) (Lamers et al., 2002) (Loeb et al., 2007). Understanding these processes and their microbial mediators are of relevance in wetland restoration. Indeed, re-wetting peat with a water quality different from the original wetland may result in complex feedbacks. pH may both increase or decrease depending on the water quality, the organic matter state and the peat iron content (Lamers et al., 2002). pH increase may increase PO_4^{3-} availability and raise O.M. decomposition (Lamers et al., 2002). On the other hand, pH decrease is expected to enhance metal mobility, like Al, but to decrease DOC solubility (Reddy and Delaune, 2008).

Within the scope of water quality degradation in the wetlands of Normandy, the present study focuses on understanding the chemical processes in the peatlands, related to two different re-wetting waters: a natural stream water and a natural groundwater.

In order to test this, a laboratory experiment was conducted in peat cores from La Bergerie. Waterlogged peat cores were kept saturated during 15 days, and peat pore water was regularly monitored for a large set of chemicals. Four replicates were used at each sampling date, resulting in a total of 56 microcosms.

2.1 Materials and methods

2.1.1 Peat sampling

The peat cores were collected close to the pumping site La Bergerie. All samples were collected on one day (end of March 2009) under dry conditions. At this time the water level was at 55 cm below soil surface. Peat was collected at randomly selected plots (10 x 10 m area) in the unsaturated zone, just above the water table. This sampling layer was chosen to be in the range of the water table fluctuation, i.e. this peat was saturated at high water level and unsaturated at low water level periods. Replicated samples were obtained directly in push cores (6.4 cm diameter, 9 cm height) that were further used in the experiment. Caution was taken to minimize the disturbance of layers during collection and storage. The peat cores were thus bulk samples, preserving the field structure. The cores were put in polyethylene bags and returned to the laboratory within 6 hours. Peat material was characterized for physical structure, chemical nutrient content and biomass. Results were reported previously in Chapter 1.5 of Part II.

2.1.2 Experiment set up and monitoring

The experiment was carried out in an open microcosm system designed to approach the field conditions. Samples were waterlogged by the two tested waters and kept saturated throughout the 15 days experiment by immersing the peat cylinders in (mason) jars (see Figure 2.2). At the top of the core, a 1 cm water stratum enabled complete peat saturation all along the 15 days period to counteract evaporation loss. For each microcosm, peat and added water weights were measured (Table 2.1). Based on these data, a volume of 32 mL on average is required to saturate the peat cores. Peat humidity (24 h oven dry at 105°CC) was also measured on six sub-samples and gives an average value of 79 $\pm$ 2 %. Water was sampled in each peat core by use of 3 soil moisture samplers (Rhizon 19.21 from Eijkelkamp), at each date of measurement: day 1, 2, 3, 4, 6, 8, 11 and 15 (see Figure 2.1). The immersion water (i.e. around the cylinder) was also sampled on days 2, 8 and 15 to allow a total mass balance on the system. It also allows to check the diffusion between the peat core and the surrounding water. Jars containing only the two waters served as control. Four replicates were used at each sampling date, with a total of 56 microcosms. In addition, the jars can be closed (air-tight) for punctual incubation to allow gas analysis.

The peats cores were waterlogged either by a surface water collected from the river (the Holerotte) and a groundwater from a well (F1) at 40 meters depth. These two waters are from the vicinity of the collected peat site in La Bergerie. Chemical characteristics of these waters are given in Table 2.2.

Major differences between the two waters are (i) groundwater is globally more enriched in ions (around 7 meq/L for groundwater with respect to 5 meq/L for surface) (ii) groundwater has higher carbonate concentrations (alkalinity is 5.08 mmol/L for groundwater and 2.87 mmol/L for surface water) and (iii) groundwater has a higher nitrate content (37 mg/L compared to 18 mg/L in the surface water). The pH values are similar. Consequently, the discriminatory factor between the two waters is mostly due to their hardness (which is 6.33 meq/L for groundwater and 4.03 meq/L for surface water) and their nitrate content.

A temperature of 15 °C was used and was intended to speed up the rate of nutrient mobilization.

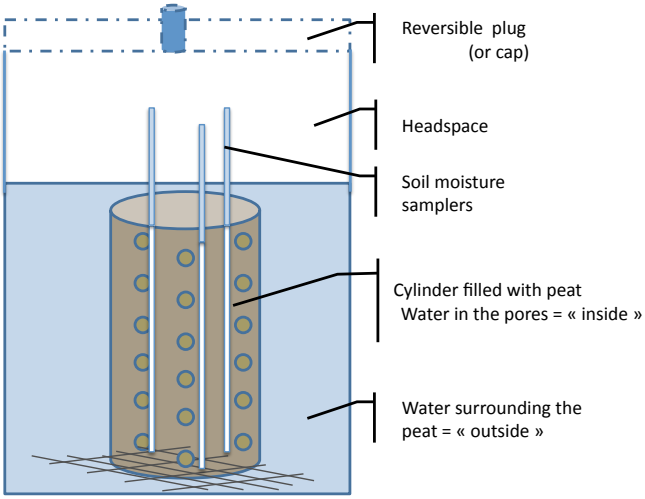

Figure 2.1: Microcosm design: peat in perforated Plexiglass cylinders is immersed in free water

Table 2.1: Volumes involved in the microcosm experiment. Values are averaged over 56 samples and are in mL

Volumes	average	standard deviation
Peat volume	289.3	9.2
Water volume into peat before saturation	212.7	8.8
Water volume into peat after saturation	244.4	9.0
Water volume to saturate the peat cores	31.7	12.5
Water volume added for immersion	570.0	10.6
Headspace (air) volume	141.3	7.4

It is somewhat higher than the average field temperature (around 12 $^{\circ}C$) but still in the field range. A three day period was used to reach stabilization in the laboratory conditions (previously checked by CO_2 analysis: after 3 days this respiration indicator has stabilized –results not shown). The two waters were also allowed to equilibrate with the atmosphere, i.e. their oxygen level is similar.

Figure 2.2: Microcosm design

Table 2.2: Surface (SW) and groundwater (GW) chemistry. In the experiments O_2 is allowed to equilibrate with the atmosphere before entering in contact with the peat microcosms, i.e. O_2 concentrations are similar in the two waters

	SW	GW		SW	GW
pH	7.54	7.65	Ca^{2+} ($mg.L^{-1}$)	57.7	110.2
EC ($\mu S.cm^{-1}$)	478	545	Mg^{2+} ($mg.L^{-1}$)	14	10
Eh (mV)	431	422	Na^{+} ($mg.L^{-1}$)	27	18
Cl^{-}($mg.L^{-1}$)	37	30.4	K^{+}($mg.L^{-1}$)	5.4	2.8
NO_3^{-}($mg.L^{-1}$)	18.3	36.6	Fe ($\mu g.L^{-1}$)	612	942
SO_4^{-} ($mg.L^{-1}$)	20.2	11.5	DIC ($mg.L^{-1}$)	40.0	70.4
O_2 ($mg.L^{-1}$)	3.2	2.2	DOC ($mg.L^{-1}$)	2.5	0

2.1.3 Chemical analysis of the water samples

Water samples were analysed for a large set of parameters and ions.

The pH was measured with a combined Mettler InLab electrode after a calibration performed with

WTW standard solutions (pH 4.01 and 7.00 at 25 C). The accuracy of the pH measurement is 0.05 pH units. The electrical conductivity (EC) was measured by a Consort electrode C533 which accuracy is of 0.01 μ S/cm. The redox potential (Eh) was measured by a Mettler Platinium 4805 electrode which accuracy is of 1 mV.

Dissolved organic carbon was analysed with a Total Organic Carbon analyser (Shimadzu TOC-5050A). The accuracy of DOC measurement was estimated at 3% (by using a standard solution of potassium hydrogen phtalate). Dissolved inorganic carbon was also measured with the Shimadzu TOC-5050A with an accuracy of 0.2%.

Major anion (Cl^-, NO_3^-, NO_2^-, PO_4^{2-}, SO_4^{2-}) concentrations were measured by ion chromatography (Dionex DX-120): the uncertainty was below 4%. Major cation (Ca^{2+}, Na^+, K^+, Mg^{2+}, Mn^{2+}, Fe) concentrations were determined by ICP-MS (Agilent 4500), using indium as an internal standard. The international geostandard SLRS-4 was used to check the validity and reproducibility of the results. Typical uncertainties including all error sources range from 2 to 5%, depending on the concentration.

Fe(II) concentration was measured by the 1.10 phenantroline colorimetric method, AFNOR NF T90-017 (AFNOR, 1997), using a UV visible spectrophotometer. Estimated uncertainty is 1%. NH_4 concentration was measured by the salicylic colorimetric method, DIN 38 406 part 23, section 2 and ISO/DIS 11732, using an automatic UV visible spectrophotometer No. G-102-93 Rev. 4 from Bran and Luebbe. Estimated uncertainty is 2%.

Finally, CO_2 was analysed by a micro gas chromatograph 3000 (from SRA Instrument) after one hour incubation. Estimated uncertainty is 1%.

2.1.4 Statistical analyses

Relationship between chemicals

A large range of chemicals were followed in our experiment to allow a comprehensive study of the inter-related reactions involved. To help finding out which reactions are likely to occur, a correlation analysis is carried out. First a principal component analysis (PCA) is carried out to help categorize the set of chemicals. Secondly, a multi-correlation matrix is calculated (by the Pearson r coefficient). This test assumes that the measurements have a bivariate normal distribution. If this assumption is not met for a large number of bivariates, a logarithmic transformation of all the data is tested. If this transformation does not improve the situation, a non parametric test is used instead on the corresponding set of data : the Spearman's rank correlation. Statistics are carried out with R (Foundation for Statistical Computing, 2010).

Comparison between the two treatments

One of the objectives of the experiment is to answer the question: is there a significant difference in reactivity between peat submitted to two different water compositions? Before running the statistical tests, the assumptions underlying these tests are checked: normal distribution of data (by Shapiro-Wilk test and histogram shape), equality of the variances (by Levene's test), similar distribution shape (by Kolmogorov-Smirnov test). On the set of data allowing a parametric test, an analysis of variance is carried out. All pair of means are then tested with the Tukey-Kramer test, using the water type

as explaining variable. On the set of data allowing only non-parametric tests, all pair of means are compared by the Mann-Whitney U-test. The level of confidence is set to 95 % . Likewise, statistics are carried out with R (Foundation for Statistical Computing, 2010).

2.2 Results

2.2.1 Chemical temporal patterns in the two treatments

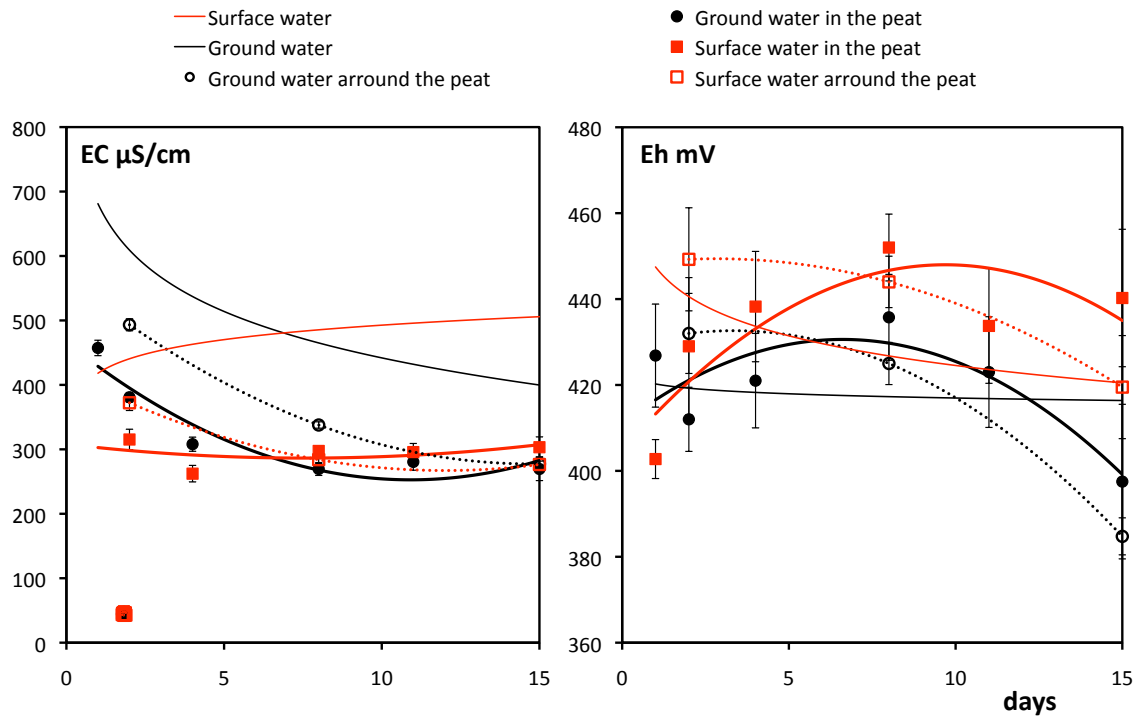

Figure 2.3: Changes in electrical conductivity (EC) and redox potential (Eh) during the 15 days incubation. Red lines : surface water; black lines: groundwater. Bold lines: peat pore water; dotted lines: ”outside” water; thin lines: controls

The two treatments show similar temporal patterns, and at first view do not reflect a high difference in peat reaction. For most of the chemicals, the 4 replicates show low standard deviation, reflecting the good ability of the peat samples and the experiment set up to control the reaction rates. However, statistical analysis will help to discriminate the two treatments.

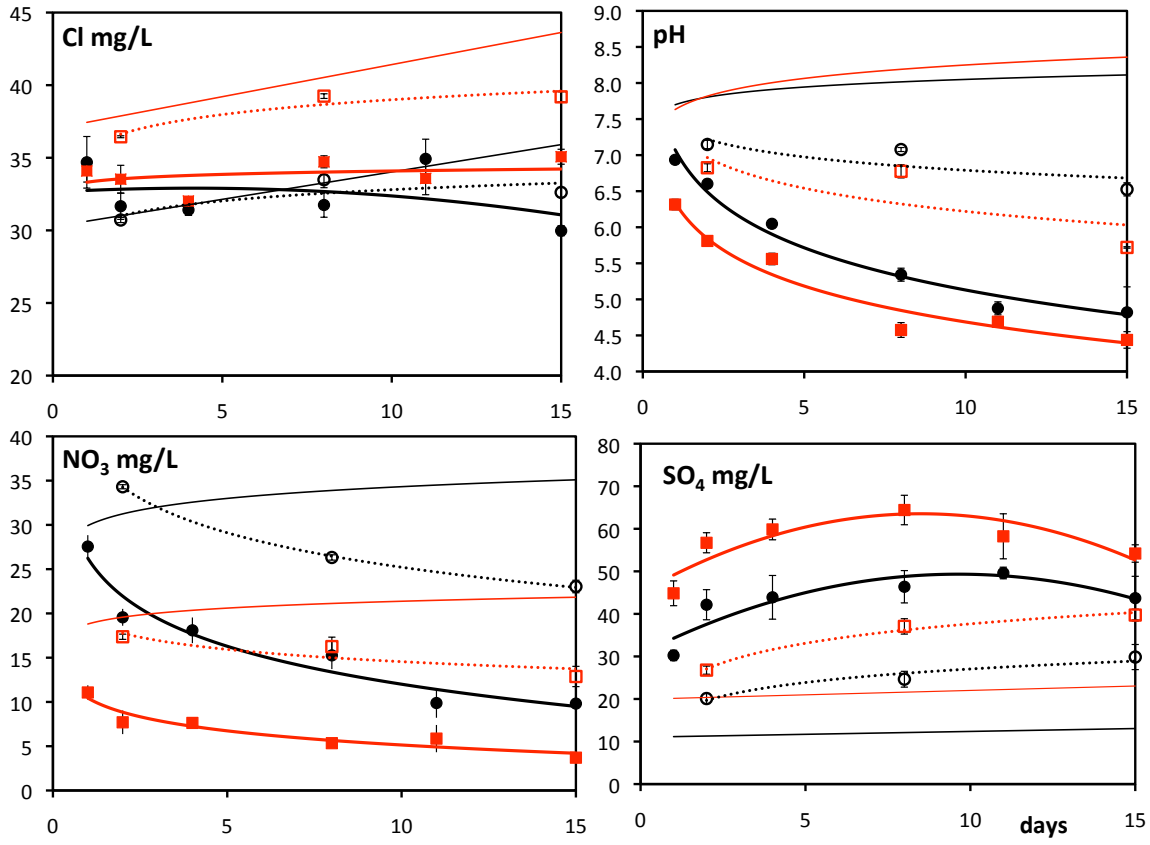

Figure 2.4: Changes in Cl, pH, NO_3 and SO_4 during the 15 days incubation. Red lines : surface water; black lines: groundwater. Bold lines: peat pore water; dotted lines: "outside" water; thin lines: controls

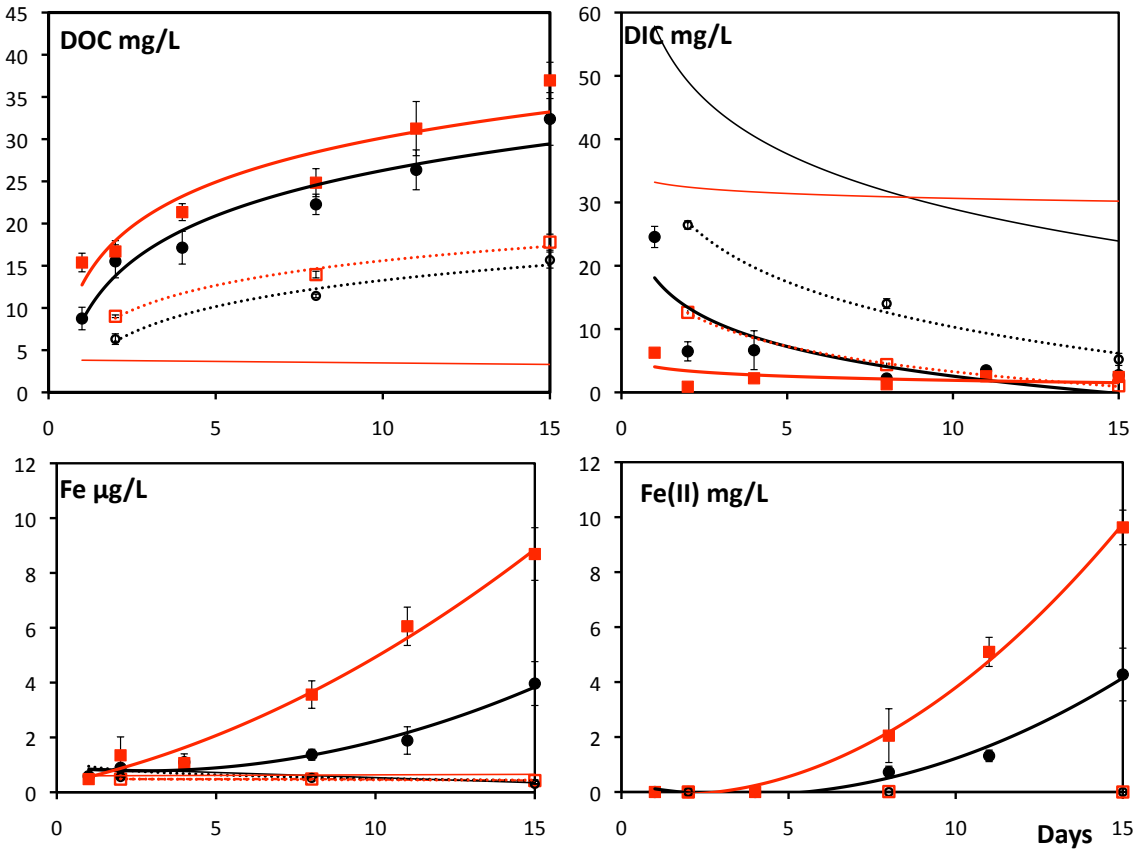

Figure 2.5: Changes in DOC, DIC, Fe(II) and Fe during the 15 days incubation. Red lines : surface water; black lines: groundwater. Bold lines: peat pore water; dotted lines: ”outside” water; thin lines: controls

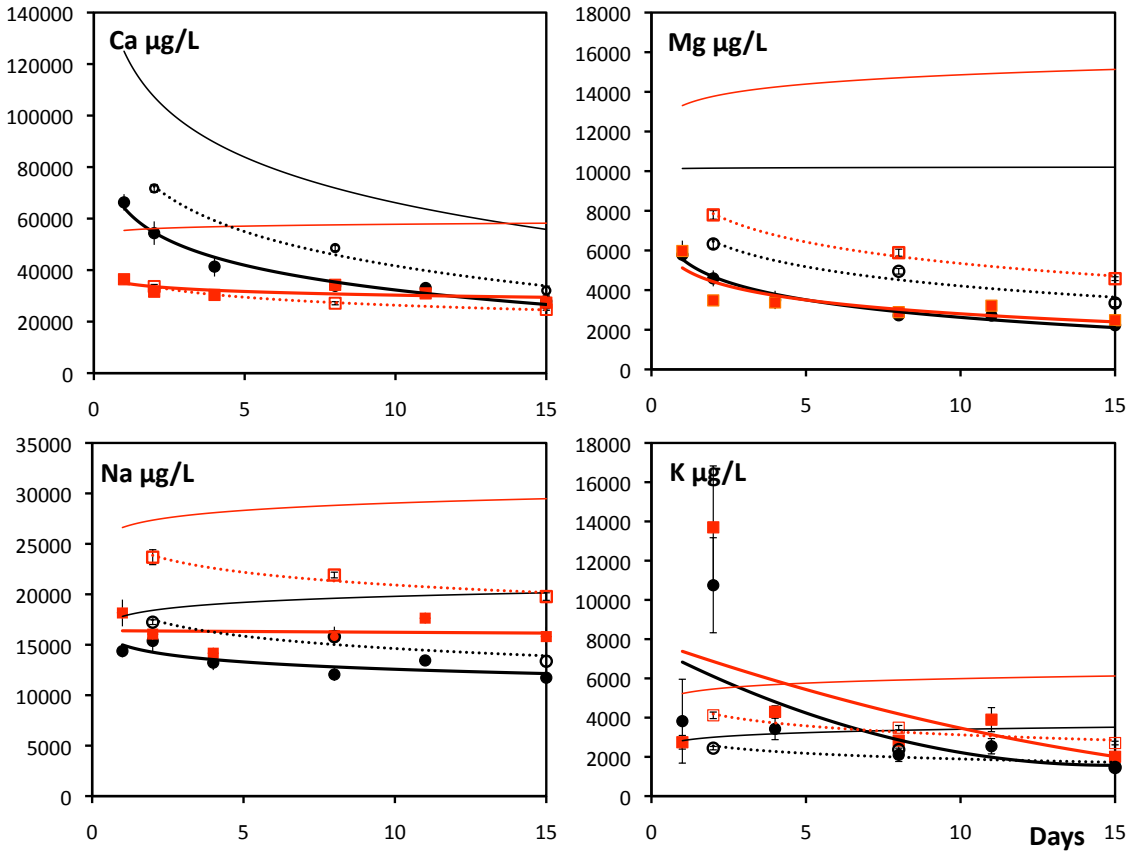

Figure 2.6: Changes in Ca, Mg, Na and K during the 15 days incubation. Red lines : surface water; black lines: groundwater. Bold lines: peat pore water; dotted lines: ”outside” water; thin lines: controls

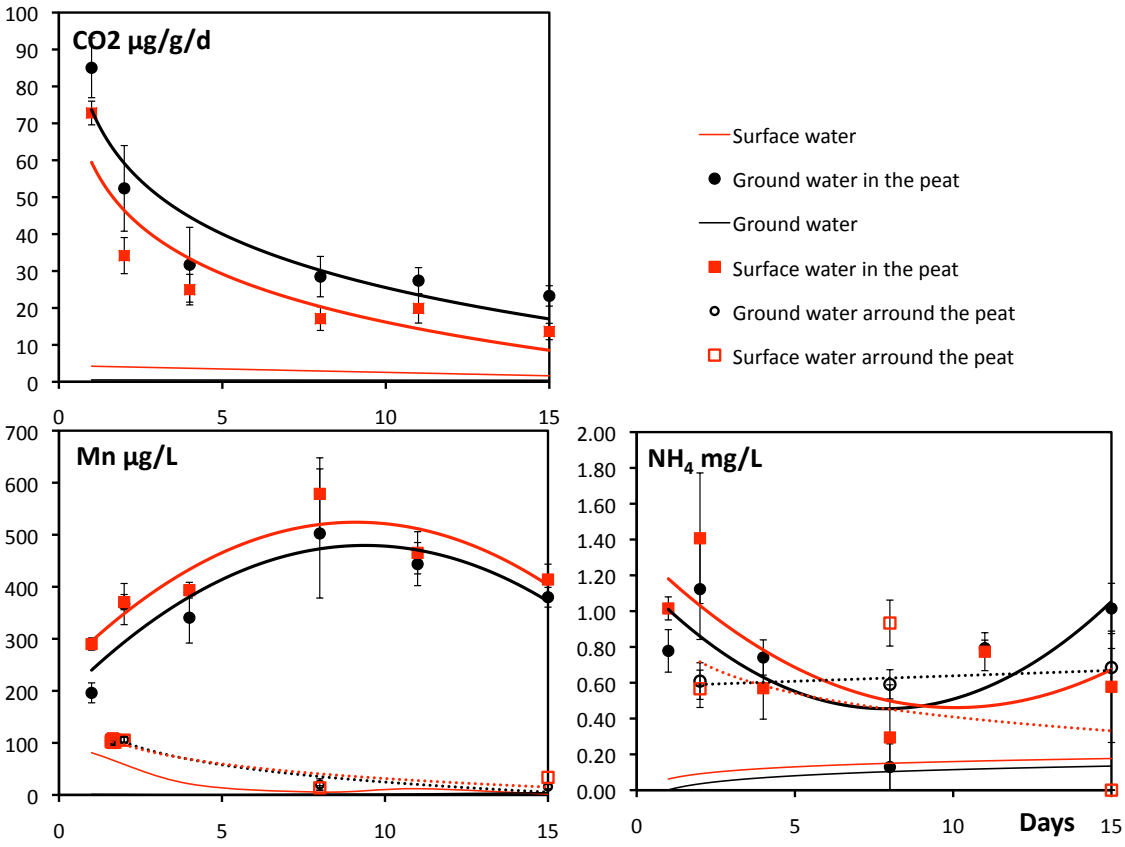

Figure 2.7: Changes in CO_2, Mn and NH_4 during the 15 days incubation. Red lines : surface water; black lines: groundwater. Bold lines: peat pore wataer; dotted lines: "outside" water; thin lines: controls

Table 2.3: Balance between day 2 and day 15 on some elements

	Surface water		Groundwater	
	inside water	outside water	inside water	outside water
NO_3^- (mg/L)	-3.99 ± 1.48	-4.49 ±1.18	-9.75 ±1.38	-11.27 ± 0.75
Mass balance total system (mg)	-3.39 ± 0.45		-8.44 ± 0.35	
SO_4^{2-} (mg/L)	-2.52 ± 7.33	12.94 ± 1.70	-4.55 ± 6.23	9.75 ± 3.19
Mass balance total system (mg)	6.35 ± 1.79		4.14 ± 1.56	
Dissolved inorganic carbon (mg/L)	1.54 ± 0.73	-11.60 ± 0.49	-3.74 ± 1.57	-21.23 ± 1.16
Mass balance total system (mg)	-5.86 ± 0.18		-12.33 ± 0.39	
Dissolved organic carbon (mg/L)	25.64 ± 6.81	8.78 ±0.96	16.87 ± 5.30	9.37 ± 1.14
Mass balance total system (mg)	10.98 ± 1.68		9.16 ± 1.31	
pH (units pH)	-1.37 ± 0.15	-1.11 ±0.23	-1.78 ± 0.36	-0.62 ± 0.11
Mass balance total system (units pH)	-0.93 ± 0.21		-0.77 ±0.20	

The temporal patterns of the main chemicals analyzed are illustrated in Figures 2.4, 2.5, 2.6 and 2.7. Each graph shows 6 curves: (1) the controls. i.e. the surface water and groundwater alone (thin lines) (2) the waters extracted from the peat for the two treatments (Figure 2.1 "inside") (bold lines) and (3) the waters around the peat cylinders (Figure 2.1 "outside") (dotted lines). For both curves (2) and (3), the 4 replicate means and standard errors are shown. In addition, a mass balance between the beginning and the end of the experiment (day 15 - day 2) is calculated for several elements and reported in Table 2.3. Mass balance on the total system is calculated by taking into account the volumes of the two water bodies in the microcosm: i.e. the "inside" water and the "outside" water (Figure 2.1 and Table 2.1) where reactions occur. This mass balance is intended to give a complete picture of the microcosm.

Electrical conductivity and redox environment (Figure 2.3)

The electrical conductivity (EC) in the peat pore water is lower than the EC in the surrounding water saturating the cylinder which is in turn lower than the EC in the control, at the beginning of the experiment. However after 15 days, for both treatments, the ECs in the microcosms become similar. ECs tend to homogenize in the total microcosm system. EC in the groundwater declines, related to carbonate precipitation (see later). The redox potential (Eh) shows high standard errors, making trends difficult to estimate. However, the surface water seems to have higher Eh, i.e. a less reductive environment than the groundwater treatment. In addition, the outside waters seems to show Eh decline in time.

Cl^-, pH, NO_3^- and SO_4^{2-} (Figure 2.4)

Cl^- Chloride concentrations show some random fluctuations in the peat water, probably reflecting the intrinsic peat heterogeneity between replicates. A linear increase is visible in the controls, due to evaporation: on average, a 1 % per day evaporation is calculated.

pH For both batch treatments, pH in the peat pore water decreases dramatically whereas no change occurs in the controls. The final pH after 15 days is 4.4 and 4.8 (on average) in the surface water and the groundwater treatments respectively. The surrounding pH water also decreases. Results of the balance between day 2 and 15 are shown in Table 2.3: surface water microcosm pH declines by 0.93 units (SD: 0.21) while groundwater microcosm pH declines by 0.77 (SD: 0.20).

NO_3^- Both treatments behave in the same way with an exponential decrease. The outside water concentrations also decrease, although the values are at least 2 orders of magnitude higher than the inside waters. Mass balance (Table 2.3) indicates a decline of 3.4 mg (SD: 0.4) in the surface water microcosm and a decline of 8.4 mg (SD: 0.3) in the groundwater microcosm. Nitrate remains unchanged in the controls.

SO_4^{2-} Sulphate is clearly produced in all the microcosms. The surface water treatment produces a maximum of 64 mg/L sulphate in the peat pore water relative to an inlet concentration of 21 mg/L. The groundwater treatment produces a maximum of 46 mg/L sulphate relative to an inlet concentration of 11 mg/L. Mass balance (Table 2.3) results in a net increase of 6.3 mg (SD: 1.8) in the surface water microcosm and 4.1 mg (SD: 1.5) in the groundwater microcosm. However, sulphate seems to decline in the peat pore waters for both treatments during the last experiment period (after day 8).

DOC, DIC, Fe and Fe(II) (Figure 2.5)

Dissolved Inorganic Carbon Dissolved inorganic carbon (DIC) decreases in both treatments. The complete microcosm is dramatically depleted in DIC, as can also be seen in the mass balance calculation (Table 2.3). It can be noticed that DIC precipitates in the groundwater control (saturation index SI relative to calcite is 10.6), while no change occurs in the surface water control (SI of 0.2).

Dissolved Organic Carbon Dissolved organic carbon (DOC) is produced in both treatments and increases exponentially (see also the mass balance on the complete microcosm in Table 2.3). At day 15 the increasing rate is still going on, reaching around 33 mg/L and 27 mg/L in the surface peat pore water and the groundwater peat pore water treatments respectively.

Iron The total Fe concentration measured by ICP-MS increases from day 4 in the peat pore water and is clearly related to the appearance of Fe (II).

The cations: Ca^{2+}, Mg^{2+}, Na^+ and K^+ (Figure 2.6)

The major cations are lower in the microcosms than in the controls. The cations of valence 2, Ca^{2+} and Mg^{2+}, show similar trends, i.e. an exponential decrease. It can be noticed that Ca^{2+} decreases exponentially in the groundwater control. This decrease can be again related to calcite precipitation like already noticed for the DIC decrease. Na^+ is also lower in the microcosms. K^+ overall trend shows a similar behaviour, however a peak concentration is observed on day 2.

CO_2, Mn and NH_4^+ (Figure 2.7)

CO_2 CO_2 production is high at day 1 (surface water 72.8 (SD 6.4), groundwater 85.0 (SD 8.1) μg/g/day) and then decreases exponentially with time. At the end of the experiment concentrations are around 20 μg/g/day. CO_2 concentration in the controls remains very low.

NH_4^+ Methane is indeed present along the experiment, but at low concentrations. No trend, but random fluctuations are observed, even in the controls.

Mn Mn increases until day 8 in the peat pore water while the surrounding water (and the control) remains at low concentrations.

2.2.2 Relationship between elements

Figure 2.8 shows a graphical view of the Principal Component Analysis (PCA) : the samples distribution, the parameters distribution on components 1 and 2 (respectively 49 and 18 % contribution to the total variance) and components 1 and 3 (10 % contribution to the total variance) and the "ward" dendogram. Pearson correlation coefficients are also computed : results are presented in Appendix C. Fe and Fe(II) are strongly correlated (r=0.979) and therefore only Fe is kept in order to not distort the analysis.

The PCA differentiates the groups DOC-Fe-Mn^{2+} and SO_4^{2-} on one side, and pH-Ca^{2+}-Mg^{2+}-DIC and NO_3^- on the other side of the first component. The first group of elements are increasing along the experiment, while the other elements are decreasing. The second component integrates the variance of Cl^-, Na^+ and K^+.

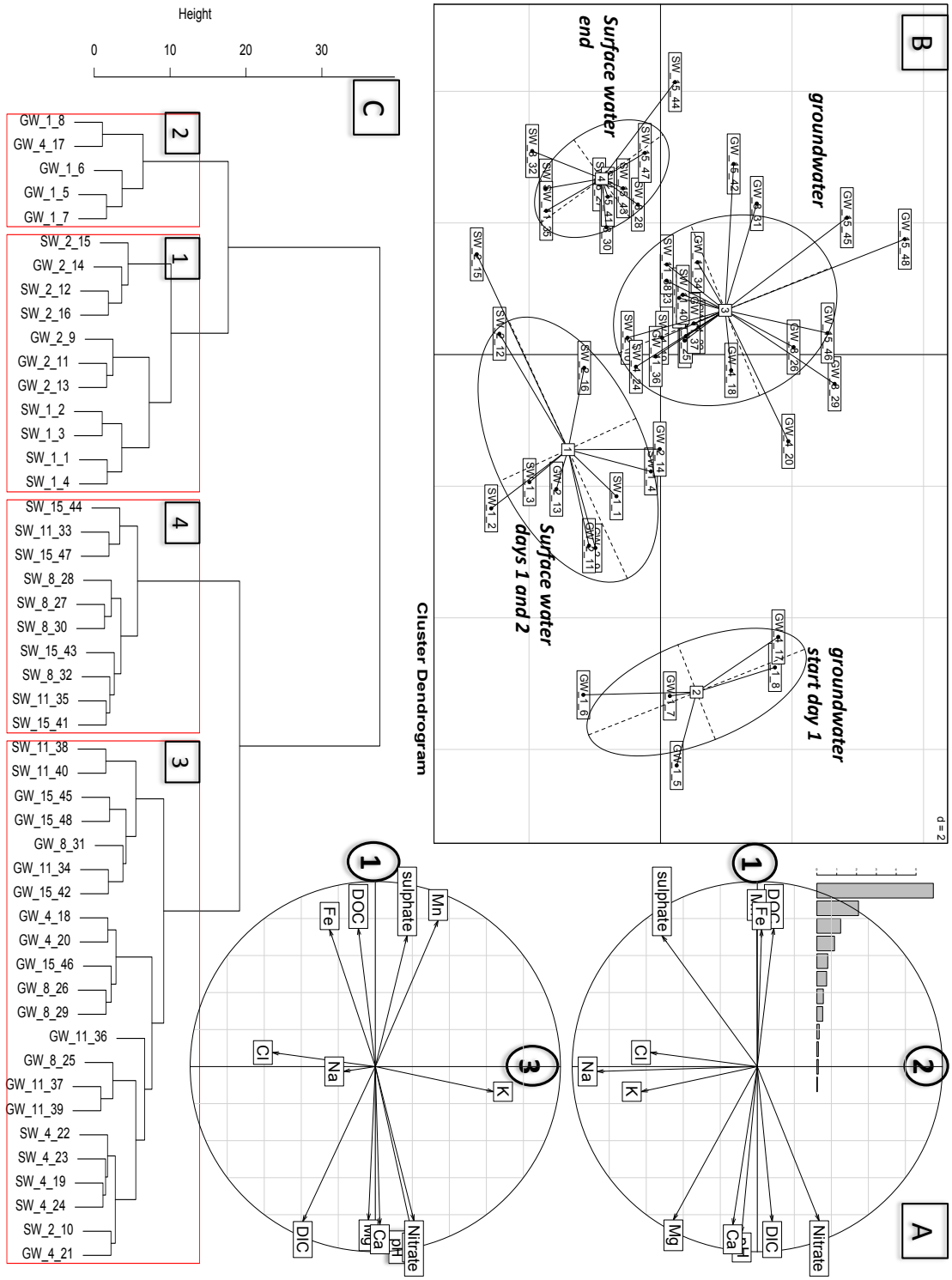

Figure 2.8: Graphical representation of the PCA analysis on the peat pore water data base from the microcosm experiment. Temporal patterns are figured by arrows in panel B

2.3 Discussion

2.3.1 Reactions involved

A major part of Fe and SO_4^{2-} concentrations may be the result of the oxidation of inorganic iron sulphur containing minerals (e.g. pyrite FeS_2). Oxidation of pyrite or other metal-sulfide minerals by oxygen or nitrate has a large environmental impact and plays a key role in the formation of acid sulphate soils resulting from drainage of lowlands (Appelo and Postma, 2005) (Rimstidt and Vaughan, 2003). Consequently, the low pH in this peat pore water may result from sulphur oxidation to SO_4^{2-} which produces H^+ (Pearson coefficient is -0.531), rather by oxygen or $NO_3{}^-$. The possible reactions involved, depending on the electron donor (O_2 or $NO_3{}^-$), are thus :

$$FeS_2 + \frac{15}{4}O_2 + \frac{7}{2}H_2O \rightleftarrows Fe(OH)_3 + 2\ SO_4^{2-} + 4\ H^+$$

$$FeS_2 + 3\ NO_3{}^- + H_2O \rightleftarrows FeOOH + \frac{3}{2}N_2 + 2\ SO_4^{2-} + H^+$$

Figure 2.9 shows a bi-variant plot of $NO_3{}^-$ versus SO_4^{2-} in meq/L. As $NO_3{}^-$ is strongly anti-correlated with SO_4^{2-} (Pearson coefficient is -0.721) it can be suggested that $NO_3{}^-$ is indeed a strong oxidizer. The stoichiometric equivalence highlighted in Figure 2.9 argues that the oxidation of pyrite is mainly driven by $NO_3{}^-$. Fe is coupled with DOC (Pearson coefficient is 0.859) which suggest that Fe is rapidly complexed with colloidal organics (Steinmann and Shotyk, 1997). DOC is increasing in both experiments: it can be suggested that the pH increase due to the peat wetting by a 7.5 water pH increases negative charges within the carboxylic or phenolic groups, leading to more hydrophilic organic carbon (Reddy and Delaune, 2008) which solubility increases (see Figure 2.10). pH is found together with Ca^{2+}, Mg^{2+} and DIC on the PCA. Surprisingly, the common solubilization of carbonates or clays in an acidic environment, resulting in cations leaching is not occurring here. Conversely, the bivalent cations entering in the peat are partly depleted in the peat pore water and the surrounding water. A possible explanation is again that the increasing negative charges within the carboxylic or phenolic groups induced by a 7.5 water pH makes cations binding more efficient (Figure 2.10) (Skyllberg and Magnusson, 1995).

K^+ and Na^+ are orthogonal to the bivalent cations. This suggest that while the bivalent cations are readily adsorbed within the peat, the mono-valent cations are more mobile. This agrees with the preferential cations order of binding to exchange sites which is : $Al^{3+} > Ca^{2+} > Mg^{2+} > K^+ = NH_4^+ > Na^+$ (Appelo and Postma, 2005).

Finally the CO_2 flush just after flooding may be explained by enhanced micro-organisms respiration.

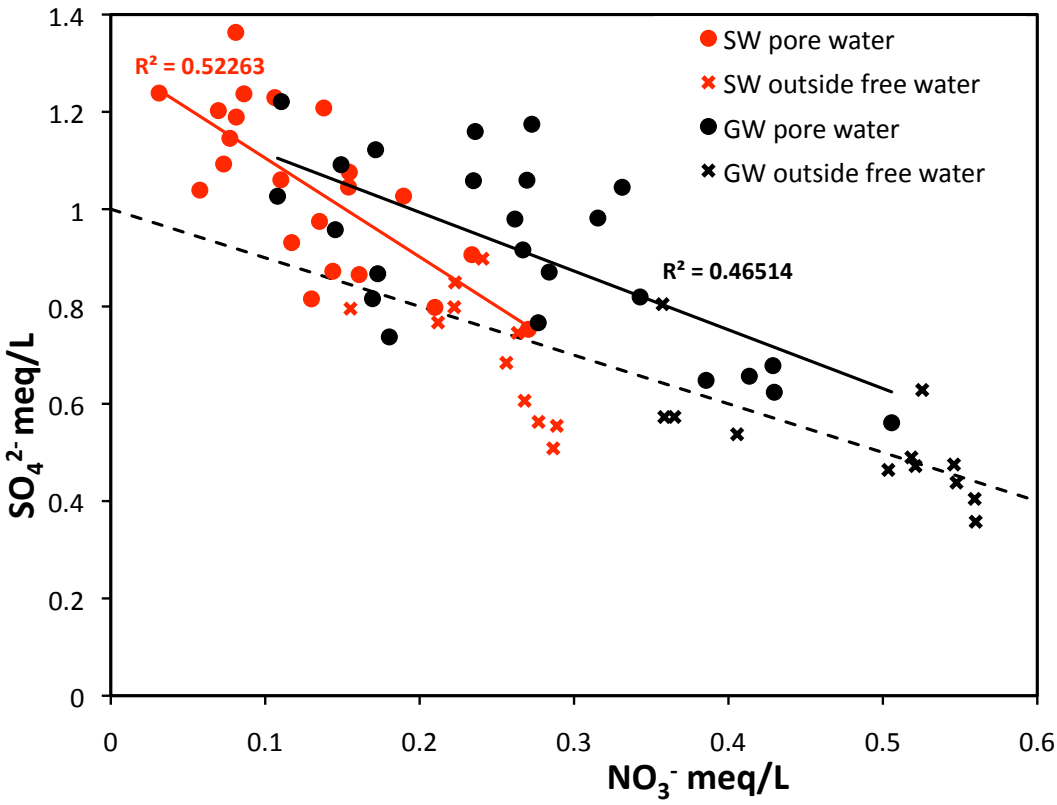

Figure 2.9: Plot of NO_3^- versus SO_4^{2-} in meq/L. Black dots are the peat pore water data and red squares the "outside" water data. The thin dotted line illustrates the stoichiometric one by one equivalence: 1 meq of NO_3^- produces 1 meq of SO_4^{2-}

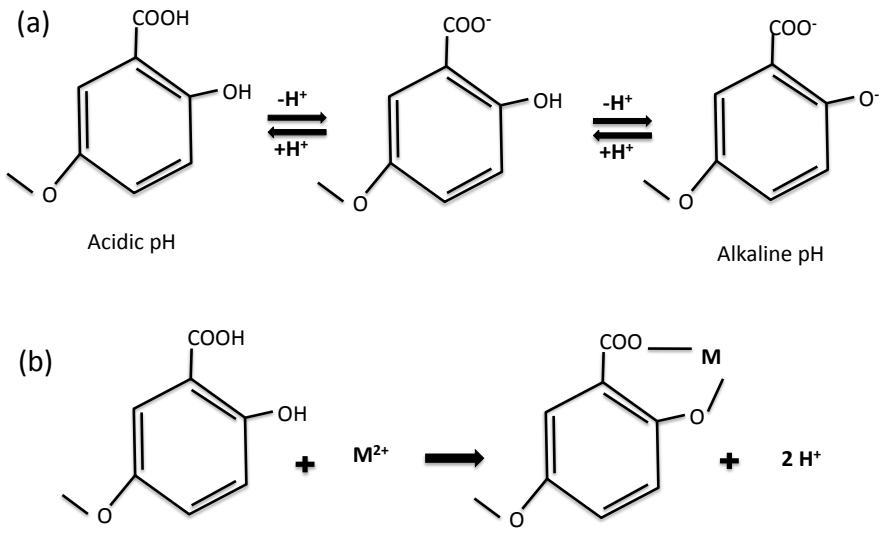

Figure 2.10: (a) Extent of negative charge in soil organic matter as a function of pH. (b) Soil organic matter complexation with metals (M = metal). After Reddy and DeLaune (Reddy and Delaune, 2008)

2.3.2 Comparison between the two treatments: surface water and groundwater

As a first insight on the overall chemical trends, the peat pore water seems mainly controlled by equilibrium states and redox constraints. The microcosms approach similar concentrations within the two water treatments, suggesting that the peat is efficient in " buffering " the water composition. However, appropriate statistics enable to point out statistical significant differences. First, the samples distribution plotted on the PCA from Figure 2.8, panel B discriminates 4 groups based on the "ward" dendogram in panel C. Surface and groundwater samples are spatially differently distributed, although there is no strict discrimination in group number 3 where some surface water samples are included. In addition, a temporal pattern, for both treatments, may be observed. Basically, the groundwater treatment starts in a "carbonated" pole and moves to a more neutral zone (no predominant variance of the chemical parameters). The surface water treatment starts in a neutral zone and moves to a "sulphate" dominated pole. This suggests that the surface water treatment induces more oxidizing conditions.

Because the PCA highlights possible differences between treatments, an analysis of variance is carried out. First the normality of each chemical variable is tested. If the data is not normal, the shape of the distributions is compared (must be similar for non parametric tests). Finally the equality of the variances is checked. Table 2.4 synthesizes these results.

Table 2.4: Test on the normality of the data and the equality of the variances

Normal				Non normal	Similar
Bold: variances are equal — *Italic*: variances are not equal					shape distribution
pH	**NO_3^-**	**K^+**	*Ca^{2+}*	*NO_2^-*	yes
Eh	**SO_4^{2-}**	**Mg^{2+}**	**CO_2**	**PO_4^{3-}**	yes
EC	**DOC**	**Si**	*Fe and Fe(II)*	**NH_4**	yes
Cl^-	**Na^+**	**Mn^{2+}**	*DIC*	Alkalinity	yes

Logarithm transformation of the data does not help to increase the number of normal distributed parameters. The non normal data has a similar distribution shape (skewed right or left) between the two treatments: a non parametric test is thus possible. For some parameters, the variances are not equal. However this assumption can be ignored, assuming the analysis of variance is not very sensitive to this violation (sample size n = 48). On the normal distributed data, an analysis of variance is carried out using the water type as explanatory variable. Results are presented in Table 2.5. Confidence interval is taken at 95 %, which means that if P-value is less than 0.05, the difference between treatments is significant. On the non normal distributed data, a Mann-Whitney U-test is carried out on each pair of variables. Results are presented in Table 2.6.

Statistical results highlight differences between treatments. The elements will be discussed from low P values to higher P values, i.e. from high absolute differences to lower absolute differences.

Firstly, NO_3^- decrease is different, probably due to different inlet concentrations: surface water inlet is 18 mg/L while groundwater inlet is 37 mg/L. It can be noticed that, in the surface water

Table 2.5: Analysis of variance to point out statistical differences between the two water treatments on the normal distributed data. Degree of freedom: 1 for the water treatment, 46 residuals. confidence interval is taken at 95 %

Variables		Sum of squares	Mean square	F	P	Difference
pH	Between treat.	3.5	3.5	4.8	0.03	yes
	Within treat.	33.1	0.7			
Eh	Between treat.	963.	9631	1.2	0.36	no
	Within treat.	1563	26			
Cl^-	Between treat.	39	39	3.0	0.009	no
	Within treat.	256	5			
NO_3^-	Between treat.	992	992	33.4	6.179e-07	yes
	Within treat.	1365	29			
SO_4^{2-}	Between treat.	904	904	9	0.003	yes
	Within treat.	4419	96			
DIC	Between treat.	309	309	8.3	0.005	yes
	Within treat.	1705	37			
DOC	Between treat.	574	574	4.7	0.034	yes
	Within treat.	5588	121			
Na^+	Between treat.	102337825	102337825	28.65	2.672e-06	yes
	Within treat.	164329530	3572381			
Mg^{2+}	Between treat.	6552	6552	0.004	0.95	no
	Within treat.	77062020	1675261			
K^+	Between treat.	9406304	9406304	0.49	0.4851	no
	Within treat.	873327281	18985376			
Ca^{2+}	Between treat.	1442304449	1442304449	12.62	0.0009	yes
	Within treat.	5255891699	114258515			
Mn^{2+}	Between treat.	26574	26574	1.60	0.21	no
	Within treat.	761429	16553			
Fe	Between treat.	25687881	25687881	9.32	0.002	yes
	Within treat.	421245666	9157514			
CO_2	Between treat.	125	125	8.05	0.009	yes
	Within treat.	963	63			

treatment, NO_3^- decrease is faster at the very beginning (day 1) of the experiment. This suggest that reduced conditions are faster established in this treatment, as agrees with the lower Eh (Figure 2.3) at this specific stage. In addition NO_3^- ends at a lower concentration after the 15 days experiment. On the other hand, NO_3^- reduction rate is higher in the groundwater treatment, which agrees with the theoretical kinetics: a higher level induces a higher reduction rate (Appelo and Postma, 2005).

Secondly, Na^+ also shows a high difference: this element has a low binding capacity (remind preferential cation binding order reported before), which makes it sensitive to the inlet level of con-

Table 2.6: Statistical significance between the two treatments on the non normal distributed data — Mann-Whitney U-test. Confidence interval is taken at 95 %

	P	Difference
NO_2^-	0.076	no
PO_4^{3-}	0.590	no
Alkalinity	0.009	yes
NH_4	0.950	no

centration. As Na^+ is quite higher in the surface water, this difference is maintained in the microcosm.

Thirdly, Ca^{2+} shows a different trend: the almost twice higher inlet concentration in the groundwater is reflected in the microcosm, in the first experimental period, and then attenuates at the end of the experiment. This suggest that the Ca^{2+} concentrations are not limited in their binding capacity to the organic matter (Figure 2.10).

Fourthly, SO_4^{2-}, DIC, Fe and Fe(II), alkalinity and CO_2 show statistical differences. Finally, pH and DOC also show differences. The surface water treatment produces more SO_4^{2-}, Fe and Fe(II) and results in lower pH values. The already discussed pyrite oxidation reaction agrees with these concentration levels. This suggest that the surface water treatment favours oxidation relative to the groundwater treatment. And this, despite a lower NO_3^- inlet concentration which was demonstrated to be a powerful pyrite oxidizer. The surface water contains 2.5 mg/L DOC while it is below detection limit in groundwater. We suggest that the surface water treatment induces more oxidizing conditions, probably related to a higher biologically catalytic efficiency.

Conclusion

This experiment tested the chemical behaviour of bulk peat cores to saturation with two different waters contributing to the peatland recharge in the field. Groundwater taken from below the wetland and river water in the close vicinity were used. These two waters are mainly differentiated by their hardness and their nitrate content, both higher in the groundwater. There are small amounts of DOC (2.5 mg/L) in the surface water, while the concentration is below detection limit in the groundwater. Oxygen and pH are similar.

Both treatments appear to involve similar reactions, mainly nitrate decrease, sulphate, (total and ferrous) iron and dissolved organic carbon production. Iron sulphide (e.g. pyrite FeS_2) oxidation produces high SO_4^{2-} concentrations. The nitrate/sulphate anti-correlation suggests that nitrate behaves as a strong oxidizer. In addition, this reaction explains the level of acidification.

Fe is coupled with DOC which suggests that Fe rapidly complexes with colloidal organics. DOC is increasing in both experiments: it can be suggested that the pH increase due to the peat wetting by a 7.5 water pH increases negative charges within the carboxylic or phenolic groups, leading to more hydrophilic organic carbon which solubility increases. Likewise, these increasing negative charges make cations binding more efficient resulting in cations decrease.

Regarding the differences between the two treatments, the surface water treatment produces more sulphate, iron and DOC which seems to demonstrate that more oxidation occurs. We argue that surface water has a slightly higher biologically catalytic efficiency.

Finally, in a wetland restoration perspective, it appears that in the Cotentin peatlands the type of water contributing to the wetland water level increase is not dramatically impacting the peat biochemical functioning, at least not in the range of the two tested waters. We may conclude that an increase of the contribution of one or the other of these water sources may not be damaging. However the laboratory experiment gives a short term perspective. The relatively higher oxidation efficiency of surface water may, on long time scales, significantly impact the peatland. This agree with the observed differences in peat state and oxidation sensitivity between Le Marais and La Bergerie reported in Chapter 2 of Part II. Surface water and stream water are indeed more contributing to the peatland recharge in La Bergerie.

Part IV

Synthèse générale

Cette étude a été initiée par le Parc Naturel Régional du Cotentin et du Bessin afin notamment de répondre aux questions suivantes: (1) mieux comprendre le fonctionnement hydrologique des zones humides dans le bassin hydrologique global, incluant la nappe souterraine et les eaux de surface (2) mesurer l'impact sur les zones humides d'une augmentation du pompage dans la nappe, et du changement climatique (3) étudier l'impact de ces changements sur le fonctionnement biochimique de la tourbe. L'objectif opérationnel est d'aider au dimensionnement des futures mesures conservatoires.

La démarche suivie est restituée en trois grandes parties.

Partie I: L'hydrologie du système

1. Une caractérisation de la zone humide complétée par une étude géophysique de l'épaisseur des tourbes.
2. Une caractérisation de l'aquifère par datation des eaux et analyses chimiques.
3. Une modélisation numérique en 3 dimensions pour déterminer les impacts respectifs d'une augmentation du pompage et du changement climatique.

Partie II: L'impact de fluctuations rapides des niveaux d'eau sur les processus biochimiques: le court terme

1. Une caractérisation des processus biochimiques dans l'eau au contact de la tourbe en réponse à une alternance de cycles aérobies/anaérobies (a l'échelle du court terme).
2. Les différences globales de comportements lors de cette dynamique de fluctuations pour estimer leurs effets bénéfiques ou non, par rapport à des conditions stagnantes.
3. Une approche préliminaire de la réponse de la biomasse et des communautés microbiennes en fonction des alternances et sites étudiés.

Partie III: L'impact de changements environnentaux sur les processus biochimiques: le long terme

1. L'impact de la dessiccation de la tourbe suite à un assèchement prolongé
2. L'impact de la recharge de la tourbière par deux types d'eau, soit une eau de cours d'eau et une eau souterraine.

Cette partie de synthèse générale récapitule les résultats majeurs obtenus en réponse à ces questions et dégage les perspectives qui pourront en être tirées dans une optique de conservation.

Chapter 1

Hydrologie du système

Les méthodes de caractérisation de l'aquifère utilisées dans cette étude (datation et chimie des eaux, géophysique, modélisation, biochimie), ont montré leurs complémentarités et permis d'acquérir une compréhension globale du système.

A: Compréhension conceptuelle du fonctionnement de l'aquifère

Une synthèse des données piézométriques disponibles depuis le début des années 1990 a tout d'abord permit de reconstruire la carte piézométrique du bassin aquifère de Sainteny-Marchésieux. Une carte synthétique est reportée dans la Figure 1.1.

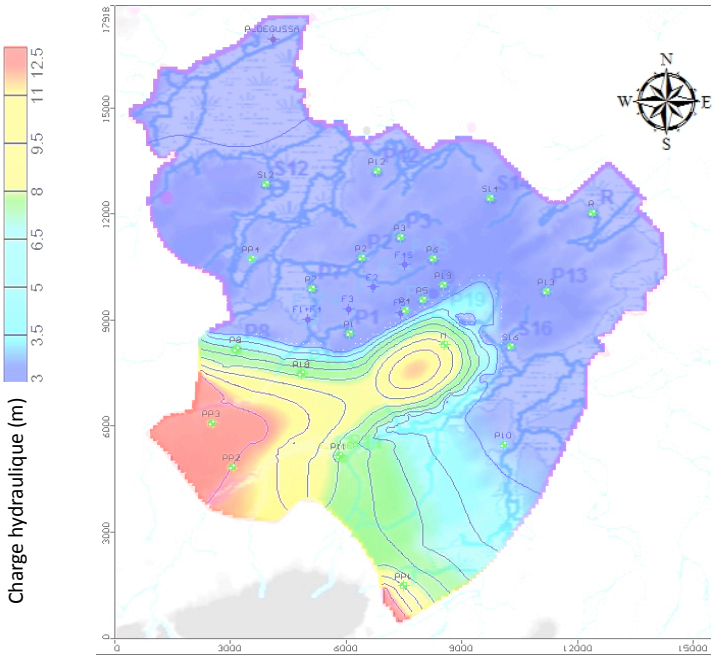

Figure 1.1: Carte piézométrique synthétique du bassin aquifère

Une première approche a utilisé la datation des eaux souterraines par le dosage de trois traceurs chlorofluorocarbonés (CFC) et de l'hexafluorure de soufre (SF_6), combinée à l'analyse chimique de ces eaux. Elle a permis d'acquérir une compréhension conceptuelle de l'aquifère. **La Figure 1.2 synthétise ce modèle conceptuel et met en évidence une bonne concordance des résultats de datation par rapport à la carte piézométrique.**

Les eaux échantillonnées réflètent une distribution verticale des temps de résidence. Des eaux plus jeunes sont captées dans les horizons supérieurs de la zone de recharge, des eaux plus agées sont captées en profondeur ou dans la zone de décharge. Cette analyse a permis d'accéder au temps de résidence moyen des eaux dans l'aquifère: il est estimé à environ 55 ans, cohérent avec une datation précédente par tritium, réalisée par les autoritées il y a quelques années.

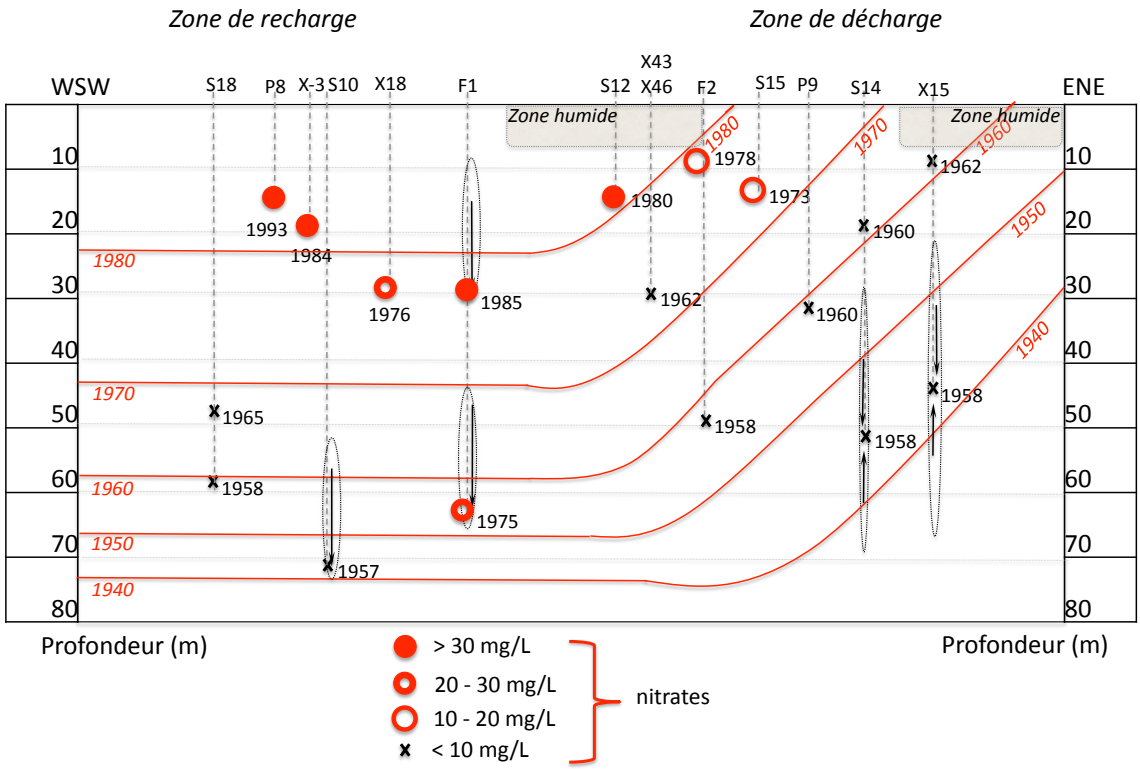

Figure 1.2: Modèle conceptuel représentant le fonctionnement de l'aquifère: une zone de recharge située à l'ouest-sud-ouest, juxtaposée à une zone confinée ou semi-deconfinée de décharge incluant la zone humide

B: Vulnérabilité de l'aquifère aux pollutions

L'analyse conjointe des âges et des nitrates met clairement en évidence la vulnérabilité de l'aquifère aux pollutions. Les eaux rechargées après les années 1970 contiennent sytématiquement

des nitrates (voir Figure 1.3). Les concentrations sont relativement importantes pour une eau souterraine. Dès les années 1980 les nitrates s'échelonnent entre 30 et 40 mg/L, atteignant 53 mg/L pour l'eau la plus récente datée de 1993. La pollution diffuse engendrée par les intrants agricoles est nette. Par conséquent, l'idée communemment répandue, que l'aquifère est protégée des pollutions grâce aux larges zones confinées (ou semi-confinées) au droit des tourbières, n'est pas correcte. En effet, la nappe souterraine est majoritairement alimentée dans le "Haut Pays".

Ce constat doit alerter sur la pérenité de l'exploitation de cet aquifère pour l'eau potable, communemment reconnue comme de très bonne qualité, car captant des eaux majoritairement âgées.

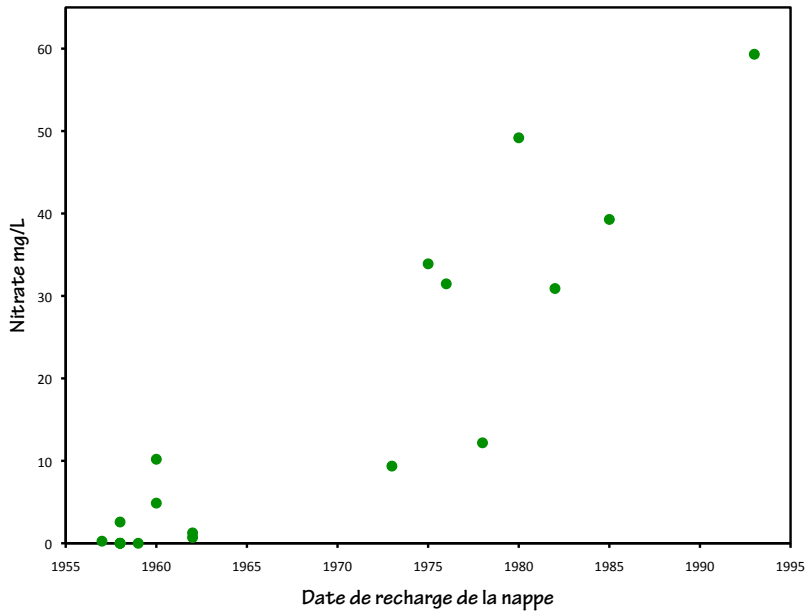

Figure 1.3: Relation entre l'âge de la nappe souterraine et les concentrations en nitrate

C: Vulnérabilité de la zone humide aux pressions anthropiques

La qualité et la quantité de données disponibles ainsi que l'élaboration du modèle conceptuel ont permis d'alimenter un modèle numérique en 3 dimensions (sous Visual MODFLOW) qui intègre une certaine complexitée. L'objectif était de tester la **vulnérabilité de la zone humide à un accroissement de l'extraction en eau potable dans l'aquifère sous-jacent et au changement climatique attendu à l'horizon 2090-2100**.

Le modèle tient compte des interactions entre l'aquifère et la zone humide, la topographie, et intègre une "limite de drainage" controlée par la topographie, qui détermine librement les aires de

drainage. Cette méthodologie a aboutit à un modèle bien calibré, notamment en reproduisant correctement l'étendue des zones humides.

Différents scénarios de diminution ou d'augmentation de pompage ont été testés. Les résultats sont synthetisés sur la Figure 1.4 pour ce qui concerne les flux entre compartiments et le Tableau 1.1 pour l'impact sur les niveaux d'eaux et les surfaces impactées dans le marais.

Les conclusions majeures sont les suivantes:

- **Les flux ascendants dominent les échanges entre la nappe souterraine et le marais**, concordant avec le postulat que le marais est majoritairement une zone de décharge de la nappe souterraine.
- Le modèle prédit toutefois des flux descendants plus importants du marais de la Sèves vers la nappe souterraine, comparées à ceux de la Taute, même dans le cas du modèle sans contrainte anthropique (sans pompage).
- **Le pompage engendre une augmentation des flux descendants** .
- **L'abaissement (et le maintien à un bas niveau) du niveau d'eau dans la tourbière de Baupte, anciennement exploitée, représente un prélèvement d'eau important** (de l'ordre de 10 Mm^3/an). Ce pompage impacte significativement le marais dans son ensemble, et plus particulièrement celui de la Sèves. Toutefois, en l'état actuel du modèle, la quantification de cet impact est hasardeux, une approche simplificatrice ayant été adoptée pour représenter le niveau d'eau à Baupte, et le modèle calibré avec cette condition.
- **Les pompages montrent un impact important sur les niveaux d'eau dans le marais de la Sèves**, bien moindre dans celui de la Taute. Ainsi, le pompage actuel de 5 Mm^3/an dans le bassin aquifère de la Sèves, aurait contribué à abaisser le niveau de la zone humide de 25 à 40 cm.
- **La quantité d'eau drainée en surface, et donc contribuant aux débits des cours d'eau, est significativement affectée dans les deux bassins**, mais plus fortement dans le bassin de la Sèves.

Différents scénarios de changement climatique ont été testés. Ces scénarios dérivent de prédictions moyennes réalisées par le G.I.E.C. (Groupement d'experts Internationaux sur l'Evolution du Climat) et appliquées aux paramètres locaux du Cotentin (latitude, conditions météorologiques locales...).

Les résultats prédisent un impact important sur les marais à l'horizon 2090. En 2090 une augmentation de température de 2.5 °C est prévue. La pluviométrie associée peut rester inchangée, ou varier de plus ou moins 5% mais dans tout les cas l'évapotranspiration est augmentée ce qui entraîne une diminution de l'alimentation de la nappe souterraine.

Table 1.1: Surfaces impactées et niveaux d'eau moyens du marais associés aux différents scénarios de pompage testés. Q: volume pompé par an.

Pompage	Surface de marais impactée	Marais Sèves - Niveaux d'eau	Marais Taute - Niveaux d'eau
Q = 0	+1.35 km^2	+25 à +40 cm	0 à +10 cm
Pompage actuel Q	/ (Total de 35 km^2)	0 cm	0 cm
Q +50% Sèves	-2.4 km^2	-20 cm	0 cm
Q +100% Sèves	-0.5 km^2	-35 à -50 cm	0 à -5 cm
Q +50% Taute	-5 km^2	0 à -10 cm	0 à 10 cm
Q +50% Taute	-2.1 km^2	-15 cm	0 à -30cm

Table 1.2: Impact de trois scénarios moyens de changement climatique sur les volumes d'eau alimentant la nappe souterraine et les surfaces de marais impactées.

Par rapport à l'alimentation et les surfaces de marais actuels (35 km^2)	Volume d'eau alimentant la nappe souterraine	Modification du fonctionnement hydrologique du marais (baisse du niveaux d'eau moyen en dessous de 50 cm/sol)
Scénario où la pluie augmente de 5 %	-22%	Impact sur 7.3 km^2
Scénario où la pluie est inchangée	-38%	Impact sur 12.5 km^2
Scénario où la pluie diminue de 5 %	-59%	Impact sur 18.4 km^2

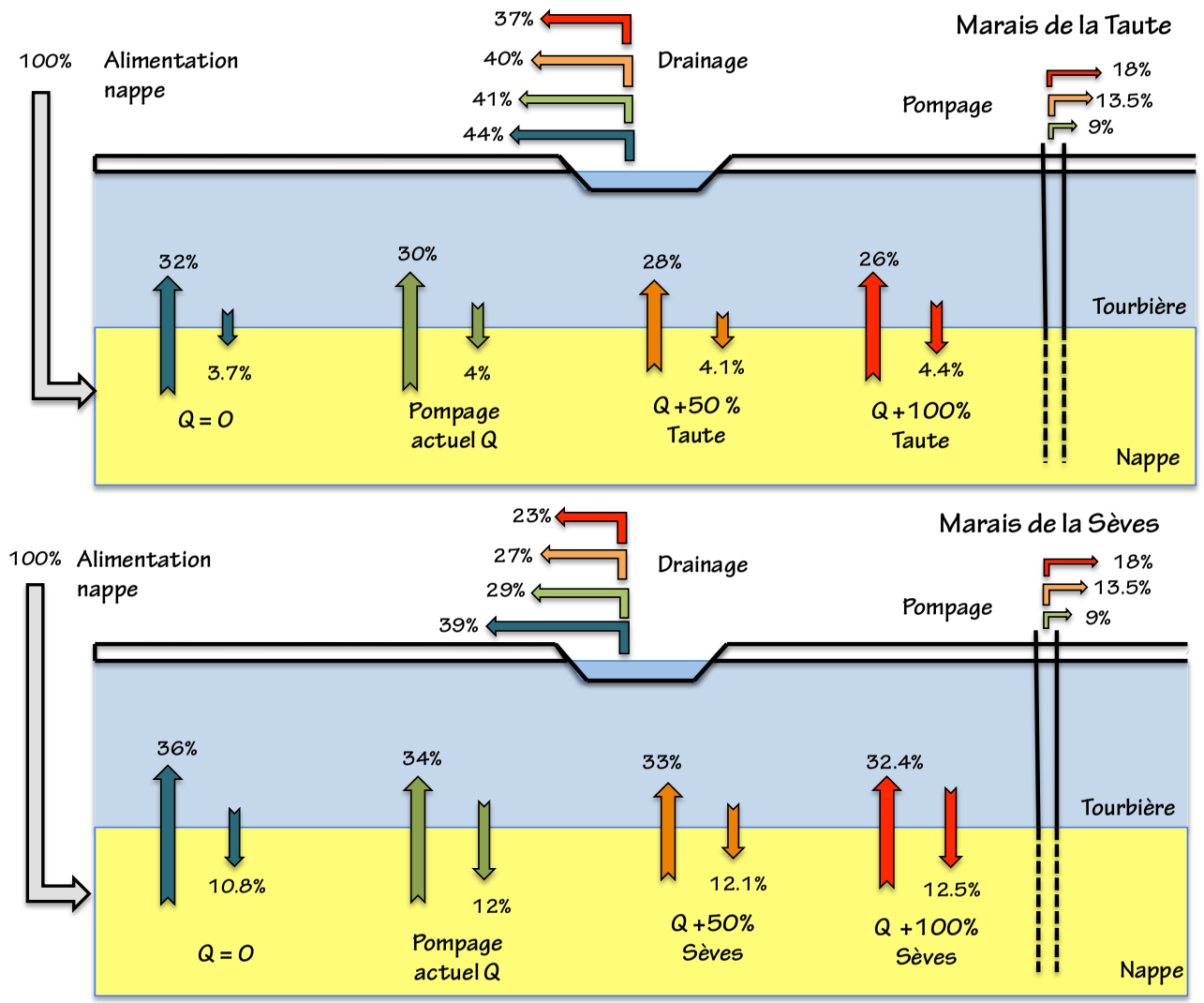

Figure 1.4: Flux entre compartiments hydrologiques en fonction des différents scénarios de pompage testés. En haut pour le bassin versant de la Taute et en bas pour celui de la Sèves

Les résultats de simulation du changement climatique (A1B) sont synthétisés dans le Tableau 1.2, du moins impactant au plus impactant à l'horizon 2090. Les probabilités de ces scénarios sont égales, l'évolution à venir rend leur date de réalisation plus ou moins proche.

Les volumes d'eau drainés sont aussi fortement impactées. Par exemple, le scénario median de changement climatique prédit une baisse du volume drainé de -17% dans le bassin de la Sèves et de -9 % dans le bassin de la Taute, par rapport au contexte actuel.

A une large échelle de temps (fin du siècle), le modèle prédit que le changement climatique a un impact plus important qu'un doublement des pompages, sur les niveaux d'eau dans le marais et plus généralement sur les flux entre compartiments. **Toutefois, ceci ne doit pas mener à sous-estimer l'impact d'un accroissement de la demande en eau souterraine. Les deux contraintes s'additionnent, et à court terme (dizaine d'années), l'extraction d'eau souterraine sera le premier processus impactant.**

L'analyse hydrologique a donc confirmé la vulnérabilité de la zone humide qui constitue un milieu en grande interconnection avec les autres compartiments hydrologiques que sont la nappe souterraine et les cours d'eau. Par conséquent, il y a un besoin de comprendre les mécanismes de réactivité biochimiques liés à ce système dynamique et ouvert.

Chapter 2

Impact de fluctuations rapides des niveaux d'eau sur les processus biochimiques de la tourbe: court terme

Par analogie avec les fluctuations de niveaux d'eau rapides sur le terrain, l'étude des processus biochimiques dans la tourbe a comparé l'effet de fluctuations de nappe rapides avec une référence en conditions stables. Une démarche expérimentale en microcosmes a été menée. De plus deux sites exposés à des conditions hydrologiques différentes dans leur passé récent sont comparés: une tourbière située à proximité d'un puits de pompage et une tourbière dite de référence. Une étude précédente avait démontré que le "site de pompage" se distingue par une modification des écoulements: les flux ascendants (nappe souterraine vers zone humide) sont diminués en faveur des flux descendants, la contribution des eaux de surface (et notamment du cours d'eau) dans l'alimentation de la zone humide étant augmentée. Par conséquent, des eaux plus oxygénées alimentent la tourbière depuis la mise en route du pompage en 1992. Une illustration des conclusions majeures est présentée dans la Figure 2.1.

A: Impact d'une alternance de cycles aérobies / anaérobies sur les processus biochimiques

- L'étude confirme que l**a vulnérabilité biochimique de la tourbe aux changements environnementaux, tel que l'état d'aération, est très dépendante de la qualité de la tourbe**. En effet, le recyclage des nutriments est fortement influencé par l'état de la tourbe, i.e. sa matière organique et minérale et sa biomasse. Une tourbe plus dégradée, où les teneurs en nutriments et biomasse sont plus faibles, est plus sensible aux processus d'oxydation qui entraînent une acidification importante, un relargage de sulfates et un lessivage de cations.

- Les pics de sulfate plus intenses sur le "site de pompage" et l'acidité engendrée, pourraient être expliqués par une plus grande disponibilité de la pyrite, un minéral abondant dans ces tourbes. L'état de dégradation de ce minéral, plutôt que la teneur totale en pyrite, est le facteur clé.

- De manière globale, les mécanismes majeurs observés dans ces tourbières sont la génération d'une acidité qui au-delà d'un certain seuil dépendant de l'état de la tourbe engendre un lessivage de cations, corrélé à un abaissement de la solubilité du carbone organique dissous.

B: Différences de comportement entre une dynamique de fluctuation et des conditions stagnantes

- La tourbe, saturée par une eau aux caractéristiques chimiques éloignées de celles de la tourbière, **maintient une bonne capacité tampon**. Autrement dit, la répétition de cycles de drainage et de mise en eau n'altère pas (ou peu) la mise en place rapide d'un milieu anaérobie et réitère les mêmes processus chimiques, comme par exemple l'abattement des nitrates et l'obtention d'un pH acide. Un gradient redox est rapidement mis en place.

- **Des fluctuations régulières de niveau d'eau**, analogues aux cycles diurnes/nocturnes ou après un évènement pluvieux, **favorisent le recyclage de nutriments**. Autrement dit, **la zone insaturée en quasi-perpétuel mouvement est un réacteur biogéochimique très efficace.**

- **Toutefois des alternances rapides et répétées** testées sur une fréquences de 3 jours **conduisent à une augmentation progressives de l'oxégénation de la tourbiére** et donc à une oxydation plus importante de celle-ci si les alternances sont maintenues à long terme.

- Les communautés microbiennes ne semblent pas affectées dans une certaine mesure par les rapides alternances de niveau d'eau. Elles apparaissent néamoins plus adaptées aux conditions anaérobies et la répétition trop fréquente et trop rapide des niveaux génère une dégradation de l'efficacité de leur fonctionnement.

- La comparaison entre l'eau à l'intrieur de la tourbe et l'eau drainée de la colonne entière semble s'accorder avec le concept de double porosité: respectivement l'eau des micro-pores et des macro-pores. L'eau des micro-pores, plus réactive, est le coeur du réacteur biogéochimique.

C: Réponse de la biomasse et des communautés microbiennes en fonction des sites et alternances étudiés.

Les deux sites étudiés (sous influence d'un pompage et plus éloigné) se distinguent nettement en terme de biomasse mais aussi de communautés microbiennes.

- Le site sous influence du pompage a **une biomasse totale et active plus faibl**e ce qui suggère que les conditions plus oxydantes subies par la tourbière ont altéré ses communautés microbiennes.

- L'analyse génomique montre une distinction nette entre communautés microbiennes entre les deux sites: **le site sous influence du pompage présente une diversité plus faible** ce qui corrobore l'hypothèse ci-avant.

- Le site sous influence du pompage présente une biomasse totale et active plus élevée dans les tourbes non remises en eau alors que l'inverse est constaté dans l'autre site. Ceci suggère que les **conditions plus oxydantes subies par la tourbière proche du pompage ont favorisé la croissance de communautés plus aérobies qui sont bien plus efficaces pour dégrader la matière organique.**

Cette partie a permis de mettre clairement en évidence les processus majeurs qui affectent la tourbe lors des variations de niveau d'eau de la nappe. La fonctionnalité de la tourbe en matière de recyclage de nutriments a également pu être quantifiée. Elle montre des signes de dégradation potentiels sur le long terme lorsque les communautés microbiennes et la matière organique adaptés aux conditions anaérobies sont soumis à de plus forts flux d'oxygène.

L'objet de la troisième partie a donc été d'évaluer plus avant le rôle à long terme des conditions d'anthropisation.

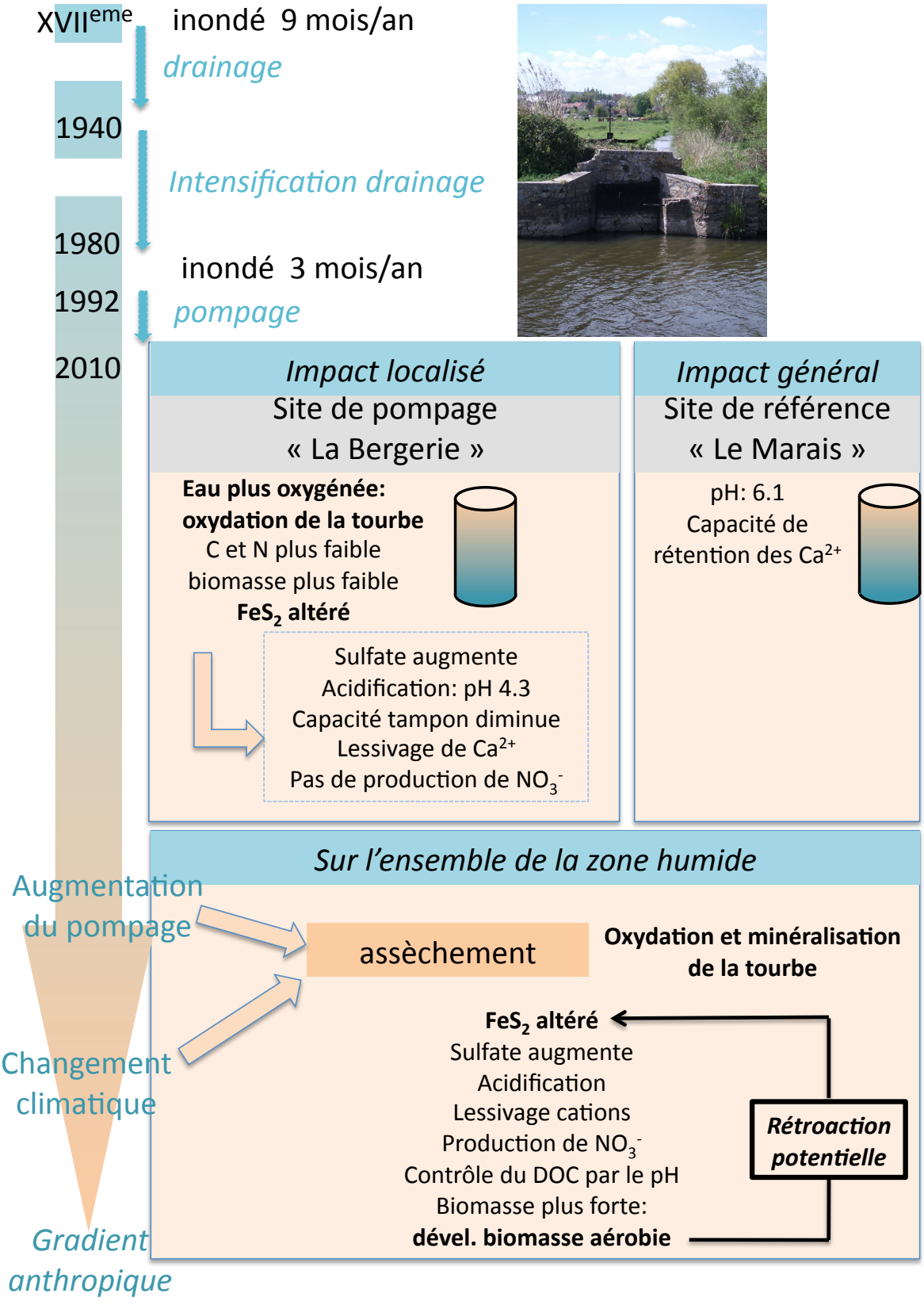

Figure 2.1: Synthèse des impacts biochimiques en fonction du degré d'anthropisation de la tourbière

Chapter 3

Impact de changements environnentaux à long terme sur les processus biochimiques

L'étude de l'impact des pressions anthropiques, objet de la première partie de ce rapport, démontre une modification du régime des écoulements, avec une baisse des niveaux d'eau dans la zone humide et des flux modifiés entre compartiments.

A long terme, l'intensification du gradient anthropique (Figure 2.1) peut engendrer un assèchement pérenne menant à la dessiccation de la tourbe. De plus, les flux modifiés entre compartiments peuvent modifier les rapports respectifs entre les sources alimentant la zone humide (Figure 1.4). Par exemple, la contribution des eaux de surface ou des eaux de pluie peut augmenter en défaveur de la contribution des eaux souterraines.

Par conséquent, nous nous sommes intéressés aux potentiels impacts de ces modifications sur la biochimie de la tourbe.

A: Impact de l'assèchement prolongé

- **La remise en eau d'une tourbe soumise à un assèchement prolongé engendre une forte production de sulfates et par conséquent une acidification importante du milieu.**
- L'acidification acrroît en partie le lessivage des cations.
- A ces pH acides, le carbone organique dissous se maintient à de faibles concentrations.
- **Des nitrates sont produits**, indiquant une minéralisation de l'azote contenue dans la tourbe.
- La dessiccation augmente la biomasse carbonée, suggérant que **l'assèchement a favorisé le développement d'une communauté microbienne aérobie**, qui rétroactivement contribue à la minéralisation (effet rétroactif).
- L'expérience en dessiccation renforce l'hypothèse que l'état de dégradation de la pyrite et non sa quantité totale explique une oxydation accrue (la dessiccation engendre une dégradation).
- **Les fortes oxydations engendrent une perte massique en éléments, qui sont majoritairement à l'origine du phénomène de subsidence de la tourbe.**

B: Impact de la qualité de l'eau de recharge

Dans un objectif de meilleure connaissance des effets biochimiques liés aux compositions des eaux sur le fonctionnement de la tourbière, et de définition de mesures conservatoires de maintien des niveaux d'eau, deux eaux ont été testées: une eau de surface et une eau souterraine.

Les deux qualités d'eau testées impliquent les mêmes type de réactions, à savoir une diminuttion rapide des nitrates, une production de sulfate, de fer et de carbone organique dissous, une rétention des cations (notamment Ca^{2+}) et une diminution du pH. L'oxydation des sulfures de fer (notamment la pyrite FeS_2) est à nouveau mise en évidence.

L'eau de surface engendre une production de sulfate, de fer et de carbone organique dissous légèrement supérieure. Une hypothèse avancée est que l'eau de surface pourrait héberger une communauté microbienne capable de légèrement plus catalyser les réactions d'oxydation.

Ces deux études ont permis d'analyser sur le long terme les effets d'une pression anthropique globalement oxydante soit à travers les effets de dessiccation, soit à travers des eaux de recharge différentes. Elles ont en particulier mis en évidence l'effet global de dégradation de la tourbe soumise aux pressions anthropiques. Elles suggèrent que ces effets puissent être non linéaires et s'accentuer au cours du temps.

Chapter 4

Quelques préconisations de mesures conservatoires

Les résultats de ce travail de recherche amènent à proposer des axes de vigilance et de préconisations générales:

1. **L'aquifère est vulnérable aux pollutions diffuses**. En première ligne, les intrants agricoles sur la totalité du bassin, sont impliqués. Si les zones humides remplissent bien leur rôle d'abattement de nitrates par exemple, le reste du bassin où se concentrent les cultures céréalières est exposé. La bonne qualité de l'eau actuellement exploitée peut s'expliquer par un captage d'eaux correspondant majoritairement aux longs temps de résidence.

2. **La mise en exploitation de nouveaux pompages d'eau potable doit privilégier le bassin de la Taute**, celui de la Sèves réagissant par une baisse plus importante des niveaux d'eau dans la zone humide (d'autant qu'il est déjà largement exploité). **Toutefois, le bassin aquifère de la Taute étant moins transmissif, il est moins intéressant à exploiter et le rayon d'influence du pompage est bien plus grand.**

3. **L'extraction d'eau souterraine a un impact sur tout le bassin hydrologique**, **mais cet impact est plus fort dans le rayon d'influence du puits, en termes de modification des sens d'écoulement**. Si cette zone est située dans une tourbière, celle-ci est exposée localement à des flux descendants plus importants, qui amènent des eaux plus oxygénées et donc accroissent les processus d'oxydation. **Si l'objectif est de préserver localement l'état d'une tourbière, l'implantation d'un pompage d'eau souterraine n'est pas conseillé.**

4. Les cycles de remise en eau conduits dans nos expériences sont analogues à des fluctuations de niveaux d'eau rapides sur le terrain. **Les résultats confirment que des conditions anaérobies doivent être favorisées dans la gestion des tourbières, mais qu'une légère fluctuation des niveaux n'altère pas son fonctionnement**. Ces résultats s'accordent avec les recommandations actuelles de restauration des tourbières qui favorisent une fluctuation dynamique des niveaux d'eau. En effet, les écoulements d'eau et les périodes courtes d'inondations favorisent

la productivité primaire et d'autres fonctions ecosystémiques comme le renouvellement de nutriments (incluant les éléments dont l'accumulation est toxique), d'énergie et de vivant. Toutefois, **quoique un certain degré de fluctuation soit bénéfique, cette étude démontre aussi que quand l'aération augmente au-delà d'un seuil critique, le recyclage d'éléments chimiques tels que le fer ou le soufre peut être drastiquement altéré. L'état extrême d'assèchement prolongé est quant à lui clairement destructeur**.

5. **A l'échelle du bassin, deux leviers possibles pour contre-balancer les effets négatifs d'un accroissement du pompage ou du changement climatique apparaissent et mériteront une analyse plus poussée. D'une part une modification de la gestion des niveaux d'eau par les ouvrages hydrauliques et d'autre part une remontée des niveaux d'eau dans la tourbière de Baupte.** En effet, un dense réseau d'ouvrages hydrauliques existe sur la zone humide, constitué de clapets anti-retour, de vannes, de portes à flot, dont la gestion est assez complexe. Par ailleurs, l'exploitation sur la tourbière de Baupte est arrêtée depuis 2006 mais le pompage est maintenu pour protéger les terres agricoles voisines. Dans le cadre de la restauration de ce site industriel, une remontée progressive des niveaux d'eau pourait favoriser les zones humides dans l'ensemble du bassin. Des réflexions sur les mesures conservatoires sont donc à mener avec le Parc Naturel dans le cadre du Schéma d'Aménagement et de Gestion des Eaux élaboré en 2012.

Chapter 5

Partie V: pour aller plus loin...

Quelques perspectives scientifiques:

- Il serait intéressant de mettre en place un équipement et un suivi à long terme des niveaux d'eau dans la zone humide. Ces données sont par exemple nécessaires pour une modélisation en régime transitoire, qui a beaucoup d'intérêt dans des zones humides sensibles aux fluctuations du niveau d'eau. Par aillleurs, le changement climatique peut engendrer des sècheresses plus accentuées en été et des hivers plus humides, une modélisation en régime transitoire est donc nécessaire pour prédire ces variations.

- Dans le cadre de la restauration du site industriel de Baupte, un affinement de la modélisation intégrant les modifications possibles du niveau d'eau, serait intéressant. Ceci afin de mesurer leurs impacts sur l'ensemble des zones humides du bassin.

- L' étude a mis en évidence une minéralisation de la tourbe, sur la base d'indicateurs chimiques. Une mesure quantitative de la minéralisation (par des méthodes classiques de mesures de perte de masse, sur le terrain ou en laboratoire) permettrait de quantifier le processus, afin de mieux estimer les risques de subsidence.

- Enfin, les expériences ont mis en évidence une dynamique du soufre qu'il serait intéressant de mieux caractériser par méthodes istopiques par exemple. Une caractérisation structurelle des phases soufrées, par rayons X par exemple, permettrait d'identifier clairement les phases en présence, mais aussi l'état d'altération de ces phases, suggéré comme facteur clé d'oxydation de la pyrite dans cette étude.

Bibliography

Jukka Alm, Narasinha J Shurpali, Kari Minkkinen, Lasse Aro, Jyrki Hytonen, Tuomas Laurila, Annalea Lohila, Marja Maljanen, Pertti J Martikainen, Paivi Makiranta, Timo Penttila, Sanna Saarnio, Niko Silvan, Eeva-Stiina Tuittila, and Jukka Laine. Emission factors and their uncertainty for the exchange of CO2, CH4 and N2O in Finnish managed peatlands. *BOREAL ENVIRONMENT RESEARCH*, 12(2):191–209, May 2007. ISSN 1239-6095.

J P E Anderson and K H Domsch. Physiological method for quantitative measurement of microbial biomass in soils. *Soil Biology & Biochemistry*, 10(3):215–221, 1978. ISSN 0038-0717. doi: 10.1016/0038-0717(78)90099-8.

M P Anderson and X X Cheng. Long-term and short-term transience in a groundwater lake system in Wisconsin, USA. *Journal of Hydrology*, 145(1-2):1–18, May 1993. ISSN 0022-1694.

C.A.J Appelo and D Postma. *Geochemistry, groundwater and pollution 2nd edition*. A.A. Balkema Publishers, 2005.

T V Armentano and E S Menges. PATTERNS OF CHANGE IN THE CARBON BALANCE OF ORGANIC SOIL-WETLANDS OF THE TEMPERATE ZONE. *JOURNAL OF ECOLOGY*, 74 (3):755–774, September 1986. ISSN 0022-0477. doi: 10.2307/2260396.

C Auterives. *Influence des flux d'eau souterraine entre une zone humide superficielle et un aquifere profond sur le fonctionnement hydrochimique des tourbieres: exemple des marais du Cotentin, Basse-Normandie*. PhD thesis, Rennes 1, 2006.

C Auterives, L Aquilina, O Bour, M Davranche, and V Paquereau. Contribution of climatic and anthropogenic effects to the hydric deficit of peatlands. *Hydrological Processes*, 25, 2011.

Virginie Ayraud, Luc Aquilina, Thierry Labasque, Helene Pauwels, Jerome Molenat, Anne-Catherine Pierson-Wickmann, Veronique Durand, Olivier Bour, Corinne Tarits, Pierre Le Corre, Elise Fourre, Philippe Merot, and Philippe Davy. Compartmentalization of physical and chemical properties in hard-rock aquifers deduced from chemical and groundwater age analyses. *APPLIED GEOCHEMISTRY*, 23(9):2686–2707, September 2008. ISSN 0883-2927. doi: 10.1016/j.apgeochem.2008.06.001.

S. Baize. *Tectonique, eustatisme et climat dans un sytème géomorphologique cotier. Le Nord-Ouest de la France au Plio-Pléistocène: exemple du Cotentin*. PhD thesis, Université de Caen, 1998.

I E Bauer. Modelling effects of litter quality and environment on peat accumulation over different time-scales. *Journal of Ecology*, 92(4):661–674, August 2004. ISSN 0022-0477. doi: 10.1111/j.0022-0477.2004.00905.x.

C Blodau, C L Roehm, and T R Moore. Iron, sulfur, and dissolved carbon dynamics in a northern peatland. *Archiv Fur Hydrobiologie*, 154:561–583, 2002.

C Blodau, N Basiliko, and T R Moore. Carbon turnover in peatland mesocosms exposed to different water table levels. *Biogeochemistry*, 67:331–351, 2004.

Ck Blodau and T R Moore. Experimental response of peatland carbon dynamics to a water table fluctuation. *Aquatic Sciences*, 65:47–62, 2003.

N Bougon, L Aquilina, M P Briand, S Coedel, and P Vandenkoornhuyse. Influence of hydrological fluxes on the structure of nitrate-reducing bacteria communities in a peatland. *SOIL BIOLOGY & BIOCHEMISTRY*, 41(6):1289–1300, June 2009. ISSN 0038-0717. doi: 10.1016/j.soilbio.2009.03.015.

E Bouillon-Launay. *Intérêt des indicateurs hydropédologiques dans la gestion raisonnée des zones humides (application aux marais du Cotentin)*. PhD thesis, Caen, 1992.

C Bradley. Simulation of the annual water table dynamics of a floodplain wetland, Narborough Bog, UK. *Journal of Hydrology*, 261:150–172, 2002.

D J Casagrange, G Idowu, A Friedman, P Rickert, K Siefert, and D Schlenz. H2S incorporation in coal precursors - Origins of of organic sulfur in coal. *Nature*, 282(5739):599–600, 1979. ISSN 0028-0836. doi: 10.1038/282599a0.

CDHAT. Piezometrie hautes eaux et basses eaux 2007. Document annexe au rapport de suivi piezometrique du bassin de Sainteny-Marchesieux. Technical report, 2008.

S J Chapman. Sulphur forms in open and afforested areas of two scottish peatlands. *Water Air and Soil Pollution*, 128:23–39, 2001.

S J Chapman and M S Davidson. S-35-sulphate reduction and transformation in peat. *Soil Biology & Biochemistry*, 33:593–602, 2001.

Jens H Christensen, Timothy R Carter, Markku Rummukainen, and Georgios Amanatidis. Evaluating the performance and utility of regional climate models: the PRUDENCE project. *CLIMATIC CHANGE*, 81(1):1–6, May 2007. ISSN 0165-0009. doi: 10.1007/s10584-006-9211-6.

J M Clark, P J Chapman, A L Heathwaite, and J K Adamson. Suppression of dissolved organic carbon by sulfate induced acidification during simulated droughts. *Environmental Science & Technology*, 40:1776–1783, 2006. doi: 10.1021/es051488c.

Clymo. Ecosystems of the world. pages 159–223. Elsevier, Amsterdam, 1983.

J C Coulson and J Butterfield. Investigation of biotic factors determining rates of plant decomposition on blanket bog. *Journal of Ecology*, 66(2):631–650, 1978. ISSN 0022-0477. doi: 10.2307/2259155.

D Dent. sulphate acidic soil: a baseline for research and development. page 204, 1986.

S J Deverel and S Rojstaczer. Subsidence of agricultural lands in the Sacramento San Joaquin Delta, California: Role of aqueous and gaseous carbon fluxes. *WATER RESOURCES RESEARCH*, 32(8): 2359–2367, August 1996. ISSN 0043-1397. doi: 10.1029/96WR01338.

K J Devito and A R Hill. Sulphate mobilization and pore water chemistry in relation to groundwater hydrology and summer drought in two conifer swamps on the Canadian Shield. *Water Air and Soil Pollution*, 113:97–114, 1999.

P.A Domenico and F.W. Schwartz. *Physical and Chemical Hydrogeology*. Wiley, 1998. ISBN 0-471-59762-7.

M C Eimers, S A Watmough, J M Buttle, and P J Dillon. Examination of the potential relationship between droughts, sulphate and dissolved organic carbon at a wetland-draining stream. *Global Change Biology*, 14:938–948, 2008. doi: 10.1111/j.1365-2486.2007.01530.x.

J W Fitzgerald, T C Strickland, and W T Swank. Metabolic-fate of inorganic sulfate in soil samples from undisturbed and managed forest ecosytems. *Soil Biology and Biochemistry*, 14(6):529–536, 1982. ISSN 0038-0717. doi: 10.1016/0038-0717(82)90082-7.

A J Francez, S Gogo, and N Josselin. Distribution of potential CO2 and CH4 productions, denitrification and microbial biomass C and N in the profile of a restored peatland in Brittany (France). *European Journal of Soil Biology*, 36:161–168, 2000.

C Freeman, G Liska, N J Ostle, M A Lock, B Reynolds, and J Hudson. Microbial activity and enzymic decomposition processes following peatland water table drawdown. *Plant and Soil*, 180:121–127, 1996.

C Freeman, N Fenner, N J Ostle, H Kang, D J Dowrick, B Reynolds, M A Lock, D Sleep, S Hughes, and J Hudson. Export of dissolved organic carbon from peatlands under elevated carbon dioxide levels. *Nature*, 430:195–198, 2004a. doi: 10.1038/nature02707.

C Freeman, N J Ostle, N Fenner, and H Kang. A regulatory role for phenol oxidase during decomposition in peatlands. *Soil Biology & Biochemistry*, 36:1663–1667, 2004b.

S Frei, G Lischeid, and J H Fleckenstein. Effects of micro-topography on surface-subsurface exchange and runoff generation in a virtual riparian wetland - A modeling study. *ADVANCES IN WATER RESOURCES*, 33(11, SI):1388–1401, November 2010. ISSN 0309-1708. doi: 10.1016/j.advwatres.2010.07.006.

Jeroen J M Geurts, Alfons J P Smolders, Artur M Banach, Jan P M van de Graaf, Jan G M Roelofs, and Leon P M Lamers. The interaction between decomposition, net N and P mineralization and their mobilization to the surface water in fens. *WATER RESEARCH*, 44(11):3487–3495, June 2010. ISSN 0043-1354. doi: 10.1016/j.watres.2010.03.030.

E. A. Ghabbour and G. Davies. *Humic Substances: Molecular Details and Applications in Land and Water Conservation*. Taylor and Francis, New York, taylor and edition, 2005.

H. Gitay, S. Brown, W. Easterling, B. Jallow, J. Antle, M. Apps, R. Beamish, T. Chapin, W. Cramer, J. Frangi, J. Laine, L. Erda, J. Magnuson, I. Noble, J. Price, T. Prowse, T. Root, E. Schulze, O. Sirotenko, B. Sohngen, J. Soussana, H. Buggman, C. Egorov, M. Finlayson, R. Fleming, W. Fraser, L. Hahn, K. Hall, M. Howden, M. Hutchins, J. Ingram, J. Hui, G. Masters, P. Megonigal, J. Morgan, N. Myers, R. Neilson, S. Page, C. Parmesan, J. Rieley, N. Roulet, G. Takle, J. van Minnen, D. Williams, T. Williamson, K. Wilson, A. Fischlin, and S. Diaz. Climate change 2001, impacts, adaptation, and vulnerability. Contribution of Working Group II to the Third Assessment Report of the Intergovernmental Panel on Climate Change. pages 235–342. Cambridge edition, 2001.

P H Glaser, J A Janssens, and D I Siegel. The response of vegetation to chemical and hydrological gradients in the Lost River peatland, Northern Minnesota. *Journal of Ecology*, 78:1021–1048, 1990.

Global Environment Centre. peat-portal.net.

T R Grapes, C Bradley, and G E Petts. Hydrodynamics of floodplain wetlands in a chalk catchment: The River Lambourn, UK. *JOURNAL OF HYDROLOGY*, 320(3-4):324–341, April 2006. ISSN 0022-1694. doi: 10.1016/j.jhydrol.2005.07.028.

M Grybos, M Davranche, G Gruau, P Petitjean, and M Pedrot. Increasing pH drives organic matter solubilization from wetland soils under reducing conditions. *Geoderma*, 154(1-2):13–19, December 2009. ISSN 0016-7061. doi: 10.1016/j.geoderma.2009.09.001.

Suzanne C M Haaijer, Leon P M Lamers, Alfons J P Smolders, Mike S M Jetten, and Huub J M Op den Camp. Iron sulfide and pyrite as potential electron donors for microbial nitrate reduction in freshwater wetlands. *GEOMICROBIOLOGY JOURNAL*, 24(5):391–401, 2007. ISSN 0149-0451. doi: 10.1080/01490450701436489.

J Holden, P J Chapman, and J C Labadz. Artificial drainage of peatlands: hydrological and hydrochemical process and wetland restoration. *Progress in Physical Geography*, 28:95–123, 2004.

J Holden, M G Evans, T P Burt, and M Horton. Impact of land drainage on peatland hydrology. *Journal of Environmental Quality*, 35:1764–1778, 2006. doi: 10.2134/jeq2005.0477.

R.H. Kadlec and A.G. Keoleian. Metal Ion Exchange on Peat. In *Peat and Water*, pages 61–93. Elsevier Applied Science Publishers Ltd, fuchsman, edition, 1986.

Klaus-Holger Knorr and Christian Blodau. Impact of experimental drought and rewetting on redox transformations and methanogenesis in mesocosms of a northern fen soil. *Soil Biology & Biochemistry*, 41(6):1187–1198, June 2009. ISSN 0038-0717. doi: 10.1016/j.soilbio.2009.02.030.

Klaus-Holger Knorr, Gunnar Lischeid, and Christian Blodau. Dynamics of redox processes in a minerotrophic fen exposed to a water table manipulation. *Geoderma*, 153(3-4):379–392, November 2009. ISSN 0016-7061. doi: 10.1016/j.geoderma.2009.08.023.

Pirkko Kortelainen, Tuija Mattsson, Leena Finer, Marketta Ahtiainen, Sari Saukkonen, and Tapani Sallantaus. Controls on the export of C, N, P and Fe from undisturbed boreal catchments, Finland. *Aquatic Sciences*, 68(4):453–468, 2006. ISSN 1015-1621. doi: 10.1007/s00027-006-0833-6.

N Krairapanond, R D Delaune, and W H Patrick. Sulfur dynamics in Louisiana coastal fresh-water marsh soils. *Soil Science*, 151:261–273, 1991.

N Krairapanond, R D Delaune, and W H Patrick. Distribution of organic and reduced sulfur forms in marsh soils of coastal Louisiana. *Organic Geochemistry*, 18:489–500, 1992.

T Labasque, V Ayraud, L Aquilina, and P Le Corre. Dosage des composes chlorofluorocarbones et du tetrachlorure de carbone dans les eaux souterraines. Application a la datation des eaux. *Cahiers techniques de Géosciences Rennes*, page 51, 2006.

R Laiho. Decomposition in peatlands: Reconciling seemingly contrasting results on the impacts of lowered water levels. *Soil Biology & Biochemistry*, 38:2011–2024, 2006.

L P M Lamers, A J P Smolders, and J G M Roelofs. The restoration of fens in the Netherlands. *Hydrobiologia*, 478:107–130, 2002.

G Lischeid, A Kolb, C Alewell, and S Paul. Impact of redox and transport processes in a riparian wetland on stream water quality in the Fichtelgebirge region, southern Germany. *HYDROLOGICAL PROCESSES*, 21(1):123–132, January 2007. ISSN 0885-6087. doi: 10.1002/hyp.6227.

Gunnar Lischeid, Marco Natkhin, Joerg Steidl, Ottfried Dietrich, Ralf Dannowski, and Christoph Merz. Assessing coupling between lakes and layered aquifers in a complex Pleistocene landscape based on water level dynamics. *ADVANCES IN WATER RESOURCES*, 33(11, SI):1331–1339, November 2010. ISSN 0309-1708. doi: 10.1016/j.advwatres.2010.08.002.

R Loeb, E van Daalen, L P M Lamers, and J G M Roelofs. How soil characteristics and water quality influence the biogeochemical response to flooding in riverine wetlands. *Biogeochemistry*, 85:289–302, 2007.

Remi Marsac, Melanie Davranche, Gerard Gruau, Martine Bouhnik-Le Coz, and Aline Dia. An improved description of the interactions between rare earth elements and humic acids by modeling: PHREEQC-Model VI coupling. *GEOCHIMICA ET COSMOCHIMICA ACTA*, 75(19):5625–5637, October 2011. ISSN 0016-7037. doi: 10.1016/j.gca.2011.07.009.

M.G. McDonald and W Harbaugh. *A Modular Three-Dimensional Finite-Difference Ground-Water Flow Model*. 1988.

Meteo France. Meteo France: convention between University of Rennes 1 and Meteo France. 2011.

J D Miller, H A Anderson, D Ray, and A R Anderson. Impact of some initial forestry practices on the drainage waters from blanket peatlands. *Forestry*, 69(3):193–203, 1996. ISSN 0015-752X.

W J Mitsch, L Zhang, C J Anderson, A E Altor, and M E Hernandez. Creating riverine wetlands: Ecological succession, nutrient retention, and pulsing effects. *Ecological Engineering*, 25:510–527, 2005. doi: 10.1016/j.ecoleng.2005.04.014.

DL Parkhurst and C.A.J Appelo. *User's guide to PHREEQC (version 2)-A computer program for speciation, batch-reaction, one-dimensional transport, and inverse geochemical calculations: Report 99-4259*. 1999.

S Paul, K Kusel, and C Alewell. Reduction processes in forest wetlands: Tracking down heterogeneity of source/sink functions with a combination of methods. *Soil Biology & Biochemistry*, 38(5):1028–1039, May 2006a. ISSN 0038-0717. doi: 10.1016/j.soilbio.2005.09.001.

S Paul, K Kusel, and C Alewell. Reduction processes in forest wetlands: Tracking down heterogeneity of source/sink functions with a combination of methods. *Soil Biology and Biochemistry*, 38(5):1028–1039, May 2006b. ISSN 00380717. doi: 10.1016/j.soilbio.2005.09.001.

J S Price and S M Schlotzhauer. Importance of shrinkage and compression in determining water storage changes in peat: the case of a mined peatland. *HYDROLOGICAL PROCESSES*, 13(16):2591–2601, November 1999. ISSN 0885-6087.

Joerg Prietzel, Juergen Thieme, Nora Tyufekchieva, David Paterson, Ian McNulty, and Ingrid Koegel-Knabner. Sulfur speciation in well-aerated and wetland soils in a forested catchment assessed by sulfur K-edge X-ray absorption near-edge spectroscopy (XANES). *Journal of Plant Nutrition and Soil Science-Zeitschrift Fur Pflanzenernahrung Und Bodenkunde*, 172(3):393–403, June 2009. ISSN 1436-8730. doi: 10.1002/jpln.200800054.

M Provost. Etude des Marais de lIsthme du Cotentin : Flore et vegetation (Study of the Cotentins Swamps : Flora and Vegetation). *D.R.A.E Basse-Normandie et CREPAN*, page 32, 1982.

M Provost. Atlas de Repartition des Plantes Vasculaires de Basse-Normandie (Atlas of the geographic distribution of the vascular plants in Basse-Normandie; France). *Presse Universitaire de Caen*, page 90, 1993.

Stefan Rahmstorf, Anny Cazenave, John A Church, James E Hansen, Ralph F Keeling, David E Parker, and Richard C J Somerville. Recent climate observations compared to projections. *SCIENCE*, 316(5825):709, May 2007. ISSN 0036-8075. doi: 10.1126/science.1136843.

K R Reddy and R D Delaune. Biogeochemistry of wetlands: science and applications. In Taylor and Francis, editors, *CRC Press*, pages 1–757. 2008. ISBN 9781566706780.

A S Reeve, D I Siegel, and P H Glaser. Simulating vertical flow in large peatlands. *JOURNAL OF HYDROLOGY*, 227(1-4):207–217, January 2000. ISSN 0022-1694. doi: 10.1016/S0022-1694(99)00183-3.

J D Rimstidt and D J Vaughan. Pyrite oxidation: A state-of-the-art assessment of the reaction mechanism. *GEOCHIMICA ET COSMOCHIMICA ACTA*, 67(5):873–880, March 2003. ISSN 0016-7037. doi: 10.1016/S0016-7037(02)01165-1.

S L Schiff, J Spoelstra, R G Semkin, and D S Jeffries. Drought induced pulses of SO42- from a Canadian shield wetland: use of delta S-34 and delta O-18 in SO42- to determine sources of sulfur. *Applied Geochemistry*, 20:691–700, 2005. doi: 10.1016/j.apgeochem.2004.11.011.

U Silins and R L Rothwell. Forest peatland drainage and subsidence affect soil water retention and transport properties in an Alberta peatland. *Soil Science Society of America Journal*, 62(4):1048–1056, 1998. ISSN 0361-5995.

J Silvola, J Alm, U Ahlholm, H Nykanen, and P J Martikainen. CO2 fluxes from peat in boreal mires under varying temperature and moisture conditions. *Journal of Ecology*, 84:219–228, 1996.

J Simunek, N J Jarvis, M T van Genuchten, and A Gardenas. Review and comparison of models for describing non-equilibrium and preferential flow and transport in the vadose zone. *JOURNAL OF HYDROLOGY*, 272(1-4):14–35, March 2003. ISSN 0022-1694.

U Skyllberg and T Magnusson. Cations adsorbed to soil organic matter - A regulatory factor for the release of organic carbon and hydrogen ions from soils to waters. *Water Air and Soil Pollution*, 85: 1095–1100, 1995.

SOGREAH PRAUD. Fourniture dun outil daide a la decision avec calage du modele hydrodynamique en regime permanent et en regime transitoire Synthese des donnees et Modelisation mathematique. Technical report, 2001.

G P Sparling, C W Felthman, J Reynolds, A W West, and P Singleton. Estimation of soil microbial C by a fumigation extraction method-Use on soils of high organic content, and a reassessment of the KEC-factor. *Soil Biology & Biochemistry*, 22(3):301–307, 1990. ISSN 0038-0717. doi: 10.1016/0038-0717(90)90104-8.

G.P. Sparling. The substrate-induced respiration method. In K Alef and P Nannipieri, editors, *Methods in applied soil microbiology and biochemistry*, pages 397–404. London, academic p edition, 1995.

P Steinmann and W Shotyk. Geochemistry, mineralogy, and geochemical mass balance on major elements in two peat bog profiles (Jura Mountains: Switzerland). *Chemical Geology*, 138:25–53, 1997.

E Sundström. Nutrient conditions in drained peatlands along a north-south climatic gradient in Sweden. *Forest Ecology and Management*, 126(2):149–161, February 2000. ISSN 03781127. doi: 10.1016/S0378-1127(99)00098-5.

C Tarits, L Aquilina, V Ayraud, H Pauwels, P Davy, F Touchard, and O Bour. Oxido-reduction sequence related to flux variations of groundwater from a fractured basement aquifer (Ploemeur area, France). *APPLIED GEOCHEMISTRY*, 21(1):29–47, January 2006. ISSN 0883-2927. doi: 10.1016/j.apgeochem.2005.09.004.

USGS. http://water.usgs.gov/lab/software/USGS_CFC/.

J Van Dijk, M Stroetenga, L Bos, P M Van Bodegom, H A Verhoef, and R Aerts. Restoring natural seepage conditions on former agricultural grasslands does not lead to reduction of organic matter decomposition and soil nutrient dynamics. *Biogeochemistry*, 71:317–337, 2004.

Lieke van Roosmalen, Torben O. Sonnenborg, and Karsten H. Jensen. Impact of climate and land use change on the hydrology of a large-scale agricultural catchment. *Water Resources Research*, 45(November 2008):1–18, March 2009. ISSN 0043-1397. doi: 10.1029/2007WR006760.

J.F. Vernoux, J.P. Deroin, P. Lebret, V. Petit, and P. Siegel. Ressources en eau souterraine de l'Isthme du Cotentin - Synthese des connaissances. *rapport BRGM*, R40824:136, 2000.

J L Weishaar, G R Aiken, B A Bergamaschi, M S Fram, R Fujii, and K Mopper. Evaluation of specific ultraviolet absorbance as an indicator of the chemical composition and reactivity of dissolved organic carbon. *Environmental Science & Technology*, 37:4702–4708, 2003. doi: 10.1021/es030360x.

R K Wieder and G E Lang. Cycling of inorganic and organic sulfur in peat from Big Run Bog, West-Virginia, USA. *BIiogeochemistry*, 5(2):221–242, 1988a. ISSN 0168-2563. doi: 10.1007/BF02180229.

R K Wieder and G E Lang. Cycling of inorganic and organic sulfur in peat from Big Run Bog, West-Virginia. *Biogeochemistry*, 5:221–242, 1988b.

R K Wieder, G E Lang, and V A Granus. Sulfur transformations in sphanium-derived peat during incubation. *Soil Biology & Biochemistry*, 19(1):101–106, 1987. ISSN 0038-0717. doi: 10.1016/0038-0717(87)90132-5.

B L Williams and D J Silcock. Nutrient and microbial changes in the peat profile beneath Sphagnum magellanicum in response to additions of ammonium nitrate. *Journal of Applied Ecology*, 34(4): 961–970, August 1997. ISSN 0021-8901. doi: 10.2307/2405286.

C J Williams, E A Shingara, and J B Yavitt. Phenol oxidase activity in peatlands in New York State: Response to summer drought and peat type. *Wetlands*, 20(2):416–421, June 2000. ISSN 0277-5212.

M M Wilsnack, D E Welter, A M Montoya, J I Restrepo, and J Obeysekera. Simulating flow in regional wetlands with the modflow wetlands package. *JOURNAL OF THE AMERICAN WATER RESOURCES ASSOCIATION*, 37(3):655–674, June 2001. ISSN 1093-474X. doi: 10.1111/j.1752-1688.2001.tb05501.x.

J H M Wosten, A B Ismail, and A L M VanWijk. Peat subsidence and its practical implications: A case study in Malaysia. *GEODERMA*, 78(1-2):25–36, July 1997. ISSN 0016-7061. doi: 10.1016/S0016-7061(97)00013-X.

List of Figures

List of Tables

Appendices

Appendix A

Chemistry in Sainteny-Marchesieux: supplement to Chapter 2 in Part I

Table A.1: Results of the chemical analysis in the wells from Sainteny-Marchesieux

Param.	Unit	117-3X-15		S15		S14 (73m)		S14 (40m)		S10	
		SAM001	SAM024	SAM002	SAM023	SAM003	SAM026	SAM004	SAM025	SAM005	SAM018
		avr.2008	oct.2008	avr.2008	oct.2008	avr.2008	oct.2008	avr.2008	oct.2008	avr.2008	oct.2008
EC	μS/cm	716	709	537	556	689	807	778	766	711	709
Oxyg	mg/L	0	0	0.80	0.01	0	0	0	1.1	0	0
T	C	12.7	13.4	12.5	12.9	13	12.4	13.3	12.9	13.1	13
pH		7.2	7.2	6.6	6.56	7.4	7.4	7.9	7.3	6.8	7.8
Eh	mV	50	195	109	388	33	73	33	317	16	238
Alc.	mol/L	0.006	/	0.004		0.006		0.007		0.006	
IC	mg/L	87.9	83.9	61.0	57.8	79.3	88.8	92.3	90.6	85.0	85.4
Cl^-	mg/L	27.1	27.4	29.2	31.7	30.1	32.8	31.7	32.6	29.6	29.7
SO_4^{2-}	mg/L	21.2	21.6	15.5	14.7	26.3	39.8	26.3	25.5	¡ 0.1	n.a.
NO_3^-	mg/L	0.30	n.a.	9.75	10.6	¡0.1	n.a.	¡0.1	5.7	0.37	0.3
NO_2^-	mg/L	0.10	0.07	¡0.07	n.a.	¡0.07	0.07	0.11	0.03	0.09	0.066
PO_4^{3-}	mg/L	¡0.1	n.a.	¡0.1	n.a.	¡0.1	n.a.	¡0.1	n.a.	0.16	0.13
Br^-	mg/L	0.10	0.11	0.11	0.13	0.10	0.09	0.11	0.10	0.13	0.11
Na^+	mg/L	26.28		35.01		32.90		24.39		74.70	
Mg^{2+}	mg/L	17.44	16.26	5.06	4.56	19.54	20.88	21.86	20.57	29.93	33.08
Al^{3+}	μg/L	1.51	7.3	0.00	7.3	3.60	8.8	1.11	6.7	2.23	12.3
Si^{4+}	mg/L	5.64		8.60		7.91		7.31		8.57	
K^+	mg/L	2.12	2.03	5.28	4.42	3.40	3.98	2.19	2.37	23.10	22.08
Ca^{2+}	mg/L	123.37	121.61	72.63	79.72	84.69	115.27	123.53	124.09	19.98	23.60
Sc	μg/L	0.872		1.277		0.991		1.175		1.188	
V	μg/L	0.12		0.18		0.15		0.08		0.09	
Cr	μg/L	0.11		0.91		0.77		0.33		0.12	
Mn	μg/L	174.94		8.16		28.46		18.39		3.15	
Fe	μg/L	2371.6		133.1		507.1		281.6		120.5	
Co	μg/L	10.88		4.98		0.78		1.19		0.44	
Ni	μg/L	1.77		3.55		2.14		2.44		0.52	
Cu	μg/L	0.38		0.27		0.40		0.46		0.47	
Zn	μg/L	1.59		1.74		11.18		2.93		1.63	
Rb	μg/L	1.69		0.65		1.80		1.60		2.53	
Sr	μg/L	1331.88		246.91		745.20		644.35		1923.76	
Cd	μg/L	0.06		0.18		0.06		0.10		0.06	
Ho	μg/L	0.0020		0.0044		0.0008		0.0006		0.0012	
Er	μg/L	0.0056		0.0125		0.0021		0.0017		0.0042	
Tm	μg/L	0.0008		0.0016		0.0003		0.0002		0.0006	
Yb	μg/L	0.0039		0.0094		0.0018		0.0017		0.0036	
Lu	μg/L	0.0007		0.0013		0.0003		0.0003		0.0006	
Pb	μg/L	0.048		0.070		0.051		0.038		0.065	
Th	μg/L	0.001		0.018		0.000		0.000		0.000	
U	μg/L	1.592		0.701		0.093		0.095		0.067	

Table A.2: Results of chemical analysis in the wells from Sainteny-Marchesieux

Param.	Unit	F4	F1(65m)		F1(32m)		117-6X-0048		S18		117-6X-003
		SAM006 avr.2008	SAM007 avr.2008	SAM034 oct.2008	SAM008 avr.2008	SAM036 oct.2008	SAM009 avr.2008	SAM031 oct.2008	SAM010 avr.2008	SAM033 oct.2008	SAM017 oct.2008
EC	μS/cm	430	631	628	592	592	570	572	418	382	392
Oxyg	mg/L	0	0.93	0	6.82	2.2	4.4	0.91	0.48	0	2.4
T	C	13.7	12.9	12.4	13.5	12.3	13.5	12.3	12.8	12.3	12.2
pH		6.8	7.0	7.2	6.8	7.3	6.5	6.8	7.1	7.34	6.3
Eh	mV	/	117	209	186	198	98	294	21	86	535
Alc.	mol/L	0.004	0.004	0.0043	0.004	0.0043	0.004	0.0040	0.003	0.0030	0.0021
IC	mg/L	49.2	62.5	60.3	61.5	59.5	58.8	56.3	44.2	20.4	28.8
Cl^-	mg/L	25.9	36.2	40.7	30.3	33.1	35.8	37.8	25.8	25.2	35.2
SO_4^{2-}	mg/L	0.5	17.1	18.0	10.9	10.6	16.1	16.7	20.2	19.0	13.7
NO_3^-	mg/L	¡0.1	31.7	33.9	37.4	39.3	25.6	31.5	2.8	0	30.9
NO_2^-	mg/L	¡0.07	0.07	0.04	0.08	0.06	¡0.07	0.05	¡0.07	¡0.07	0.05
PO_4^{3-}	mg/L	¡0.1	¡0.1	¡0.1	0.12	0.04	¡0.1	¡0.1	¡0.1	¡0.1	¡0.1
Br^-	mg/L	0.13	0.11	0.11	0.11	0.11	0.14	0.15	0.08	0.08	n.a.
Na^+	mg/L	19.951	21.335		15.970	16.17	20.735		19.262	17.52	
Mg^{2+}	mg/L	7.350	9.176	9.93	7.503	8.26	10.105	11.17	4.019	4.66	10.32
Al^{3+}	μg/L	0.939	0.991	7.9	3.038	10.4	0.238	6.7	2.618	9.8	7.7
Si^{4+}	mg/L	1.417	7.567		4.743		7.242		6.659		
K^+	mg/L	1.613	1.735	1.844	2.109	2.61	1.080	1.17	1.379	2.148	2.001
Ca^{2+}	mg/L	61.261	83.817	95.62	85.818	98.32	72.546	85.91	52.076	67.28	48.22
Sc	μg/L	0.267	0.741		0.694		0.957		0.817		
V	μg/L	0.13	0.34		0.54		0.22		0.21		
Cr	μg/L	0.04	0.10		1.07		0.62		0.05		
Mn	μg/L	112.41	18.93		0.74		1.23		78.93		
Fe	μg/L	741.7	203.4		185.6		150.3		509.9		
Co	μg/L	1.18	0.53		0.31		0.38		0.41		
Ni	μg/L	1.48	1.36		1.96		1.55		4.40		
Cu	μg/L	0.34	0.32		1.25		0.36		0.28		
Zn	μg/L	1.49	1.60		4.43		2.05		3.48		
Rb	μg/L	1.34	0.52		0.36		0.40		1.02		
Sr	μg/L	116.25	264.07		136.14		183.07		150.37		
Cd	μg/L	0.05	0.10		0.69		0.06		0.06		
Ho	μg/L	0.0002	0.0002		0.0004		0.0011		0.0006		
Er	μg/L	0.0005	0.0005		0.0011		0.0030		0.0016		
Tm	μg/L	0.0001	0.0001		0.0001		0.0004		0.0003		
Yb	μg/L	0.0004	0.0006		0.0010		0.0026		0.0014		
Lu	μg/L	0.0001	0.0001		0.0001		0.0004		0.0002		
Pb	μg/L	0.076	0.052		0.105		0.044		0.092		
Th	μg/L	0.007	0.002		0.000		0.000		0.001		
U	μg/L	0.227	7.084		0.344		0.223		0.037		

Table A.3: Results of chemical analysis from the wells in Sainteny-Marchesieux

Param.	Unit	117-6X-0046		S12		F2(55m)		117-6X-0043		P9	P8
		SAM011 avr.2008	SAM021 oct.2008	SAM012 avr.2008	SAM037 oct.2008	SAM013 avr.2008	SAM030 oct.2008	SAM014 avr.2008	SAM020 oct.2008	SAM027 oct.2008	SAM032 oct.2008
EC	μS/cm	711	713	650	585	654	658	451	446	524	380
Oxyg	mg/L	0.6	0	1.17	0.45	0.2	0	0.34	0	1.4	3.1
T	C	12.7	12.5	12.7	12.8	12.3	12.5	13.4	13	11.9	13.2
pH		7.2	7.1	7.1	6.7	7	7.1	7.1	7.6	7.5	6
Eh	mV	27	304	109	334	77	187	71	69	403	395
Alc.	mol/L	0.006	0.006	0.004	0.003	0.006	0.005	0.003	0.003	0.004	0.0007
IC	mg/L	80.7	80.4	58.8	42.5	80.0	75.3	44.9	43.2	57.6	9.4
Cl^-	mg/L	37.4	34.9	45.1	46.8	31.1	33.2	26.9	25.7	28.1	46.8
SO_4^{2-}	mg/L	32.4	28.8	39.7	31.3	14.3	16.3	18.2	21.6	8.7	17.0
NO_3^-	mg/L	0.97	1.5	30.2	49.2	¡0.1	3.1	2.9	0.8	11.5	53.6
NO_2^-	mg/L	¡0.07	20	¡0.07	¡0.07	¡0.07	0.05	0.08	n.a.	n.a.	n.a.
PO_4^{3-}	mg/L	¡0.1	n.a.	¡0.1	0.04	¡0.1	n.a.	¡0.1	n.a.	n.a.	n.a.
Br^-	mg/L	0.16	0.14	0.2	0.2	0.1	0.11	0.07	0.07	0.0988	0.12
Na^+	mg/L	30.33		26.21	20.02	22.08		19.27		20.76	
Mg^{2+}	mg/L	9.04	9.63	7.81	5.912	13.26	14.53	8.09	7.94	11.75	5.61
Al^{3+}	μg/L	1.475	9.3	5.084	7.3	0.000	8.0	1.619	10.6	8.3	10.3
Si^{4+}	mg/L	8.48		4.64		5.91		6.59			
K^+	mg/L	0.94	1.068	9.46	3.361	2.16	2.361	1.07	1.429	1.942	0.461
Ca^{2+}	mg/L	108.99	126.48	85.24	87.93	99.55	108.39	64.47	71.84	78.50	42.02
Sc	μg/L	0.94		0.62		0.90		0.61			
V	μg/L	0.16		1.63		0.24		0.12			
Cr	μg/L	0.32		0.68		0.12		0.11			
Mn	μg/L	85.72		7.07		113.86		26.53			
Fe	μg/L	1472.5		184.6		817.1		239.3			
Co	μg/L	0.66		0.65		0.46		0.36			
Ni	μg/L	2.06		2.48		1.72		1.07			
Cu	μg/L	0.35		1.35		0.37		0.38			
Zn	μg/L	1.47		11.59		3.67		3.75			
Rb	μg/L	0.72		3.17		0.45		0.69			
Sr	μg/L	246.57		178.12		283.85		3200.36			
Cd	μg/L	0.08		0.11		0.23		0.09			
Ho	μg/L	0.0008		0.0081		0.0001		0.0003			
Er	μg/L	0.0017		0.0230		0.0002		0.0011			
Tm	μg/L	0.0004		0.0034		0.0000		0.0001			
Yb	μg/L	0.0015		0.0173		0.0000		0.0008			
Lu	μg/L	0.0005		0.0033		0.0002		0.0001			
Pb	μg/L	0.047		0.068		0.074		0.057			
Th	μg/L	0.009		0.003		0.015		0.000			
U	μg/L	0.048		0.272		0.751		1.158			

Table A.4: Result of chemical analysis in the rain water and stream water from Sainteny-Marchesieux

Param.	Unité	Rain water			Sreams			
		mar.2004	nov.2004	jan.2005	SW1	SW2	SW3	SW4
Cond.	μS/cm	95	n.c	88	361	463	425	461
Oxyg	mg/L	n.c.	n.c.	n.c.	3.4	4	1.7	4.5
T	C	n.c.	n.c.	n.c.	12	12.7	12.0	11.3
pH		7.4	n.c.	7.3	7.4	7.9	7.3	7.4
Alc.	mol/L	0.00045	n.c.	0.00012	0.00167	0.00298	0.00237	0.00269
IC	mg/L	6.4	n.c.	n.d	23.2	41.5	33.0	37.5
Cl^-	mg/L	10.3	9.3	19.2	35.0	34.7	36.4	39.4
SO_4^{2-}	mg/L	4.2	4.1	3.9	19.0	17.1	15.6	19.1
NO_3^-	mg/L	4.8	11.4	7.6	9.1	1.7	7.3	7.4
NO_2^-	mg/L	n.c.	n.c.	n.c.	0.2	n.a.	0.3	0
PO_4^{3-}	mg/L	n.c.	n.c.	n.c.	0.3	n.a.	0.1	0
Br^-	mg/L	n.c.	n.c.	n.c.	0.07	0.11	0.09	0.11
Na^+	mg/L	6.05	5.83	12.12	20.35		19.34	21.54
Mg^{2+}	mg/L	0.76	0.77	1.43	10.52	9.38	13.96	9.03
Al^{3+}	μg/L	0.02	0.02	0.02	34.6	6.4	37.2	14.4
Si^{4+}	mg/L	n.c.	n.c.	n.c.	6.54	5.72	3.24	6.18
K^+	mg/L	0.45	0.12	0.04	8.55	3.38	13.79	5.05
Ca^{2+}	mg/L	12.26	1.18	1.65	34.14	63.97	41.78	57.42

Appendix B

Gases and noble gases in Sainteny-Marchesieux: supplement to Chapter 2 in Part I

Table B.1: Noble gases results

Well	Ne mol/L	Ar mol/L	O_2 mol/L	N_2 mol/L	CH_4 mol/L	CO_2 mol/L	N_2O mol/L
F1	1.1816E-08	1.8213E-05	1.0716E-05	8.4948E-04	1.2780E-07	5.1621E-04	2.0137E-06
F4	1.37E-08	1.904E-05	6.48E-05	0.00088479	1.58768E-05	8.98505E-05	0
F4	1.13002E-08	1.7406E-05	1.3154E-05	7.5447E-04	0.3329E-06	9.4445E-05	0.0000E+00
F2	1.25E-08	1.90E-05	9.60E-07	0.000914817	0	0.000718554	0
F2	1.24 E-08	1.96E-05	1.33E-05	0.000966074	0	0.000746508	0
48	1.27E-08	2.024E-05	1.26E-05	8.6625E-05	0	0.001340439	4.69575E-07
48	1.1767E-08	1.9706E-05	2.1072E-05	8.5023E-04	0.0000E+00	1.3504E-03	1.2819E-06
S12	1.12E-08	1.88E-05	8.75E-06	0.000847756	9.40267E-08	0.00244337	2.63713E-06
S12	1.2946E-08	1.9050E-05	9.9985E-06	4881E-04	0.0000E+00	2.4129E-3	2.4613E-06
43	1.15E-08	2.05E-05	9.66E-06	0.000963897	1.72929E-08	0.000214892	0
46	1.36707E-08	1.931E-05	1.23994E-05	0.000906181	0	0.001487458	0
46	1.3371E-08	1.8968E-05	1.1001E-05	8.8774E-04	2.9193E-08	1.5507E-03	0.0000E+00
S18	1.3678E-08	1.9404E-05	1.0657E-05	9.0927E-04	4.1954E-07	1.9087E-04	0.0000E+00
S18	1.3370E-08	1.9286E-05	9.48551E-06	9.0094E-04	3.085E-07	2.3794E-04	0.0000E+00
S10	1.52832E-08	2.3829E-05	1.6946E-05	2.1683E-04	1.1558E-05	2.6120E-04	0.0000E+00
S10	1.3490E-08	2.3374E-05	9.9163E-06	1.0874E-03	1.1620E-05	2.4004E-04	0.0000E+00
15	1.0869E-08	1.8224E-05	8.7607E-06	8.4848E-04	5.1393E-08	9.7482E-04	0.0000E+00
15	1.0392E-08	1.7821E-05	8.7396E-06	8.2559E-04	5.3331E-08	9.8953E-04	0.0000E+00
S15	1.10934E-08	1.8934E-05	1.3583E-05	8.5183E-04	0.0000E+00	2.9750E-03	1.3432E-05
S15	1.4730E-08	1.9283E-05	1.4789E-05	8.4076E-04	0.0000E+00	2.5299E-03	1.1467E-05
S14	1.1260E-08	1.7451E-05	1.0827E-05	8.5999E-04	1.1106E-06	1.2185E-03	0.0000E+00
S14	1.1659E-08	1.8507E-05	8.5613E-06	9.0091E-04	2.2795E-05	7.1487E-04	0.0000E+00

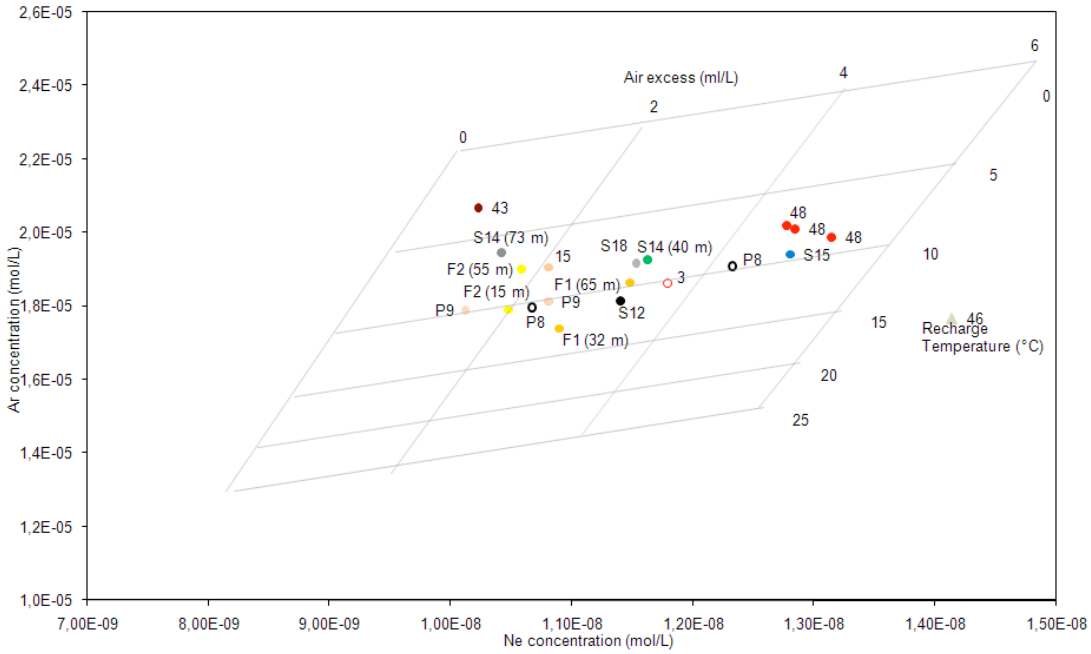

Figure B.1: Ne against Ar, excess air and recharge temperature

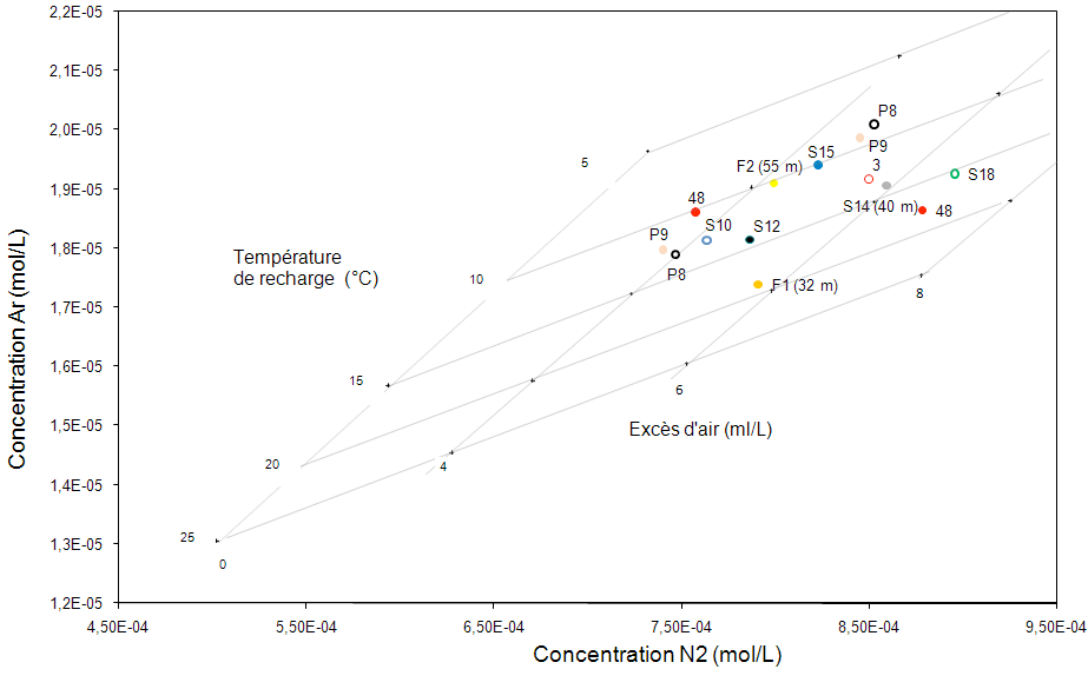

Figure B.2: N_2 against Ar, excess air and recharge temperature

Appendix C

Pearson correlation coefficient : supplement to Chapter 2 in Part II

	pH	Eh	EC	Cl^-	NO_2^-	NO_3^-	$SO_4{}^{2-}$	alk.	Fe^2+	NH_4	DIC	DOC	Na^+	Mg^2+	K^+	Ca^2+	Mn^2+	Fe	CO_2
Eh	-0.482	1	-0.204	0.270	0.133	-0.179	0.153	0.108	-0.079	-0.369	-0.155	-0.017	0.014	-0.275	-0.189	-0.170	0.465	-0.136	-0.278
EC	0.610	-0.204	1	0.128	-0.194	0.667	-0.245	0.154	-0.134	0.265	0.804	-0.383	0.252	0.676	0.257	0.860	-0.470	-0.135	0.691
Cl^-	-0.133	0.270	0.128	1	0.121	-0.240	0.210	0.185	0.132	-0.048	0.135	0.020	0.363	0.128	0.067	0.011	0.011	0.108	0.067
NO_2^-	-0.138	0.133	-0.194	0.121	1	-0.187	0.148	-0.133	-0.063	-0.171	-0.157	0.105	0.150	-0.052	-0.164	-0.173	0.164	-0.054	-0.099
NO_3^-	0.711	-0.179	0.667	-0.240	-0.187	1	-0.721	0.211	-0.450	0.009	0.771	-0.605	-0.208	0.551	0.043	0.822	-0.478	-0.478	0.687
$SO_4{}^{2-}$	-0.531	0.153	-0.245	0.210	0.148	-0.721	1	-0.085	0.294	0.116	-0.599	0.343	0.374	-0.340	0.185	-0.410	0.510	0.361	-0.519
alkalinity	-0.060	0.108	0.154	0.185	-0.133	0.211	-0.085	1	-0.108	0.051	0.175	-0.352	-0.016	0.041	-0.078	0.140	0.065	-0.121	0.101
Fe^2+	-0.523	-0.079	-0.134	0.132	-0.063	-0.450	0.294	-0.108	1	-0.111	-0.189	0.843	0.108	-0.391	-0.228	-0.369	0.152	0.979	-0.374
NH_4	0.262	-0.369	0.265	-0.048	-0.171	0.009	0.116	-0.108	-0.111	1	0.054	-0.145	0.132	0.275	0.354	0.195	-0.177	-0.080	0.229
DIC	0.667	-0.155	0.804	0.135	-0.157	0.771	-0.599	0.175	-0.189	0.054	1	-0.436	-0.011	0.681	-0.073	0.852	-0.612	-0.220	0.799
DOC	-0.628	-0.017	-0.383	0.020	0.105	-0.605	0.343	-0.352	0.843	-0.14	-0.436	1	0.013	-0.550	-0.200	-0.551	0.328	0.859	-0.566
Na^+	0.012	0.014	0.252	0.363	0.150	-0.208	0.374	-0.016	0.108	0.132	-0.011	0.013	1	0.470	0.184	0.076	-0.145	0.145	0.079
Mg^2+	0.791	-0.275	0.676	0.128	-0.052	0.551	-0.340	0.041	-0.391	0.275	0.681	-0.550	0.470	1	0.177	0.744	-0.569	-0.395	0.789
K^+	0.334	-0.189	0.257	0.067	-0.164	0.043	0.185	-0.078	-0.228	0.354	-0.073	-0.200	0.184	0.177	1	0.154	-0.048	-0.156	0.062
Ca^2+	0.746	-0.170	0.860	0.011	-0.173	0.822	-0.410	0.140	-0.369	0.195	0.852	-0.551	0.076	0.744	0.154	1	-0.454	-0.375	0.755
Mn^2+	-0.680	0.465	-0.470	0.011	0.164	-0.478	0.510	0.065	0.152	-0.177	-0.612	0.328	-0.145	-0.569	-0.048	-0.454	1	0.173	-0.589
Fe	-0.516	-0.136	-0.135	0.108	-0.054	-0.478	0.361	-0.121	0.979	-0.080	-0.220	0.859	0.145	-0.395	-0.156	-0.375	0.173	1	-0.400
CO_2	0.774	-0.278	0.691	0.067	-0.099	0.687	-0.519	0.101	-0.374	0.229	0.799	-0.566	0.079	0.789	0.062	0.755	-0.589	-0.400	1

Appendix D

Statistical results : supplement to Chapter 2 in Part II

Table D.1: Summary table for analysis of variance of pH relative to the 3 treatments at day 45. P Le Marais = 0.84; P La Bergerie = 0.0007

Source	**Degrees of freedom**		**Sum of squares**		**Mean square**		**F ratio**	
	Le Marais	La Bergerie	Le Mar.	La Berg.	Le Mar.	La Berg.	Le Mar.	La Berg.
Between treatments	2	2	0.0367	4.8362	0.0183	2.4180		11.88
Within treatments	18	18	1.6875	3.2554	0.1054	0.2034		
Total	20	20						

Table D.2: Summary table for analysis of variance of SO_4^{2-} relative to the 3 treatments at day 45. P Le Marais =0.14; P La Bergerie =0.0011

Source	**Degrees of freedom**		**Sum of squares**		**Mean square**		**F ratio**	
	Le Marais	La Bergerie	Le Mar.	La Berg.	Le Mar.	La Berg.	Le Mar.	La Berg.
Between treatments	2	2	2696	298778	1348	149389	2.254	10.202
Within treatments	18	18	8973	263574	598	14643		
Total	20	20						

Table D.3: Summary table for analysis of variance of DOC relative to the 3 treatments at day 45. P Le Marais =0.00061; P La Bergerie = 0.0011

Source	**Degrees of freedom**		**Sum of squares**		**Mean square**		**F ratio**	
	Le Marais	La Bergerie	Le Mar.	La Berg.	Le Mar.	La Berg.	Le Mar.	La Berg.
Between treatments	2	2	6741.5	298778	3370	149389	12.64	10.202
Within treatments	18	18	3998.8	263574	266	279		
Total	20	20	10740	8684.8	1818	1052		

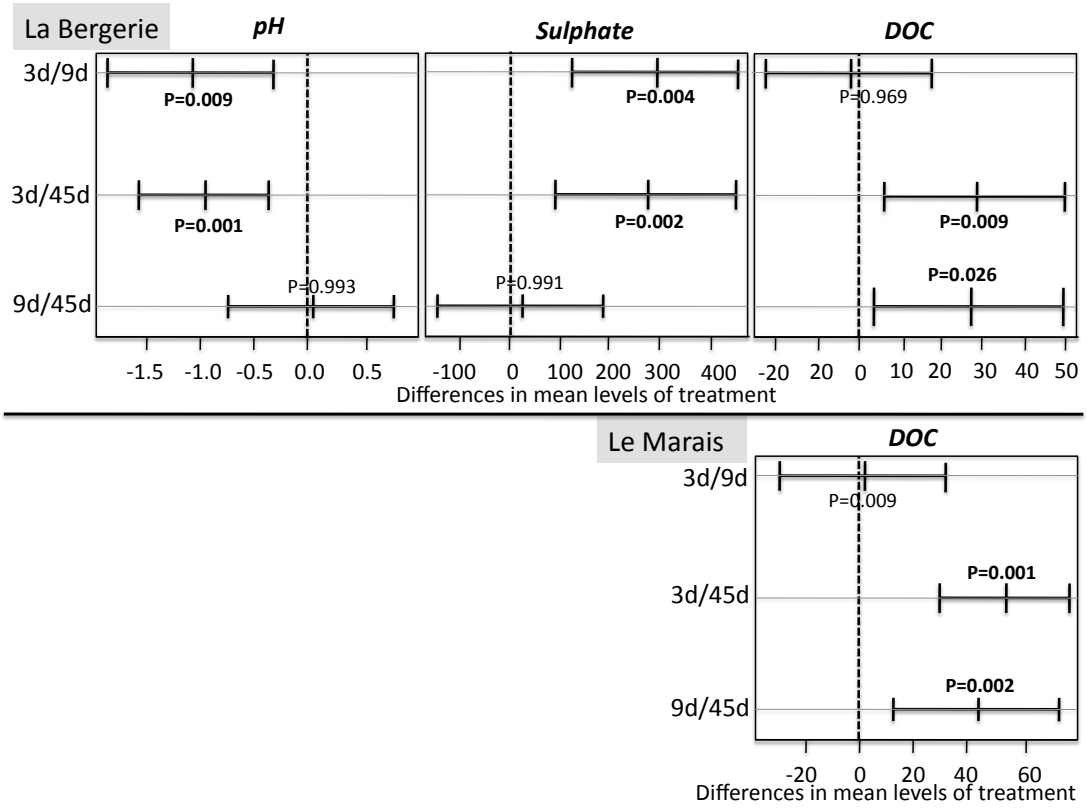

Figure D.1: Plot illustrating the Tukey Kramer test on the parameters found statistically different in the variance analysis. Treatments are different if P value is less than 0.05 (bold type). 3d = 3 days frequency; 9d = 9 days frequency; 45d = permanently saturated

MEMOIRES DE GEOSCIENCES RENNES
Université de Rennes 1 - Campus de Beaulieu
F-35042 - RENNES Cedex
Tél : (33) 02 23 23 65 43 - Fax (33) 02 23 23 67 80
http://www.geosciences.univ-rennes1.fr

N° l - H. MARTIN - Nature, origine et évolution d'un segment de croûte continentale archéenne : contraintes chimiques et isotopiques. Exemple de la Finlande orientale. 392 p., 183 fig., 51 tabl., 4 pl. (1985).	**21,34 €**
N° 2 - G. QUERRE - Palingénèse de la croûte continentale à l'Archéen : Les granitoïdes tardifs (2,5-2,4 Ga) de Finlande Orientale. Pétrologie et géochimie. 226 p., 74, fig., 41 tabl., 3 pl. (1985).	**12,96 €**
N° 3 - J. DURAND - Le Grès Armoricain. Sédimentologie. Traces fossiles. Milieux de dépôt. 150 p., 76 fig., 9, tabl., 19 pl. (1985).	**8,38 €**
N° 4 - D. PRIOUR - Genèse des zones de cisaillement : Application de la méthode des éléments finis à la simulation numérique de la déformation des roches. 157 p., 106 fig., 7 tabl. (1985).	**8,38 €**
N° 5 - V. NGAKO - Evolution métamorphique et structurale de la bordure sud-ouest de la "série de Poli", segment camerounais de la chaîne panafricaine. 185 p., 76 fig., 16, tabl., 12 pl. (1986).	**10,67 €**
N° 6 - J. DE POULPIQUET - Etude géophysique d'un marqueur magnétique situé sur la marge continentale sud-armoricaine.159 p., 121 fig., 5 tabl. (1986).	**8,38 €**
N° 7 - P. BARBEY - Signification géodynamique des domaines granulitiques. La ceinture des granulites de Laponie : une suture de collision continentale d'âge protérozoique inférieur (1,9-2,4 Ga). 324 p., 89 fig., 46 tabl., 11 pl. (1986).	**17,53 €**
N° 8 - Ph. DAVY - Modélisation thermo-mécanique de la collision continentale. 233 p., 72 fig., 2 tabl. (1986).	**Epuisé**
N° 9 - Y. GEORGET - Nature et origine des granites peralumineux à cordiérite et des roches associées. Exemple des granitoïdes du Massif Armoricain (France) : Pétrologie et géochimie. 250 p., 140 fig., 67 tabl. (1986).	**Epuisé**
N° 10 - D. MARQUER - Transfert de matière et déformation progressive des granitoïdes. Exemple des massifs de l'Aar et du Gothard (Alpes Centrales Suisses). 287 p., 134 fig., 52 tabl., 5 cartes hors-texte (1987).	**Epuisé**
N° 11 - J.S. SALIS - Variation séculaire du champ magnétique terrestre. Direction et Paléointensité sur la période 7,000-70,000 BP dans la Chaîne des Puys. 190 p., 73 fig., 28 tabl., I carte hors-texte (1987).	**13,72 €**
N° 12 - Y. GERARD - Etude expérimentale des interactions entre déformation et transformation de phase. Exemple de la transition calcite-aragonite. 126 p., 42 fig., 3 tabl., 10 pl. (1987).	**11,43 €**
N° 13 - H. TATTEVIN - Déformation et transformation de phases induites par ondes de choc dans les silicates. Caractérisation par la microscopie électronique en transmission. 150 p., 50 fig., I tabl., 13 pl. (1987).	**14,48 €**

N° 14 - J.L. PAQUETTE - Comportement des systèmes isotopiques U-Pb et Sm-Nd dans le métamorphisme éclogitique. Chaîne hercynienne et chaîne alpîne. 190 p., 88 fig., 39 tab., 2 pl. (1987).	**14,48 €**
N° 15 - B. VENDEVILLE - Champs de failles et tectonique en extension; modélisation expérimentale. 392 p., 181 fig., I, tabl., 82 pl. (1987).	**Epuisé**
N° 16 - E. TAILLEBOIS - Cadre géologique des indices sulfurés à Zn, Pb, Cu, Fe du secteur de Gouézec-St-Thois : Dévono-Carbonifère du flanc Sud du Bassin de Châteaulin (Finistère). 195 p., 64 fig., 41 tabl., 8 pl. photo., 8 pl. h.texte. (1987).	**16,77 €**
N° 17 - J.P. COGNE - Contribution a l'étude paléomagnétique des roches déformées. 204 p., 86 fig., 17 tabl. (1987).	**13,72 €**
N° 18 - E. DENIS - Les sédiments briovériens (Protérozoïque supérieur) de Bretagne septentrionale et occidentale : Nature, mise en place et évolution. 263 p., 148 fig., 26 tab., 8 pl. (1988).	**21,34 €**
N° 19 - M. BALLEVRE - Collision continentale et chemins P-T : l'Unité pennique du Grand Paradis (Alpes Occidentales). 340 p., 146 fig., 10 tabl., (1988).	**Epuisé**
N° 20 - J.P. GRATIER - L'équilibrage des coupes géologiques. Buts, méthodes et applications. Atelier du Groupe d'Etudes Tectoniques le 8 Avril 1987 à Rennes. 165 p., 82 fig., 2 tabl. (1988).	**12,96 €**
N° 21 - R.P. MENOT - Magmatismes paléozoïques et structuration carbonifère du Massif de Belledonne (Alpes Françaises). Contraintes nouvelles pour les schémas d'évolution de la chaîne varisque ouest-européenne. 465 p., 101 fig., 31 tab., 6 pl., (1988).	**Epuisé**
N° 22 - S. BLAIS - Les ceintures de roches vertes archéennes de Finlande Orientale : Géologie, pétrologie, géochimie et évolution géodynamique. 312 p., 107 fig., 98, tab., 11 pl. photo, 1 pl. h.texte, (1989).	**24,39 €**
N° 23 - A. CHAUVIN - Intensité du champ magnétique terrestre en période stable de transition, enregistrée par des séquences de coulées volcaniques du Quaternaire. 217 p., 100 fig., 13 tab. (1989).	**15,24 €**
N° 24 - J.P. VUICHARD- La marge austroalpine durant la collision alpine; évolution tectonométamorphique de la zone de Sesia-Lanzo. 307 p., 143 fig., 26 tab., 6 pl. hors-texte. (1989).	**25,95 €**
N° 25 - C. GUERROT - Archéen et Protérozoïque dans la chaîne hercynienne ouest-européenne : géochimie isotopique (Sr-Nd-Pb) et géochronologie U-Pb sur zircons. 180 p., 68 fig., 29 tab., I pl. (1989).	**13,72 €**
N° 26 - J.L. LAGARDE - Granites tardi-carbonifères et déformation crustale. L'exemple de la Méseta marocaine. 353 p., 244 fig., 15pl. (1989).	**32,01 €**
N° 27 - Ph. BARDY - L'orogène cadomien dans le Nord-Est du Massif Armoricain et en Manche Occidentale. Etude tectonométamorphique et géophysique. 395 p., 142 fig., 7 tab., I pl. hors-texte. (1989).	**26,68 €**
N° 28 - D. GAPAIS - Les Orthogneiss : Structures, mécanismes de déformation et analyse cinématique. 377 p., 184 fig., 3 tab. (1989).	**Epuisé**

N° 29 - E. LE GOFF - Conditions pression-température de la déformation dans les orthogneiss : Modèle thermodynamique et exemples naturels. 321 p., 146 fig., 42 tab. (1989).	**22,87 €**
N° 30 - D. KHATTACH - Paléomagnétisme de formations paléozoiques du Maroc. 220 p., 97 fig., 35 tab., (1989).	**15,24 €**
N° 31 - A. HAIDER - Géologie de la formation ferrifère précambrienne et du complexe granulitique encaissant de Buur (Sud de la Somalie). Implications sur l'évolution crustale du socle de Buur. 215 p., 18 fig., 42 tab., 7 pl. (1989).	**19,82 €**
N° 32 - T. DANIEL - Traitement numérique d'image appliqué à l'analyse texturale de roches déformées. 186 p., 121 fig., 4 tab. (1989).	**32,01 €**
N° 33 - C. LECUYER - Hydrothermalisme fossile dans une paléocroûte océanique associée à un centre d'expansion lent : Le complexe ophiolitique de Trinity (N. Californie, U.S.A). 342 p., 109 fig., 73 tab. (1989).	**30,49 €**
N° 34 - P. RICHARD - Champs de failles au dessus d'un décrochement de socle: modélisation expérimentale. 382 p., 137 fig. (1989).	**60,98 €**
N° 35 - J. de BREMOND d'ARS - Estimation des propriétés rhéologiques des magmas par l'étude des instabilités gravitaires. Pétrologie du complexe plutonique lité de Guernesey. 370 p., 128 fig., 64 tabl. (1989).	**27,44 €**
N° 36 - A. LE CLEAC'H - Contribution à l'étude des propriétés physiques des minéraux à haute pression : Spectroscopie et calcul des grandeurs thermodynamiques de la lawsonite, des épidotes et des polymorphes de SiO2, 190 p., 72 fig., 37 tabl. (1989).	**15,24 €**
N° 37 - O. MERLE - Cinématique des nappes superficielles et profondes dans une chaîne de collision. 280 p., 165 fig., 3 tabl. (1990).	**24,39 €**
N° 38 - P. ALLEMAND - Approche expérimentale de la mécanique du rifting continental. 205 p., 106 fig., 13 tabl. (1990).	**24,39 €**
N° 39 - Ch. BASILE - Analyse structurale et modélisation analogique d'une marge transformante : l'exemple de la marge de Côte-d'Ivoire - Ghana. 230 p., 161 fig., 7 tabl. (1990).	**31,65 €**
N° 40 - M. AUDIBERT - Déformation discontinue et rotations de blocs. Méthodes numériques de restauration. Application à la Galilée. 250 p., 80 fig., 5 tabl., (1991).	**22,87 €**
N° 41 - G. RUFFET - Paléomagnétisme et 40Ar/39Ar : étude combinée sur des intrusions précambriennes et paléozoïques du Trégor (Massif Armoricain). 261 p., 80 fig., 19 tabl. (1991).	**18,29 €**
N° 42 - P. SUZANNE - Extrusion latérale de l'Anatolie : Géométrie et mécanisme de la fracturation. 262 p., 100 fig., 12 pl., 5 tabl. (1991).	**32,01 €**
N° 43 - G. FIQUET - Propriétés thermodynamiques de minéraux du manteau supérieur. Calorimétrie à haute température et spectroscopie Raman à haute pression et haute température. 274 p., 101 fig., 53 tabl. (1991).	**19,82 €**
N° 44 - J. MARTINOD - Instabilités périodiques de la lithosphère (Flambage, Boudinage en compression et en extension). 283 p., 117 fig., 3 tabl., 2 pl. couleur. (1991).	**25,92 €**

N° 45 - M.O. BESLIER - Formation des marges passives et remontée du manteau: Modélisation expérimentale et exemple de la marge de la Galice. 257 p., 86 fig., 5 tab., 2 pl. noir/blanc, 2 Pl. couleur. (1991). **Epuisé**

N° 46 - J.B.L. FRANCOLIN - Analyse structurale du Bassin du Rio Do Peixe. (Brésil). 250 p., 83 fig., 3 tab., 9 pl. couleur. (1992). **45,73 €**

N° 47 - S. TOURPIN - Perte des mémoires isotopiques (Nd, Sr, O) et géochimiques (REE) primaires des komatiites au cours du métamorphisme : exemple de la Finlande Orientale. 85 p., 53 fig., 23 tabl. (1992). **15,24 €**

N° 48 - J.A. BARRAT - Genèse des magmas associés à l'ouverture d'un domaine océanique : Géochimie des laves du Nord-Est de l'Afrique (Mer Rouge - Afar) et d'Arabie. 175 p., 47 fig., 23 tab. (1992). **15,24 €**

N° 49 - E. HALLOT - Injection dans les réservoirs magmatiques. Contraintes pétrologiques (Massifs de Fort La Latte et de Saint Brieuc, Bretagne Nord) et modélisation analogique. 331 p., 101 fig., 30 tabl. (1993). **27,44 €**

N° 50 - T. SOURIOT - Cinématique de l'extension post-pliocène en Afar. Imagerie SPOT et modélisation analogique. 225 p., 2 pl. coul., I tabl., 91 fig., 16 pl. photo., I carte H.Texte. (1993). **28,97 €**

N° 51 - T. EUZEN - Pétrogenèse des granites de collision post- épaississement. Le cas des granites crustaux et mantelliques du Complexe de Pontivy-Rostrenen (Massif Armoricain, France). 350 p., 2 pl. coul., 34 tabl. En annexe, (1993). **28,97 €**

N° 52 - J. LE GALL - Reconstitution des dynamismes éruptifs d'une province paléovolcanique : l'exemple du graben cambrien du Maine (Est du Massif Armoricain). Pétrogenèse des magmas andésitiques et ignimbritiques et leur signification dans l'évolution géodynamique cadomienne. 370 p., 30pl. photo., I pl. coul. (1993). **Epuisé**

N° 53 - J.C. THOMAS - Cinématique tertiaire et rotations de blocs dans l'ouest de l'Asie Centrale (Tien Shan Kirghiz et dépression Tadjik). Etude structurale paléomagnétique. 330 p., 107 fig., 2 pl. coul., 18 tabl., 1 carte, annexes. (1993). **33,54 €**

N° 54 - F. LAFONT - Influences relatives de la subsidence et de l'eustatisme sur la localisation et la géométrie des réservoirs d'un système deltaïque. Exemple de l'Eocène du bassin de Jaca, Pyrénées Orientales. 270 p., 115 fig., dont 17 pl. couleur. (1994). **22,87 €**

N° 55 - C. BIELLMANN - Stabilité et réactivité des carbonates à très hautes pression et température. Implications pour le stockage du Carbone dans le manteau terrestre. 230 p., 74 fig., 11 tabl., 1 pl. couleur (1993). **26,68 €**

N° 56 - A. POTREL - Evolution tectono-métamorphique d'un segment de croûte continentale archéenne. Exemple de l'Amsaga (R.I. Mauritanie), dorsale Réguibat (Craton Ouest Africain). 400 p., (dont annexes) 125 fig., 21 tabl., 1 pl. couleur, 43 pl. photo (1994). **41,16 €**

N° 57 - M. KUNTZ - Approche expérimentale de la déformation dans les systèmes préfracturés : Contribution à l'étude de l'inversion tectonique des bassins sédimentaires. 220 p., 19 pl., 87 fig., 3 tabl. (1994). **23,63 €**

N° 58 - D. ROUBY - Restauration en carte des domaines faillés en extension. Méthode et applications. 266 p., 98 fig. dont annexes (1994). **27,44 €**

N° 59 - J.J. TONDJI-BIYO - Chevauchements et bassins compressifs. Influence de l'érosion et de la sédimentation. Modélisation analogique et exemples naturels. 426 p., 141, fig., 4 pl. couleur, 21 tableaux, dont annexes (1995). **41,16 €**

N° 60 - H. BOUHALLIER - Evolution structurale et métamorphique de la croûte continentale archéenne (Craton de Dharwar, Inde du Sud). 277 p., 100 fig., dont 5 pl. coul., 7 tab., dont annexes (1995).	**22,87 €**
N° 61 - P. GAUTIER - Géométrie crustale et cinématique de l'extension tardi-orogénique dans la domaine centre-égéen îles des Cyclades et d'Eubée, Grèce). 430 p., 89 fig., dont 4 pl. coul., 1 tabl., dont annexes (1995).	**33,54 €**
N° 62 - M.T. ROMAN BERDIEL - Mécanismes d'intrusion des granites supracrustaux. Modèles analogiques et exemples naturels. 270 p., 75 fig., 5 pl. laser, 9 tabl. (1995).	**24,39 €**
N° 63 - M. JULLIEN - Polytypisme, ordre d'empilement et interstratification dans la cookéite et les phyllosilicates non micacés du métamorphisme. Influence de la pression. 226 p., 61 fig., 8 tabl. (1995).	**22,87 €**
N° 64 - Y. LAHAYE - L'altération des komatiites. 224 p., 70 fig., 29 tabl., + annexes (1995).	**22,87 €**
N° 65 - A. CRAVE - Quantification de l'Organisation des réseaux hydrographiques. 210 p., 68 fig., dont annexe (1995).	**Epuisé**
N° 66 - A. ESSAIFI - Relations entre magmatisme-déformation et altération hydrothermale : L'exemple des Jebilet centrales (Hercynien, Maroc). 331 p., 248 fig., 4 tabl., dont annexes (1995).	**25,92 €**
N° 67 - M. LE RAVALEC - Vitesses et perméabilité des roches : modélisation du rôle des fluides et des fissures. 276 p., 119 fig. 3 pl. couleur, 5 tabl., dont annexe (1996).	**21,34 €**
N° 68 - A. SEMIANI - Métallogénie de la zone de cisaillement aurifère est-ouzzalienne : structure, pétrologie et géochimie des gisements d'or de Tirek-Amesmessa (Hoggar occidental, Algérie). 262 p.,72 fig., 36 tabl., 4 pl. couleur + annexes, (1996).	**19,82 €**
N° 69 - F. MOREAU - Méthodes de traitement de données géophysiques par transformée en ondelettes. 177 p., 57 fig., + annexes. (1996).	**15,24 €**
N° 70 - B. TOURNERIE - Imagerie de réflecteurs électromagnétiques en régime diffusif : Méthode et applications en Géophysique. 165 p., 45 fig., 8 tabl., + annexes, (1996).	**15,24 €**
N° 71 - T. NALPAS - Inversion des grabens du Sud de la Mer du Nord. Données de sub-surface et modélisation analogique. 245 p., 110 fig., dont 10 pl. coul, (1996).	**18,29 €**
N° 72 - M. URREIZTIETA - Tectonique néogène et bassins transpressifs en bordure méridionale de l'Altiplano-Puna (27°S), Nord-Ouest argentin. 311 p., 111 fig., 5 tabl., 6 pl. couleur, dont annexe. (1996).	**30,49 €**
N° 73 - A.N. KOUAMELAN - Géochronologie et Géochimie des Formations Archéennes et Protérozoïques de la Dorsale de Man en Côte d'Ivoire. Implications pour la Transition Archéen-Protéorozoïque. 290 p., 99 fig., 23 tabl., 2 pl. couleur, dont annexe (1996).	**18,29 €**
N° 74 - Y. GARCIA - Variation de l'intensité du champ magnétique en France durant les deux derniers millénaires. 331 p., 122 fig., 35 tab., dont annexe. (1996).	**22,87 €**
N° 75 - M. A. SANTOS PINTO - Le recyclage de la croûte continentale archéenne : Exemple du bloc du Gavião- Bahia, Brésil. 193 p., 102 fig., 51 tab. (1996).	**15,24 €**
N° 76 - D. CHARDON - Les déformations continentales archéennes : Exemples naturels et modélisation hermomécanique. 300 p., 127 fig., 6 tabl., 4 pl. photo; dont annexes. (1997).	**19,82 €**

N° 77 - C. ROBIN - Mesure stratigraphique de la déformation : Application à l'évolution jurassique du Bassin de Paris. 293 p., 129 fig., 9 pl. couleur, dont annexes. (1997).	**27,44 €**
N° 78 - D. GRANJEON - Modélisation stratigraphique déterministe : Conception et applications d'un modèle diffusif 3D multilithologique. 197 p., 56 fig., 22 tabl., 8 pl. couleur. (1997).	**15,24 €**
Hors Série N°1 - P. DAVY, F. GUILLOCHEAU, B. HAMELIN (Coordinateurs) - Géomorphologie : Processus et modélisation. Ecole thématique du CNRS, 146 p., 69 fig., 2 tab., Lumigny, Juillet (1997).	**7,62 €**
N° 79 - A. JAFFREZIC - Géochimie des éléments métalliques, des nitrates et du carbone organique dissous dans les eaux et les sols hydromorphes. Agriculture intensive et qualité des eaux dans les zones humides en Bretagne. 296 p., 143 fig., 46 tabl., 1 pl. coul., dont annexes (1997).	**Epuisé**
N° 80 - O. BOUR - Transferts de fluides dans les milieux fracturés : Effets d'échelle. 272 p., 100 fig., 1 tabl., (1997).	**15,24 €**
N° 81 - E. BONNET - La localisation de la déformation dans les milieux fragile-ductile : Approche expérimentale et application à la lithosphère continentale. 183 p., 85 fig., 4 tabl., (1997).	**12,96 €**
N° 82 - S. GESSA - Le genre Nowakia (Dacryoconarides) dans le Praguien de la République Tchèque : Biométrie, systématique, phylogénie, paléoenvironnements. 256 p., 132, fig., 8 pl., + annexes. (1997).	**19,06 €**
N° 83 - T. MAUDUIT - Déformation gravitaire synsédimentaire sur une marge passive : modélisation analogique et application au Golfe de Guinée. 260 p., 96 fig., dont 12 pl. coul., (1998).	**15,24 €**
N° 84 - G. QUEREL - Cristallochimie des éléments traces dans les phases du manteau terrestre : applications de la spectroscopie de luminescence à haute pression et haute température. 241 p., 101 fig., 23 tabl., (1998).	**14,48 €**
N° 85 - M. DIRAISON - Evolution cénozoïque du Bassin de Magellan et tectonique des Andes australes. 333 p., 119 fig., dont 6 pl. coul., 2 pl. hors-texte, 7 tabl., (1998).	**19,82 €**
N° 86 - S. BONNET - Tectonique et dynamique du relief : le socle armoricain au Pléistocène. 352 p., 144 fig., dont 7pl. coul., +1 pl. coul. et 3 transparents en annexe, (1998).	**Epuisé**
N° 87 - F. TOUCHARD - Caractérisation hydrogéologique d'un aquifère en socle fracturé : site de Ploëmeur (Morbihan). 271 p., 103 fig., dont 5 coul., 37 tabl., annexe. (1999).	**17,53 €**
N° 88 - T.V. LE - Stratigraphie sismique et modélisation stratigraphique : application à l'évolution tectonique oligo-miocène du Bassin du Fleuve Rouge (Vietnam). 229 p., 131 fig., dont 16 pl. coul. + annexes (1999).	**16,77 €**
N° 89 - V. CHAVAGNAC - Behaviour of the Sm-Nd isotopic system during metamorphism : examples from the HT-LP metamorphic terrane of the Limpopo Belt, South Africa and the UHP metamorphic terrane of Dabieshan, Central China. 405 p., 126 fig., 47 tabl. (1999).	**22,87 €**
N° 90 - J. MOLENAT - Rôle de la nappe sur les transferts d'eau de nitrate dans un bassin versant agricole. Etude expérimentale et modélisation. 272 p., 87 fig., 19 tabl., 3 pl. couleur. (1999).	**15,24 €**

N° 91 - C. RIOU - Géochimie des terres rares et des éléments traces associés dans les nappes et l'eau des sols hydromorphes : Application au traçage hydrologique. 293 p., 74 fig., 17 tabl., + annexes. (1999).	**15,24 €**
N° 92 - I. COUTAND - Tectonique Cénozoïque du Haut Plateau de la Puna, Nord Ouest Argentin, Andes Centrales. 381 p., 125 fig., 10 tabl., 6 pl. coul., 1 pl. hors-texte + annexes. (1999).	**22,87 €**
N° 93 - F. DARBOUX - Modélisations numérique et expérimentale du ruissellement. Effet de la rugosité sur les distances de transfert. 170 pages., 56 fig., 4 tabl. (1999).	**12,20 €**
N° 94 - J.R. De DREUZY - Analyse des propriétés hydrauliques des réseaux de fractures. Discussion des modèles d'écoulement compatibles avec les principales propriétés géométriques. 217 pages, 118 fig., 9 tabl., (2000).	**13,72 €**
Hors-Série n° 2 - G. BADARCH & B.M. JAHN - IGCP-420 Continental Growth in the Phanerozoïc : Evidence from Central Asia. Second Workshop. Abstracts and Excursion Guidebook. (Geotraverse through a terrane collage in Southern Khangay). July 25 - August 3, 1999, Ulaanbaatar, Mongolia. 190 pages. (2000).	**9,91 €**
N° 96 – O. BOURGEOIS - Processus d'extension lithosphérique en Islande. Interactions avec les calottes glaciaires quaternaires. 280 pages, 95 fig., dont 2 planches couleur, 2 tabl. (2000).	**12,20 €**
N° 97 - S. REVILLON – Origine et composition du Plateau Océanique Caraïbe. 358 pages, 77 fig., 24 tabl. (2000).	**18,29 €**
Hors-Série n° 3 - J.P. BRUN & M.A. OLLIVIER – 150 ans de Géologie à Rennes. 105 p., 13 pl. coul. (2000).	**10,67 €**
N° 98 – M. PESSEL - Tomographie électrique : Développements méthodologiques et applications. 129 pages, 59 fig, dont 7 planches couleur, 1 tab. (2001).	**11,43 €**
N° 99 – L. MICHON – Dynamique de l'extension continentale – Application au Rift Ouest-Européen par l'étude de la province du Massif Central. 266 pages, 134 fig., dont 6 planches couleur.(2001).	**14,48 €**
N° 100 – M. BULOURDE - Processus d'altération des basaltes du Mont Cameroun : approche géochimique. 270 p., 67 fig., 32 tabl. (2001).	**16,77 €**
N° 101 – O. SERRANO - Le Crétacé supérieur - Paléogène du bassin compressif Nord-pyrénéen (Bassin de l'Adour). Sédimentologie, stratigraphie, géodynamique. 173 p., 72 fig., dont 3 pl. couleur, 9 pl. photos., 1 CD-ROM. (2001).	**19,06 €**
Hors-Série n° 4 – D. GAPAIS et J.P. BRUN (Ed.) - Deformation, mechanisms, rheology and tectonics, Saint-Malo, France, April, 14-16, 2003, 183 p. (2003).	**Epuisé**
N° 102 – C. DARCEL – Corrélations dans les réseaux de fractures : caractérisation et conséquences sur les propriétés hydrauliques. 224 p. (2003).	**22,50 €**
N° 103 – L. BARRIER – Interactions déformation – sédimentation dans les systèmes compressifs supra-crustaux. Exemples naturels et modélisation analogique. 219 p. (2003).	**27,75 €**
N° 104 – S. CASTELLTORT - Origine et modification des cycles stratigraphiques à haute-fréquence (10's à 100's ka). Rôle des déformations courte longueur d'onde et modélisation du comportement des systèmes fluviatiles. 193 p. (2003).	**23,41 €**

N° 105 – S. POCHAT - Escarpement de faille synsédimentaire. Perturbation des écoulements gravitaires sous-marins et détermination de la cinématique des failles. 282 p. (2003).	**26,82 €**
N° 106 – C. GUMIAUX - Modélisation du cisaillement hercynien de Bretagne centrale : déformation crustale et implications lithosphériques**.** 266 p. (2003).	**13,56 €**
N° 107 – C. ARRIAGADA - Rotations tectoniques et déformation de l'avant arc des Andes centrales au cours du Cénozoïque = Rotaciones tectónicas y deformación del antearco en los Andes centrales durante el cenozoico**.** 308 p. (2004).	**19,50 €**
N° 108 – B. VIDET - Dynamique des paléoenvironnements à huîtres du Crétacé Supérieur nord-aquitain (SO France) et du Mio-Pliocène andalou (SE Espagne) : biodiversité, analyse séquentielle, biogéochimie. 288 p. (2004).	**19,60 €**
N° 109 – O. BROUCKE - Relations Déformation - Sédimentation en contexte de sédimentation gravitaire. Exemples sismiques (marge angolaise) et de terrain (Grès d'Annot). 354 p. (2004).	**Epuisé**
N° 110 – D. MENIER - Morphologie et remplissage des vallées fossiles sud-armoricaines : apport de la stratigraphie sismique. 202 p. (2004).	**16,71 €**
N° 111 – H. BOUKERBOUT - Analyse en ondelettes et prolongement des champs de potentiel. Développement d'une théorie 3-D et application en géophysique. 134 p. (2004)	**17,46 €**
N° 112 – J. BABAULT - Dynamique de l'érosion dans une chaîne de montagnes : influence de la sédimentation de piedmont. L'exemple des Pyrénées. 218 p. (2004).	**14,54 €**
N° 113 – R. MOURGUES - Surpressions de fluide et décollements. Modélisations analogique et numérique. 264 p. (2004)	**24,79 €**
N° 114 – M. LEROY - Mécanismes de déformation post-rifting des marges passives. Exemple des marges péri-atlantiques et modélisation. 244 p. (2005)	**20,38 €**
N° 115 – C. TIREL - Dynamique de l'extension des domaines continentaux épaissis : dômes métamorphiques et écoulement de la croûte ductile. 248 p. (2005)	**17,28 €**
N° 116 – O. GALLAND - Interactions mécaniques entre la tectonique compressive et le magmatisme : expériences analogiques et exemple naturel. 423 p. (2005)	**32,38 €**
N° 117 – S. SCHULLER - Localisation de la déformation et fracturation associée. Etude expérimentale et numérique sur des analogues de la lithosphère continentale. 350 p. (2005)	**18,37 €**
N° 118 – V. PERRICHOT - Environnements paraliques à ambre et à végétaux du Crétacé Nord-Aquitain (Charentes, Sud-Ouest de la France). 310 p. (2005)	**27 €**
N° 119 – N. LOGET - Dynamique de l'érosion fluviatile consécutive à une chute du niveau de base. L'exemple de la crise de salinité messinienne. 226 p. (2005)	**21 €**
N° 120 – A. GRISLIN-MOUEZY - Caractérisation de l'endommagement de parois de galeries par tomographie électrique : application en laboratoire souterrain. 192 p. (2006)	**32,10 €**
N° 121 – B. LE BAYON - Evolution structurale et métamorphique d'une croûte continentale subductée (Grand Paradis, Alpes occidentales). 385 p. (2006)	**32,10 €**

N° 122 – M. GOMEZ PACCARD - Étude de la variation de la direction et de l'intensité du champ géomagnétique en Espagne durant les deux derniers millénaires. 194 p. + 1 CD-ROM (2006)	**32,10 €**
N° 123 – F. CAGNARD - Compression des lithosphères continentales "chaudes". Application à la tectonique précambrienne. 339 p. (2006)	**32,10 €**
Hors-Série n° 5 – S. BOURQUIN et M. DURAND - Pan-European correlation of the epicontinental Triassic International Field Workshop on 'The Triassic of eastern France' October 2 - 7, 2006. 80 p. (2007)	**32,10 €**
N° 124 – S. ROHAIS - Architecture stratigraphique et flux sédimentaires sur la marge sud du golfe de Corinthe (Grèce) : Analyse de terrain, modélisations expérimentales et numériques. 386 p. (2007)	**32,10 €**
N° 125 – R. VULLO - Les vertébrés du Crétacé supérieur des Charentes (Sud-Ouest de la France) : Biodiversité, Taphonomie, Paléoécologie et Paléobiogéographie. 357 p. (2007)	**32,10 €**
N° 126 – N. CARRY - De la subduction continentale à l'exhumation dans les Alpes Penniques. Modélisations thermo-mécanique et paléogéographique. 311 p. (2007)	**32,10 €**
Hors-Série n° 6 – O. DUGUÉ – Le Massif Armoricain dans l'évolution mésozoïque et cénozoïque du nord-ouest de l'Europe. Contrôles tectonique, eustatique et climatique d'un bassin intracratonique (Normandie, Mer de la Manche, France). 335 p. (2007)	**Epuisé**
C. ROBIN, D. ROUBY, M. SIMOES, J.-J. TIERCELIN – International Workshop - *Abstract Book :* TOPOAFRICA - Evolution of African Topography over the last 250My from the sedimentary record to mantle dynamics - Rennes November 13-16, 2007. 90 p. (2007)	**Epuisé**
N° 127 – N. BRAULT - Ressources du sous-sol et environnement en Bretagne. Genèse, géométrie et propriétés de différents types d'aquifères. 240 p. + 1 CD-ROM (2008)	**32,10 €**
N° 128 – F. PAQUET – Evolution morphostructurale des bassins de marge active en subduction : l'exemple du bassin avant arc de Hawke Bay en Nouvelle-Zélande = Morphostructural evolution of active subduction margin basins : the example of the Hawke Bay forearc basin, New Zealand. 228 p. (2008)	**32,10 €**
N° 129 – E. LASSEUR – La Craie du Bassin de Paris (Cénomanien-Campanien, Crétacé supérieur). Sédimentologie de faciès, stratigraphie séquentielle et géométrie 3D. 409 p. + 1 CD-ROM (2008)	**32,10 €**
N° 130 – J. PRECIGOUT – La localisation de la déformation dans le manteau sous-continental. Origine à travers l'étude du massif de Ronda (Espagne) et implications sur la résistance de la lithosphère. 154 p. (2009)	**32,10 €**
N° 131 – M. FAKIH – Biogéochimie du fer et des éléments associés : exemple de l'arsenic (V). 161 p. (2009)	**32,10 €**
N° 132 – C. LOISELET – Devenir d'une lithosphère en subduction dans le manteau terrestre : Etude de sa déformation et des flux mantelliques associés. 206 p. (2011)	**32,10 €**
N° 133 – G. BIESSY – Quantification et caractérisation des mouvements verticaux aux courtes échelles de temps dans les zones dites stables. 216 p. (2010)	**32,10 €**

N° 134 – V. GIRARD – Microcénoses des ambres medio-crétacés français. Taphonomie, systématique, paléoécologie et reconstitution du paléoenvironnement 294 p. (2010)	**32,10 €**
N° 135 – C. DUCASSOU – Age et origine des premiers reliefs de la chaîne hercynienne Le Dévono-Carbonifère du Bassin d'Ancenis. 513 p. (2010)	**32,10 €**
N° 136 – M. PÉDROT – Colloïdes et compositions élémentaires des solutions de sols. 221 p. (2010)	**32,10 €**
N° 137 – F. MVONDO OWONO – Surrection cénozoïque de l'Ouest de l'Afrique à partir de deux exemples : le plateau sud-namibien et la marge nord camerounaise. 324 p. (2011)	**32,10 €**
N° 138 – R. MARSAC – Contrôle de la spéciation des terres rares par les acides humiques : rôle de l'hétérogénéité des sites de complexation et de la compétition entre cations. 151 p. (2012)	**32,10 €**
N° 139 – C. ANDERMANN – Climate, topography and erosion in the Nepal Himalayas. 185 p. (2012)	**32,10 €**
N° 140 – C. MALFILATRE – Mise au point d'une méthodologie analytique d'identification des pierres naturelles de construction. 465 p. (2012)	**32,10 €**
N° 141 – E. LE BRETON – Differential spreading along the NE Atlantic ridge system and post-breakup deformation of the adjacent continental margins. 316 p. (2012)	**32,10 €**
N° 142 – H. POUDEROUX – Sédimentation gravitaire et paléosismicité d'une marge active : exemple de la marge en subduction Hikurangi en Nouvelle-Zélande. 353 p. (2012)	**32,10 €**
N° 143 – J. DE RIDDER – Réponse des processus biochimiques d'une tourbière soumise à des fluctuations du niveau d'eau. 222 p. (2012)	**32,10 €**
N° 144 – E. BRESCIANI – Modélisation des contrôles climatiques, topographiques, géologiques et anthropiques sur les écoulements souterrains en domaine de socle. 213 p. (2012)	**32,10 €**

CAHIERS TECHNIQUES DE GEOSCIENCES RENNES

Université de Rennes 1 - Campus de Beaulieu
F-35042 - RENNES Cedex
Tél : (33) 02 23 23 65 43 - Fax (33) 02 23 23 67 80
http://www.geosciences.univ-rennes1.fr

N° l – M. BOUHNIK-LE COZ, P. PETITJEAN, E. SERRAT et G. GRUAU - Validation d'un protocole permettant le dosage simultané des cations majeurs et traces dans les eaux douces naturelles par ICP-MS. 84 p. (2001) **7,62 €**

N° 2 – P. PETITJEAN, O. HENIN, S. ELLIAS et G. GRUAU - Application de l'électrophorèse capillaire au dosage des anions et des cations majeurs en solution dans les eaux douces naturelles. 49 p. (2001) **9,15 €**

N° 3 – P. PETITJEAN, O. HENIN, G. GRUAU - Dosage du carbone organique dissous dans les eaux douces naturelles. Intérêt, principe, mise en oeuvre et précautions opératoires. 61 p. (2004) **8,74 €**

N° 4 – T. LABASQUE, V. AYRAUD, L. AQUILINA, P. LE CORRE - Dosage des composés chlorofluorocarbonés et du tétrachlorure de carbone dans les eaux souterraines. Application à la datation des eaux. 51 p. (2006) **15,82 €**

MEMOIRES DU CAREN

Université de Rennes 1 - Campus de Beaulieu
F-35042 - RENNES Cedex
Tél : (33) 02 23 23 60 75 - Fax (33) 02 23 23 67 80
http://www.caren.univ-rennes1.fr

N° 1 – D. LAGUE - Dynamique de l'érosion continentale aux grandes échelles de temps et d'espace : modélisation expérimentale, numérique et théorique. 155 p. (2003).	**17,80 €**
N° 2 – H. VANDEN BOSSCHE – Devenir du phosphore apporté sur les sols et risques de contamination des eaux de surface. Cas des boues de stations d'épuration. 338 p. (2003).	**28,46 €**
N° 3 – P. DAVY, Y. LAGADEUC (coord.) – Centre Armoricain de Recherches en Environnement : rapport d'activité 2000-2002, prospective 2004-2007, 145 p. (2003)	**épuisé**
N° 4 - C. MARTIN – Mécanismes hydrologiques et hydrochimiques impliqués dans les variations saisonnières des teneurs en nitrate dans les bassins versants agricoles. Approche expérimentale et modélisation. 267 p. (2003).	**21,67 €**
N° 5 - K. BESNARD – Modélisation du transport réactif dans les milieux poreux hétérogènes. Application aux processus d'adsorption cinétique non linéaire. 251 p. (2004)	**22,56 €**
N° 6 – V. VIAUD – Organisation spatiale des paysages bocagers et flux d'eau et de nutriments. Approche empirique et modélisations. 283 p. (2004).	**12,10 €**
N° 7 – G. PERES – Identification et quantification in situ des interactions entre la diversité lombricienne et la macro-bioporosité dans le contexte polyculture breton. Influence sur le fonctionnement hydrique du sol. 268 p. (2004).	**26,49 €**
N° 8 – F. ABLAIN – Rôle des activités lombriciennes sur la redistribution des éléments traces métalliques issus de boue de station d'épuration dans un sol agricole. 152 p. (2004).	**21,31 €**
N° 9 – A. KERSANTE – Rôle régulateur de la macrofaune lombricienne dans la dynamique de l'herbicide atrazine en sol cultivé tempéré. 189 p. (2004).	**22,20 €**
N° 10 – S. ABIVEN – Relations entre caractéristiques des matières organiques apportées, dynamique de leur décomposition et évolution de la stabilité structurale du sol. 262 p. (2005).	**22,28 €**
N° 11 – C. BASSET-MENS - Propositions pour une adaptation de l'analyse de cycle de vie aux systèmes de production agricole. Mise en œuvre pour l'évaluation environnementale de la production porcine. 242 p. (2005)	**25,97 €**
N° 12 – F. TORTRAT - Modélisation orientée décision des processus de transfert par ruissellement et subsurface des herbicides dans les bassins versants agricoles. 219 p. (2005)	**14,33 €**
N° 13 – T. LE BORGNE - Mesure *in situ* et modélisation de l'hétérogénéité des écoulements dans les milieux géologiques. 175 p. (2005)	**21 €**
N° 14 – V. AYRAUD - Détermination du temps de résidence des eaux souterraines : application au transfert d'azote dans les aquifères fracturés hétérogènes. 298 p. (2006)	**32,10 €**

N° 15 – S. FOLLAIN - Effet du réseau bocager sur l'organisation des sols. Redistributions des sols et stockage en carbone organique. 244 p. (2006)	**22 €**
N° 16 - C. LEGOUT - Etude des mécanismes hydrologiques et biogéochimiques de la recharge des nappes à surface libre. 180 p. (2006)	**22 €**
N° 17 - C. AUTERIVES - Influence des flux d'eau souterraine entre une zone humide superficielle et un aquifère profond sur le fonctionnement hydrochimique des tourbières : Exemple des marais du Cotentin, Basse-Normandie. 261 p. (2007)	**32,10 €**
N° 18 - O. POURRET - Impact de la matière organique sur le comportement des terres rares en solution : étude expérimentale et modélisation. 172 p. (2007)	**32,10 €**
N° 19 - J. LEFRANÇOIS - Dynamiques et origines des matières en suspension sur de petits bassins versants agricoles sur schistes. 273 p. (2007)	**22 €**
N° 20 - A.H. LE GALL et Y. LAGADEUC - Pour des connaissances et une culture partagées en environnement. Rapport d'activités CST du CAREN, 2003-2006. 60 p. (2007)	**Epuisé**
N° 21 – P. LAGUIONIE - Mesures in situ et modélisation du transport des sédiments en rivière. Application au bassin versant de la Vilaine. 349 p. (2007)	**32,10 €**
N° 22 – N. BOUGON – L'influence des circulations hydrologiques sur la structure des communautés bactériennes à l'interface sol-nappe. 338 p. (2008)	**32,10 €**
N° 23 – L. SOREL – Paysages virtuels et analyse de scénarios pour évaluer les impacts environnementaux des systèmes de production agricole = Virtual landscapes and scenario analysis to assess the environmental impacts of agrosystems. 211 p. (2008)	**22,00 €**
N° 24 – B. MOREL – Transport de carbone organique dissous dans un bassin versant agricole à nappe superficielle. 208 p. (2009)	**22,00 €**
N° 25 – R. LE GOC – Caractérisation et modélisation des écoulements dans les milieux fracturés. 182 p. (2010)	**32,10 €**
N° 26 – L. MICHEL – Transport en fracture et interaction avec la matrice : une expérience analogique. 255 p. (2010)	**32,10 €**
N° 27 – N. BOTTINELLI – Evolution de la structure et de la perméabilité d'un sol en contexte de non labour associé à l'apport d'effluent d'élevage : rôle de l'activité lombricienne. 152 p. (2011)	**22,00 €**
N° 28 – O. MONTREUIL – Relation entre l'ordre des bassins versants, l'organisation spatiale et le fonctionnement hydrologique et hydrochimique des zones humides riveraines. 230 p. (2011)	**22,00 €**
N° 29 – D. ROUBINET – Impact des structures géologiques sur les échanges entre fractures et matrice dans les milieux poreux fracturés. 166 p. (2011)	**32,10 €**
N° 30 – S. RUELLEU – Caractérisation hydrogéophysique des milieux fracturés : développement instrumental et modélisation des vitesses d'écoulement en forage. 265 p. (2011)	**non publié**
N° 31 – I. ACOSTA-ALBA – Quelles valeurs de référence pour l'analyse de la durabilité environnementale des systèmes de production animale ? Méthode de détermination et application aux exploitations laitières de Bretagne. 158 p. (2011)	**22,00 €**

N° 32 – A. BOISSON – Etude multi-échelles des réactions de dénitrification dans les aquifères hétérogènes : Approches expérimentales de l'influence des écoulements sur la réactivité biogéochimique. 293 p. (2011) **32,10 €**

POUR PASSER COMMANDE

S'adresser à :

Catherine Bertin
Géosciences Rennes
Université de Rennes 1
Bâtiment 14 B – Centre de documentation
F-35042 Rennes cedex

Tel : 02 23 23 65 43
Fax : 02 23 23 67 80
mail : catherine.bertin@univ-rennes1.fr

Votre commande doit être accompagnée :

- de votre bon de commande
- de votre règlement par chèque à l'ordre de : *Agent comptable du CNRS*

BON DE COMMANDE

.NOM	
.ORGANISME	
.ADRESSE	

Veuillez me faire parvenir les ouvrages suivants (cocher la collection concernée):

☐ dans la collection des Mémoires

☐ dans la collection des Cahiers techniques

N°	**Auteur – Titre**	**Nombre d'ex**	**Prix unitaire**	**Total 1**
Frais de port : ***Nous consulter***			**Total 2**	
	TOTAL DE LA COMMANDE		**Total 1 + Total 2**	

Imprimé à l'Université de Rennes 1

Dépôt Légal

4° trimestre 2012